



HAL
open science

Gravitational Bremsstrahlung in the Worldline Effective Field Theory Approach

Massimiliano Maria Riva

► **To cite this version:**

Massimiliano Maria Riva. Gravitational Bremsstrahlung in the Worldline Effective Field Theory Approach. High Energy Physics - Theory [hep-th]. Université Paris-Saclay, 2022. English. NNT : 2022UPASP078 . tel-03895254

HAL Id: tel-03895254

<https://theses.hal.science/tel-03895254>

Submitted on 12 Dec 2022

HAL is a multi-disciplinary open access archive for the deposit and dissemination of scientific research documents, whether they are published or not. The documents may come from teaching and research institutions in France or abroad, or from public or private research centers.

L'archive ouverte pluridisciplinaire **HAL**, est destinée au dépôt et à la diffusion de documents scientifiques de niveau recherche, publiés ou non, émanant des établissements d'enseignement et de recherche français ou étrangers, des laboratoires publics ou privés.

Gravitational Bremsstrahlung in the Worldline Effective Field Theory Approach

*Bremsstrahlung gravitationnelle dans l'approche
"worldline" de la théorie des champs effective*

Thèse de doctorat de l'université Paris-Saclay

École doctorale n° 564, Physique en Ile-de-France (PIF)
Spécialité de doctorat: Physique
Graduate School : Physique, Référent : Faculté des sciences d'Orsay

Thèse préparée dans l'unité de recherche « Institut de physique théorique, (Université Paris-Saclay, CNRS, CEA) »,
sous la direction de Filippo Vernizzi, Directeur de recherche CEA, Université Paris-Saclay.

Thèse soutenue à Paris-Saclay, le 30 septembre 2022, par

Massimiliano Maria RIVA

Composition du jury

Luc BLANCHET Directeur de recherche (HDR), <i>Institut d'Astrophysique de Paris</i> , Sorbonne Université, CNRS.	President
Walter GOLDBERGER Maître de conférences (HDR), Physics Department, <i>Yale University</i> (USA).	Rapporteur & Examineur
Rodolfo RUSSO Maître de conférences (HDR), <i>Centre for Theoretical Physics</i> , Department of Physics and Astronomy, Queen Mary University of London (UK).	Rapporteur & Examineur
Brando BELLAZZINI Chargé de recherche, <i>Institut de Physique Théorique</i> , Université Paris-Saclay, CNRS, CEA.	Examineur
Federico PIAZZA Professeur des universités, <i>Centre de Physique Théorique</i> , Aix-Marseille Université, Université de Toulon, CNRS.	Examineur
Rafael Alejandro PORTO Chargé de recherche, <i>Deutsches Elektronen-Synchrotron</i> , University of Hamburg (DE).	Examineur
Danièle STEER Professeure des universités, <i>Astroparticule et Cosmologie</i> , Université Paris Cité, CNRS.	Examinatrice
Filippo VERNIZZI Directeur de recherche, <i>Institut de Physique Théorique</i> , Université Paris-Saclay, CNRS, CEA.	Directeur de thèse

Titre: Bremsstrahlung gravitationnelle dans l'approche "worldline" de la théorie des champs effective
Mots clés: Ondes Gravitationnelles – Problème à deux corps – Relativité Générale – Théorie des Champs Effective – Formalisme "Worldline" – Intégration par boucles

Résumé : La nécessité d'améliorer la connaissance analytique des ondes gravitationnelles émises par les systèmes binaires d'objets compacts a suscité une activité fervente dans l'étude du problème gravitationnel à deux corps. En particulier, grâce à l'emploi des techniques d'intégration empruntées à la physique des particules, des progrès ont été réalisés dans le cadre post-Minkowskien : étendre la dynamique gravitationnelle dans la constante de Newton G , tout en gardant les vitesses entièrement relativistes. Dans le corps de cette thèse, est étudiée la diffusion classique de deux objets massifs en utilisant une approche worldline de la théorie des champs effectifs dans le cadre post-Minkowskien. Après une introduction qui porte sur les principaux ingrédients

de cette méthode et les techniques d'intégration modernes utilisées dans les calculs, notamment les identités d'intégration par parties, l'unitarité inversée et les équations différentielles pour la résolution des intégrals de Feynman, on se concentre sur la dérivation des quantités rayonnées pour plusieurs cas de figure. Tout d'abord, sont calculées l'amplitude de l'onde gravitationnelle et la quadri-impulsion émises dans le cas de deux objets massifs ponctuels sans spin, représentant deux trous noirs de Schwarzschild. Ensuite, on étend ces études en incluant les modifications dues à l'influence de la structure interne des composants binaires, comme les effets de marée et de spin, qui sont pertinents pour décrire les étoiles et les trous noirs en rotation.

Title: Gravitational Bremsstrahlung in the Worldline Effective Field Theory Approach

Keywords: Gravitational waves – Two-body problem – General Relativity – Effective Field Theory – Worldline Formalism – Loop Integration

Abstract : The need to improve the analytical knowledge of the gravitational waveforms emitted by binary systems of compact objects has sparked a fervent activity in the study of the gravitational two-body problem. In particular, thanks to the use of integration techniques borrowed from particle physics, progresses have been made in the post-Minkowskian framework, which consists in expanding the gravitational dynamics in the Newton constant G , while keeping the velocities fully relativistic. In this thesis, I study the classical scattering of two massive objects using an effective field theory worldline approach in the post-Minkowskian framework. After an introduction

on the main ingredients of this method and on the modern integration techniques used in the calculations, such as integration-by-parts identities, reverse unitarity and differential equation for Feynman integrals, I focus on the derivation of radiated quantities for several scenarios. First, I derive the gravitational wave amplitude and the associated emitted four-momentum in the case of two massive point-like spinless objects, describing two Schwarzschild black holes. Then, I extend these studies by including modifications due to the influence of the internal structure of the binary components, such as tidal and spin effects, which are relevant for rotating stars and black holes.

Acknowledgements

First, the biggest thank goes to Filippo Vernizzi. Thank you for all your mentorship, guidance and all the time you gave to construct this project. I want to thank you also for all the support you gave me, necessary to safely navigate through the difficult pandemic time, that (unfortunately) characterized most of the last three years.

I would like to send a huge thank also to all my collaborators and friends for all their exceptional works: Stavros Mougiakakos, Leong Khim Wong, Giulia Isabella and Brando Bellazzini. I hope that there will be many occasions to discuss, work and spend a wonderful time together in the future. A special thank to all the people at IPhT that make our lab a wonderful place; so thanks Raquel Galazo García, Alexis Boudon, Natalie Hogg and Pierre Fleury.

A huge thank to all my friends that, even at distance, were always very close to me. Thank you Celeste, Giulia and Silvia for all the precious time and laughs we had together; you helped me more than you can imagine. Thank you to my dear friend Ilenia for being incredibly close to me all these years. Thank you Elena and Raffaele for all the long discussions and the amazing food and experiences we had (and will have) together. Thank you Beatriz for being a wonderful person and an even more wonderful friend.

I would like to deeply thank my family for all their unconditional love; to my parents Giuseppe and Annunciata, my brothers and sisters, Francesco, Erica, Maddalena, Giovanni and Stefano. Words cannot explain what you mean to me. Thanks also to what I consider to be my second family, Renata and Paolo, for all your care and help.

Finally, my warmest thanks go to Umberto. You have been the biggest support and the main source of happiness in all these years. I really could not have done it without you and all your love.

Contents

Introduction	9
Introduction en français	15
Conventions and definitions	21
1 The Post-Minkowskian Effective field theory	23
1.1 The scattering set-up	23
1.2 Action for the sources	24
1.3 The effective action	25
1.3.1 Potential and radiation modes	29
1.3.2 Effective action for the radiative sector	29
1.4 Computing Observables	31
1.4.1 The total impulse	31
1.4.2 The emitted momentum	33
1.4.3 The deflection angle	34
1.5 Boundary-to-Bound Map	35
1.5.1 From observables to Hamiltonian	35
1.5.2 Connecting hyperbolae and ellipses	36
1.5.3 Connecting Observables	38
1.6 Summary of the chapter	38
2 Integration techniques	41
2.1 PM EFT at $\mathcal{O}(G^2)$	41
2.1.1 Effective action and EOM	41
2.1.2 1PM order impulse	42
2.2 $\Delta^{(2)}p_1^\mu$ as a one loop computation	43
2.3 Computing $\Delta^{(2)}p_1^\mu$: the integration methods	46
2.3.1 Integration-By-Parts Identities and Reverse Unitarity	46
2.3.2 IBP reduction of the $\mathcal{O}(G^2)$ impulse	48
2.3.3 Differential equations	49
2.3.4 Canonical basis and solution	50
2.3.5 Relating cut and uncut integrals	51
2.4 The $\mathcal{O}(G^2)$ impulse and deflection angle	54
2.5 Summary of the chapter	55
3 Stress-energy tensor and Waveform	57
3.1 Explicit Feynman rules	57
3.2 Stress-energy tensor at order $\mathcal{O}(G)$	58

3.3	Amplitude and Waveform at $O(G^{3/2})$	61
3.3.1	Integrals involved in the amplitude	62
3.4	Results in the rest frame of one of the body	66
3.4.1	Asymptotic waveform in direct space	67
3.5	Radiative observables	68
3.5.1	Emitted momentum in the small velocity limit	69
3.5.2	Energy spectrum in the soft limit	70
3.5.3	Emitted angular momentum	70
3.6	Summary of the chapter	72
4	Leading order radiated momentum	73
4.1	Radiated four-momentum as a two-loop integral	73
4.2	Solving the integral	75
4.2.1	Master integrals	75
4.2.2	Boundary conditions and solutions for the MIs	78
4.3	Computing the four topologies	80
4.3.1	M topology	81
4.3.2	N topology	82
4.3.3	IY topology	82
4.3.4	H topology	83
4.4	Final result	83
4.5	Summary of the chapter	84
5	Beyond point-particle: Tidal deformations	85
5.1	Tidal deformations in the worldline action	85
5.2	Tidal effects in the radiative sector	88
5.2.1	Stress-energy tensor with tides	89
5.2.2	Asymptotic waveform	91
5.3	Radiated four-momentum with tides	92
5.3.1	Radiated energy and instantaneous flux	95
5.3.2	Consistency checks	98
5.4	Summary of the chapter	99
6	Beyond point-particle: Spin effects	101
6.1	Spin effects in the wordline action	101
6.1.1	Degrees of freedom	101
6.1.2	Consistency condition	104
6.1.3	Constructing the Routhian	106
6.2	Spin effects in the radiative sector	107
6.2.1	Stress-energy tensor up to $\mathcal{O}(S^2)$	109
6.3	Radiated four-momentum with spins	110
6.3.1	Loop integral decomposition and IBP reduction	111
6.3.2	The radiated four-momentum	112

6.3.3 Consistency checks	114
6.4 Summary of the chapter	115
Conclusions	117
Appendices	120
A Derivation of the Cutkosky rules	123
A.1 The largest time equation	123
A.2 Largest time equation in momentum space and the Curkosky rules	125
B Boundary conditions	129
B.1 Connecting cut and uncut integrals	129
B.2 Integrals in the near-static limit	131
C Explicit expressions	136
C.1 Radiated Four momentum	136
C.2 Stress-energy tensor for spinning object up to $\mathcal{O}(s^2)$	140
C.3 Feynman rules	145
Bibliography	149

Introduction

Gravitational waves (GWs) will provide an unprecedented source of information about astrophysics, cosmology and fundamental physics. The increase in sensitivity of future detectors, such as LISA [1], Einstein Telescope [2] or Cosmic Explorer [3], will offer new opportunities to explore questions in fundamental physics, test the nature of strong-field gravity, and constrain various binary formation and evolution channels [4–10]. Currently, waveform templates are modeled using semi-analytical approaches such as the effective-one-body (EOB) formalism [11–13]. These methods require blending information coming from both numerical relativity simulations [14–17], and purely analytic perturbative studies. It is then crucial to have an increasingly accurate knowledge of the physical system producing GWs [18, 19].

As of today, the main sources of GWs signals are binary systems of compact objects, i.e. black holes or neutron stars. For this reason, the study of the gravitational two-body problem in General Relativity (GR) has recently gain renew attention. Traditionally, this problem has been tackled using the so-called post-Newtonian (PN) approximation, which considers the constituents of the binary to move non relativistically, thus performing a joint expansion in the small gravitational potential Gm/r , G being the Newton constant, m the typical mass of the two objects and r their relative distance, and small relative velocity v/c , with c the velocity of light. See Refs. [20–28] and references therein for reviews of the different methods employed in this perturbative scheme. Dating back to the early days of GR [29, 30], this approach turned out to be remarkably efficient, recently obtaining the complete description of the dynamics of binary bound systems at 4PN order (i.e. order $(v/c)^8$ beyond Newton’s approximation) [31–40]. Regarding radiation, the PN approximation managed to reach the precision of 4.5PN order beyond the quadrupole formula [41–47]. Together with partial known results up to 6PN order [48–53] and the inclusion of spin and tidal effects, see e.g. [54–63], this constitutes the current state-of-the-art. Another successful perturbative approach to the two-body problem is the self-force formalism [64–66], designed to study extreme-mass-ratio binary systems in which the masses of the constituents m_1 and m_2 are such that $m_2 \ll m_1$. In contrast with the PN approach, this consists in expanding in the mass ratio m_2/m_1 , while keeping all orders in the Newton constant G . See Refs. [67–70] for some recent results.

The main subject of this work is yet another analytic perturbative scheme, called the post-Minkowskian (PM) approximation. In this framework, one studies the gravitational two-body system expanding in the Newton constant G while keeping the velocities fully relativistic. In this sense, this approach is complementary to the PN one. As it can be seen in figure 1, each order of the PM expansion, represented on the vertical line, contains a tower of infinite (incomplete) terms of the PN series (horizontal line). Moreover, while the PN approach is suitable for the study of gravitationally bound systems — after all, the gravitational potential and relative velocity are related by the virial theorem — the PM scheme naturally applies to the unbound case, such as the scattering of two

	0PN	1PN	2PN	3PN	4PN	5PN	6PN		
1PM	1	v^2	v^4	v^6	v^8	v^{10}	v^{12}	...	G^1
2PM		1	v^2	v^4	v^6	v^8	v^{10}	...	G^2
3PM			1	v^2	v^4	v^6	v^8	...	G^3
4PM				1	v^2	v^4	v^6	...	G^4
5PM					1	v^2	v^4	...	G^5
									\vdots

Figure 1: Comparison of PM (vertical line) and PN (horizontal line) expansions. For spinless case, the pink and light-blue boxes are the current state-of-the-art including radiation for the PM and PN series respectively. The 4PN radiation sector is almost complete. The 4PM order (purple box) is known only in part, as the 5PN and 6PN (dark-blue box). For simplicity, in this picture $c = 1$ and only even power of v are represented.

compact objects. It has been employed in the past, especially in the analysis of an elastic scattering [71–77], with pioneering studies of radiation effects such as [76, 78–83], and [84, 85] in the Regge limit (i.e., when the center-of-mass energy is much larger than the momentum transfer).

In recent years, rapid progress in the PM program has been driven by modern computational tools mixing quantum field theory (QFT), effective field theory (EFT), on-shell amplitude techniques and integration methods. The scattering of two massive compact objects interacting via gravity is clearly a classical problem, hence quantum effects are highly suppressed. Nonetheless, using the long-time well-established QFT description of gravity [86–93], information about the dynamics can be efficiently extracted by modelling the system quantum mechanically and taking the appropriate classical limit. This has led to the developments of two broad systematic frameworks to study the gravitational two-body problem within the PM approximation, based either on quantum scattering amplitudes or on worldline approaches. The main distinction between these two methods consists in taking the aforementioned classical limit at different stages in the computations.

In the first approach, one computes the full quantum amplitude describing the scattering system, a task that can be achieved efficiently exploiting all the modern techniques developed within the particle physics community, such as the double copy [94–97] and generalized unitarity [98–100]. Then, one must understand how to isolate the classical physics from this quantum amplitude; advancements in this sense have been reached in various contests, see Refs. [101–105].

If we stick to the gravitational two-body problem, one quickly realizes that there are

essentially three length scales in the problem: the Compton wavelength of the massive objects $\ell_c = \hbar/(mc)$, their typical size $R_S = Gm/c^2$ and their separation given by the impact parameter b , see figure 3, page 24 . The classical limit is enforced by considering the following hierarchy,

$$\ell_c \ll R_S \ll b. \quad (1)$$

The first inequality ensures that quantum effects are suppressed¹, while the second is the classical PM expansion governed by the small parameter

$$\frac{R_S}{b} = \frac{Gm}{c^2 b} \ll 1. \quad (2)$$

Since the leading-order scattering angle is essentially R_S/b , from the above equation we understand that, by computing higher order corrections in R_S/b , the PM approximation can study only the near-forward scattering.

In Fourier space, the hierarchy in eq. (1) becomes

$$\frac{q}{mc} \ll \frac{Gmq}{\hbar c^2} \ll 1, \quad q \sim \frac{\hbar}{b}, \quad (3)$$

where q is the exchanged momentum, the conjugate variable of b . From here, we see that the classical limit is obtained by expanding the computed amplitude for small values of q , i.e. performing the so-called soft expansion, familiar from the method of regions [106].

Once this limit of the amplitude is computed, there are several ways of extracting the relevant classical information. One can either perform a matching with an EFT to find the classical Hamiltonian of the system [107, 108], or use the amplitude data to compute the classical eikonal phase [109–112] or radial action [113, 114], from which one then derives observables such as the scattering angle. Alternatively, one can also follow the method presented in Refs. [115, 116] and directly take the classical limit of well defined quantum observables (e.g. the total impulse or radiated momentum) making a careful \hbar counting to isolate classical and quantum contributions.

Using this framework, the knowledge of the two-body conservative and radiative dynamics has been pushed to include increasingly higher PM orders. In particular, the 3PM order full dynamics is now well known [110, 117–128] and part of the 4PM order was recently derived in [129, 130] using the methods briefly presented in the previous paragraphs. Tidal deformations [131–136] and spin effects [137–143] have also been included within this approach.

Alternatively, worldline EFT methods have been developed to study the PM expansion of the gravitational scattering; one of these methods constitutes the main subject of this work. Inspired by Non-Relativistic-General-Relativity (NRGR) [20, 144] — an EFT approach to the PN analysis of the two-body problem, see [23–27, 145] for reviews — this approach considers the two compact objects as localized external non-propagating

¹Note that the first inequality enforces also $\ell_{\text{Pl}} \ll R_S$, where $\ell_{\text{Pl}} = \sqrt{\hbar G/c^3}$ is the Planck length.

sources of the gravitational field. Their recoil is of the order of the exchanged momentum q , hence it is suppressed with respect to their initial momentum $p \sim mv$ by

$$\frac{\hbar}{J} = \frac{\hbar}{pb} \sim \frac{q}{p} \ll 1, \quad (4)$$

with $J = pb$ the asymptotic angular momentum of the system. Then, one can compute an effective action for the two bodies by “integrating-out” the gravitational degrees of freedom. This can be achieved by computing all the connected Feynman diagrams order per order in the perturbative parameter G . In this process, one discards all the diagrams containing closed graviton loops as these are suppressed by a factor [20]

$$\frac{\hbar}{pb} \sim \frac{q}{p} \ll 1. \quad (5)$$

We shall see this explicitly in chapter 1.

One main advantage of this method with respect to the one relying on on-shell amplitudes is that, by considering the aforementioned simplifications, the classical limit is enforced from the beginning, dispensing one from the \hbar counting or small q expansion. This EFT was used already in [146–148], systematized for the study of the scattering in the PM expansion in Ref. [149] and recently extended in Ref. [150] to include dissipative effects using the *in-in* formalism [151]. Initially applied to the conservative sector of the scattering problem up to 2PM order, this approach has been then employed to compute the 3PM [152] and 4PM orders [153, 154] concurrently with the results coming from quantum amplitude methods. Tidal [149, 155–158] and spin [159–161] effects have also been included in this formalism.

A variation of this approach consists in quantizing also the worldlines describing the compact objects, as presented in Ref. [162], thus constructing a worldline QFT. One then computes the connected Feynman diagrams as described before, this time with worldline propagators, and take the classical limit from the beginning, discarding again all graphs that contain a closed graviton loops. This has been applied in [163] to the study of the leading-order gravitational radiation, then extended to spinning bodies in Ref. [164–166] up to 3PM order. Dissipative effects have also been included recently in Ref. [167].

Both worldline and quantum amplitude methods greatly benefit from modern integration techniques, developed in the context of high energy physics. In both approaches, one eventually needs to solve n -loop integrals to find an explicit expression for the $(n + 1)$ PM order quantities. These integrals contain (on-shell) delta functions which can be regarded as cut propagators through a procedure called reverse unitarity [121, 168–171]. Then, one can simplify the computations using integration-by-parts (IBP) identities [172–176], which have been automatized in many ways, such as in the *Mathematica* package LiteRed [177, 178] or in the program FIRE6 [179]. Applying IBP identities allows one to reduce the problem of computing a complicated n -loop integral to just a set of simpler scalar (n -loop) integrals, commonly referred to as master integrals. Finally, one can write a differential equation satisfied by the latter, as shown in Refs. [180–183]. This equation can be put in the so-called canonical form [184, 185], for

which the solution is known. Therefore, rather than solving these master integrals one-by-one, one just needs to consider them in a particular (simpler) limit to find appropriate boundary conditions for the differential equation [110, 112, 184].

As mentioned above, the PM approximation is more adapted to study the hyperbolic encounter of two massive objects. However, the main sources that produce detectable GWs are bound systems of two compact bodies². It is thus important to find a way to connect unbound and bound orbits' information. One can relate the two physical systems by means of the EOB formalism, as shown in [190, 191]. A more direct way consists in performing a suitable analytic continuation to connect hyperbolic and elliptic motion. This map was dubbed Boundary-to-Bound (B2B) and has been extensively developed in Refs. [114, 192, 193]. With this procedure, one can either reconstruct a Hamiltonian describing the two systems, or connect directly unbound observables (e.g. the scattering angle) with bound ones (e.g. the periastron advance). This approach, however, still misses the inclusion of the non-universal non-local part of such Hamiltonian, which is due to radiation modes that are re-absorbed by the binary system after their emission. These contributions are well understood in the PN formalism, see e.g. [31, 34, 194–196], and in the PM scheme they first appeared in the recently obtained 4PM order results [129, 130, 153, 154].

In this work, we first review the main ingredients of the worldline EFT following closely Ref. [149]. In particular in chapter 2 we include an extensive discussion on the integration techniques used throughout the thesis, by considering a simple example at 2PM order. The other chapters are devoted to the treatment of radiative observables in different scenarios, such as the total four-momentum carried away by the GWs, that was not computed before using this formalism.

In chapter 3, we study the case of an encounter of two massive point-particles. We lay out the Feynman rules and compute, at $\mathcal{O}(G)$, the pseudo stress-energy tensor — the source of the gravitational radiation — via a matching procedure involving Feynman diagrams. From there, we are able to compute the radiation amplitude (i.e. the asymptotic waveform in Fourier space), from which one can extract the leading-order radiated angular momentum [122, 128, 163, 197]. To the best of our knowledge, the order $\mathcal{O}(G^{3/2})$ amplitude cannot be written in terms of analytic known functions. As a consequence, the radiated four-momentum cannot be computed using only this information due to the multiscale nature of the resulting integrals, which have so far proven to be intractable without performing a low-velocity expansion.

In the subsequent chapter, we see how to bypass the problem of not having an explicit solution for the amplitude by rewriting the phase-space integral of the four-momentum as a (cut) two-loop integral. In particular, we organize our calculations in terms of four topologies that come out naturally from our Feynman rules for the gravitons. We solve each topology, one by one. Then, we apply the integration techniques presented in chapter 2, finding that the final result can be written as a linear combination of four cut

²For current detectors, signals from hyperbolic encounters of astrophysical objects are expected to be rare [186–189].

two-loop master integrals. Solving these through the differential equations method, we are able to obtain the result found using amplitude-based approaches [110, 120, 121].

The remaining part of this work is devoted to the extension of these computations beyond the point-particle approximation, by including the influence of the internal structure of the two bodies. In chapter 5, we explain how tidal deformations are incorporated in the EFT [20, 144, 149, 155, 198, 199], and then compute the leading-order radiated waveform, emitted four-momentum and energy flux. The obtained expression for the emitted energy is analytically continued to the bound case, and found to be consistent with the state-of-the-art results available from the PN computations [59–61].

Finally, in chapter 6 we include the effect of spins. After an introduction to the worldline EFT formalism adapt to describe rotating objects [26, 57, 58, 159–161, 200–202], we compute once again the radiated four-momentum in this context, finding agreement with the existing PN literature up to 4PN order [63, 193, 203]. Remarkably, the derivation of the emitted momentum in the case of point-particles, tidally deformed objects, and rotating bodies requires the knowledge of only the four master integrals computed in chapter 4.

We collect all the (lengthy) explicit expressions found in this dissertation in appendix C. Appendices A and B are devoted respectively to a re-derivation of the Cutkosky cutting rules [204, 205] and the computation of the boundary conditions needed to solve the differential equation satisfied by the four master integrals.

This thesis is based on [206–209].

Introduction en français

Les ondes gravitationnelles sont amenées à devenir une source d'information sans précédent pour l'astrophysique, la cosmologie et la physique fondamentale. L'amélioration de la sensibilité des futurs détecteurs, comme LISA [1], le télescope Einstein [2], et le Cosmic Explorer [3], offre de nouvelles opportunités pour explorer les nouveaux enjeux de la physique fondamentale, mettre à l'épreuve la nature de la gravité en champ fort, et contraindre diverses formations binaires et cas d'évolution [4–10]. Actuellement, les modèles de forme d'onde sont façonnés en employant des approches semi-analytiques, comme le formalisme “effective-one-body” (EOB) [11–13]. Ces méthodes utilisent à la fois des simulations de relativité numérique [14–17], et des études analytiques en théorie des perturbations. Il est donc nécessaire de posséder une connaissance de plus en plus précise du système physique qui produit les ondes gravitationnelles [18, 19].

À présent, les principales sources des signaux d'ondes gravitationnelles sont les systèmes binaires d'objet compacts, à savoir des trous noirs ou des étoiles à neutrons. C'est pourquoi l'étude du problème à deux corps en relativité générale (RG) a récemment reçu un renouveau d'attention. Traditionnellement, ce problème a été affronté en utilisant l'approximation post-Newtonienne (PN), selon laquelle les constituants du système binaire sont non-relativistes, menant à la fois à un développement en puissances du potentiel gravitationnel Gm/r , G étant la constante de Newton, m la masse typique de deux objets et r leur distance relative, mais aussi en la petite vitesse relative v/c , c étant la vitesse de la lumière. On réfère le lecteur aux travaux [20–28] et leurs références pour une revue des différentes méthodes employées dans ce schéma de perturbation.

Dès l'aube de la RG [29, 30], cette approche s'est montrée très efficace, et on a récemment obtenu la description (quasiment) complète de la dynamique des systèmes binaires liés à l'ordre 4 PN (à savoir un ordre $(v/c)^8$ au-delà de l'approximation Newtonienne) [31–40]. En ajoutant les résultats obtenus pour le rayonnement gravitationnel [41–47] et les résultats partiellement connus jusqu'à l'ordre 6PN [48–53], et avec l'inclusion des effets de spin et de marée, cf. par exemple [54–63], tout cela constitue l'état de l'art. Une autre approche de perturbation efficace pour le problème à deux corps est le formalisme “self-force” [64–66], conçu pour l'étude des systèmes binaires à différence extrême de masse où les masses des constituants m_1 et m_2 sont tels que $m_2 \ll m_1$. Contrairement à l'approche PN, celle-ci met en jeu un développement en puissances du rapport des masses m_2/m_1 , en gardant toutes les puissances de la constante de Newton G . Les références [67–70] contiennent des résultats récents.

Le sujet principal de ce travail de thèse est un autre schéma analytique de perturbation, dit approximation post-Minkowskienne (PM). Dans ce cadre, nous étudierons un système gravitationnel à deux corps à travers son développement en la constante G de Newton, tout en maintenant les vitesses complètement relativistes. Cette approche est ainsi complémentaire à la susmentionnée PN. Comme on peut le voir sur la figure 2, chaque ordre du développement PM, représenté verticalement, contient une suite de

	0PN	1PN	2PN	3PN	4PN	5PN	6PN		
1PM	1	v^2	v^4	v^6	v^8	v^{10}	v^{12}	...	G^1
2PM		1	v^2	v^4	v^6	v^8	v^{10}	...	G^2
3PM			1	v^2	v^4	v^6	v^8	...	G^3
4PM				1	v^2	v^4	v^6	...	G^4
5PM					1	v^2	v^4	...	G^5
									\vdots

Figure 2: Comparaison des développements PM (ligne verticale), et PN (ligne horizontale). Pour le cas sans spin, les cases roses et bleu clair représentent l'état de l'art actuel, qui inclut la radiation pour les séries PM et PN respectivement. Le secteur de radiation 4PN est quasiment complet. L'ordre 4PM (la case violette) est connu seulement en partie, comme pour les ordres 5PN et 6PN (case bleu foncé). Par simplicité, $c = 1$ sur la figure et seuls les ordres pairs de v sont représentés.

termes infinis (incomplets) de la série PN, sur la ligne horizontale. Si l'approche PN est adaptée à l'étude des systèmes liés gravitationnellement — après tout, le potentiel gravitationnel et la vitesse relative sont reliés par le théorème du viriel —, le schéma PM s'applique naturellement au cas de figure non-lié, comme la diffusion de deux objets compacts. Cela a été employé par le passé dans l'analyse d'une diffusion élastique [71–77], avec des études novatrices sur l'effet de radiation comme [76, 78–83], et [84, 85] dans la limite de Regge, à savoir quand l'énergie du centre de masse est bien plus importante que le moment transféré.

Récemment, les avancées rapides de la méthode PM ont été accomplies grâce à des outils numériques modernes qui mêlent la théorie quantique des champs (QFT), les théories des champs efficace (EFT), les techniques d'amplitude “on-shell” et les méthodes d'intégration. La diffusion de deux objets compacts massifs qui interagissent gravitationnellement constitue un problème classique, et nous négligeons donc les effets quantiques. Toutefois, en employant des descriptions bien connues en QFT de la gravité [86–93], on peut obtenir efficacement des informations sur la dynamique à partir de la modélisation quantique et en considérant les limites classiques appropriées. Cela a conduit au développement de deux cadres systématiques destinés à l'étude du problème à deux corps en utilisant l'approximation PM, à savoir les techniques d'amplitude de diffusion quantique et “wordline”. La différence principale entre ces deux méthodes vient du moment du calcul auquel on prend la limite classique susmentionné.

Dans la première approche, on calcule l'amplitude quantique en décrivant le système de diffusion, une tâche que l'on peut atteindre efficacement grâce à l'exploitation de

toutes les techniques modernes développées par la communauté de la physique des particules, par exemple la double copie [94–97] et l’unitarité généralisée [98–100]. Il faut par la suite comprendre comment isoler la physique classique de cette amplitude quantique. Des progrès en ce sens ont récemment été accomplis dans différents contextes [101–105].

Si l’on se concentre sur le problème gravitationnel à deux corps, on s’aperçoit rapidement qu’il y a essentiellement trois échelles de longueur : la longueur d’onde de Compton des objets massifs $\ell_c = \hbar/(mc)$, leur dimension typique $R_S = Gm/c^2$ et leur séparation donnée par le paramètre d’impact b , voir la figure 3, page 24. La limite classique est imposée par la hiérarchie suivante:

$$\ell_c \ll R_S \ll b. \quad (1)$$

La première inégalité a pour but d’assurer que les effets quantiques soient supprimés³, alors que la seconde correspond au développement PM gouvernée par le petit paramètre

$$\frac{R_S}{b} = \frac{Gm}{c^2 b} \ll 1. \quad (2)$$

Puisque l’angle de diffusion au premier ordre est essentiellement R_S/b , on peut déduire de l’équation précédente, en calculant les corrections d’ordre supérieur en R_S/b , que l’approximation PM peut seulement étudier des diffusions quasi-droites.

Dans l’espace de Fourier, la hiérarchie de l’équation (1) devient

$$\frac{q}{mc} \ll \frac{Gmq}{\hbar c^2} \ll 1, \quad q \sim \frac{\hbar}{b}, \quad (3)$$

où q est le moment échangé, la variable conjuguée de b . De là, on peut constater que la limite classique est obtenue en développant l’amplitude calculée pour des petites valeurs de q , c’est-à-dire en accomplissant un développement dit mou, commune dans la méthode des régions [106]. Une fois la limite de cette amplitude calculée, il y a de nombreuses manières d’extraire l’information classique. On peut soit ajuster les résultats avec une EFT afin de trouver le Hamiltonien classique du système [107,108], soit utiliser les données de l’amplitude pour calculer la phase eikonale classique [109–112] ou l’action radiale [113,114], d’où on peut extraire des observables telles que l’angle de diffusion. De manière alternative, on peut suivre la méthode présentée dans [115,116] et prendre directement la limite classique des observables quantiques bien définies, comme l’impulsion totale ou le moment irradié, en comptant attentivement les puissances de \hbar pour isoler les contributions classiques et quantiques.

Dans ce cadre, la connaissance de la dynamique à deux corps conservative et radiative a été étendue afin d’inclure des ordres PM de plus en plus élevés. En particulier, la dynamique complète à l’ordre 3PM est à présent bien connue [110,117–126,128], et une partie de l’ordre 4PM a été naguère dérivée dans [129,130] en utilisant des méthodes brièvement énoncées dans les paragraphes précédents. Les effets de marée [131–136] et de spin [137–143] ont également été pris en compte dans cette approche.

³Il faut noter que la première inégalité impose également $\ell_{\text{Pl}} \ll R_S$, où $\ell_{\text{Pl}} = \sqrt{\hbar G/c^3}$ est la longueur de Planck.

De manière alternative, les méthodes “wordline” EFT ont été développées en visant l’étude du développement PM des problèmes de diffusion gravitationnelle. C’est là le principal objet de ce travail. Cette méthode, inspirée par la théorie nommée Non-Relativistic-General-Relativity (NRGR) [20, 144] — une approche EFT de l’analyse PN du problème à deux corps, voir [23–27, 145] pour une revue —, considère les deux objets compacts comme des sources localisées extérieures sans propagation du champ gravitationnel. Leur recul est du même ordre de grandeur que le moment échangé q , c’est pourquoi il est négligeable par rapport au moment initial p à cause de

$$\frac{\hbar}{J} = \frac{\hbar}{pb} \sim \frac{q}{p} \ll 1, \quad (4)$$

où $J = pb$ est le moment angulaire asymptotique du système. Ensuite, on peut calculer l’action effective pour les deux corps en “intégrant” les degrés de liberté gravitationnels. Cela peut être effectué en calculant tous les diagrammes de Feynman connectés ordre par ordre en le paramètre de perturbation G . Dans ce procédé, on écarte tous les diagrammes contenant des boucles de gravitons fermées. Ceux-ci sont négligeables puisqu’ils sont atténués par un facteur [20] :

$$\frac{\hbar}{pb} \sim \frac{q}{p} \ll 1. \quad (5)$$

Nous exposerons cela plus en détail dans le premier chapitre.

L’un des principaux avantages de cette méthode par rapport à celle qui s’appuie sur les amplitudes “on-shell” est que, si l’on considère les simplifications susmentionnées, la limite classique est imposée dès le début, et cela dispense de compter les \hbar ou de faire un développement en q . Cette EFT avait déjà été employée dans [146–148], puis systématisée pour l’étude de la diffusion dans le développement PM dans [149], et récemment étendue dans [150] pour inclure des effets de dissipation en utilisant le formalisme “in-in” [151]. Initialement appliquée au secteur conservatif du problème de la diffusion jusqu’à l’ordre 2PM, cette approche a par la suite été employée pour calculer les ordres 3PM [152] et 4PM [153, 154]. Les effets de marée [149, 155–158] et de spin [159–161] ont également été inclus dans ce formalisme.

On peut suivre une approche légèrement différente et quantifier les lignes d’univers qui décrivent les objets compacts en construisant ainsi une QFT “wordline” [162]. Il faut ensuite calculer les diagrammes de Feynman connectés susmentionnés, cette fois avec des propagateurs “wordline”, et prendre la limite classique au début, en écartant de nouveau tous les diagrammes qui contiennent des boucles de gravitons fermées. Cela a été mis en œuvre dans [163] pour l’étude de la radiation gravitationnelle au premier ordre, et ensuite étendu aux objets en rotation jusqu’à l’ordre 3PM dans [164–166]. Les effets de dissipation ont également été inclus récemment dans [167].

Les méthodes à la fois quantique et “wordline” tirent un grand bénéfice des techniques d’intégration modernes, développées dans le contexte de la physique des hautes énergies. Dans les deux approches, il faut résoudre des intégrales à n boucles afin de trouver une expression explicite pour les quantités d’ordre $(n+1)$ PM. Ces intégrales contiennent des fonctions delta “on-shell” qui peuvent être considérées comme des propagateurs coupés

en employant une procédure appelée unitarité inversée [121, 168–171]. On peut simplifier les calculs en utilisant des identités d’intégration par parties (IPP) [172–176], qui ont été automatisées par de nombreuses manières, voir par exemple le package *Mathematica LiteRed* [177, 178] et le programme FIRE6 [179]. Le fait d’appliquer les identités IPP permet de réduire le problème du calcul d’intégrales compliquées à n boucles, à un ensemble d’intégrales scalaires plus simples (à n boucles), communément appelées intégrales “master”. Enfin, on peut écrire une équation différentielle pour ces dernières, comme montré dans [180–183], équation qui peut être mise sous la forme dite canonique, cf. [184, 185], dont la solution est connue. Donc, sans devoir résoudre les intégrales “master” une par une, il faut simplement trouver une solution pour un cas limite plus simple afin de trouver les conditions aux limites de l’équation différentielle [110, 112, 184].

Comme nous l’avons dit, l’approximation PM est plus adaptée à l’étude des trajectoires hyperboliques de deux objets massifs. Toutefois, les sources principales des signaux détectables d’ondes gravitationnelles sont des systèmes liés de deux objets compacts⁴. En ce sens, le fait de trouver un moyen pour connecter les informations d’orbites liées et non-liées est un objectif théorique important. On peut relier les deux systèmes physiques à travers le formalisme EOB, comme montré dans [190, 191]. En prenant un prolongement analytique pour connecter les mouvements hyperbolique et elliptique, on obtient une solution plus directe. Cette méthode a été appelée “Boundary-to-Bound” (B2B) et a été étudiée en profondeur dans [114, 192, 193]. En suivant ce procédé, on peut soit reconstruire un Hamiltonien décrivant les deux systèmes, soit connecter directement des observables non-liées, comme l’angle de diffusion, et liées, comme la précession du périastre. Il manque toutefois dans cette approche l’inclusion de la partie non-universelle et non-locale du Hamiltonien, qui vient des modes de radiation réabsorbés par le système binaire après leur émission. Ces contributions sont bien contrôlées dans le formalisme PN, voir par exemple [31, 34, 194–196], et apparaissent pour la première fois dans le schéma PM à l’ordre 4PM récemment obtenu [129, 130, 153, 154].

Dans le cadre de cette thèse, nous allons d’abord passer en revue les principaux éléments de l’EFT “wordline” en nous appuyant sur [149]. Dans le deuxième chapitre, nous présentons une discussion approfondie des techniques d’intégration utilisées tout au long du corps de la thèse, grâce à un exemple simple à l’ordre 2PM. Dans les autres chapitres, nous nous concentrerons sur le traitement des observables radiatives dans différents cas de figure, par exemple le quadri-moment total transporté par les ondes gravitationnelles, ce qui n’avait jamais été calculé auparavant en suivant ce formalisme.

Dans le troisième chapitre, nous étudierons le cas de figure d’une rencontre de deux objets ponctuels. Nous introduirons les règles de Feynman et calculerons, à l’ordre $\mathcal{O}(G)$, le pseudo-tenseur énergie-impulsion — la source des ondes gravitationnelles — à travers un ajustement avec les diagrammes de Feynman. Grâce à cela, nous pourrions calculer l’amplitude de radiation, à savoir la forme d’onde asymptotique dans l’espace de Fourier, à partir de laquelle l’on peut extraire l’émission du moment angulaire au premier ordre

⁴On estime que, vu la sensibilité actuelle des détecteurs, les signaux produits par les orbites elliptiques d’objets astrophysiques seront rares [186–189].

[122,128,163,197]. En l'état actuel de nos connaissances, l'amplitude à l'ordre $\mathcal{O}(G^2)$ ne peut pas être écrite en employant des fonctions analytiques connues. Par conséquent, le quadri-moment irradié ne peut pas être calculé en employant seulement ces informations, à cause de la nature multiscalaire des intégrales qui en résultent, qui, comme cela a été montré jusqu'à présent, ne sont pas tractables sans effectuer un développement à basse vitesse.

Dans le quatrième chapitre, nous verrons comment on peut éviter le problème du manque de solution explicite pour l'amplitude en réécrivant l'intégrale dans l'espace des phases du quadri-moment comme une intégrale coupée à deux boucles. En particulier, nous présenterons nos calculs selon quatre topologies qui découlent naturellement de nos règles de Feynman pour les gravitons. Nous résoudrons ces topologies une par une. Par la suite, nous appliquerons les techniques d'intégration présentées au deuxième chapitre et nous montrerons que le résultat final peut être écrit comme une combinaison linéaire de quatre intégrales "master" coupées à deux boucles. En les résolvant selon la méthode des équations différentielles, nous pouvons obtenir le résultat que l'on retrouve dans [110,120,121] en employant les approches fondées sur les amplitudes.

Le reste de ce travail est dévoué à l'extension de ces calculs au-delà de l'approximation d'une particule ponctuelle, en incluant l'influence de la structure interne des deux corps. Dans le cinquième chapitre, nous expliquerons comment les déformations de marée sont incorporées dans l'EFT [20,144,149,198,199], et nous calculerons au premier ordre la forme d'onde irradiée, le quadri-moment émis, et le flux d'énergie. L'expression obtenue pour l'énergie émise est prolongée analytiquement au cas lié, et elle est cohérente avec les résultats de l'état de l'art accessibles par les calculs PN [59–61].

Enfin, au chapitre sixième, nous inclurons les effets de spin. Après une introduction du formalisme EFT "wordline" apte à décrire les objets en rotation [26,57,58,161,200–202], nous calculerons de nouveau le quadri-moment dans ce contexte, et nous serons en accord avec la littérature sur l'approche PN jusqu'à l'ordre 4PN [63,193,203]. Remarquablement, le calcul du moment émis dans le cas des particules ponctuelles, d'objets déformés par les effets de marée, et de corps en rotation, requiert seulement la connaissance des quatre intégrales "master" calculés au chapitre quatrième.

Nous recueillons toutes les longues expressions explicites trouvées dans cette thèse dans l'appendice C. Les appendices A et B sont consacrées, pour l'une, au calcul des règles de coupe de Cutkosky [204,205] et, pour l'autre, au calcul des conditions limites nécessaires à la résolution de l'équation différentielle satisfaite par les quatre intégrales "master".

Cette thèse se fonde sur [206–209].

Conventions and definitions

- From now on, we work with natural units $\hbar = c = 1$, unless otherwise noted, and define the Planck mass as $m_{\text{Pl}} \equiv (32\pi G)^{-1/2}$, where G is the Newton constant.
- We use Einstein's summation over repeated indices. Greek and Latin indices ranges are $\mu, \nu, \dots = 0, 1, 2, 3$ and $i, j, \dots = 1, 2, 3$.
- We use round and square brackets to respectively symmetrize and anti-symmetrize indices, e.g.

$$A^{(\mu\nu)} \equiv \frac{1}{2} (A^{\mu\nu} + A^{\nu\mu}) , \quad A^{[\mu\nu]} \equiv \frac{1}{2} (A^{\mu\nu} - A^{\nu\mu}) .$$

If the indices are not contiguous, we put straight lines to highlight them, e.g.

$$A^{(\mu|\sigma\rho|\nu)} = \frac{1}{2} (A^{\mu\sigma\rho\nu} + A^{\nu\sigma\rho\mu}) , \quad A^{[\mu|\sigma\rho|\nu]} = \frac{1}{2} (A^{\mu\sigma\rho\nu} - A^{\nu\sigma\rho\mu}) .$$

- We use mostly-minus convention for the metric, i.e. the four-dimensional Minkowski metric is given by $\eta_{\mu\nu} = \text{diag}(1, -1, -1, -1)$. A generic metric $g_{\mu\nu}$ then keeps the same signature. We define $g \equiv \det g_{\mu\nu}$.
- We denote 3-vectors in boldface, e.g. $\mathbf{x}, \mathbf{y}, \dots$, while we use non boldface plus a Latin index to denote a component of the 3-vector, e.g. x^i, y^i, \dots .
- We define the Riemann tensor as $R^\rho{}_{\mu\sigma\nu} \equiv 2\partial_{[\sigma}\Gamma^\rho{}_{\mu|\nu]} + 2\Gamma^\rho{}_{\lambda[\sigma}\Gamma^\lambda{}_{\mu|\nu]}$, where $\Gamma^\rho{}_{\mu\nu}$ is the torsion-free Levi-Civita connection. The Ricci tensor and scalar are then respectively defined as follows $R_{\mu\nu} \equiv R^\sigma{}_{\mu\sigma\nu}$, $R \equiv R_{\mu\nu}g^{\mu\nu}$. Finally, pulling down all indices for convenience, we defined the Weyl tensor in four dimensions as

$$C_{\rho\sigma\mu\nu} \equiv R_{\rho\sigma\mu\nu} - (g_{\rho[\mu}R_{\nu]\sigma} - g_{\sigma[\mu}R_{\nu]\rho}) + \frac{1}{3}g_{\rho[\mu}g_{\nu]\sigma}R .$$

- We use the compact notation

$$\int \frac{d^4k}{(2\pi)^4} \frac{d^4q}{(2\pi)^4} \dots \equiv \int_{k,q,\dots} .$$

When working in d dimension, $\int_{k,q,\dots}$ denotes the d dimensional version of the above integrals.

- We define $\delta^n(x) \equiv (2\pi)^n \delta^n(x)$, where $\delta^n(x)$ is the n dimensional delta function. For massive and massless field, we define the on-shell delta functions respectively as

$$\delta_\pm(k^2 - m^2) \equiv \vartheta(\pm k^0) \delta(k^2 - m^2) , \quad \delta_\pm(k^2) \equiv \vartheta(\pm k^0) \delta(k^2) .$$

where $\vartheta(x)$ is the Heaviside step function.

1 - The Post-Minkowskian Effective field theory

In this chapter we review the worldline PM EFT first established in [149]. Originally constructed to study the conservative part of the two-body problem, this can be extended to include radiative effects¹, following [206, 207]. We conclude the chapter with a brief discussion of the powerful Boundary-to-Bound (B2B) map described in [114, 192, 193], that allows us to connect the scattering and the bound two-body problem.

1.1 . The scattering set-up

In what follows, we study the scattering process between two classical spinless massive objects with masses m_1 and m_2 , see figure 3 in the next page. In the center of mass (COM) frame, we can parametrize the two incoming four-momenta p_1 and p_2 as

$$p_1^\mu = m_1 u_1^\mu = (E_1, \mathbf{p}), \quad p_2^\mu = m_2 u_2^\mu = (E_2, -\mathbf{p}), \quad (1.1.1)$$

where u_1^μ and u_2^μ are the two incoming four-velocities and $E_a = \sqrt{m_a^2 + \mathbf{p}^2}$, for $a = 1, 2$, the incoming energies. We call the absolute value of the impact parameter b , and, following a standard notation, we define the total mass M and the symmetric mass ratio ν as

$$M \equiv m_1 + m_2, \quad \nu \equiv \frac{m_1 m_2}{M^2}. \quad (1.1.2)$$

These allow us to introduce the following quantities useful to parametrize the problem:

- The total incoming energy E and the reduced non relativistic energy \mathcal{E}

$$E = E_1 + E_2 = M(1 + \nu\mathcal{E}), \quad \mathcal{E} = \frac{E - M}{M\nu} \quad (1.1.3)$$

- The relative Lorentz factor γ and the ratio $\Gamma = E/M$

$$\gamma = u_1 \cdot u_2 = 1 + \mathcal{E} + \frac{\nu}{2}\mathcal{E}^2, \quad \Gamma = \frac{E}{M} = \sqrt{1 + 2\nu(\gamma - 1)} \quad (1.1.4)$$

- The modulo of the asymptotic three-momentum p_∞ and the total asymptotic angular momentum J

$$p_\infty \equiv |\mathbf{p}| = M\nu \frac{\sqrt{\gamma^2 - 1}}{\Gamma}, \quad J = p_\infty b \quad (1.1.5)$$

As discussed in the introduction, defining the Compton wavelength ℓ_c and the Schwarzschild radius R_S of the scattering objects with a typical mass m

$$\ell_c \equiv \frac{1}{m}, \quad R_S \equiv Gm, \quad (1.1.6)$$

¹An implementation of the *in-in* formalism in the worldline EFT and QFT approaches has been recently proposed in Refs. [150] and [167] respectively.

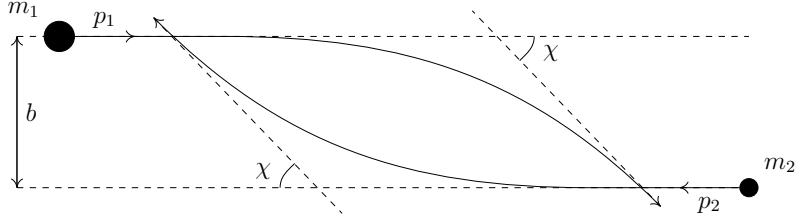


Figure 3: The scattering problem in the center of mass frame. b is the impact parameter and χ is the scattering angle.

the classical regime and PM expansion are ensured by considering the following hierarchy of scales (in direct and Fourier space respectively),

$$\frac{\ell_c}{b} \ll \frac{R_S}{b} \ll 1, \quad \frac{q}{m} \ll Gmq \ll 1. \quad (1.1.7)$$

In the above equations, q is the modulo of the exchanged momentum q^μ , that is the conjugate variable of b^μ . The first inequality ensures the suppression of the quantum contributions, while the second one is the classical PM expansion. Moreover, we stress that $1/(mb) \ll Gm/b$ implies $\ell_{P1}/(Gm) \ll 1$, where $\ell_{P1} = \sqrt{G}$. Indeed

$$\frac{\ell_{P1}^2}{R_S^2} = \frac{\ell_c}{b} \left(\frac{b}{R_S} \right) \ll 1. \quad (1.1.8)$$

Therefore the previous hierarchy can be equivalently rewritten as

$$\frac{\sqrt{G}}{b} \ll \frac{Gm}{b} \ll 1, \quad \sqrt{G}q \ll Gmq \ll 1. \quad (1.1.9)$$

In what follows, we should employ either eq. (1.1.7) or (1.1.9) to justify the approximations we make to obtain the classical limit.

1.2 . Action for the sources

Let us now be more explicit and introduce the action that describes the two compact objects in the EFT formalism. In this thesis, we follow the approach of [20] (reviewed in [23–27, 145]) and consider the massive objects as external non-propagating sources of the gravitational field. To construct their action, let us first consider the case of just one object. In first approximation, this can be taken to be a point-particle described by its worldline coordinates $x^\mu(\lambda)$, with λ an affine parameter. Let us introduce the conjugate momentum, defined as

$$p_\mu \equiv -\frac{\delta S_{pp}}{\delta \dot{x}^\mu}, \quad (1.2.1)$$

where $\dot{x}^\mu(\lambda) = dx^\mu(\lambda)/d\lambda$, and we raise and lower indices with the metric $g_{\mu\nu}$. We can then write the action of this object using first-order forms, i.e.

$$S_{pp} = \int d\lambda (-g_{\mu\nu} \dot{x}^\mu p^\nu - \mathcal{H}_{pp}). \quad (1.2.2)$$

We know that only three of the four components of $x^\mu(\lambda)$ are necessary to uniquely determine the position of the object; therefore, we must impose a constraint to remove one of them. An obvious one is the on-shell condition, i.e. if m is the mass of the body

$$\mathcal{H}_{\text{pp}} = -\frac{e(\lambda)}{2m}(p^2 - m^2), \quad (1.2.3)$$

with $e(\lambda)$ a Lagrange multiplier and $p^2 = g_{\mu\nu}p^\mu p^\nu$. Notice that the Hamiltonian for a generally covariant system typically vanishes [210], that is why \mathcal{H}_{pp} is purely a constraint term. We can remove the dependence of the action on p_μ using its equations of motion (EOM), finding eventually

$$S_{\text{pp}} = -\frac{m}{2} \int d\lambda \frac{1}{e(\lambda)} [g_{\mu\nu}(x(\lambda))\dot{x}^\mu(\lambda)\dot{x}^\nu(\lambda) + e^2(\lambda)]. \quad (1.2.4)$$

This is sometimes referred to as the Polyakov form of the point-particle action, see also Ref. [211]. Notice that now the EOM for the Lagrange multiplier are

$$e^2(\lambda) = g_{\mu\nu}(x(\lambda))\dot{x}^\mu(\lambda)\dot{x}^\nu(\lambda); \quad (1.2.5)$$

substituting this in (1.2.4) gives the more familiar Lagrangian $\mathcal{L}_{\text{pp}} = -m\sqrt{g_{\mu\nu}\dot{x}^\mu\dot{x}^\nu}$. In chapters 5 and 6 we shall see how this derivation can be modified to include respectively finite-size effects, e.g. [20, 212], and spins, e.g. [26, 201].

Finally, notice that the action (1.2.4) is invariant under re-parametrization of the worldline $\lambda \rightarrow \lambda'(\lambda)$ which implies that $e(\lambda)$ transforms as

$$e(\lambda) \rightarrow e'(\lambda') = \frac{d\lambda}{d\lambda'} e(\lambda). \quad (1.2.6)$$

The Lagrange multiplier $e(\lambda)$ is there to precisely ensure this gauge symmetry. It is then sometimes convenient to describe the worldline using the proper time of the object $d\tau^2 = g_{\mu\nu}dx^\mu dx^\nu$ which is equivalent to fix $e(\lambda) = 1$. In this case, the point-particle action becomes

$$S_{\text{pp}} = -\frac{m}{2} \int d\tau [g_{\mu\nu}(x(\tau))\mathcal{U}^\mu(\tau)\mathcal{U}^\nu(\tau) + 1], \quad (1.2.7)$$

with $\mathcal{U}^\mu = dx^\mu/d\tau$ the four-velocity of the body. As we shall see in the next sections, having fixed $e(\lambda)$, one must impose the condition $g_{\mu\nu}(x(\tau))\mathcal{U}^\mu(\tau)\mathcal{U}^\nu(\tau) = 1$ after having computed observables in this formalism. Note that compared to the “traditional” action [20], this parametrization allows to simplify the coupling between matter and gravity [149, 213, 214].

1.3 . The effective action

Let us go back to the two-body problem and introduce the gravitational interaction. This system is described by the action

$$S_{\text{eff},1} = -2m_{\text{P}1}^2 \int d^4x \sqrt{-g} R - \sum_{a=1,2} \frac{m_a}{2} \int d\tau_a [g_{\mu\nu}(x_a)\mathcal{U}_a^\mu(\tau_a)\mathcal{U}_a^\nu(\tau_a) + 1], \quad (1.3.1)$$

where $g_{\mu\nu}$ is the metric parametrizing the gravitational interaction. For the two point-particles, we choose to parametrize the worldlines with their proper time τ_a , $a = 1, 2$, thus their action has the form (1.2.7).

We want to study a classical scattering process in which the two bodies deviate from their initial straight trajectories due to the gravitational interaction. We do this in the weak field regime, i.e. we expand the metric around Minkowsky spacetime as

$$g_{\mu\nu} = \eta_{\mu\nu} + \frac{h_{\mu\nu}}{m_{\text{Pl}}}. \quad (1.3.2)$$

Using QFT language, we can compute the effective action describing the objects starting from eq. (1.3.1) and integrating out the gravitational degrees of freedom $h_{\mu\nu}$ [20, 23–27, 145], i.e.

$$e^{iS_{\text{eff}}} = \int \mathcal{D}h_{\mu\nu} e^{iS + iS_{\text{GF}}}, \quad (1.3.3)$$

where S_{GF} is the usual gauge-fixing term arising from a Faddeev-Popov procedure that determines the gravitational field unambiguously [215–217]. We shall discuss the absence of ghosts fields in the next paragraph.

The way of computing the effective action as in eq. (1.3.3) is known as the *top-down* approach. As explained before, we consider the two massive objects as external non-propagating sources of the gravitational field. Indeed, in our approximation, all the momenta k^μ of the exchanged gravitons scale like $|k^\mu| \sim 1/b \sim q$, while the momentum of the sources is clearly $|\mathbf{p}| \sim m$. The sources then recoil by $|\Delta\mathbf{p}| \sim q$ [20], hence

$$\frac{|\Delta\mathbf{p}|}{|\mathbf{p}|} \sim \frac{q}{m} \ll 1, \quad (1.3.4)$$

as per the scaling in (1.1.7). Therefore, eq. (1.3.3) is equivalent to the so-called vacuum-to-vacuum amplitude in the presence of sources. Then, S_{eff} can be computed efficiently at each order in the perturbative expansion by considering all connected Feynman diagrams having the same power of G . More explicitly, introducing the following diagrammatic conventions

$$\begin{aligned} \text{---} \circ \text{---} &\longrightarrow \text{Point-particle sourcing the field,} \\ \text{---} \text{---} &\longrightarrow \text{graviton propagator,} \end{aligned}$$

and deriving the corresponding Feynman rules from eq. (1.3.1), one can compute the effective action as

$$iS_{\text{eff}} = \begin{array}{c} \text{---} \circ \text{---} \\ | \\ \text{---} \circ \text{---} \end{array} + \begin{array}{c} \text{---} \circ \text{---} \\ \text{---} \text{---} \end{array} + \begin{array}{c} \text{---} \circ \text{---} \\ | \\ \text{---} \circ \text{---} \\ | \\ \text{---} \circ \text{---} \end{array} + \begin{array}{c} \text{---} \circ \text{---} \\ \text{---} \text{---} \\ | \\ \text{---} \circ \text{---} \\ \text{---} \text{---} \end{array} + \mathcal{O}(G^3). \quad (1.3.5)$$

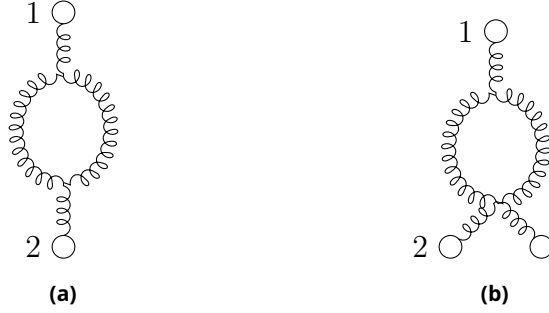


Figure 4: Example of topologies giving quantum contributions to S_{eff} at order (a) $\mathcal{O}(G^2)$ and (b) $\mathcal{O}(G^3)$.

One must also add the analogous diagrams with bodies 1 and 2 exchanged. Notice that the approximation of the two bodies as point-particles may produce ultraviolet (UV) divergent contributions. These can be easily handled in the EFT language through the use of dimensional regularization and counter terms [20, 23, 25, 216, 217].

In order to be more explicit, let us first write the Feynman rules relevant for the computations done in the first three chapters of this work. Due to the use of the Polyakov-like parametrization, from the matter part of eq. (1.3.1) we see that we have only one way in which we can source the gravitational field,

$$\tau_a \begin{array}{c} \rightarrow \\ \text{wavy line} \end{array}^{\mu\nu} = -\frac{im_a}{2m_{\text{Pl}}} \int d\tau_a e^{ik \cdot x_a(\tau_a)} \mathcal{U}_a^\mu(\tau_a) \mathcal{U}_a^\nu(\tau_a). \quad (1.3.6)$$

For the gravitational sector, we choose to work in the usual De Donder gauge, hence in eq. (1.3.3) we set

$$S_{\text{GF}} = \int d^4x \left(\partial^\rho h_{\rho\mu} - \frac{1}{2} \partial_\mu h \right) \left(\partial_\sigma h^{\sigma\mu} - \frac{1}{2} \partial^\mu h \right), \quad (1.3.7)$$

where we defined $h \equiv h_{\mu\nu} \eta^{\mu\nu}$. Summing this to the Einstein-Hilbert action, we obtain

$$S_{\text{EH}} + S_{\text{GF}} = \frac{1}{2} \int d^4x \left(\partial_\mu h^{\alpha\beta} \partial^\mu h_{\alpha\beta} - \frac{1}{2} \partial_\mu h \partial^\mu h \right) + \mathcal{O}(h^3). \quad (1.3.8)$$

We can then derive the Feynman rules for the graviton propagator as well as the self-interaction vertices, i.e.

$$\begin{array}{c} \mu\nu \\ \text{wavy line} \end{array}^k \begin{array}{c} \rho\sigma \\ \text{wavy line} \end{array} = \frac{i}{k^2} P_{\mu\nu\rho\sigma}, \quad P_{\mu\nu\rho\sigma} = \eta_{\mu(\rho} \eta_{\sigma)\nu} - \frac{1}{2} \eta_{\mu\nu} \eta_{\rho\sigma}, \quad (1.3.9)$$

$$\begin{array}{c} \alpha_1\beta_1 \\ \text{wavy line} \end{array}^k \begin{array}{c} \alpha_3\beta_3 \\ \text{wavy line} \end{array}^k \begin{array}{c} \alpha_2\beta_2 \\ \text{wavy line} \end{array}^k = \frac{i}{m_{\text{Pl}}} \delta^4(k_1 + k_2 + k_3) V_3^{\alpha_1\beta_1\alpha_2\beta_2\alpha_3\beta_3}(k_1, k_2, k_3). \quad (1.3.10)$$

Due to its length, we display the rules for the self interaction vertex in appendix C. Expressions such as this one are more efficiently handled with symbolic softwares, e.g. Mathematica².

As we discussed in the introduction, even though we are using QFT language, we are actually interested only in the classical contributions to the effective action. We must then find a way to identify and ignore any quantum effect. One can use an equivalent scaling reasoning as before — as explained in Ref. [20] — to see that all quantum contributions to S_{eff} are given by closed-graviton-loop diagrams. Indeed, since at leading order the two bodies move freely in empty space, we can say that the four-velocities scale as³

$$U_a^\mu(\tau_a) \sim 1 + \mathcal{O}(G). \quad (1.3.11)$$

Together with the fact that all gravitons scale as q , one obtains

$$\text{Oself} \times \sim \sqrt{G} \frac{m}{q} + \mathcal{O}(G), \quad \text{self} \sim \frac{1}{q^2}, \quad \text{self} \sim \frac{\sqrt{G}}{q^2}. \quad (1.3.12)$$

The first diagram giving Newtonian physics in (1.3.5) scales as

$$\begin{array}{c} 1 \text{ } \circ \\ \text{---} \\ \text{---} \\ \text{---} \\ \text{---} \\ \text{---} \\ \text{---} \\ \text{---} \\ \text{---} \\ \text{---} \\ 2 \text{ } \circ \end{array} \sim Gm^2. \quad (1.3.13)$$

(To obtain this scaling, one must include the integration measure of the exchanged graviton momenta.) The graph in figure 4 (a) is, instead,

$$\begin{array}{c} 1 \text{ } \circ \\ \text{---} \\ \text{---} \\ \text{---} \\ \text{---} \\ \text{---} \\ \text{---} \\ \text{---} \\ \text{---} \\ \text{---} \\ 2 \text{ } \circ \end{array} \sim G^2 m^2 q^2 = Gm^2 (Gq^2) \ll 1. \quad (1.3.14)$$

Compared to eq. (1.3.13), this scales as Gq^2 , hence precisely as a quantum contribution; see the hierarchy in eq. (1.1.9). On the other hand, the third graph of (1.3.5) scales as

$$\begin{array}{c} 1 \text{ } \circ \\ \text{---} \\ \text{---} \\ \text{---} \\ \text{---} \\ \text{---} \\ \text{---} \\ \text{---} \\ \text{---} \\ \text{---} \\ 2 \text{ } \circ \end{array} \sim Gm^2 (Gmq), \quad (1.3.15)$$

²See for instance packages `xTensor` and `xPert` [218, 219].

³This will be clearer in section 1.4.1, see the paragraph before eqs. (1.4.7) and (1.4.8).

thus encoding the first PM correction to the effective action. To conclude, in order to ignore all quantum contributions, it is enough to discard graphs such as the ones depicted in figure 4. This is the reason why we do not need to include any ghost field in eq. (1.3.3). Computing the effective action in this way is actually equivalent to solve perturbatively the Einstein equations for $h_{\mu\nu}$ and insert the solution in the original action (1.3.1), a procedure known as the construction of the Fokker-action (see [21] and references therein for a review).

1.3.1 . Potential and radiation modes

Note that in eq. (1.3.9), we have left implicit the $i0^+$ prescription in the denominator appearing to specify the contour of integration in the complex k^0 plane. In general, any integral appearing in (1.3.5) receives contributions from two physical regions:

- The *potential* region, responsible for the conservative part of the problem that in a scattering process makes the two bodies deviate from their initial trajectories. All gravitons in this regions are off-shell, i.e. $k^2 \neq 0$ in (1.3.9).
- The *radiation* region that incorporates on-shell momenta, i.e. $k^2 = 0$ in (1.3.9). These gravitons carry the signal that we can detect on earth.

For potential modes the $i0^+$ prescription is thus irrelevant, and one can safely use the usual Feynman time-symmetric propagator. On the other hand, for radiation modes the contribution of the pole is essential. In the typical scattering process we want to analyze, the two bodies are initially moving along straight trajectories in vacuum, hence there is no incoming radiation. Thus, in order to take into account only outgoing radiation, one should impose retarded boundary conditions, e.g.

$$\underbrace{\mu\nu \quad k \quad \rho\sigma}_{\text{Ret}} = \frac{i}{(k^0 + i0^+)^2 - |\mathbf{k}|^2} P_{\mu\nu\rho\sigma}. \quad (1.3.16)$$

In particular, the way to correctly implement this in an EFT language is through the use of the *in-in* formalism [151, 220, 221], which allows to describe systems that are no longer time-symmetric. This has been recently applied in the context of the study of the two-body problem in the PM framework in Refs. [150, 167].

As we shall see, splitting in potential and radiation modes allows us to simplify the computation of the Feynman integrals encountered at each perturbative order. However, when doing such decomposition, spurious infrared (IR) and UV divergences may occur in intermediate steps of the computation. These are naturally handles in the EFT language through the use of dimensional regularization, and are expected to eventually cancel against each other in the final result for physical observables. See [34, 35, 37] and references therein for a thorough discussion on this matter.

1.3.2 . Effective action for the radiative sector

In principle, the procedure outlined in the previous sections can be carried out for both the conservative and radiation sector. However, here we introduce an equivalent

way of computing the previous effective action that, as we shall see in the next sections and chapters, turns out to be very useful when one wants to focus on the radiative part of the problem.

The idea is to match our theory described by eq. (1.3.1) with the following effective action [20, 88, 222]

$$\Gamma[x_a, h_{\mu\nu}] = \int d^4x \left[\frac{1}{2} \left(\partial_\mu h^{\alpha\beta} \partial^\mu h_{\alpha\beta} - \frac{1}{2} \partial_\mu h \partial^\mu h \right) - \frac{1}{2m_{\text{Pl}}} T^{\mu\nu}(x) h_{\mu\nu}(x) \right]. \quad (1.3.17)$$

The gravitational part of the above equation is the quadratic gauge-fixed part of the Einstein-Hilbert action, see eq. (1.3.8). We parametrize the source of the gravitational field with an unknown pseudo stress-energy tensor $T^{\mu\nu}$. This contains the contributions coming from both the two massive objects and all the gravitational self-interactions.

We can compute $T^{\mu\nu}$ via a matching procedure as follows: we expand again (1.3.1) for small $h_{\mu\nu}$ and use this to compute the one-point expectation value $\langle h_{\mu\nu} \rangle$, i.e. considering all the Feynman diagrams with one external graviton

$$\langle \tilde{h}_{\mu\nu}(k) \rangle = \begin{array}{c} 1 \\ \circ \end{array} \begin{array}{c} \nearrow k \\ \text{wavy} \\ \searrow \mu\nu \end{array} + \begin{array}{c} \nearrow k \\ \text{wavy} \\ \searrow \mu\nu \\ 2 \\ \circ \end{array} + \begin{array}{c} 1 \\ \circ \\ \text{wavy} \\ \searrow k \\ \text{wavy} \\ \mu\nu \\ 2 \\ \circ \end{array} + \dots, \quad (1.3.18)$$

where we have denoted the Fourier transform with a tilde. We can do the same computation starting from eq. (1.3.17). Then, we match the two results obtaining the following equation

$$\frac{P_{\mu\nu\rho\sigma} \tilde{T}^{\rho\sigma}(k)}{k^2 2m_{\text{Pl}}} = \begin{array}{c} 1 \\ \circ \end{array} \begin{array}{c} \nearrow k \\ \text{wavy} \\ \searrow \mu\nu \end{array} + \begin{array}{c} \nearrow k \\ \text{wavy} \\ \searrow \mu\nu \\ 2 \\ \circ \end{array} + \begin{array}{c} 1 \\ \circ \\ \text{wavy} \\ \searrow k \\ \text{wavy} \\ \mu\nu \\ 2 \\ \circ \end{array} + \dots, \quad (1.3.19)$$

which allows us to find an explicit expression for $\tilde{T}^{\mu\nu}$ at each order in the perturbative expansion. This procedure is known as *bottom-up* approach.

If we are interested in the radiative sector, we can consider the external graviton to be on-shell and impose $k^2 = 0$. Then, $\tilde{T}^{\rho\sigma}(k)$ contains all the relevant information needed to compute physical observables, as we shall see in the next sections. Finally, let us stress that in principle one can have more than one graviton that is emitted, see e.g. the diagram in figure 5. This would require an extra term in (1.3.17) of the form

$$\Gamma[x_a, h_{\mu\nu}] \supset -\frac{1}{2m_{\text{Pl}}} \int d^4x J^{\mu\nu\rho\sigma}(x) h_{\mu\nu}(x) h_{\rho\sigma}(x). \quad (1.3.20)$$

Since they enter at an higher order in the perturbative expansion, these terms will not appear in the computations done in this work, and we can then ignore them.

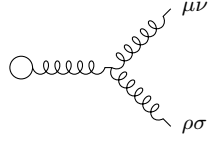


Figure 5: Example a diagram contributing to $J^{\mu\nu\rho\sigma}$.

1.4 . Computing Observables

Now that we have introduced the general set-up of the PM EFT, let us be more concrete, and explain how the PM series is arranged. One feature that distinguishes this EFT approach from the original PN description of [20] is that, rather than computing explicitly the effective action introduced in (1.3.3), it focuses on directly computing observables such as the scattering angle. There are two main reasons for this: first of all, observables are gauge invariants, therefore, their expressions are more compact and more easily comparable with results obtained with other approaches. Secondly, the recently established B2B dictionary [114, 192, 193] has shown that certain observables can be used to reconstruct gauge-dependent quantities such as the action, meaning that their expression is enough to reconstruct the dynamics of the system. Moreover, the B2B mapping finds a direct link between the scattering observables that we can compute with our EFT framework, and the corresponding bound-case observables that are of greater interest for the current and future gravitational wave detectors.

We shall briefly present the B2B dictionary at the end of this chapter, redirecting the reader to [114, 192, 193] for a more complete description. For the reasons that we have just outlined, in the next few sections we focus on two main observables:

- The total impulse Δp_a^μ , i.e. the change in the four-momentum of the two objects $a = 1, 2$. This can be used to compute the deflection angle.
- The emitted momentum P_{rad}^μ , i.e. the momentum carried away by the GWs during the scattering. From here, we shall obtain the radiated energy.

We postpone any explicit computation to chapter 2, where we shall see how to compute the total impulse at next-to-leading-order (NLO), i.e. $\mathcal{O}(G^2)$, recovering results known in the literature [76, 118, 149, 162]. This rather simple computation allows us to introduce in an extensive way the main integration techniques routinely applied in the study of the two-body problem. The leading-order (LO) emitted momentum will be instead the subject of the other chapters of this thesis.

1.4.1 . The total impulse

Since the description of body 1 is completely equivalent to the one of body 2, let us focus on the former. The effective action (1.3.3) can be written as

$$S_{\text{eff}} = \sum_{n=0}^{\infty} \int d\tau_1 \mathcal{L}_n [x_1(\tau_1), x_2(\tau_2)] , \quad (1.4.1)$$

where the label n stands for the order $\mathcal{O}(G^n)$ in the perturbative expansion. The lowest order $n = 0$ is simply the Lagrangian for a particle moving freely in flat spacetime, i.e.

$$\mathcal{L}_0 = -\frac{m_1}{2}\eta_{\mu\nu}\mathcal{U}_1^\mu\mathcal{U}_1^\nu. \quad (1.4.2)$$

By varying eq. (1.4.1), we obtain the usual EOM

$$\sum_{n=0}^{\infty} \left[\frac{d}{d\tau_1} \left(\frac{\partial \mathcal{L}_n}{\partial \mathcal{U}_1^\nu} \right) - \frac{\partial \mathcal{L}_n}{\partial x_1^\nu} \right] = 0. \quad (1.4.3)$$

Since \mathcal{L}_0 does not depend explicitly on x_1^μ , we can see that

$$\eta^{\mu\nu} \frac{d}{d\tau_1} \left(\frac{\partial \mathcal{L}_0}{\partial \mathcal{U}_1^\nu} \right) = -m_1 \frac{d\mathcal{U}_1^\mu}{d\tau_1} = -\frac{dp_1^\mu}{d\tau_1}. \quad (1.4.4)$$

If we isolate this terms in eq. (1.4.3) and integrate over τ_1 one eventually obtains

$$\Delta p_1^\mu = \int_{-\infty}^{\infty} d\tau_1 \frac{dp_1^\mu}{d\tau_1} = -\eta^{\mu\nu} \sum_{n=1}^{\infty} \int_{-\infty}^{\infty} d\tau_1 \frac{\partial \mathcal{L}_n}{\partial x_1^\nu}. \quad (1.4.5)$$

In order to get the above equation, we have assumed that the two bodies are moving freely both at incoming and outgoing infinity, i.e.

$$\mathcal{L}_n \xrightarrow[\tau_a \rightarrow \pm\infty]{} 0, \quad \text{for } n > 0. \quad (1.4.6)$$

The right-hand side of eq. (1.4.5) depends on both the worldline positions and velocities of the two bodies $x_a^\mu(\tau_a)$ and $\mathcal{U}_a^\mu(\tau_a)$. In a gravitational scattering these quantities change due to the mutual gravitational interaction between the two masses, hence they depend on the Newton constant. Therefore, in order to completely isolate the power of G , we expand them around straight motion variables [115, 149, 152, 223], i.e. for each body $a = 1, 2$

$$x_a^\mu(\tau_a) = b_a^\mu + u_a^\mu \tau_a + \delta^{(1)} x_a^\mu(\tau_a) + \delta^{(2)} x_a^\mu(\tau_a) \dots, \quad (1.4.7)$$

$$\mathcal{U}_a^\mu(\tau_a) = u_a^\mu + \delta^{(1)} u_a^\mu(\tau_a) + \delta^{(2)} u_a^\mu(\tau_a) \dots. \quad (1.4.8)$$

Here u_a is the constant asymptotic incoming velocity, b_a is the body displacement orthogonal to it, $b_a \cdot u_a = 0$ and the $\delta^{(n)} x_a^\mu$ and $\delta^{(n)} u_a^\mu$ are the order $\mathcal{O}(G^n)$ deviation from straight motion that can be computed from the $(n-1)$ -th order effective action. Finally, we see that $b^\mu \equiv b_1^\mu - b_2^\mu$ is the impact parameter of the system. Notice that in our scattering set up

$$\delta^{(n)} x_a^\mu(\tau_a) \xrightarrow[\tau_a \rightarrow \pm\infty]{} 0, \quad \delta^{(n)} u_a^\mu(\tau_a) \xrightarrow[\tau_a \rightarrow \pm\infty]{} 0. \quad (1.4.9)$$

We can then compute the n PM order impulse as follows [149]

$$\begin{aligned} \Delta^{(n)} p_1^\mu \equiv & -\eta^{\mu\nu} \int_{-\infty}^{\infty} d\tau_1 \left\{ \frac{\partial}{\partial x_1^\nu} \mathcal{L}_n [b_a + u_a \tau_a] \right. \\ & \left. + \sum_{k=1}^{n-1} \frac{\partial}{\partial x_1^\nu} \mathcal{L}_k [b_a + u_a \tau_a + \delta^{(1)} x_a^\mu + \dots + \delta^{(n-k)} x_a^\mu] \Big|_{\mathcal{O}(G^n)} \right\}. \end{aligned} \quad (1.4.10)$$

In the above equation we left implicit the dependence on the four-velocities to simplify the final expression. The second line of (1.4.10) means that we need to expand the derivative of the Lagrangian at order k , with $k < n$, up to order $n - k$ in the worldline trajectories and velocities and then take the term of order $\mathcal{O}(G^n)$. Once again, we see that in order to compute the $\mathcal{O}(G^n)$, we just need to know the $\mathcal{O}(G^{n-1})$ deviations from straight motion, so the procedure can be carried out iteratively.

1.4.2 . The emitted momentum

Let us now illustrate how we can compute an observable in the radiative sector. In section 1.3.2 we saw how to obtain the pseudo stress-energy tensor of the two-body system. If we consider the emitted radiation to be on-shell, i.e. $k^2 = 0$, then we can compute the total (classical) probability amplitude of emitting one graviton with helicity λ and momentum k as

$$i\mathcal{A}_\lambda(k) = -\frac{i}{2m_{\text{Pl}}} \epsilon_{\mu\nu}^{*\lambda}(\mathbf{k}) \tilde{T}^{\mu\nu}(k) \Big|_{k^2=0} . \quad (1.4.11)$$

In the above equation $\lambda = \pm 2$, and we introduced the polarization tensors $\epsilon_{\mu\nu}^\lambda$ normalized as $\epsilon_{\mu\nu}^{*\lambda}(\mathbf{k}) \epsilon_{\lambda'}^{\mu\nu}(\mathbf{k}) = \delta_{\lambda'}^\lambda$. The amplitude in eq. (1.4.11) can then be used to compute radiative observables such as the asymptotic waveform [224],

$$h_{\mu\nu}(x) = -\frac{1}{4\pi r} \sum_{\lambda=\pm 2} \int \frac{dk^0}{2\pi} e^{-ik^0 t_r} \epsilon_{\mu\nu}^\lambda(\mathbf{k}) \mathcal{A}_\lambda(k) \Big|_{k^\mu = k^0 n^\mu} , \quad (1.4.12)$$

where r is a distance much larger than the interaction region, $t_r = t - r$ is the retarder time and $n^\mu = (1, \mathbf{n})$ with \mathbf{n} the unitary vector pointing along the direction of propagation of the emitted graviton.

Eq. (1.4.11) can also be used to compute the total momentum loss in gravitational waves by the system as [146]

$$P_{\text{rad}}^\mu = \sum_{\lambda=\pm 2} \int_k \delta_+(k^2) k^\mu |\mathcal{A}_\lambda(k)|^2 , \quad (1.4.13)$$

where the $\delta_+(k^2)$ ensures that the emitted radiation is on-shell. This is basically the integration over all momenta k weighted with the differential probability of emission of one graviton with polarization λ and momentum k^μ ,

$$dN_\lambda = \frac{d^3 k}{(2\pi)^3} \int \frac{dk^0}{2\pi} \delta_+(k^2) |\mathcal{A}_\lambda(k)|^2 . \quad (1.4.14)$$

This quantity is not well-defined classically: if we interpret \mathbf{k} and k^0 in these expressions as classical wave-vector and frequency, respectively, and we restore $\hbar \neq 1$, the right-hand side becomes proportional to \hbar^{-1} , which shows that the number of emitted gravitons

⁴Restoring $\hbar \neq 1$, the amplitude is defined as $i\mathcal{A}_\lambda(k) = -i\sqrt{8\pi G} \epsilon_{\mu\nu}^{*\lambda} \tilde{T}^{\mu\nu}(k)$. Distinguishing units of energy and length, denoted respectively by $[M]$ and $[L]$, it has units $[M]^{1/2} [L]^{3/2}$. The needed factor \hbar^{-1} in eq. (1.4.14) restores the correct dimensions of the right-hand side, making it dimensionless.

is divergent in the classical limit $\hbar \rightarrow 0$. However, inserting the four-momentum of the graviton $\hbar k^\mu$ gives a finite quantity in the classical limit and integrating over all gravitons we obtain the total classical emitted momentum.

The computation of this observable will be the main subject of chapters 4, 5 and 6. From this we can compute the radiated energy in the COM

$$\Delta E_{\text{hyp}} = P_{\text{rad}} \cdot u_{\text{COM}}, \quad (1.4.15)$$

where

$$u_{\text{COM}}^\mu = \frac{m_1 u_1^\mu + m_2 u_2^\mu}{M\Gamma}, \quad (1.4.16)$$

is the four velocity of the initial COM frame.

1.4.3 . The deflection angle

The deflection angle is defined as the angle between the initial and the final directions of propagation for each of the two bodies. Usually, one considers the value of the scattering angle in the COM frame χ , see figure 3, page 24.

If the total energy is conserved, the COM is an inertial frame. Then, we can parametrize the incoming four-momenta p_1^μ and p_2^μ as in eq. (1.1.1), and momentum conservation requires that

$$\Delta p_1^\mu + \Delta p_2^\mu = 0, \quad \Delta p_1^\mu = -\Delta p_2^\mu \equiv \Delta p^\mu \quad (1.4.17)$$

The outgoing momentum are then given by

$$p_1'^\mu = (E_1, \mathbf{p}') \quad p_2'^\mu = (E_2, -\mathbf{p}'), \quad \text{where } |\mathbf{p}'| = |\mathbf{p} + \Delta\mathbf{p}| = p_\infty. \quad (1.4.18)$$

Note that the total impulse is $\Delta p^\mu = (0, \mathbf{p}' - \mathbf{p})$. The scattering angle χ satisfies

$$\mathbf{p} \cdot \mathbf{p}' = p_\infty^2 \cos(\chi), \quad (1.4.19)$$

here a dot stands for the standard three-dimensional euclidean product. Using the expression for the impulse and some trivial trigonometric identities, one eventually finds [149, 223]

$$\sin\left(\frac{\chi}{2}\right) = \frac{|\Delta\mathbf{p}|}{2p_\infty} = \frac{\sqrt{-\Delta p^2}}{2p_\infty}. \quad (1.4.20)$$

When the energy of the system is not conserved, things are more subtle. The COM frame is no longer inertial, momentum conservation is now given by the relation

$$\Delta p_1^\mu + \Delta p_2^\mu + P_{\text{rad}}^\mu = 0, \quad (1.4.21)$$

that illustrates that the radiative problem is actually a multi-body problem. The final momenta are no longer in the COM, they can be parametrised as follows

$$p_1'^\mu = (E_1', \mathbf{p} + \Delta\mathbf{p}_1) \quad p_2'^\mu = (E_2', -\mathbf{p} + \Delta\mathbf{p}_2) \quad (1.4.22)$$

Nonetheless, one can define the scattering angle as before, this time computed in the initial COM frame. The relation between χ and Δp_1^μ becomes slightly more involved because now $|\mathbf{p} + \Delta\mathbf{p}_1| \neq p_\infty$. Explicitly one gets

$$\cos(\chi) = \frac{\mathbf{p} \cdot (\mathbf{p} + \Delta\mathbf{p}_1)}{p_\infty |\mathbf{p} + \Delta\mathbf{p}_1|} = \frac{p_\infty^2 + |\mathbf{p} + \Delta\mathbf{p}_1|^2 - |\Delta\mathbf{p}_1|^2}{2p_\infty |\mathbf{p} + \Delta\mathbf{p}_1|}. \quad (1.4.23)$$

It is not hard to see that going back to the conservative case, i.e. for $P_{\text{rad}} = 0$ which implies $|\mathbf{p} + \Delta\mathbf{p}_1| = p_\infty$, and using $\cos(\chi) = 1 - 2\sin^2(\chi/2)$, one recovers the simpler eq. (1.4.20).

In both cases, what we can compute is the PM expanded deflection angle which is customarily defined as [149]

$$\frac{\chi}{2} = \sum_{n=1}^{\infty} \chi_b^{(n)} \left(\frac{GM}{b} \right)^n. \quad (1.4.24)$$

The computation of the coefficients $\chi_b^{(n)}$ is one of the main results of the PM EFT theory, as it will become clearer in the next section.

1.5 . Boundary-to-Bound Map

The PM EFT is able to efficiently solve the classical scattering problem of two massive objects interacting via gravity in the perturbative regime $GM/b \ll 1$. To use this analytic solution to improve waveform models, it is therefore necessary to find a way of connecting the scattering problem studied so far with the bound case. As we shall see, the B2B map originally introduced in [114] and further developed in [192, 193] does exactly this. In this brief section we present the original derivation of [114] on how to reconstruct a Hamiltonian starting from the scattering angle, proving that the observables actually contain all the information of the dynamics of the system. Then, as shown in [192, 193], one can see how this concept can be pushed even further to link scattering observables directly with bound ones through analytic continuation, bypassing the need to compute the intermediate quantities.

1.5.1 . From observables to Hamiltonian

Let us consider a generic Hamiltonian describing two massive spinless objects in a central potential in the COM,

$$H(r, |\mathbf{p}|^2) = \sqrt{|\mathbf{p}|^2 + m_1^2} + \sqrt{|\mathbf{p}|^2 + m_2^2} + V(r, |\mathbf{p}|^2). \quad (1.5.1)$$

Written in this way, the potential is in the so-called isotropic gauge. Working in polar coordinates, we know that the angular component of the momentum \mathbf{p} is the conserved angular momentum $J = p_\infty b$. Therefore the only unknown is the radial momentum

$$p_r^2(r, E) = |\mathbf{p}|^2(r, E, J) - \frac{J^2}{r^2}, \quad (1.5.2)$$

where r is the relative position in the COM frame. We can use the conservation of energy and solve $H = E$ for p_r , from which one can obtain the scattering angle as

$$\chi = -\pi + 2J \int_{r_{\min}}^{\infty} \frac{dr}{r^2 \sqrt{|\mathbf{p}|^2(r, E, J) - J^2/r^2}}, \quad (1.5.3)$$

where r_{\min} is the point of closest approach, which is the solution of $p_r^2(r, E) = 0$.

In the previous sections, we saw how we can directly compute the quantity on the left-hand side of this equation as a perturbative series in GM/b , see eq. (1.4.24). The above equation can be inverted exactly, as done many years ago in [225, 226], obtaining

$$|\bar{\mathbf{p}}|^2(r, E) = \exp \left[\frac{2}{\pi} \int_{r|\bar{\mathbf{p}}|(r, E)}^{\infty} \frac{\chi(\tilde{b}, E) d\tilde{b}}{\sqrt{\tilde{b}^2 - r^2 |\bar{\mathbf{p}}|^2(r, E)}} \right], \quad \bar{\mathbf{p}} \equiv \frac{\mathbf{p}}{p_{\infty}}. \quad (1.5.4)$$

This means that plugging in the above equation the expression (1.4.24) for the scattering angle computed before, we can obtain a similar series expansion for the momentum in the COM,

$$|\mathbf{p}|^2(r, E) = p_{\infty}^2(E) \left(1 + \sum_{n=1}^{\infty} f_n(E) \left(\frac{GM}{r} \right)^n \right). \quad (1.5.5)$$

Here the coefficients $f_n(E)$ are completely determined by the known coefficients of the deflection angle.

At this point, we can make the following ansatz for the central potential appearing in eq (1.5.1):

$$V(r, |\mathbf{p}|^2) = \sum_{n=1}^{\infty} \frac{c_n(|\mathbf{p}|^2)}{n!} \left(\frac{G}{r} \right)^n, \quad (1.5.6)$$

Using this expression and eq. (1.5.5), we can use the conservation of energy to impose that

$$p_{\infty} \sum_{a=1,2} \sqrt{|\bar{\mathbf{p}}|^2 - \sum_{n=1}^{\infty} f_n \left(\frac{GM}{r} \right)^n} + m_a^2 = \sum_{n=0}^{\infty} \frac{c_n}{n!} \left(\frac{G}{r} \right)^n, \quad (1.5.7)$$

which uniquely fixes the coefficients of the potential order-by-order in the PM expansion. As shown in [114], this allows to reconstruct the PM potential matching the results obtained through other methods [107, 118]. This potential can then be used to compute observables in the bound case, i.e. the case in which the total energy of the system is negative.

1.5.2 . Connecting hyperbolae and ellipses

The procedure outlined above is in principle sufficient to connect unbound and bound systems. However, the coefficients of the potential defined in eq. (1.5.6) are gauge-dependent quantities and their complexity can rapidly increase with the order of the perturbative expansion. On the other hand, the coefficients of the deflection angle remain compact and, as we saw, are enough to reconstruct the entire dynamics of the system.

There is a more geometrical way of connecting hyperbolic and elliptic motions without going through the procedure outlined in the previous section. Consider the reduced non-relativistic energy \mathcal{E} defined in eq. (1.1.3). For both unbound ($\mathcal{E} > 0$) and bound ($\mathcal{E} < 0$) motion, the extrema of the relative position r are given by the solution of $p_r^2(r, \mathcal{E}) = 0$, i.e., in the PM expansion,

$$r^2 \left(1 + \sum_{n=1}^{\infty} f_n(\mathcal{E}) \left(\frac{GM}{r} \right)^n \right) = b^2. \quad (1.5.8)$$

Suppose we have reconstructed $f_1(\mathcal{E})$ through the scattering angle χ_1 . Then, the previous equation becomes

$$r^2 \left(1 + \frac{GM}{r} f_1(\mathcal{E}) \right) = b^2. \quad (1.5.9)$$

In the hyperbolic case, $f_1 > 0$ [114]; therefore, since $r > 0$, we have only one valid root which is the point of closest approach,

$$r_{\min} = -\frac{GM}{2} f_1 + \sqrt{\frac{G^2 M^2 f_1^2}{4} + b^2}. \quad (1.5.10)$$

On the other hand, for a bound orbit $f_1 < 0$, hence we get two possible roots corresponding to the periastron and apastron of the ellipse. We can reconstruct these two solutions via an analytic continuation of (1.5.10). In particular, the periastron r_- can be found as

$$r_-(b, \mathcal{E}) = r_{\min}(ib, \mathcal{E}) = -\frac{GM f_1}{2} + \sqrt{\frac{G^2 M^2 f_1^2}{4} - b^2}, \quad b > 0, \mathcal{E} < 0. \quad (1.5.11)$$

The other root is found as

$$r_+(b, \mathcal{E}) = r_-(-b, \mathcal{E}) = r_{\min}(-ib, \mathcal{E}), \quad b > 0, \mathcal{E} < 0. \quad (1.5.12)$$

As shown explicitly in [114], this procedure can be extended to all order in the PM expansion using eq. (1.5.4). Hence, one can actually compute the extrema of the two motions directly using once again only the coefficients of the PM expanded scattering angle.

Finally, notice that under the analytic continuation $\mathcal{E} < 0$, $p_{\infty} \rightarrow -ip_{\infty}$, which implies that

$$J = bp_{\infty} \rightarrow (ib)(-ip_{\infty}) = J > 0. \quad (1.5.13)$$

Hence we conclude that we can equivalently write

$$r_{\mp}(J, \mathcal{E}) = r_{\min}(\pm J, \mathcal{E}), \quad J > 0, \mathcal{E} < 0. \quad (1.5.14)$$

1.5.3 . Connecting Observables

Let us now go back to connecting bound and unbound observables. In particular let us consider the scattering angle χ for an hyperbolic motion computed as in eq. (1.5.3), and the periastron advance $\Delta\Phi$ for an elliptic one, given by [192]

$$\Delta\Phi = -2\pi + 2J \int_{r_-}^{r_+} \frac{dr}{r^2 \sqrt{|\mathbf{p}|^2(r, \mathcal{E}, J) - J^2/r^2}}. \quad (1.5.15)$$

The resemblance between this equation and (1.5.3) is not a coincidence; indeed these two quantities are closely related. In light of eq. (1.5.14), let us consider the following combination

$$\chi(J, \mathcal{E}) + \chi(-J, \mathcal{E}) + 2\pi = 2J \int_{r_{\min}(J, \mathcal{E})}^{r_{\min}(-J, \mathcal{E})} \frac{dr}{r^2 \sqrt{|\mathbf{p}|^2(r, \mathcal{E}, J) - J^2/r^2}}, \quad (1.5.16)$$

where we needed to use that $|\mathbf{p}|^2(r, \mathcal{E}, J) = |\mathbf{p}|^2(r, \mathcal{E}, -J)$, valid for spinless particles. Upon the analytic continuation $\mathcal{E} < 0$, one finds the remarkably compact formula [192]

$$\Delta\Phi(J, \mathcal{E}) = \chi(J, \mathcal{E}) + \chi(-J, \mathcal{E}), \quad (1.5.17)$$

which shows that it is possible to connect directly observables in a simple way.

This was further developed in [193] to include radiation effects and radiated observables. For example, in the following we shall need the connection between the emitted energy in the COM for an hyperbolic encounter ΔE_{hyp} and the average radiate energy over a period of an elliptic motion ΔE_{ell} which is

$$\Delta E_{\text{ell}}(\mathcal{E}, J) = \Delta E_{\text{hyp}}(\gamma, J) - \Delta E_{\text{hyp}}(\mathcal{E}, -J), \quad \mathcal{E} < 0. \quad (1.5.18)$$

The right-hand side can be computed in the PM expansion using eq. (1.4.16).

As discussed in [193], this map does not seem to capture the (non-universal) non-local terms coming from the radiation modes that are re-absorbed by the binary system at a later time than their emission, see e.g. [31, 34, 194–196]. In the PM scheme they first appear in the recently obtained 4PM (incomplete) order [129, 130, 153, 154]; therefore, finding a complete map between unbound and bound motion is still an open problem.

1.6 . Summary of the chapter

In this chapter, we presented the worldline EFT approach to the gravitational two-body problem. Building on NRGR [20, 144], this EFT allowed us to study the scattering of two massive objects within the PM expansion. The two objects are considered as external sources of the gravitational field. With this approximation, we were able to perturbatively compute a classical effective action for the two bodies by considering all connected Feynman diagrams at a certain order in the PM expansion. Diagrams containing closed graviton loops encoded only quantum effects and could then be neglected.

Rather than computing the effective action, we focused in computing directly observables such as the impulse and emitted momentum, from which one can extract respectively the deflection angle and radiated energy. The results for the scattering problem can then be analytically continued to the bound case using the B2B map [114, 192, 193] briefly presented in section 1.5.

We shall now proceed and show an explicit computation using the tools just described in this chapter.

2 - Integration techniques

In the previous chapter we reviewed the general features of the PM EFT approach. Now, we shall present the main techniques used to solve Feynman integrals throughout this dissertation, i.e. reverse unitarity [168–171], Integration-by-Parts (IBP) identities [172, 173, 176], differential equations to solve loop integrals [180–185] and the Cutkosky rules [204, 205, 227, 228]. For this purpose, we consider a simple example: the computation of the total impulse at $\mathcal{O}(G^2)$.

2.1 . PM EFT at $\mathcal{O}(G^2)$

Up to 2PM order, the energy of the two-body system is conserved; therefore, the only non trivial observable that we can compute is the total impulse. As explained in 1.4.1, see eq. (1.4.10), in order to compute the $\mathcal{O}(G^2)$ impulse, we need the effective Lagrangian at $\mathcal{O}(G^2)$, and the LO deviation from straight motion $\delta^{(1)}x_a^\mu$ and $\delta^{(1)}u_a^\mu$ for the two bodies, as defined in eqs. (1.4.7) and (1.4.8). This section shows how to compute these quantities and the 1PM impulse.

2.1.1 . Effective action and EOM

Since the energy is conserved, the effective Lagrangian can be computed by simply taking the diagrams in eq. (1.3.5) plus their symmetric version in the exchange of the two objects, and ignoring the ones where the graviton lines start and end at the same worldline. In the conservative sector, this type of diagrams produce scaleless divergent terms that can be handled with dimensional regularization [20, 149]. More explicitly, using the rules established in section 1.3.1, we obtain, at LO,

$$\mathcal{L}_1 = -\frac{m_1 m_2}{4m_{\text{Pl}}^2} \int d\tau_2 \left(\mathcal{U}_1(\tau_1) \cdot \mathcal{U}_2(\tau_2) - \frac{1}{2} \mathcal{U}_1^2(\tau_1) \mathcal{U}_2^2(\tau_2) \right) \int_k \frac{e^{ik \cdot (x_1(\tau_1) - x_2(\tau_2))}}{k^2}. \quad (2.1.1)$$

The NLO Lagrangian as defined in eq. (1.4.1) is given by the cubic diagram¹ depicted in (1.3.5)

$$\begin{aligned} \mathcal{L}_2 = & \frac{m_1 m_2^2}{16m_{\text{Pl}}^4} \int d\tau_2 d\tau_2' \mathcal{U}_1^\alpha(\tau_1) \mathcal{U}_1^\beta(\tau_1) \mathcal{U}_2^\rho(\tau_2) \mathcal{U}_2^\sigma(\tau_2) \mathcal{U}_2^\mu(\tau_2') \mathcal{U}_2^\nu(\tau_2') P_{\alpha\beta\alpha_1\beta_1} P_{\rho\sigma\alpha_2\beta_2} P_{\mu\nu\alpha_3\beta_3} \\ & \times \int_{k_1, k_2, k_3} \delta^4(k_1 + k_2 + k_3) \frac{e^{ik_1 \cdot x_1(\tau_1)} e^{ik_2 \cdot x_2(\tau_2)} e^{ik_3 \cdot x_2(\tau_2')}}{k_1^2 k_2^2 k_3^3} V_3^{\alpha_1\beta_1\alpha_2\beta_2\alpha_3\beta_3}(k_1, k_2, k_3) \\ & + (1 \leftrightarrow 2), \end{aligned} \quad (2.1.2)$$

where $(1 \leftrightarrow 2)$ means that we exchange only the label 1 and 2 of the two objects. Note that at this point these quantities do not have a unique power of G , since they depend

¹Note that we use a different gauge for the graviton with respect to reference [149].

on the full four-velocities $\mathcal{U}_a(\tau_a)$ and positions $x_a(\tau_a)$. As explained in eq. (1.4.10), the expansion around straight-motion variables introduced in eqs. (1.4.8) and (1.4.7) has to be done after taking the necessary derivatives of the Lagrangians.

For instance, taking derivatives of eq. (2.1.1) and then expanding $\mathcal{U}_a(\tau_a)$ and $x_a(\tau_a)$, we can obtain the first order deviations $\delta^{(1)}x_a^\mu$ and $\delta^{(1)}u_a^\mu$ [149]

$$\delta^{(1)}u_1^\mu(\tau) = \frac{m_2}{4m_{\text{P}1}^2} \int_q \frac{\delta(q \cdot u_2) e^{iq \cdot b + iq \cdot u_1 \tau}}{q^2 (q \cdot u_1 - i0^+)} \left[\frac{2\gamma^2 - 1}{2} q^\mu - (q \cdot u_1) (2\gamma u_2^\mu - u_1^\mu) \right], \quad (2.1.3)$$

$$\delta^{(1)}x_1^\mu(\tau) = -\frac{im_2}{4m_{\text{P}1}^2} \int_q \frac{\delta(q \cdot u_2) e^{iq \cdot b + iq \cdot u_1 \tau}}{q^2 (q \cdot u_1 - i0^+)^2} \left[\frac{2\gamma^2 - 1}{2} q^\mu - (q \cdot u_1) (2\gamma u_2^\mu - u_1^\mu) \right]. \quad (2.1.4)$$

In eqs. (2.1.3) and (2.1.4) we have introduced a Feynman regulator $-i0^+$ to ensure that the deviations from straight motion vanish as $\tau \rightarrow -\infty$, as in (1.4.9). The EOM for body 2 can be obtained by performing again the exchange ($1 \leftrightarrow 2$). Note that this step implies $b^\mu \rightarrow -b^\mu$.

2.1.2 . 1PM order impulse

The LO impulse follows from eq. (1.4.10) using the expression of (2.1.1) evaluated along straight motion variables. One eventually obtains

$$\Delta^{(1)}p_1^\mu = i \frac{m_1 m_2}{8m_{\text{P}1}^2} (2\gamma^2 - 1) \int_k \delta(k \cdot u_1) \delta(k \cdot u_2) k^\mu \frac{e^{ik \cdot b}}{k^2}. \quad (2.1.5)$$

In order to compute this quantity, we need the following family of d dimensional Fourier transforms ($\int_q \equiv \int d^d q / (2\pi)^d$)

$$I_\alpha \equiv \int_q \delta(q \cdot u_1) \delta(q \cdot u_2) \frac{e^{iq \cdot b}}{(q^2)^\alpha}. \quad (2.1.6)$$

Introducing the projector to the $(d-2)$ -dimensional hypersurface orthogonal to u_1 and u_2

$$P_{12}^{\mu\nu} = \eta^{\mu\nu} - \left(\frac{u_1^\mu - \gamma u_2^\mu}{1 - \gamma^2} \right) u_1^\nu - \left(\frac{u_2^\mu - \gamma u_1^\mu}{1 - \gamma^2} \right) u_2^\nu, \quad (2.1.7)$$

the solution of eq. (2.1.6) can be written as

$$I_\alpha = \frac{2^{-2\alpha}}{\pi^{(d-2)/2} \sqrt{\gamma^2 - 1}} \frac{\Gamma\left(\frac{d-2}{2} - \alpha\right)}{\Gamma(\alpha)} (-b \cdot P_{12} \cdot b)^{\alpha - \frac{d-2}{2}}. \quad (2.1.8)$$

From this scalar result, we can solve the following vectorial integrals

$$I_\alpha^{\mu_1 \dots \mu_n} \equiv \int_q \delta(q \cdot u_1) \delta(q \cdot u_2) \frac{q^{\mu_1} \dots q^{\mu_n}}{(q^2)^\alpha} e^{iq \cdot b}, \quad (2.1.9)$$

by taking derivatives w.r.t. b^μ , i.e.

$$I_\alpha^{\mu_1 \dots \mu_n} = (-i)^n \frac{\partial}{\partial b_{\mu_1}} \dots \frac{\partial}{\partial b_{\mu_n}} I_\alpha. \quad (2.1.10)$$

These results will be useful throughout the entire thesis.

Going back to eq. (2.1.5), using eqs. (2.1.10) and (2.1.8), we eventually obtain

$$\Delta^{(1)} p_1^\mu = -2Gm_1 m_2 \frac{2\gamma^2 - 1}{\sqrt{\gamma^2 - 1}} \frac{b^\mu}{b^2}. \quad (2.1.11)$$

Using the expression (2.1.11), we can compute the LO deflection angle in the COM frame. Expanding eq. (1.4.20) up to order G and using eq. (1.4.24) we get

$$\frac{GM}{b} \chi_b^{(1)} = \frac{|\Delta^{(1)} \mathbf{p}_1|}{2p_\infty}, \quad (2.1.12)$$

with p_∞ defined in eq. (1.1.5). Hence, we get explicitly

$$\frac{\chi_b^{(1)}}{\Gamma} = \frac{2\gamma^2 - 1}{\gamma^2 - 1}, \quad (2.1.13)$$

in agreement with known results in the literature [76, 118, 149, 223].

2.2 . $\Delta^{(2)} p_1^\mu$ as a one loop computation

According to (1.4.10), the 2PM order impulse is composed of two contributions: one is coming from \mathcal{L}_2 evaluated along straight-line trajectories, and the other from \mathcal{L}_1 expanded up to first order in $\delta^{(1)} x_a^\mu$ and $\delta^{(1)} u_a^\mu$. Explicitly we have

$$\begin{aligned} \Delta^{(2)} p_1^\mu &= \frac{m_1 m_2}{4m_{\text{Pl}}^2} \int d\tau_1 d\tau_2 \int_k \frac{ik^\mu}{k^2} e^{ik \cdot b} e^{ik \cdot (u_1 \tau_1 - u_2 \tau_2)} \\ &\times \left\{ \frac{m_2}{16m_{\text{Pl}}^2} \int_p \delta(p \cdot u_2) \frac{k^2 + 2(p \cdot u_1)^2 + (2\gamma^2 - 1)(p^2 + (p - k)^2)}{p^2(k - p)^2} \right. \\ &\left. + \left[\frac{2\gamma - 1}{2} ik \cdot \delta^{(1)} x_1(\tau_1) + (2\gamma u_2 - u_1) \cdot \delta^{(1)} u_1(\tau_1) \right] \right\} + (1 \leftrightarrow 2). \quad (2.2.1) \end{aligned}$$

We are going to ignore the symmetric contribution ($1 \leftrightarrow 2$) because the steps to be performed on this term are exactly the same we show now. Using eqs. (2.1.3) and (2.1.4), one eventually gets

$$\begin{aligned} \Delta^{(2)} p_1^\mu &= \frac{m_1 m_2^2}{16m_{\text{Pl}}^2} \int_{k,p} \delta(p \cdot u_2) \frac{ik^\mu}{k^2 p^2} e^{ik \cdot b} \left\{ \delta(k \cdot u_1) \delta(k \cdot u_2) \frac{\mathcal{N}_{c,1}}{k^2(p - k)^2} \right. \\ &\left. + e^{ip \cdot b} \delta((k + p) \cdot u_1) \delta(k \cdot u_2) \frac{\mathcal{N}_1}{(p \cdot u_1 - i0^+)^2} \right\}, \quad (2.2.2) \end{aligned}$$

where we have defined, for simplicity,

$$\mathcal{N}_1 = \frac{1}{4} [(2\gamma^2 - 1)k \cdot p - 8\gamma^2 p \cdot u_1] , \quad (2.2.3)$$

$$\mathcal{N}_{c,1} = \frac{1}{4} [k^2 + 2(p \cdot u_1)^2 + (2\gamma^2 - 1)(p^2 + (k - p)^2)] . \quad (2.2.4)$$

Now, for a reason that will be clear momentarily, we rename $k = q$ and $p = \ell$ in the first line of (2.2.2), while we change variable $k = \ell$ and $p = q - \ell$ for its second line. The result can then be rewritten as

$$\begin{aligned} \Delta^{(2)} p_1^\mu &= i \frac{m_1 m_2^2}{16m_{\text{Pl}}^4} \int_q \delta(q \cdot u_1) \delta(q \cdot u_2) e^{iq \cdot b} \\ &\quad \times \int_\ell \frac{\delta(\ell \cdot u_2)}{\ell^2(\ell - q)^2} \left[\frac{\ell^\mu}{(\ell \cdot u_1 + i0^+)^2} \mathcal{N}_1 + \frac{q^\mu}{q^2} \mathcal{N}_{c,1} \right] . \end{aligned} \quad (2.2.5)$$

Finally, adding the symmetric contribution we obtain

$$\Delta^{(2)} p_1^\mu = i \frac{m_1 m_2}{16m_{\text{Pl}}^4} \int_q \delta(q \cdot u_1) \delta(q \cdot u_2) e^{iq \cdot b} \mathcal{Q}_1^\mu(q) , \quad (2.2.6)$$

$$\begin{aligned} \mathcal{Q}_1^\mu(q) &\equiv m_2 \int_\ell \frac{\delta(\ell \cdot u_2)}{\ell^2(\ell - q)^2} \left[\frac{\ell^\mu}{(\ell \cdot u_1 + i0^+)^2} \mathcal{N}_1 + \frac{q^\mu}{q^2} \mathcal{N}_{c,1} \right] + \\ &\quad + m_1 \int_\ell \frac{\delta(\ell \cdot u_1)}{\ell^2(\ell - q)^2} \left[\frac{\ell^\mu}{(-\ell \cdot u_2 + i0^+)^2} \mathcal{N}_2 + \frac{q^\mu}{q^2} \mathcal{N}_{c,2} \right] , \end{aligned} \quad (2.2.7)$$

where, in eq. (2.2.7), $\mathcal{N}_2 = \mathcal{N}_1|_{1 \leftrightarrow 2}$ and $\mathcal{N}_{c,2} = \mathcal{N}_{c,1}|_{1 \leftrightarrow 2}$. We can now understand why we have performed such a change of integration variables: the problem is now reduced to a one-loop integral \mathcal{Q}_1^μ followed by a Fourier transform from q to b space of the form of eqs. (2.1.8) and (2.1.10). This is convenient because we can then apply all the powerful techniques developed specifically to solve loop integrals, as we shall see explicitly in the rest of this chapter.

Before proceeding however, it is convenient to perform one last step. It is always more practical to work with scalar rather than vector-valued integrals. Therefore, to get rid of the free index in eq. (2.2.6), we introduce the following basis of vectors in four dimensions

$$\hat{b}^\mu \equiv \frac{b^\mu}{\sqrt{-b^2}} , \quad \check{u}_1^\mu \equiv \frac{\gamma u_2^\mu - u_1^\mu}{\gamma^2 - 1} , \quad \check{u}_2^\mu \equiv \frac{\gamma u_1^\mu - u_2^\mu}{\gamma^2 - 1} , \quad \hat{l}^\mu \equiv \frac{\epsilon^\mu{}_{\nu\rho\sigma} u_1^\nu u_2^\rho \hat{b}^\sigma}{\sqrt{\gamma^2 - 1}} . \quad (2.2.8)$$

It is straightforward to see that these form a complete basis in four dimensions and have the advantage that $u_a \cdot \check{u}_b = \delta_{ab}$. One can also realize that \hat{l}^μ is nothing but the unitary vector pointing in the direction of the (orbital) angular momentum of the system. We can then decompose $\Delta^{(2)} p_1^\mu$ along this four components, i.e.

$$\Delta^{(2)} p_1^\mu \equiv G^2 m_1 m_2 [c_1 \check{u}^\mu + c_2 \check{u}^\mu - c_b \hat{b}^\mu] . \quad (2.2.9)$$

We recall that, in this case, the scattering happens on a plane orthogonal to the angular momentum of the system and for this reason we do not have any component of the impulse in the \hat{l}^μ direction. We are left with the computation of

$$c_V \equiv i64\pi^2 \int_q \delta(q \cdot u_1) \delta(q \cdot u_2) e^{iq \cdot b} \mathcal{Q}_1(q) \cdot V, \quad \text{where } V \in \{\hat{b}, u_1, u_2\}. \quad (2.2.10)$$

and $\mathcal{Q}_1(q) \cdot V$ are just three scalar one-loop integrals.

Adopting a standard notation, we introduce the following definitions for the propagators [110, 112, 121]:

$$\begin{aligned} \rho_1 &= 2\ell \cdot u_1 + i0^+, & \rho_2 &= -2\ell \cdot u_2 + i0^+, \\ \rho_3 &= \ell^2 + i0^+, & \rho_4 &= (\ell - q)^2 + i0^+. \end{aligned} \quad (2.2.11)$$

The linear propagators ρ_1 and ρ_2 can be thought of as the LO expansion in small momentum of a standard quadratic propagator as it happens for instance in heavy-quark EFT [229], or in the scattering-amplitude approach to the two-body problem (see e.g. [110, 112, 118, 124] and references therein for an incomplete set of reference of this approach). We shall come back on this at the end of section 2.3.5. With these definitions, we can explicitly write

$$\mathcal{Q}_1 \cdot \hat{b} = 2m_2 \int_\ell \frac{\delta(\rho_2)}{\rho_3 \rho_4} \left[4 \frac{\ell \cdot \hat{b}}{\rho_1^2} \mathcal{N}_1 + \frac{q \cdot \hat{b}}{q^2} \mathcal{N}_{c,1} \right] - (1 \leftrightarrow 2), \quad (2.2.12)$$

$$\mathcal{Q}_1 \cdot u_1 = 4m_2 \int_\ell \frac{\delta(\rho_2)}{\rho_1 \rho_3 \rho_4} \mathcal{N}_1, \quad (2.2.13)$$

$$\mathcal{Q}_1 \cdot u_2 = 4m_1 \int_\ell \frac{\delta(\rho_1)}{\rho_2 \rho_3 \rho_4} \mathcal{N}_2. \quad (2.2.14)$$

Note that $\hat{b}^\mu \rightarrow -\hat{b}^\mu$ when taking the symmetric contribution in eq. (2.2.12).

There are still some simplifications we can perform. To get rid of $\ell \cdot \hat{b}$ in eq. (2.2.12), we decompose the loop momentum as

$$\ell^\mu = (\ell \cdot u_1) \check{u}_1^\mu + (\ell \cdot u_2) \check{u}_2^\mu + \frac{(\ell \cdot q)}{q^2} q^\mu + \ell_\perp^\mu, \quad (2.2.15)$$

where ℓ_\perp^μ is a four-vector orthogonal to \check{u}_1^μ , \check{u}_2^μ and q^μ . Then we see that

$$\hat{b} \cdot \ell = \frac{(\ell \cdot q)}{q^2} q \cdot \hat{b} + \ell_\perp \cdot \hat{b}. \quad (2.2.16)$$

It is not hard to see that the integration in (2.2.12) is odd with respect to $\ell_\perp^\mu \rightarrow -\ell_\perp^\mu$. Thus, the terms proportional to $\ell_\perp \cdot \hat{b}$ do not contribute to the integral in eq. (2.2.12). Moreover, $\ell \cdot q = (\rho_4 - \rho_3 - q^2)/2$. Therefore, eq. (2.2.12) becomes

$$\mathcal{Q}_1 \cdot \hat{b} = 2m_2 \frac{q \cdot \hat{b}}{q^2} \int_\ell \frac{\delta(\rho_2)}{\rho_3 \rho_4} \left[2 \frac{\rho_3 + q^2 - \rho_4}{\rho_1^2} \mathcal{N}_1 + \mathcal{N}_{c,1} \right] - (1 \leftrightarrow 2). \quad (2.2.17)$$

Finally, we can rewrite eq. (2.2.13) as

$$\mathcal{Q}_1 \cdot u_1 = 2m_2 \int_{\ell} \delta(\rho_2) \frac{\mathcal{N}_1}{\rho_3 \rho_4} \left(\frac{1}{2\ell \cdot u_1 + i0^+} + \frac{1}{2\ell \cdot u_1 + i0^+} \right). \quad (2.2.18)$$

Performing the shift $\ell \rightarrow q - \ell$ in the second term of the round bracket, using the fact that q is orthogonal to both u_1 and u_2 (see eq. (2.2.10)) and recalling the relation

$$\delta(x) = \frac{i}{x + i0^+} - \frac{i}{x - i0^+}, \quad (2.2.19)$$

one eventually obtains

$$\mathcal{Q}_1 \cdot u_1 = -2im_2 \int_{\ell} \delta(\rho_1) \delta(\rho_2) \frac{\mathcal{N}_1}{\rho_3 \rho_4}, \quad (2.2.20)$$

$$\mathcal{Q}_1 \cdot u_2 = -2im_1 \int_{\ell} \delta(\rho_1) \delta(\rho_2) \frac{\mathcal{N}_2}{\rho_3 \rho_4}. \quad (2.2.21)$$

Here we have performed similar simplification on the second term of (2.2.13).

To summarize, in this section we saw step-by-step how to rewrite the classical impulse at $\mathcal{O}(G^2)$ as a one-loop integral, landing on eqs (2.2.17), (2.2.20) and (2.2.21). Even though these integrals can be solved without too much effort, we shall use them as guiding examples to present the various loop integration methods that we need to go beyond this PM order.

2.3 . Computing $\Delta^{(2)} p_1^\mu$: the integration methods

The rest of this chapter is devoted to an explicit computation of the total impulse at $\mathcal{O}(G^2)$. This simple example allows us to introduce and explain all the main integration techniques used throughout this dissertation.

2.3.1 . Integration-By-Parts Identities and Reverse Unitarity

The first tool that allows us to greatly simplify the computation of loop integrals are IBP identities [172, 173, 176]. The idea is to find non-trivial relations that reduce the computation of a complicated loop integral to a much simpler one.

As a warm-up activity and to explicitly show how the procedure works, let us consider the following family of one-loop integrals in d dimensions,

$$I_{a,b} \equiv \int_{\ell} \frac{1}{(\ell^2 - s + i0^+)^a (2\ell \cdot u + i0^+)^b}, \quad a, b \in \mathbb{N}. \quad (2.3.1)$$

Starting from the following identities (omitting the $i0^+$ prescriptions for simplicity),

$$\int_{\ell} \frac{\partial}{\partial \ell^\mu} \left(\frac{\ell^\mu}{(\ell^2 - s)^a (2\ell \cdot u)^b} \right) = 0, \quad \int_{\ell} \frac{\partial}{\partial \ell^\mu} \left(\frac{u^\mu}{(\ell^2 - s)^a (2\ell \cdot u)^b} \right) = 0, \quad (2.3.2)$$

one can develop the derivatives obtaining the system of equations

$$\begin{cases} (d - 2a - b)I_{a,b} - 2asI_{a+1,b} = 0 \\ aI_{a+1,b-1} + 2b(u \cdot u)sI_{a,b+1} = 0 \end{cases}. \quad (2.3.3)$$

As long as $a > 1$, we can rewrite the previous system in a more suggestive way

$$\begin{cases} I_{a,b} = \frac{d-2a-b+2}{2s(a-1)} = I_{a-1,b} \\ I_{a,b} = -\frac{1}{4s(u \cdot u)} \frac{d-2a-b+2}{(b-1)} I_{a,b-2} \end{cases} . \quad (2.3.4)$$

Using the simple identities (2.3.2), we have found non trivial relations that connect the original $I_{a,b}$ with a simpler integral with less powers at the denominator.

This system can be solve iteratively. Indeed, for b fixed, the first equation of (2.3.4) gives us

$$I_{a,b} = \frac{1}{(a-1)!s^{a-1}} \frac{\Gamma\left(\frac{d-b}{2}\right)}{\Gamma\left(\frac{d-b}{2} - a + 1\right)} I_{1,b} . \quad (2.3.5)$$

This completely solves the reduction for the exponent a . We can then choose $a = 1$ in the second equation of (2.3.2) and focus on b . It is not too hard to see that we have two distinct cases: when b is even and when it is odd. Solving again iteratively we find that

$$I_{1,b} = \begin{cases} \frac{1}{(b-1)!!} \left(-\frac{1}{2su \cdot u}\right)^{b/2} \frac{\Gamma\left(\frac{d}{2}\right)}{\Gamma\left(\frac{d-b}{2}\right)} I_{1,0} & b \text{ even} , \\ \frac{1}{(b-1)!!} \left(-\frac{1}{2su \cdot u}\right)^{(b-1)/2} \frac{\Gamma\left(\frac{d-1}{2}\right)}{\Gamma\left(\frac{d-b}{2}\right)} I_{1,1} & b \text{ odd} . \end{cases} \quad (2.3.6)$$

Putting together this and (2.3.5), we finally find

$$I_{a,b} = \begin{cases} \frac{(-1)^{b/2} s^{1-a-b/2}}{(2u \cdot u)^{b/2} (b-1)!!} \frac{\Gamma\left(\frac{d}{2}\right)}{\Gamma(a) \Gamma\left(\frac{d-b}{2} - a + 1\right)} I_{1,0} & b \text{ even} , \\ \frac{(-1)^{(b-1)/2} s^{1-a-(b-1)/2}}{(2u \cdot u)^{(b-1)/2} (b-1)!!} \frac{\Gamma\left(\frac{d-1}{2}\right)}{\Gamma(a) \Gamma\left(\frac{d-b}{2} - a + 1\right)} I_{1,1} & b \text{ odd} . \end{cases} \quad (2.3.7)$$

To summarize, the IBP identities in eq. (2.3.2) allow us to reduce the computation of an entire family of loop integrals $I_{a,b}$ to just two simpler master integrals (MIs) $\{I_{1,0}, I_{1,1}\}$. This procedure can be generalized to arbitrary number of loop momenta, and it has been automatized in algorithmic codes such as LiteRed [177, 178] and FIRE6 [179].

It would be convenient to apply the IBP reduction process to simplify eqs. (2.2.17), (2.2.20) and (2.2.21), however, we can see a clear difference with the procedure described in the previous paragraph: the loop integrals contain a delta-function. Luckily, IBP identities can still be applied in this case thanks to the use of the so-called reverse unitarity [168–171]. Suppose we want to IBP reduce the following integral,

$$\int_{\ell} \frac{\delta(2\ell \cdot u)}{(\ell^2 - s)^a} . \quad (2.3.8)$$

The idea is to treat $\delta(2\ell \cdot u)$ as a propagator that has been cut, which means that it is evaluated on the pole, or equivalently, it is on-shell. We can formally replace

$$\delta(2\ell \cdot u) \rightarrow \frac{1}{\underline{2\ell \cdot u}} . \quad (2.3.9)$$

From now on, an underlined propagators means that it is in fact cut. One can see that in this way we are back to the family $I_{a,b}$. Here the cut propagator to the power b simply means the $(b-1)$ -th derivative of a delta function.

We can implement the IBP procedure as explained previously. Developing the second identities of (2.3.2), one finds

$$-\int_{\ell} \left[\frac{2a\ell \cdot u}{(\ell^2 - s)^{a+1} \underline{2\ell \cdot u}} + \frac{2u \cdot u}{(\ell^2 - s)^a (\underline{2\ell \cdot u})^2} \right] = 0. \quad (2.3.10)$$

Looking at the first term of this equation, we would be tempted to simplify the numerator with the last term in the denominator. However, one must keep in mind that the underline propagator is cut, so that term is explicitly

$$\int_{\ell} \frac{2a\ell \cdot u}{(\ell^2 - s)^{a+1} \underline{2\ell \cdot u}} \rightarrow a \int_{\ell} \frac{\delta(2\ell \cdot u) 2\ell \cdot u}{(\ell^2 - s)^{a+1}} = 0. \quad (2.3.11)$$

This means that whenever we use reverse unitarity, during the IBP process we need to discard all integrals in which the cut propagators disappear. This step can be implemented automatically in LiteRed [177, 178] through the option CutDS.

Looking at eq. (2.3.7), we immediately understand that all the integrals in the family $I_{a,b}$ with b even vanish because they can always be reduced to an integral in which the cut propagator has been simplified. Therefore

$$I_{a,b} = \begin{cases} 0 & b \text{ even,} \\ (-1)^{(b-1)/2} s^{1-a-(b-1)/2} \frac{\Gamma(\frac{d-1}{2})}{(2u \cdot u)^{(b-1)/2} (b-1)!! \Gamma(a) \Gamma(\frac{d-b}{2} - a + 1)} I_{1,1} & b \text{ odd.} \end{cases} \quad (2.3.12)$$

Finally, to find the correct result for $I_{1,1}$, one must replace the underlined propagator with its original expression as delta-function and then solve it.

2.3.2 . IBP reduction of the $\mathcal{O}(G^2)$ impulse

We are now ready to apply what we have described in the previous section to the three loop integrals needed for the computation of the $\mathcal{O}(G^2)$ impulse, eqs. (2.2.17), (2.2.20) and (2.2.21). Introducing the following family of one-loop integrals,

$$G_{n_1, n_2, n_3, n_4} \equiv \int_{\ell} \frac{1}{\rho_1^{n_1} \rho_2^{n_2} \rho_3^{n_3} \rho_4^{n_4}}, \quad (2.3.13)$$

it is easy to see that eqs. (2.2.17), (2.2.20) and (2.2.21) can be written as a linear combination of these integrals. Using reverse unitarity and LiteRed [177, 178] to perform the IBP reduction, this time in $d = 4$ dimensions, we find that

$$\mathcal{Q} \cdot \hat{b} = -\frac{3q \cdot \hat{b}}{8} (5\gamma^2 - 1) (m_2 G_{0,1,1,1} + m_1 G_{1,0,1,1}), \quad (2.3.14)$$

$$\mathcal{Q} \cdot u_1 = -im_2 \frac{q^2}{4} (2\gamma^2 - 1)^2 G_{1,1,1,1}, \quad (2.3.15)$$

$$\mathcal{Q} \cdot u_2 = im_1 \frac{q^2}{4} (2\gamma^2 - 1)^2 G_{1,1,1,1}, \quad (2.3.16)$$

where we recall that an underlined lower index means that the propagator is cut. Once again, the advantages of this procedure is clear. Rather than solving three loop integrals with a complicated numerator structure, we just need to solve three MIs. Notice that using Feynman parametrization and the fact that $q \cdot u_1 = 0$, one can rewrite

$$G_{\underline{1},0,1,1} = \int_0^1 dz \int_\ell \frac{\delta(2\ell \cdot u_1)}{(\ell^2 - (-q^2)z(1-z))^2} = \int_0^1 dz I_{2,\underline{1}}(z). \quad (2.3.17)$$

Hence, imposing $s = (-q^2)z(1-z)$ we could use the IBP identities found earlier to solve this integral.

In practice, all these integrals can be solved using standard Feynman parametrization or equivalent methods [176]. However, we are going to describe another approach that turns out to be very efficient for more complicated higher-loop computations.

2.3.3 . Differential equations

In the following, we use the method of differential equations to solve the MIs obtained after the IBP reduction process. Introduced in [180–183], this method has been systematized in [184, 185]. The idea is the following: the Feynman loop integrals are functions of the external kinematic variables. Therefore we can write an appropriate differential equation by taking derivatives with respect to the external momenta.

To be concrete, let us consider the family of (uncut) Feynman integrals G_{n_1, n_2, n_3, n_4} defined in eq (2.3.13) in $d = 4 - 2\varepsilon$ dimensions. We consider the same kinematic that we have in the loop integrals (2.2.17), (2.2.20) and (2.2.21) i.e.

$$q \cdot u_1 = 0 = q \cdot u_2, \quad u_1 \cdot u_1 = 1 = u_2 \cdot u_2 \quad u_1 \cdot u_2 = \gamma. \quad (2.3.18)$$

Using once again LiteRed [177, 178], we find that all integrals of this family can be written as the linear combination of the following three MIs

$$f_1 \equiv G_{0,0,1,1}, \quad f_2 \equiv \sqrt{-q^2} G_{1,0,1,1}, \quad f_3 \equiv (-q^2) G_{1,1,1,1}. \quad (2.3.19)$$

Here we have multiplied them by an appropriate power of q^2 in order to make them dimensionless in four dimensions². Looking at eq. (2.3.18), we understand that q^2 is the only dimensionful external variable. Therefore we can fix its dependence in the MIs by dimensional analysis. The MIs are only non trivial functions of³ the Lorentz factor γ , and the dimensional regularization parameter ε . For instance, we can construct a differential equation for f_2 by taking its derivative with respect to γ , i.e.

$$\frac{df_2}{d\gamma} = \frac{\gamma u_1^\mu - u_2^\mu}{\gamma^2 - 1} \frac{\partial f_2}{\partial u_1^\mu} = -\frac{\sqrt{-q^2}}{\gamma^2 - 1} (G_{1,0,1,1} + G_{2,-1,1,1}). \quad (2.3.20)$$

The right-hand side of this equation can be IBP reduced to go back to an expression given in terms of the integrals of the basis (2.3.19), thus constructing a close system

²Note that, from eq. (2.3.18), q is space-like, therefore $-q^2 = |\mathbf{q}|^2$.

³Actually, another Lorentz invariant quantity is the sign of the zero component of the four-velocities $\text{Sign}(u_a^0)$, $a = 1, 2$. In what follows we shall always consider $u_a^0 > 0$. See [150] for a thorough discussion on this point.

of differential equations for f_1, f_2 and f_3 . To get rid of the square-roots that inevitably appear in the computations, it is convenient to introduce the (equivalent) kinematic variable x [112]

$$x \equiv \gamma - \sqrt{\gamma^2 - 1}, \quad \gamma = \frac{1 + x^2}{2x}, \quad \sqrt{\gamma^2 - 1} = \frac{1 - x^2}{2x}. \quad (2.3.21)$$

In this variable, the differential equations for the three MIs take the following form

$$\frac{d}{dx} \vec{f}(x, \varepsilon) = \begin{pmatrix} 0 & 0 & 0 \\ 0 & 0 & 0 \\ \frac{(2-4\varepsilon)}{x^2-1} & 0 & \frac{(x^2+1)}{x-x^3} \end{pmatrix} \vec{f}(x, \varepsilon), \quad \vec{f} = \begin{pmatrix} f_1 \\ f_2 \\ f_3 \end{pmatrix}, \quad (2.3.22)$$

The properties of Feynman integrals ensure that the above system has only regular singularities, i.e. it is a Fuchsian system of differential equations.

2.3.4 . Canonical basis and solution

The choice of the basis of MIs is clearly not unique. Is there a convenient basis in which the differential equations are simpler? The answer to this question is yes. In [184, 185], it has been shown that it is always possible to find a basis of MIs $\{g_1, g_2, g_3\}$ that satisfies the following canonical differential equation,

$$\frac{d}{dx} \vec{g}(x, \varepsilon) = \varepsilon A(x) \vec{g}(x, \varepsilon). \quad (2.3.23)$$

The advantages of reaching this form are evident. Indeed, not only the previous equation can actually be formally solved as a path-ordered exponential [184], but also, since one is ultimately interested in the solution at $\varepsilon = 0$, eq (2.3.23) can be more easily solved by performing a Laurent expansion in ε and truncate it at the desired order. In our example, the transformation between the basis \vec{f} and \vec{g} can be obtained with the help of the package Fuchsia [230, 231], implementing the Lee algorithm [232]. One eventually obtains

$$g_1 \equiv \frac{2\varepsilon - 1}{\varepsilon} G_{0,0,1,1}, \quad g_2 \equiv \sqrt{-q^2} G_{1,0,1,1}, \quad g_3 \equiv (-q^2) \sqrt{\gamma^2 - 1} G_{1,1,1,1}. \quad (2.3.24)$$

These integrals satisfy an equation of the form (2.3.23), where

$$A(x) = \frac{1}{x} \begin{pmatrix} 0 & 0 & 0 \\ 0 & 0 & 0 \\ 1 & 0 & 0 \end{pmatrix}. \quad (2.3.25)$$

A solution to this equation can be found trivially, but here we are going to follow a procedure that will be necessary for the computations in the next chapters. As we mentioned before, a solution to (2.3.23) can be found as Laurent series in $\varepsilon = 0$. Therefore, let us expand the MIs as follows,

$$\vec{g}(\varepsilon, x) = \frac{1}{(-q^2)^\varepsilon} \sum_k \vec{g}^{(k)}(x) \varepsilon^k, \quad (2.3.26)$$

where we have isolated a factor of $(-q^2)^\varepsilon$ coming from the dimensional analysis of the MIs in $d = 4 - 2\varepsilon$ dimensions. By inserting this expansion in (2.3.23), we get

$$\frac{d}{dx} \vec{g}^{(k)}(x) = \frac{1}{x} \begin{pmatrix} 0 & 0 & 0 \\ 0 & 0 & 0 \\ 1 & 0 & 0 \end{pmatrix} \vec{g}^{(k-1)}(x). \quad (2.3.27)$$

We then understand that we can solve the differential equation order-by-order in ε , and truncate this process once we have reached the desired precision.

To fix the final solution for the MIs, we still miss their boundary conditions. One can either study the analytic properties of the MIs [121, 184, 185], or solve the MIs in a particular physical limit. In this simple example, we use the value of the integrals in the static limit $\gamma \rightarrow 1$ (or equivalently $x \rightarrow 1$). The one-loop integrals \vec{g} can be easily solved following standard procedures, see e.g. [176]. One eventually obtains

$$g_1|_{x \rightarrow 1} = \frac{1}{(-q^2)^\varepsilon} \frac{i}{(4\pi)^{2-\varepsilon}} \frac{2\varepsilon - 1}{\varepsilon} \frac{\Gamma(1-\varepsilon)^2 \Gamma(\varepsilon)}{\Gamma(2-2\varepsilon)}, \quad (2.3.28)$$

$$g_2|_{x \rightarrow 1} = -\frac{1}{(-q^2)^\varepsilon} \frac{i}{(4\pi)^{2-\varepsilon}} \frac{2^{2\varepsilon-1} \pi \Gamma(\frac{1}{2} + \varepsilon) \Gamma(\frac{1}{2} - \varepsilon)}{\Gamma(1-\varepsilon)}, \quad (2.3.29)$$

$$g_3|_{x \rightarrow 1} = \frac{1}{(-q^2)^\varepsilon} \frac{\pi}{(4\pi)^{2-\varepsilon}} \frac{\Gamma(-\varepsilon)^2 \Gamma(1+\varepsilon)}{2\Gamma(-2\varepsilon)}. \quad (2.3.30)$$

Expanding these boundary conditions around $\varepsilon = 0$, we see that $\vec{g}^{(k)}(x) = 0, \forall k < -2$. Moreover, from the structure of (2.3.25), we understand that g_1 and g_2 do not depend on γ (or x). Thus eqs. (2.3.28) and (2.3.29) are actually the exact solutions. The only non trivial solution is the one for g_3 , for which we find $g_3^{(k)}(x) = 0, \forall k < -1$, and

$$g_3^{(-1)} = -\frac{i}{16\pi^2} (\log(x) + i\pi) \quad g_3^{(0)} = i \frac{\gamma_E - \log(4\pi)}{16\pi^2} (\log(x) + i\pi), \quad (2.3.31)$$

plus higher order terms in ε . In the above expression, γ_E is the Euler-Mascheroni constant.

2.3.5 . Relating cut and uncut integrals

In the previous section, we have seen how to write a differential equation of the MIs of the family G_{n_1, n_2, n_3, n_4} . However, in the computation of $\Delta^{(2)} p_1^\mu$ after the IBP reduction process, we found MIs of this family but with delta functions, i.e. cut propagators, see eqs. (2.3.14), (2.3.15) and (2.3.16). Most of the time, uncut loop integrals are more easily solvable than cut ones. In this section, we introduce a tool that allows us to relate complicated cut integrals with their uncut version: the so-called Cutkosky rules. These were originally derived in [204] and later in [205] through Veltman's largest time equation (see also [227, 228]). Here, we shall briefly introduce them and give a useful example, leaving an explicit derivation in appendix A.

As a warm up example, let us consider the following scalar one-loop integral,

$$I_\square \equiv \int_\ell \frac{(-i)^4 i^4}{((p_1 + \ell - q/2)^2 - m_1^2) ((p_2 - \ell + q/2)^2 - m_2^2) \ell^2 (\ell - q)^2}, \quad (2.3.32)$$

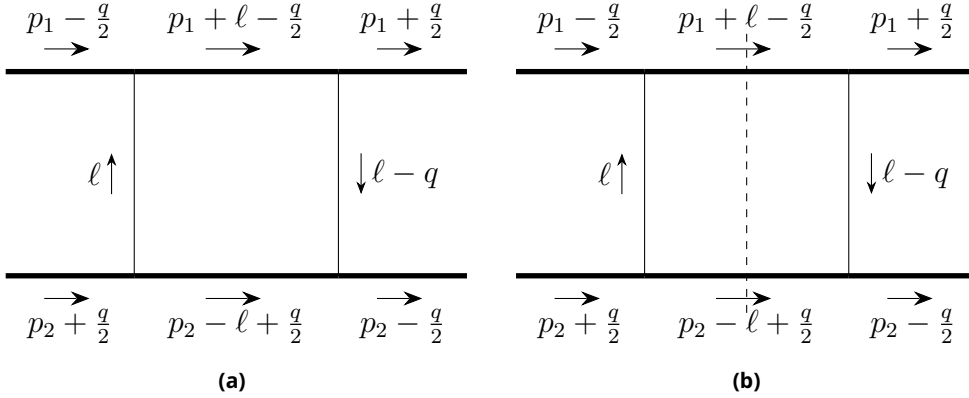


Figure 6: Feynman diagrams representing the integral (a) I_{\square} and (b) I_{\square} .

which describes two massive objects with incoming momenta $p_1^\mu - q^\mu/2$ and $p_2^\mu + q^\mu/2$ that interact by exchanging massless mediators with momenta ℓ^μ and $\ell^\mu - q^\mu$. It can be depicted as the diagram in figure 6 (a) where thick lines are massive scalar fields, while thin lines represent massless scalars. We also consider the external legs to be on-shell, e.g. $(p_1 - q/2)^2 = m_1^2$. To be more explicit, in eq (2.3.32) we have included the factors of $-i$ and i coming respectively from the vertices and the propagators. Once we have depicted the integral in this way, Cutkosky's cutting rules tell us how to relate the cut and uncut diagrams following these prescriptions:

- The sum of all cuts in a given channel is zero.
- All uncut propagators and vertices on the left-hand side of the cut are unaltered, while the ones on the right-hand side are replaced by the complex conjugate of their usual expressions.
- Cut propagators are replaced by on-shell delta functions.

The last rule means that, as we said already, a cut propagator is put on-shell, i.e. for a massive and a massless propagator we have respectively

$$\overline{\underset{|}{\underset{|}{\xrightarrow{k}}}}} = \delta_+(k^2 - m^2), \quad \overline{\underset{|}{\xrightarrow{k}}} = \delta_+(k^2). \quad (2.3.33)$$

Applying the last two rules, we can write the explicit expression of figure 6 (b)

$$I_{\square} \equiv \int_{\ell} \frac{\delta_+((p_1 + \ell - q/2)^2 - m_1^2) \delta_+((p_2 - \ell + q/2)^2 - m_2^2)}{\ell^2 (\ell - q)^2}. \quad (2.3.34)$$

Finally, the first rule tells us that the sum of all cuts in the s -channel of figure 6 (a) has to be zero. This translates in the following pictorial equation

$$\overline{\underset{|}{\underset{|}{\xrightarrow{k}}}}} + \overline{\underset{|}{\xrightarrow{k}}} + \overline{\underset{|}{\underset{|}{\xrightarrow{k}}}}} = 0. \quad (2.3.35)$$

It is straightforward to see that the first and the last diagrams of the above equation are respectively $(I_{\square})^*$ and I_{\square} , where the star denotes the complex conjugate. Therefore, from eq. (2.3.35) we can write

$$I_{\square} = -2\text{Re}(I_{\square}) . \quad (2.3.36)$$

We shall see in the next chapter some more non-trivial examples in which applying these rules is essential to find a solution for cut Feynman integrals.

At this point, however, we must explain how this discussion is related to the integrals we have considered so far, that, as we briefly mentioned in section 2.2, contain linearized propagators. The answer is that the integrals we obtained previously within our EFT set-up are an expanded version of I_{\square} and I_{\square} , in a sense that will be clear momentarily.

As we explained in sections 1.1 and 1.3, in order to take the classical limit, we need to consider the regime in which all the exchanged gravitons are *soft*, i.e. their momenta are small compared to the ones of the external bodies. Suppose now that we want to take the classical limit of I_{\square} . If we consider the external massive bodies to be on-shell, the incoming momenta scale as $|p_1^\mu| \sim m_1$ and $|p_2^\mu| \sim m_2$. It is straightforward to see that the fact that they are on-shell implies also that $q \cdot p_1 = 0 = q \cdot p_2$. Then, the soft or classical regime means that

$$|\ell^\mu| \sim q, \quad q \ll m_1, m_2 . \quad (2.3.37)$$

We can then expand the massive propagators in eq. (2.3.32) in q/m_a , for $a = 1, 2$ obtaining, at leading order,

$$I_{\square} = \int_{\ell} \frac{1}{(2\ell \cdot p_1)(-2\ell \cdot p_2)\ell^2(\ell - q)^2} + \dots . \quad (2.3.38)$$

If we now consider⁴ $p_1^\mu = m_1 u_1^\mu$ and $p_2^\mu = m_2 u_2^\mu$, then we see that

$$I_{\square} = \frac{1}{m_1 m_2} G_{1,1,1,1} + \dots , \quad (2.3.39)$$

which are exactly the family of integrals we obtained in our EFT computations, see eqs. (2.3.14), (2.3.15) and (2.3.16). This brief discussion is also an explicit example of what we said in the introduction: in the PM EFT approach one takes the classical limit from the beginning. Indeed, we landed directly on integrals of the form G_{n_1, n_2, n_3, n_4} which, as we have just explained, are a one-loop integral expanded in the classical regime. In order not to deviate too much from the subject of the chapter, we redirect the reader to [106, 110, 112, 115, 124] and references therein for a more thorough discussion on the method of regions, the soft-expansion and the connection with classical observables.

This expansion can be performed also in the case of cut propagators as in I_{\square} . Let us consider for example the cut propagator for p_2 . In the regime defined by eq. (2.3.37), this can be expanded as follows,

$$\vartheta(p_2^0 - \ell^0) \delta((p_2 - \ell + q/2)^2 - m_2^2) \sim \frac{1}{m_2} \delta(-2\ell \cdot u_2) + \dots . \quad (2.3.40)$$

⁴To be precise for both $a = 1, 2$, $p_a^\mu = m_a u_a^\mu + \mathcal{O}(q^2)$ [112]. Here we ignore these extra terms, as they do not change the above discussion.

We dropped the positive energy condition because, being $p_2^0 \sim m_2 > 0$ and $\ell^0 \ll p_2^0$, it is automatically satisfied. Therefore

$$I_{\square} = \frac{1}{m_1 m_2} G_{\underline{1}, \underline{1}, 1, 1} + \dots \quad (2.3.41)$$

The crucial point is that the cutting rules we have previously described are non-perturbative relations between the integrals I_{\square} and I_{\square} . Therefore, they must be valid order-by-order in the soft expansion, which implies for example that

$$G_{\underline{1}, \underline{1}, 1, 1} = -2\text{Re}(G_{1, 1, 1, 1}) \quad (2.3.42)$$

Cut loop integrals are typically more complicated than their uncut version. Therefore, in chapter 4, to find the value of the MIs in the near-static limit, we shall first solve the non cut loop integrals and then relate their solution to the cut version employing the rules explained in this section.

2.4 . The $\mathcal{O}(G^2)$ impulse and deflection angle

Finally, we now exploit all the techniques explained in the previous sections to find an explicit solution for the $\mathcal{O}(G^2)$ impulse given in eq. (2.2.9), using the IBP-reduced expressions (2.3.14), (2.3.15) and (2.3.16).

For the transverse contribution $\mathcal{Q} \cdot \hat{b}$ we can use (2.2.19) and write

$$G_{\underline{1}, 0, 1, 1} = 2iG_{1, 0, 1, 1} = \frac{2i}{\sqrt{-q^2}} g_2, \quad (2.4.1)$$

where in the second equation we have applied the definition of g_2 as in eq. (2.3.24). Its solution is given in eq. (2.3.29). It is also easy to see that $G_{0, \underline{1}, 1, 1}$ is just g_2 in which one exchanges u_1^μ with u_2^μ . Since the final solution does not depend on the four-velocities, we conclude that $G_{\underline{1}, 0, 1, 1} = G_{0, \underline{1}, 1, 1}$. Inserting these solutions in (2.3.14) and taking $\varepsilon \rightarrow 0$, we finally find

$$\mathcal{Q}_1 \cdot \hat{b} = -\frac{3M}{128} (5\gamma^2 - 1) \frac{q \cdot \hat{b}}{\sqrt{-q^2}}. \quad (2.4.2)$$

Taking then eq. (2.2.10) and performing the Fourier transform of the above quantity using (2.1.10), we get

$$c_b = \frac{3\pi}{4} M \frac{5\gamma^2 - 1}{\sqrt{\gamma^2 - 1}} \frac{1}{b^2}. \quad (2.4.3)$$

For the longitudinal contributions, $\mathcal{Q}_1 \cdot u_1$ and $\mathcal{Q}_1 \cdot u_2$, we can use Cutkosky's rules; from eq. (2.3.42),

$$G_{\underline{1}, \underline{1}, 1, 1} = -2\text{Re}(G_{1, 1, 1, 1}) = -\frac{2}{(-q)^2 \sqrt{\gamma^2 - 1}} \text{Re}(g_3), \quad (2.4.4)$$

where g_3 is defined in eq. (2.3.24). Recalling the expansion in eq. (2.3.26) and the solution in eq. (2.3.31), we find that

$$\mathcal{Q}_1 \cdot u_1 = \frac{im_2 (2\gamma^2 - 1)^2}{32\pi^2 \sqrt{\gamma^2 - 1}} \left[-\frac{1}{\varepsilon} + \gamma_E - \log(4\pi) + \log(-q^2) \right], \quad (2.4.5)$$

and similarly for $\mathcal{Q}_1 \cdot u_2$. Notice that we have a seemingly divergent term in four dimension, i.e. when $\varepsilon \rightarrow 0$. However, once we insert this solution in (2.2.10), the first three terms in the above square brackets lead to the following Fourier transform

$$\int_q \delta(q \cdot u_1) \delta(q \cdot u_2) e^{iq \cdot b} = \frac{\delta^2(\mathbf{b})}{\sqrt{\gamma^2 - 1}}. \quad (2.4.6)$$

This represents a contact-term contribution, i.e. a case in which the impact parameter goes to zero and the two objects collide head-on. This is outside the regime of validity of our EFT because we are considering $b \gg GM$, see eq. (1.1.7). Therefore, we can safely discard it. Only the last term in eq. (2.4.5) contributes to the coefficient c_1 of the impulse (2.2.9), giving explicitly

$$c_1 = 2m_2 \frac{(2\gamma^2 - 1)^2}{\gamma^2 - 1} \frac{1}{b^2}. \quad (2.4.7)$$

Similarly, we obtain

$$c_2 = -2m_1 \frac{(2\gamma^2 - 1)^2}{\gamma^2 - 1} \frac{1}{b^2}. \quad (2.4.8)$$

Putting all together, we finally find

$$\Delta^{(2)} p_1^\mu = \frac{G^2 M^3 \nu}{b^2} \left[-\frac{3\pi}{4} \frac{5\gamma^2 - 1}{\sqrt{\gamma^2 - 1}} \hat{b}^\mu + 2 \frac{(2\gamma^2 - 1)^2}{\gamma^2 - 1} \left(\frac{m_2}{M} \check{u}_1 - \frac{m_1}{M} \check{u}_2 \right) \right], \quad (2.4.9)$$

which agrees with results in the literature [118, 149].

Since the system is conservative, we can use eq. (1.4.20) to compute the $\mathcal{O}(G^2)$ deflection angle, obtaining

$$\frac{\chi_b^{(2)}}{\Gamma} = \frac{3\pi}{8} \frac{5\gamma^2 - 1}{\gamma^2 - 1}, \quad (2.4.10)$$

Once again, we find agreement with previously known results [76, 118, 149].

2.5 . Summary of the chapter

All the steps that we have outlined in this chapter can be applied systematically in the PM EFT approach, at every order in the perturbative expansion. In general, in order to compute any observable in our EFT we can follow the steps that are sketched in figure 7.

First we recast the problem as a cut loop integral by making a suitable change of variables, as we saw in section 2.2. Once that done, we can use reverse unitarity and apply IBP identities as explained in section 2.3.1. This step greatly simplify the task of

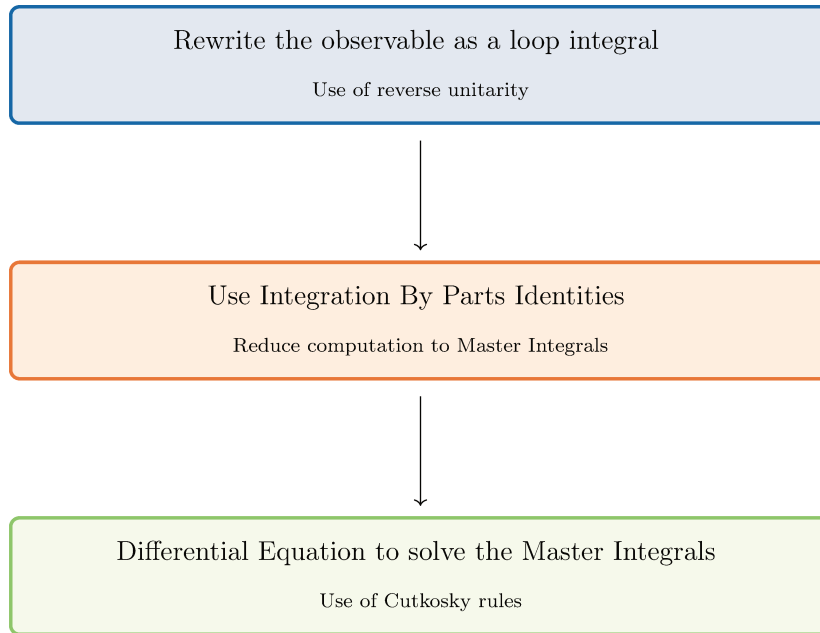


Figure 7: Schematic roadmap use to compute observables in the PM EFT.

solving the aforementioned loop integral, reducing the problem to just a set of MIs. As we saw in sections 2.3.3 and 2.3.4, we can efficiently solve these MIs by writing a (canonical) differential equation, for which the solution is known. The only unknowns at this point are the boundary conditions for this differential equation, i.e. the value of the MIs in a particular point. In this dissertation, we shall always use the value of the MIs in the near static limit as boundary conditions. In order to find these, we can first solve the simpler non-cut version of the integrals, and then relate the results to the cut ones using the cutting rules introduced in section 2.3.5.

We shall see an explicit step-by-step application of this roadmap in chapter 4, where we will compute the LO radiated four-momentum emitted by a binary system of point-particles.

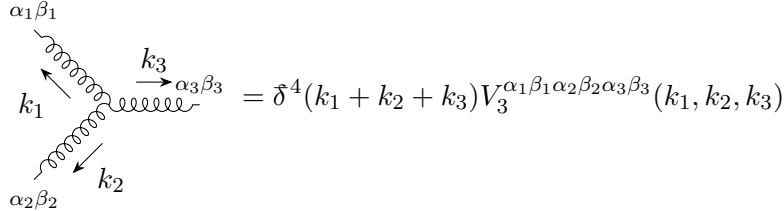
3 - Stress-energy tensor and Waveform

In this chapter we shall see explicitly how the PM EFT illustrated so far works in the radiative sector. In particular, following the discussion in section 1.3.2, we implement the matching procedure of eq. (1.3.19) to obtain the $\mathcal{O}(G)$ conserved pseudo stress energy tensor [146, 206, 207]. This result can then be used to compute the classical probability amplitude defined in eq. (1.4.11) [206] or, equivalently, the asymptotic emitted waveform at $\mathcal{O}(G^{3/2})$ [82, 163, 206]. We shall finally see how, as of today and to the best of our knowledge, the integrals appearing in the computation of the amplitude cannot be solved in terms of known analytic functions, leading to even more complicated integrals in the computation of the emitted momentum, see eq. (1.4.13). We will show how to solve this problem in the next chapter.

3.1 . Explicit Feynman rules

Let us first consider the gravitational sector of the effective action. All the Feynman rules we need for the following computations are actually written in section 1.3. We redisplay them here for convenience:

$$\text{wavy line }^{\mu\nu} \xrightarrow{k} \text{wavy line }^{\rho\sigma} = \frac{i}{k^2} P_{\mu\nu\rho\sigma}, \quad P_{\mu\nu\rho\sigma} = \eta_{\mu(\rho}\eta_{\sigma)\nu} - \frac{1}{2}\eta_{\mu\nu}\eta_{\rho\sigma}, \quad (3.1.1)$$



$$\text{Diagram} = \delta^4(k_1 + k_2 + k_3) V_3^{\alpha_1 \beta_1 \alpha_2 \beta_2 \alpha_3 \beta_3}(k_1, k_2, k_3). \quad (3.1.2)$$

Recall that we are working in De Donder gauge, see eq. (1.3.7). Due to its length, the cubic vertex tensorial structure is displayed in appendix C. $V_3^{\alpha_1 \beta_1 \alpha_2 \beta_2 \alpha_3 \beta_3}$ is bilinear in the momenta, symmetric in α_a and β_a , for $a = 1, 2, 3$, and symmetric in the exchange of $(p_1, \alpha_1 \beta_1)$, $(p_2, \alpha_2 \beta_2)$ and $(p_3, \alpha_3 \beta_3)$.

In the previous chapter we also saw that, by using the linear parametrization of the point-particle action (1.3.1), we have only one way of sourcing the gravitational field, that we rewrite here for convenience,

$$\text{wavy line }^{\tau_a} \xrightarrow{k} \text{wavy line }^{\mu\nu} = -\frac{im_a}{2m_{\text{Pl}}} \int d\tau_a e^{ik \cdot x_a(\tau_a)} \mathcal{U}_a^\mu \mathcal{U}_a^\nu, \quad (3.1.3)$$

with $a = 1, 2$. However, as in the computation of the impulse in section 1.4.1, we need to completely isolate the powers of the Newton constant G ; therefore, we perform the usual expansion of the trajectories and four-velocities around straight motion, see eqs. (1.4.7) and (1.4.8). In practice, plugging these expressions in eq. (3.1.3) results in having a

tower of Feynman rules, each of which has a definite power of G . In what follows we shall need the LO Feynman rule,

$$\begin{array}{c} \tau_a \\ \bullet \end{array} \begin{array}{c} \nearrow k \\ \mu\nu \\ \searrow \end{array} = -\frac{im_a}{2m_{\text{Pl}}} u_a^\mu u_a^\nu \int d\tau_a e^{ik \cdot (b_a + u_a \tau_a)}, \quad (3.1.4)$$

which describes a particle moving freely and sourcing the gravitational field, and the NLO rule

$$\begin{array}{c} \tau_a \\ \bullet \end{array} \begin{array}{c} \nearrow k \\ \mu\nu \\ \searrow \end{array} = -\frac{im_a}{2m_{\text{Pl}}} \int d\tau_a e^{ik \cdot (b_a + u_a \tau_a)} \left(2\delta^{(1)} u_a^{(\mu}(\tau_a) u_a^{\nu)} + i(k \cdot \delta^{(1)} x_a(\tau_a)) u_a^\mu u_a^\nu \right). \quad (3.1.5)$$

The meaning of the above picture is this: the gravitational interaction bends the trajectory of body a which then emits a graviton with momentum k^μ .

With the above Feynman rules, we can rewrite the matching procedure presented in section 1.3.2 up to order G explicitly as

$$\frac{P_{\mu\nu\rho\sigma}}{k^2} \frac{\tilde{T}^{\rho\sigma}(k)}{2m_{\text{Pl}}} = \begin{array}{c} 1 \\ \bullet \end{array} \begin{array}{c} \nearrow k \\ \mu\nu \\ \searrow \end{array} + \begin{array}{c} \nearrow k \\ \mu\nu \\ \searrow \\ 2 \\ \bullet \end{array} + \begin{array}{c} 1 \\ \bullet \end{array} \begin{array}{c} \nearrow k \\ \mu\nu \\ \searrow \\ 2 \\ \bullet \end{array} + \begin{array}{c} 1 \\ \bullet \end{array} \begin{array}{c} \nearrow k \\ \mu\nu \\ \searrow \\ 2 \\ \bullet \end{array} + \begin{array}{c} 1 \\ \bullet \end{array} \begin{array}{c} \nearrow k \\ \mu\nu \\ \searrow \\ 2 \\ \bullet \end{array}. \quad (3.1.6)$$

We compute each of these diagrams in the next section.

3.2 . Stress-energy tensor at order $O(G)$

At leading order in G , particles move along straight trajectories, generating a static term. Using the Feynman rule written in eq. (3.1.4), for body 1 we have

$$\begin{array}{c} 1 \\ \bullet \end{array} \begin{array}{c} \nearrow k \\ \mu\nu \\ \searrow \end{array} = \frac{m_1}{2m_{\text{Pl}}} u_1^\rho u_1^\sigma \delta(k \cdot u_1) e^{ik \cdot b_1} \frac{P_{\rho\sigma\mu\nu}}{k^2}. \quad (3.2.1)$$

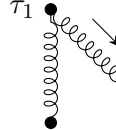
Therefore, adding the symmetric contribution, we immediately find that

$$\tilde{T}_{\text{LO}}^{\mu\nu}(k) = \sum_a m_a u_a^\mu u_a^\nu e^{ik \cdot b_a} \delta(k \cdot u_a). \quad (3.2.2)$$

The non-radiating nature of this piece is manifest by the presence of the delta function $\delta(k \cdot u_a)$. Indeed, a massless vector k^μ cannot be at the same time on-shell and orthogonal to a time-like vector such as u_a^μ .

At the next order, the stress-energy tensor $\tilde{T}_{\text{NLO}}^{\mu\nu}$ is given by the sum of the last three contributions of eq. (3.2.1). The first one is obtained when the worldline of the first

body is deflected by the second one. Using the rule (3.1.5), we obtain



$$\mu\nu = \frac{m_1}{2m_{\text{Pl}}} \int d\tau_1 e^{ik \cdot b_1 + k \cdot u_1 \tau_1} \left(2\delta^{(1)} u_1^{(\rho}(\tau_1) u_1^{\sigma)} + i(k \cdot \delta^{(1)} x_1(\tau_1)) u_1^\rho u_1^\sigma \right) \frac{P_{\rho\sigma\mu\nu}}{k^2}. \quad (3.2.3)$$

The second term contributing to $\tilde{T}_{\text{NLO}}^{\mu\nu}$ is analogous to the first one, with the roles of the two bodies exchanged. Defining for convenience

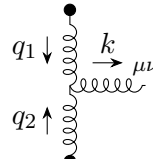
$$\mu_{1,2}(k) \equiv e^{i(q_1 \cdot b_1 + q_2 \cdot b_2)} \delta^4(k - q_1 - q_2) \delta(q_1 \cdot u_1) \delta(q_2 \cdot u_2), \quad (3.2.4)$$

one explicitly gets

$$\tilde{T}_{\uparrow}^{\mu\nu}(k) = \frac{m_1 m_2}{4m_{\text{Pl}}^2} \int_{q_1, q_2} \mu_{1,2}(k) \frac{1}{q_1^2 q_2^2} \left\{ \frac{2\gamma^2 - 1}{k \cdot u_1} q_2^{(\mu} u_1^{\nu)} - 4\gamma u_1^{(\mu} u_2^{\nu)} - \left[\frac{2\gamma^2 - 1}{2} \frac{k \cdot q_2}{(k \cdot u_1)^2} - 2\gamma \frac{k \cdot u_2}{k \cdot u_1} - 1 \right] u_1^\mu u_1^\nu \right\}, \quad (3.2.5)$$

$$\tilde{T}_{\downarrow}^{\mu\nu}(k) = \tilde{T}_{\uparrow}^{\mu\nu}(k)|_{1 \leftrightarrow 2}. \quad (3.2.6)$$

The last piece involves the cubic gravitational vertex and comes from evaluating the following diagram,



$$q_1 \downarrow \quad q_2 \uparrow \quad \mu\nu = -\frac{m_1 m_2}{4m_{\text{Pl}}^3} \int_{q_1, q_2} \delta(q_1 \cdot u_1) \delta(q_2 \cdot u_2) \delta^4(q_1 + q_2 - k) \frac{e^{iq_1 \cdot b_1 + iq_2 \cdot b_2}}{q_1^2 q_2^2} \times u_1^\alpha u_1^\beta P_{\alpha\beta\alpha_1\beta_1} u_2^\rho u_2^\sigma P_{\rho\sigma\alpha_2\beta_2} V_3^{\alpha_1\beta_1\alpha_2\beta_2\alpha_3\beta_3} \frac{P_{\alpha_3\beta_3\mu\nu}}{k^2}. \quad (3.2.7)$$

Performing the matching procedure one last time results in

$$\begin{aligned} \tilde{T}_{\uparrow}^{\mu\nu}(k) = & \frac{m_1 m_2}{4m_{\text{Pl}}^2} \int_{q_1, q_2} \mu_{1,2}(k) \frac{1}{q_1^2 q_2^2} \left\{ \frac{2\gamma^2 - 1}{2} (q_1^\mu q_1^\nu + q_2^\mu q_2^\nu + k^\mu k^\nu) + 4\gamma (k \cdot u_2) q_2^{(\mu} u_1^{\nu)} \right. \\ & + 2 \left((k \cdot u_2)^2 - \frac{k^2 + q_1^2}{2} \right) u_1^\mu u_1^\nu + 2 \left((k \cdot u_1)^2 - \frac{k^2 + q_2^2}{2} \right) u_2^\mu u_2^\nu \\ & - \eta^{\mu\nu} \left[(k \cdot u_1)^2 + (k \cdot u_2)^2 - 2\gamma (k \cdot u_1)(k \cdot u_2) + \frac{2\gamma^2 - 1}{4} (3k^2 + q_1^2 + q_2^2) \right] \\ & + 2 [\gamma (q_1^2 + q_2^2 + k^2) - 2(k \cdot u_1)(k \cdot u_2)] u_1^{(\mu} u_2^{\nu)} + 4\gamma (k \cdot u_1) q_1^{(\mu} u_2^{\nu)} \\ & \left. + 4 \left(\frac{k \cdot u_1}{2} - \gamma k \cdot u_2 \right) k^{(\mu} u_1^{\nu)} + 4 \left(\frac{k \cdot u_2}{2} - \gamma k \cdot u_1 \right) k^{(\mu} u_2^{\nu)} \right\}. \quad (3.2.8) \end{aligned}$$

Note that this separation in three contributions is only for convenience and depends on the chosen gauge. It can be verified that the total NLO stress-energy tensor is conserved, i.e. for any momentum k^μ of the external graviton

$$k_\mu \left(\tilde{T}_\top^{\mu\nu}(k) + \tilde{T}_\perp^{\mu\nu}(k) + \tilde{T}_+^{\mu\nu}(k) \right) = 0. \quad (3.2.9)$$

For the computations we do in the next part of this work, we only need this pseudo stress-energy tensor evaluated on-shell, i.e. for $k^2 = 0$. Imposing this, using momentum conservation as well as harmonic gauge conditions, i.e. for any four-vector vector w^ν one has $k^\mu w^\nu = (k \cdot w/2)\eta^{\mu\nu}$, we can simplify its final expression to

$$\begin{aligned} \tilde{T}_{\text{NLO}}^{\mu\nu}(k) = \frac{m_1 m_2}{4m_{\text{Pl}}^2} \int_q \delta(q \cdot u_1) \delta(q \cdot u_2 - k \cdot u_2) \frac{e^{iq \cdot b} e^{ik \cdot b_2}}{q^2 (q - k)^2} \\ \times [t_\top^{\mu\nu}(q, k) + t_\perp^{\mu\nu}(q, k) + t_+^{\mu\nu}(q, k)], \end{aligned} \quad (3.2.10)$$

where $t_\top^{\mu\nu}$, $t_\perp^{\mu\nu}$ and $t_+^{\mu\nu}$ are explicitly given by

$$\begin{aligned} t_\top^{\mu\nu}(q, k) \equiv q^2 \left\{ \frac{2\gamma^2 - 1}{k \cdot u_1} (k - q)^{(\mu} u_1^{\nu)} - 4\gamma u_1^{(\mu} u_2^{\nu)} \right. \\ \left. + \left[\frac{2\gamma^2 - 1}{2} \frac{k \cdot q}{(k \cdot u_1)^2} + 2\gamma \frac{k \cdot u_2}{k \cdot u_1} + 1 \right] u_1^\mu u_1^\nu \right\}, \end{aligned} \quad (3.2.11)$$

$$\begin{aligned} t_\perp^{\mu\nu}(q, k) \equiv (k - q)^2 \left\{ \frac{2\gamma^2 - 1}{k \cdot u_2} q^{(\mu} u_2^{\nu)} - 4\gamma u_2^{(\mu} u_1^{\nu)} \right. \\ \left. - \left[\frac{2\gamma^2 - 1}{2} \frac{k \cdot q}{(k \cdot u_2)^2} - 2\gamma \frac{k \cdot u_1}{k \cdot u_2} - 1 \right] u_2^\mu u_2^\nu \right\}, \end{aligned} \quad (3.2.12)$$

$$\begin{aligned} t_+^{\mu\nu}(q, k) \equiv \frac{2\gamma^2 - 1}{2} \left[k^\mu k^\nu - 2k^{(\mu} q^{\nu)} + 2q^\mu q^\nu \right] + \left[2(k \cdot u_2)^2 - q^2 \right] u_1^\mu u_1^\nu \\ + \left[2(k \cdot u_1)^2 - (k - q)^2 \right] u_2^\mu u_2^\nu + 4\gamma(k \cdot u_2)(k - q)^{(\mu} u_1^{\nu)} \\ + 4\gamma(k \cdot u_1)q^{(\mu} u_2^{\nu)} - \eta^{\mu\nu} \left[2\gamma(k \cdot u_1)(k \cdot u_2) + \frac{2\gamma^2 - 1}{4} ((k - q)^2 + q^2) \right] \\ + 2 \left[\gamma((k - q)^2 + q^2) - 2(k \cdot u_1)(k \cdot u_2) \right] u_1^{(\mu} u_2^{\nu)}. \end{aligned} \quad (3.2.13)$$

Here we have integrated over q_2 so that the integration in eq. (3.2.10) is over the momentum of the graviton exchanged by the two bodies. One can verify that the total stress-energy tensor in eq. (3.2.10) is transverse only for on-shell momenta. The two delta functions arise from the fact that we are taking the two bodies as non-propagating external sources. Note that similar integrals and delta functions appear when taking the classical limit of quantum observables in the scattering process between two massive particles. In this case, the integration variable q is the difference between the momentum within the wavefunction and that in its conjugate (the so-called momentum mismatch [115]) while the delta functions arise from the on-shell constraints on the momenta of the scattering particles.

Finally, we stress that we have left implicit all the $i0^+$ prescriptions in the denominators appearing either from the graviton propagator to specify the contour of integration in the complex k^0 plane or from the corrections to the straight motion of the two bodies, see eqs. (2.1.3) and (2.1.4). Concerning the gravitons, in order to take into account only outgoing radiation one should impose retarded boundary conditions¹, e.g. $[(q^0 + i0^+)^2 - |\mathbf{q}|^2]^{-1}$. In our case, however, these prescriptions are irrelevant because, as displayed by eq. (3.2.10), the two delta functions ensure that the momenta q^μ and $q^\mu - k^\mu$ are orthogonal to one of the two four-velocities. Thus, these two momenta can hit the pole only in the trivial case $q^\mu - k^\mu = 0 = q^\mu$. This means that at this order the only graviton that can be on-shell is the external one with momentum k^μ .

Similarly, all the matter linear propagators $[k \cdot u_a]^{-1}$ in eqs. (3.2.11) and (3.2.12) can hit the poles only if k is off-shell. In order to take into account possible static contributions at this order, one should consider the off-shell stress-energy tensor and insert back the $i0^+$ prescription. Comparing eqs. (3.2.5) and (3.2.6) with their on-shell versions (3.2.11) and (3.2.12), one sees that the dependence on $[k \cdot u_a]^{-1}$ does not change. Then we can take into account these static pieces by taking the on-shell $\tilde{T}^{\mu\nu}(k)$ with $[k \cdot u_a]^{-1} \rightarrow [k \cdot u_a + i0^+]^{-1}$ for $a = 1, 2$.

3.3 . Amplitude and Waveform at $O(G^{3/2})$

We can now compute the classical amplitude \mathcal{A}_λ perturbatively in G using eq. (1.4.11). The LO term is obtained from the static contribution in eq. (3.2.2),

$$\mathcal{A}_\lambda^{\text{LO}}(k) = - \sum_a \frac{m_a}{2m_{\text{Pl}}} \epsilon_{\mu\nu}^{\lambda*} u_a^\mu u_a^\nu e^{ik \cdot b_a} \delta(k \cdot u_a). \quad (3.3.1)$$

The NLO amplitude is of order $G^{3/2}$. Analogously to what we did for the stress-energy tensor in eq. (3.2.10), we can separate it in three pieces for convenience,

$$\mathcal{A}_\lambda^{\text{NLO}}(k) = - \frac{m_1 m_2}{8m_{\text{Pl}}^3} \left(\mathcal{A}_\lambda^{\text{R}}(k) + \mathcal{A}_\lambda^{\text{V}}(k) + \mathcal{A}_\lambda^{\text{T}}(k) \right), \quad (3.3.2)$$

where the labels refer to the contribution with the same name given in eqs. (3.2.11), (3.2.12) and (3.2.13). Introducing the following set of integrals,

$$I_{(n)}^{\mu_1 \dots \mu_n} \equiv \int_q \delta(q \cdot u_1 - k \cdot u_1) \delta(q \cdot u_2) \frac{e^{-iq \cdot b}}{q^2} q^{\mu_1} \dots q^{\mu_n}, \quad (3.3.3)$$

$$J_{(n)}^{\mu_1 \dots \mu_n} \equiv \int_q \delta(q \cdot u_1 - k \cdot u_1) \delta(q \cdot u_2) \frac{e^{-iq \cdot b}}{q^2 (k - q)^2} q^{\mu_1} \dots q^{\mu_n}, \quad (3.3.4)$$

¹For instance, radiation poles play a key role for hereditary effects at higher orders [233]. See also [150, 167].

we have explicitly that

$$\mathcal{A}_\lambda^\dagger(k) = \epsilon_{\mu\nu}^{\lambda*} \left\{ - \left[\frac{2\gamma^2 - 1}{2} \frac{k \cdot I_{(1)}}{(k \cdot u_1 + i0^+)^2} - \left(2\gamma \frac{k \cdot u_2}{k \cdot u_1 + i0^+} + 1 \right) I_{(0)} \right] u_1^\mu u_1^\nu \right. \\ \left. + \frac{2\gamma^2 - 1}{k \cdot u_1 + i0^+} I_{(1)}^\mu u_1^\nu - 4I_{(0)} \gamma u_1^\mu u_2^\nu \right\} e^{ik \cdot b_1}, \quad (3.3.5)$$

$$\mathcal{A}_\lambda^\vee(k) = \mathcal{A}_\lambda^\dagger(k)|_{1 \leftrightarrow 2}, \quad (3.3.6)$$

$$\mathcal{A}_\lambda^\dagger(k) = \epsilon_{\mu\nu}^{\lambda*} \left\{ \frac{2\gamma^2 - 1}{2} J_{(2)}^{\mu\nu} + (2(k \cdot u_2)^2 J_{(0)} - I_{(0)}) u_1^\mu u_1^\nu \right. \\ \left. - \eta^{\mu\nu} \left[\gamma(k \cdot u_1)(k \cdot u_2) J_{(0)} + \frac{2\gamma^2 - 1}{4} I_{(0)} \right] + 4\gamma k \cdot u_2 J_{(1)}^\mu u_1^\nu \right. \\ \left. + 2 [\gamma I_{(0)} - (k \cdot u_1)(k \cdot u_2) J_{(0)}] u_1^\mu u_2^\nu \right\} e^{ik \cdot b_1} + (1 \leftrightarrow 2). \quad (3.3.7)$$

We stress that in eqs. (3.3.6) and (3.3.7) one needs to exchange the label $1 \leftrightarrow 2$ also inside the definitions of $I_{(n)}^{\mu_1 \dots \mu_n}$ and $J_{(n)}^{\mu_1 \dots \mu_n}$. At this point, we are left with solving the integrals in eqs. (3.3.3) and (3.3.4). As we shall see, for the set $I_{(n)}^{\mu_1 \dots \mu_n}$ it is possible to find an analytic solution in terms on known functions while for the set $J_{(n)}^{\mu_1 \dots \mu_n}$ the best we can do is to write them as one-dimensional integrals over a Feynman parameter [110,206].

3.3.1 . Integrals involved in the amplitude

Let us start with the scalar integral $I_{(0)}$. Since the final result will be in terms of Lorentz invariants, we can solve this integral in a particular frame. It is convenient to pick the frame in which one of the two bodies, say body 2, is at rest, i.e.

$$u_2^\mu = \delta_0^\mu, \quad u_1^\mu = \gamma v^\mu = (\gamma, \sqrt{\gamma^2 - 1} \mathbf{e}_v), \\ b_2^\mu = 0, \quad b_1^\mu = b^\mu = (0, b \mathbf{e}_b). \quad (3.3.8)$$

Solving the two delta functions, we reduce $I_{(0)}$ to a two-dimensional integral over the components \mathbf{q}_\perp that lie on the plane perpendicular to the direction of the scattering bodies. Hence

$$I_{(0)} = - \frac{1}{\sqrt{\gamma^2 - 1}} \int \frac{d^2 \mathbf{q}_\perp}{(2\pi)^2} \frac{e^{i \mathbf{q}_\perp \cdot \mathbf{b}}}{\mathbf{q}_\perp^2 + \frac{(k \cdot u_1)^2}{\gamma^2 - 1}} \\ = - \frac{1}{\sqrt{\gamma^2 - 1}} \int_0^\infty dt \int \frac{d^2 \mathbf{q}_\perp}{(2\pi)^2} \exp \left[-t \mathbf{q}_\perp^2 + i \mathbf{q}_\perp \cdot \mathbf{b} - t \frac{(k \cdot u_1)^2}{\gamma^2 - 1} \right], \quad (3.3.9)$$

where in the second step we introduced a Schwinger parameter t . Solving the Gaussian integral in \mathbf{q}_\perp eventually gives the final result, i.e.

$$I_{(0)} = - \frac{1}{4\pi \sqrt{\gamma^2 - 1}} \int_0^\infty dt \frac{1}{t} \exp \left[-\frac{b^2}{4t} - t \frac{(k \cdot u_1)^2}{\gamma^2 - 1} \right] \\ = - \frac{K_0(z_1)}{2\pi \sqrt{\gamma^2 - 1}}, \quad (3.3.10)$$

where K_n are modified Bessel functions of the second kind and we defined

$$z_a \equiv \frac{\sqrt{-b^2}(k \cdot u_a)}{\sqrt{\gamma^2 - 1}}, \quad a = 1, 2. \quad (3.3.11)$$

Once the scalar integral is solved, the vectorial $I_{(1)}^\mu$ can be computed decomposing it on a complete basis, i.e.

$$I_{(1)}^\mu = A_b b^\mu + A_u (u_1^\mu - \gamma u_2^\mu), \quad (3.3.12)$$

where the dependence on the combination $u_1^\mu - \gamma u_2^\mu$ comes from the fact that $u_2 \cdot I_{(1)} = 0$. Contracting both sides with b^μ and u_1^μ , one eventually obtains

$$\begin{aligned} A_b &= \frac{b \cdot I_{(1)}}{b^2} = \frac{i b^\mu \partial I_{(0)}}{b^2 \partial b^\mu} = -\frac{i}{2\pi \sqrt{\gamma^2 - 1}} \frac{z_1 K_1(z_1)}{|b^2|}, \\ A_u &= -\frac{u_1 \cdot I_{(1)}}{\gamma^2 - 1} = -\frac{k \cdot u_1}{\gamma^2 - 1} I_{(0)} = \frac{k \cdot u_1}{2\pi(\gamma^2 - 1)^{3/2}} K_0(z_1). \end{aligned} \quad (3.3.13)$$

Finally, we need to comment about contributions that appear in the amplitude as $I_{(n)}^{\mu_1 \dots \mu_n} / (k \cdot u_1 + i0^+)$, with $n = 1, 2$. These can be rewritten as

$$\frac{I_{(n)}^{\mu_1 \dots \mu_n}}{(k \cdot u_1 + i0^+)} = \text{P} \left(\frac{I_{(n)}^{\mu_1 \dots \mu_n}}{k \cdot u_1} \right) - i\pi I_{(n)}^{\mu_1 \dots \mu_n} \delta(k \cdot u_1). \quad (3.3.14)$$

where P denote the principal value. The first term of the previous equation gives the solutions we have found before, i.e. eqs. (3.3.10) and (3.3.13), while the second contributes to the amplitude as

$$i\pi \delta(k \cdot u_1) I_{(n)}^{\mu_1 \dots \mu_n} = i\pi \delta(k \cdot u_1) \int_q \delta(q \cdot u_1) (q \cdot u_2) \frac{e^{-iq \cdot b}}{q^2} q^{\mu_1 - 1} \dots q^{\mu_n}. \quad (3.3.15)$$

For this computation we need

$$i\pi \delta(k \cdot u_1) I_{(0)} = 0, \quad (3.3.16)$$

$$i\pi \delta(k \cdot u_1) I_{(1)}^\mu = i\pi \delta(k \cdot u_1) \frac{b^\mu}{2\pi \gamma v b^2}. \quad (3.3.17)$$

The last equation is again a static piece that we include for completeness.

The second set of integrals, defined in eq. (3.3.4), is more involved due to the presence of a second massless propagator. These integrals appear only in the contributions coming from the self-interaction term $t_+^{\mu\nu}$ of eq. (3.2.13), which means that we do not get any possible static contribution coming from $k \cdot u_a + i0^+$. Therefore we can always safely set $k^2 = 0$. We first solve again the scalar integral $J_{(0)}$, and use Feynman parametrization to rewrite it in terms of only one massless propagator,

$$\begin{aligned} J_{(0)} &= \int_0^1 dy \int_q \delta(q \cdot u_1 - k \cdot u_1) \delta(q \cdot u_2) \frac{e^{-iq \cdot b}}{(q - yk)^4} \\ &= \int_0^1 dy e^{-iyk \cdot b} \int_q \delta(q \cdot u_1 - (1-y)k \cdot u_1) \delta(q \cdot u_2 + yk \cdot u_2) \frac{e^{-iq \cdot b}}{q^4}. \end{aligned} \quad (3.3.18)$$

To get to the second line we have performed the shift $q^\mu \rightarrow q^\mu + yk^\mu$ and we have imposed $k^2 = 0$. At this point we can follow a procedure analogous to the one we used for $I_{(0)}$. Choosing again the frame (3.3.8), we use the two delta functions to reduce the computation to a two-dimensional integral over \mathbf{q}_\perp , that we can solve using Schwinger parametrization. This yields

$$J_{(0)} = \int_0^1 dy \frac{e^{-iyk \cdot b}}{\sqrt{\gamma^2 - 1}} \int_0^\infty dt t \int \frac{d^2 \mathbf{q}_\perp}{(2\pi)^2} \exp \left[-t \mathbf{q}_\perp^2 + i \mathbf{q}_\perp \cdot b - t \frac{s^2(y)}{\gamma^2 - 1} \right], \quad (3.3.19)$$

where we have defined

$$s(y) \equiv \sqrt{(1-y)^2(k \cdot u_1)^2 + 2\gamma y(1-y)(k \cdot u_1)(k \cdot u_2) + y^2(k \cdot u_2)^2}. \quad (3.3.20)$$

Notice that $s(y)$ changes when computing the symmetric contribution $1 \leftrightarrow 2$. At this point, the integral over \mathbf{q}_\perp in eq. (3.3.19) is Gaussian and can be easily solved,

$$J_{(0)} = \frac{\sqrt{-b^2}}{4\pi} \int_0^1 dy e^{-iyk \cdot b} \frac{K_1(w(y))}{s(y)}, \quad (3.3.21)$$

where we introduced the shorthand notation

$$w(y) \equiv \frac{\sqrt{-b^2} s(y)}{\sqrt{\gamma^2 - 1}}. \quad (3.3.22)$$

We can solve $J_{(1)}^\mu$ and $J_{(2)}^{\mu\nu}$ analogously to what we did for $I_{(1)}^\mu$ with the difference that, before decomposing on a complete basis as in eq. (3.3.12), we find it convenient to use again Feynman parametrization. For instance, for $J_{(1)}^\mu$ we have

$$J_{(1)}^\mu = \int_0^1 dy e^{-iyk \cdot b} \int_q \delta(q \cdot u_1 - (1-y)k \cdot u_1) \delta(q \cdot u_2 + yk \cdot u_2) \frac{e^{-iq \cdot b}}{q^4} (q^\mu + yk^\mu), \quad (3.3.23)$$

where we performed again the shift $q^\mu \rightarrow q^\mu + yk^\mu$. The contribution proportional to k^μ can be computed using the result of $J_{(0)}$, while the one proportional to q^μ must be decomposed on a complete basis. The very same procedure can be carried out for $J_{(2)}^{\mu\nu}$, yielding to

$$J_{(1)}^\mu = \int_0^1 dy e^{-iyk \cdot b} [B_b b^\mu + B_1 u_1^\mu + B_2 u_2^\mu], \quad (3.3.24)$$

$$J_{(2)}^{\mu\nu} = \int_0^1 dy e^{-iyk \cdot b} [C_\eta \eta^{\mu\nu} + C_b b^\mu b^\nu + C_1 b^{(\mu} u_1^{\nu)} + C_2 b^{(\mu} u_2^{\nu)} + C_3 u_1^{(\mu} u_2^{\nu)} + C_4 u_1^\mu u_1^\nu + C_5 u_2^\mu u_2^\nu], \quad (3.3.25)$$

where we omitted terms proportional to k^μ . As we shall see in the next section, these terms are actually irrelevant for the final computation of the amplitude.

To find the coefficients B_i in eq. (3.3.24) we must solve

$$\begin{aligned} B_b &= \frac{ib^\mu}{b^2} \frac{\partial J_{(0)}}{\partial b^\mu}, & B_1 &= \frac{(y-1)k \cdot u_1 - y\gamma k \cdot u_2}{\gamma^2 - 1} J_{(0)}, \\ B_2 &= \frac{yk \cdot u_2 - (y-1)\gamma k \cdot u_1}{\gamma^2 - 1} J_{(0)}. \end{aligned} \quad (3.3.26)$$

Using eq. (3.3.21), the solutions are

$$\begin{aligned} B_b &= \frac{i}{4\pi\sqrt{\gamma^2 - 1}} K_0(w(y)), \\ B_1 &= \frac{\sqrt{-b^2}}{4\pi(\gamma^2 - 1)} \frac{(y-1)k \cdot u_1 - y\gamma k \cdot u_2}{s(y)} K_1(w(y)), \\ B_2 &= \frac{\sqrt{-b^2}}{4\pi(\gamma^2 - 1)} \frac{yk \cdot u_2 - (y-1)\gamma k \cdot u_1}{s(y)} K_1(w(y)). \end{aligned} \quad (3.3.27)$$

Then contracting eq. (3.3.25) with the tensor structure on the right-hand side, we obtain the following system for the C_i coefficients,

$$\begin{aligned} b^2 (C_\eta + C_b b^2) &= -b^\mu b^\nu \frac{\partial^2 J_{(0)}}{\partial b^\mu \partial b^\nu}, \\ \frac{b^2}{2} (\gamma C_1 + C_2) &= -b^2 yk \cdot u_2 B_b, \\ \frac{b^2}{2} (C_1 + \gamma C_2) &= -b^2 (y-1)k \cdot u_1 B_b, \\ C_\eta + \gamma C_3 + C_4 + \gamma^2 C_5 &= (y-1)^2 (k \cdot u_1)^2 J_{(0)}, \\ C_\eta + \gamma C_3 + \gamma^2 C_4 + C_5 &= y^2 (k \cdot u_2)^2 J_{(0)}, \\ \gamma C_\eta + \frac{C_3}{2} (\gamma^2 + 1) + \gamma (C_4 + C_5) &= (y-1)y (k \cdot u_1)(k \cdot u_2) J_{(0)}, \\ 4C_\eta + b^2 C_b + \gamma C_3 + C_4 + C_5 &= -\frac{1}{2\pi\sqrt{\gamma^2 - 1}} K_0(w(y)), \end{aligned} \quad (3.3.28)$$

where the right-hand side of the last equation can be computed following the same procedure we used to solve $J_{(0)}$, i.e.

$$\int_q \delta(q \cdot u_1 - (1-y)k \cdot u_1) \delta(q \cdot u_2 + yk \cdot u_2) \frac{e^{-iq \cdot b}}{q^2} = -\frac{1}{2\pi\sqrt{\gamma^2 - 1}} K_0(w(y)). \quad (3.3.29)$$

Solving the previous system, we finally obtain

$$\begin{aligned} C_\eta &= -\frac{1}{4\pi\sqrt{\gamma^2 - 1}} K_0(w(y)), \\ C_b &= -\frac{1}{4\pi(\gamma^2 - 1)} \frac{s(y)}{\sqrt{-b^2}} K_1(w(y)), \end{aligned} \quad (3.3.30)$$

$$\begin{aligned}
C_1 &= \frac{i}{2\pi(\gamma^2 - 1)} \frac{(y-1)k \cdot u_1 - y\gamma k \cdot u_2}{\sqrt{\gamma^2 - 1}} K_0(w(y)) , \\
C_2 &= \frac{i}{2\pi(\gamma^2 - 1)} \frac{yk \cdot u_2 - (y-1)\gamma k \cdot u_1}{\sqrt{\gamma^2 - 1}} K_0(w(y)) , \\
C_3 &= \frac{1}{2\pi(\gamma^2 - 1)^{3/2}} \left\{ \gamma K_0(w(y)) \right. \\
&\quad \left. - w(y)K_1(w(y)) \left[\gamma + \frac{(\gamma^2 - 1)}{s^2(y)} y(y-1)k \cdot u_1 k \cdot u_2 \right] \right\} , \\
C_4 &= \frac{1}{4\pi(\gamma^2 - 1)^{3/2}} \left\{ -K_0(w(y)) \right. \\
&\quad \left. + w(y)K_1(w(y)) \left[1 + \frac{(\gamma^2 - 1)}{s^2(y)} y^2(k \cdot u_2)^2 \right] \right\} , \\
C_5 &= \frac{1}{4\pi(\gamma^2 - 1)^{3/2}} \left\{ -K_0(w(y)) \right. \\
&\quad \left. + w(y)K_1(w(y)) \left[1 + \frac{(\gamma^2 - 1)}{s^2(y)} (y-1)^2(k \cdot u_1)^2 \right] \right\} .
\end{aligned} \tag{3.3.31}$$

These solutions completely determined the NLO amplitude defined in (3.3.2).

3.4 . Results in the rest frame of one of the body

The NLO amplitude takes a rather compact form if we consider the polarization tensor in the transverse-traceless (TT) gauge, i.e.,

$$\epsilon_{0\mu}^\lambda = 0 , \quad k^\nu \epsilon_{\mu\nu}^\lambda = 0 , \quad \epsilon_{\mu\nu}^\lambda \eta^{\mu\nu} = 0 , \tag{3.4.1}$$

and we choose again the frame defined in eq. (3.3.8). With this choice $\mathcal{A}_\lambda^k(k) = 0$ and all but one term in the symmetric contribution in eq. (3.3.7) drop. Finally, parametrizing the graviton four-momentum as $k^\mu = \omega n^\mu$, with $n^\mu = (1, \mathbf{n})$ the four-vector pointing along the direction of propagation of the graviton normalized as $\mathbf{n} \cdot \mathbf{n} = 1$, and defining

$$z \equiv \frac{\gamma b \omega}{\sqrt{\gamma^2 - 1}} , \quad f(y) \equiv \sqrt{(1-y)^2(n \cdot v)^2 + 2y(1-y)(n \cdot v) + y^2/\gamma^2} , \tag{3.4.2}$$

one can write the NLO amplitude in a compact form as

$$\mathcal{A}_\lambda^{\text{NLO}}(k) = -\frac{Gm_1m_2}{m_{\text{Pl}}\sqrt{\gamma^2 - 1}} \epsilon_{ij}^{*\lambda} e_I^i e_J^j A_{IJ}(k) e^{ik \cdot b} , \tag{3.4.3}$$

where $I, J = v, b$ and the coefficients A_{IJ} are explicitly given by [206]

$$A_{vv} = c_1 K_0(z(n \cdot v)) + ic_2 \left[K_1(z(n \cdot v)) - i\pi\delta(z(n \cdot v)) \right] + \int_0^1 dy e^{iy\mathbf{k} \cdot \mathbf{b}} \left[d_1(y) z K_1(zf(y)) + c_0 K_0(zf(y)) \right], \quad (3.4.4)$$

$$A_{vb} = ic_0 \left[K_1(z(n \cdot v)) - i\pi\delta(z(n \cdot v)) \right] + i \int_0^1 dy e^{iy\mathbf{k} \cdot \mathbf{b}} d_2(y) z K_0(zf(y)), \quad (3.4.5)$$

$$A_{bb} = \int_0^1 dy e^{iy\mathbf{k} \cdot \mathbf{b}} d_0(y) z K_1(zf(y)). \quad (3.4.6)$$

The coefficients c and d are

$$c_0 = 1 - 2\gamma^2, \quad c_1 = -c_0 + \frac{3 - 2\gamma^2}{n \cdot v}, \quad c_2 = \frac{\sqrt{\gamma^2 - 1}}{\gamma} c_0 \frac{\mathbf{n} \cdot \mathbf{e}_b}{n \cdot v},$$

$$d_0(y) = f(y)c_0, \quad (3.4.7)$$

$$d_1(y) = \frac{\gamma^2 - 1}{\gamma^2} \frac{4\gamma^2(y-1)(n \cdot v) - c_0(y-1)^2 - 2y - 1}{f(y)} - d_0(y),$$

$$d_2(y) = -1 + (1-y)c_0(n \cdot v - 1).$$

For small-velocities we find agreement between our amplitude and the waveform in Fourier space of Ref. [82]. In this limit $f(y) \rightarrow 1$, $e^{iy\mathbf{k} \cdot \mathbf{b}} \rightarrow 1$, $\gamma \rightarrow 1$, and thus²

$$A_{vv} \xrightarrow{v \rightarrow 0} zK_1(z) + K_0(z), \quad (3.4.8)$$

$$A_{vb} \xrightarrow{v \rightarrow 0} -i [K_1(z) + zK_0(z) - i\pi\delta(z)], \quad (3.4.9)$$

$$A_{bb} \xrightarrow{v \rightarrow 0} -zK_1(z). \quad (3.4.10)$$

We have also checked that we recover their amplitude in the forward and backward limit (i.e. \mathbf{n} along the direction of \mathbf{e}_v), for which $\mathbf{n} \cdot \mathbf{e}_b \rightarrow 0$ and the integral in y can be solved exactly.

3.4.1 . Asymptotic waveform in direct space

While it was not possible to find a solution in terms of analytic functions for the NLO amplitude, one can find an explicit expression for the NLO asymptotic waveform in direct space as shown in Ref. [163]. In terms of our classical amplitude, one can compute the waveform using eq. (1.4.12). Since we are interested in on-shell propagating degrees of freedom, we work again in the TT gauge (3.4.1). We can then split the computation as follows

$$h_{ij}(x) = \frac{1}{r} \left[\epsilon_{ij}^+ f_{\text{NLO}}^{(+)} + \epsilon_{ij}^- f_{\text{NLO}}^{(-)} \right] + \mathcal{O}(G^{5/2}). \quad (3.4.11)$$

where we have defined

$$f_{\text{NLO}}^{(\pm)} \equiv -\frac{1}{4\pi} \int \frac{d\omega}{2\pi} e^{-i\omega t_r} \mathcal{A}_{\pm}^{\text{NLO}}(k) \Big|_{k^\mu = \omega n^\mu}, \quad (3.4.12)$$

²The signs in front of K_0 and K_1 of the last term of eqs. (2.9b) and (2.9c) of [82] are opposite to ours because of a different convention in the definition of the Fourier Transform.

To simplify the computations, we work again in the rest frame of body 2 defined in eq. (3.3.8). Using the definitions given in eqs. (3.3.3) and (3.3.4) we have

$$\begin{aligned} \mathcal{A}_{\pm}^{\text{NLO}} = & -\frac{m_1 m_2}{8m_{\text{Pl}}^3} \epsilon_{ij}^{\pm*} e^{i\omega n \cdot b} \left[\left(\frac{2\gamma^2 - 1}{\gamma\omega n \cdot v + i0^+} I_{(1)}^i + 4\gamma\omega J_{(1)}^i \right) u_1^j + (2\gamma^2 - 1) J_{(2)}^{ij} \right. \\ & \left. + \left(\frac{1 - 2\gamma^2}{2} \frac{\omega n \cdot I_{(1)}}{(\gamma\omega n \cdot v + i0^+)^2} + \frac{2\gamma\omega}{\gamma\omega n \cdot v + i0^+} I_{(0)} + 2\omega^2 J_{(0)} \right) u_1^i u_1^j \right]. \end{aligned} \quad (3.4.13)$$

We need to solve essentially the following two sets of integrals

$$\int \frac{d\omega}{2\pi} \int_q I_{(n)}^{\mu_1 \dots \mu_n} \mathcal{F}(\omega) e^{-i\omega(t_r - n \cdot b)} = \int_q \delta(q^0) \mathcal{F}\left(\frac{q \cdot v}{n \cdot v}\right) \frac{e^{-iq \cdot \tilde{b}}}{q^2} q^{\mu_1} \dots q^{\mu_n}, \quad (3.4.14)$$

$$\int \frac{d\omega}{2\pi} \int_q J_{(n)}^{\mu_1 \dots \mu_n} \mathcal{F}(\omega) e^{-i\omega(t_r - n \cdot b)} = \int_q \delta(q^0) \mathcal{F}\left(\frac{q \cdot v}{n \cdot v}\right) \frac{e^{-iq \cdot \tilde{b}}}{q^2 (q^2 - q_\rho M^{\rho\sigma} q_\sigma)} q^{\mu_1} \dots q^{\mu_n}, \quad (3.4.15)$$

where $\mathcal{F}(\omega)$ represent any pre-factor of either $I_{(n)}^{\mu_1 \dots \mu_n}$ or $J_{(n)}^{\mu_1 \dots \mu_n}$ coming from eq. (3.4.13). In the above equation we have defined

$$\tilde{b}^\mu \equiv b^\mu + \frac{v^\mu}{n \cdot v} (t_r - n \cdot b), \quad M^{\mu\nu} \equiv 2 \frac{n^{(\mu} v^{\nu)}}{n \cdot v}. \quad (3.4.16)$$

Therefore, plugging eq. (3.4.13) into (3.4.12) and using the manipulations just described, one eventually obtains

$$f_{\text{NLO}}^{(\pm)} = \frac{Gm_1 m_2}{m_{\text{Pl}}} \int_q e^{iq \cdot \tilde{b}} \left[\frac{\mathcal{N}_{(\pm)}^i q_i}{q^2 (q \cdot e_v - i0^+)} + \frac{\mathcal{M}_{(\pm)}^{ij} q_i q_j}{q^2 (q^2 + q^k M_{k\ell} q^\ell)} \right]. \quad (3.4.17)$$

Here we have introduced

$$\mathcal{N}_{(\pm)}^i \equiv \frac{2\gamma^2 - 1}{\gamma(n \cdot v)} \left[\left(\frac{\sqrt{\gamma^2 - 1}}{2} n^i - \frac{2\gamma^2 - 2}{2\gamma^2 - 1} e_v^i \right) \frac{\epsilon_{kl}^{\pm*} e_v^k e_v^\ell}{\gamma(n \cdot v)} + \epsilon_{\pm}^{*ij} e_v^j \right], \quad (3.4.18)$$

$$\mathcal{M}_{(\pm)}^{ij} \equiv \frac{2\gamma^2 - 1}{\gamma n \cdot v} \epsilon_{\pm}^{*ij} + 2 \frac{(\gamma^2 - 1)^2}{\gamma^3 (n \cdot v)^3} (\epsilon_{kl}^{\pm*} e_v^k e_v^\ell) e_v^i e_v^j - 4 \frac{\gamma^2 - 1}{\gamma (n \cdot v)^2} e_v^i \epsilon_{\pm}^{*j} e_v^k. \quad (3.4.19)$$

One can now solve the remaining integrals as shown in [163] to obtain an explicit and compact expression for the asymptotic waveform in direct space. This is in agreement with the computation done in [81, 82].

3.5 . Radiative observables

In this final section we see how to use the NLO amplitude we have just derived to compute radiative observables such as the emitted linear and angular momentum.

3.5.1 . Emitted momentum in the small velocity limit

The emitted linear momentum can be computed using eq. (1.4.13). Similarly to what happened for the impulse, we can decompose this integral on a complete basis in order to get rid of the free index. Using again the vectors defined in eq. (2.2.8), one obtains the general structure

$$P_{\text{rad}}^\mu = \frac{G^3 m_1^2 m_2^2}{b^3} \left(\mathcal{C}_{u_1} \check{u}_1^\mu + \mathcal{C}_{u_2} \check{u}_2^\mu - \mathcal{C}_l \hat{l}^\mu - \mathcal{C}_b \hat{b}^\mu \right), \quad (3.5.1)$$

where we collected an overall dimensionful factor so that the coefficients inside the round brackets are dimensionless. The modulo square of the amplitude is actually symmetric under $k \cdot \hat{b} \rightarrow -k \cdot \hat{b}$ and $k \cdot \hat{l} \rightarrow -k \cdot \hat{l}$, therefore $\mathcal{C}_l = \mathcal{C}_b = 0$. Moreover, at this order the energy measured in the frame of one body is the same as the one measured in the frame of the other one, hence $\mathcal{C}_{u_1} = \mathcal{C}_{u_2}$ and the final result must be proportional to $u_1^\mu + u_2^\mu$. Therefore, we can write the emitted momentum as

$$P_{\text{rad}}^\mu = \frac{G^3 m_1^2 m_2^2}{b^3} \frac{u_1^\mu + u_2^\mu}{\gamma + 1} \mathcal{E}_{\text{pp}}(\gamma) + \mathcal{O}(G^4), \quad (3.5.2)$$

which confirms that at this order the result has homogeneous mass dependence and is thus fixed by the probe limit [82, 120, 234]. The function $\mathcal{E}_{\text{pp}}(\gamma)$ can be found by integrating the modulo squared of the amplitude written in eq. (3.4.3) over the phase space, i.e.

$$\mathcal{E}_{\text{pp}}(\gamma) = \int d\Omega \int_0^\infty dz \frac{d\mathcal{E}_{\text{pp}}}{dz d\Omega}(z, \Omega; \gamma) \quad (3.5.3)$$

with

$$\frac{d\mathcal{E}_{\text{pp}}}{dz d\Omega}(z, \Omega; \gamma) \equiv \frac{2\sqrt{\gamma^2 - 1} z^2}{\pi^2 \gamma^3} \sum_\lambda |\epsilon_{ij}^{*\lambda} e_I^i e_J^j A_{IJ}(z, \Omega)|^2. \quad (3.5.4)$$

Due to the involved structure of the y integrals in eq. (3.4.3), we were unable to compute \mathcal{E}_{pp} explicitly in this way. We shall see in the next chapter an alternative way of computing this quantity which dispenses with the need for an analytical expression of $\mathcal{A}_\lambda^{\text{NLO}}$ and which leads directly to the full emitted momentum. Nevertheless, introducing the relative velocity $v \equiv \sqrt{\gamma^2 - 1}$, we can first compute the integrals in y in the $v \ll 1$ regime at any order. After this, the phase-space integration can be performed once we fix a particular direction for the orthogonal normalized vectors e_v and e_b . We have computed the energy up to order $\mathcal{O}(v^8)$, obtaining

$$\frac{\mathcal{E}_{\text{pp}}(\gamma)}{\pi} = \frac{37}{15} v + \frac{2393}{840} v^3 + \frac{61703}{10080} v^5 + \frac{3131839}{354816} v^7 + \mathcal{O}(v^9). \quad (3.5.5)$$

As explained in section 1.4.2, we can project this result with u_{COM} to obtain the emitted energy in the COM frame, see eq (1.4.16). This quantity agrees with the 2PN results of [41, 82, 234] while eq. (3.5.5) matches the expansion of the fully relativistic result found in [111, 120, 121, 207]. This is a non-trivial check of our NLO amplitude (3.4.3).

3.5.2 . Energy spectrum in the soft limit

As an extra check, we can compute the LO energy spectrum in the soft limit, which is obtained by considering only wavelengths of the emitted gravitons much larger than the interaction region, i.e. $b\omega/v \ll 1$. In this limit the amplitude at order $G^{3/2}$ does not receive any contributions from the cubic-vertex term in eq. (3.3.7), hence it is not affected by the gravitational self-interactions. This means that we can discard all the terms proportional to the family of integrals $J_{(n)}^{\mu_1 \dots \mu_n}$ that we could not solve and the amplitude can be written just in terms of Bessel functions. Taking the limit $\omega \rightarrow 0$ and ignoring (sub-leading) $\log(\omega)$ terms we get

$$i\mathcal{A}_\lambda(k)_{\omega \rightarrow 0} = \frac{2Gm_1m_2}{b^2m_{\text{Pl}}} \frac{2\gamma^2 - 1}{\sqrt{\gamma^2 - 1}} \frac{\epsilon_{ij}^{*\lambda}}{\omega + i0^+} \left[-\frac{b^i u_1^j}{n \cdot u_1} + \frac{b^i u_2^j}{n \cdot u_2} + n \cdot b \left(\frac{u_1^i u_1^j}{2(n \cdot u_1)^2} - \frac{u_2^i u_2^j}{2(n \cdot u_2)^2} \right) \right]. \quad (3.5.6)$$

We verified that this is in agreement with Weinberg's soft graviton theorem [235, 236].

At this point, we can compute the energy spectrum in this limit as

$$\frac{dE_{\text{rad}}}{d\omega} \Big|_{\omega \rightarrow 0} = \frac{1}{2(2\pi)^3} \sum_{\lambda=\pm} \int d\Omega |\omega \mathcal{A}_\lambda(k)_{\omega \rightarrow 0}|^2. \quad (3.5.7)$$

In particular, working again in the rest frame of body 2, the soft limit amplitude written in (3.5.6) simplifies to

$$i\mathcal{A}_\lambda^{(2)}(k)_{\omega \rightarrow 0} = \frac{Gm_1m_2}{m_{\text{Pl}}b} \frac{1}{\gamma\omega n \cdot v} \epsilon_{ij}^{*\lambda} (c_2 e_v^i e_v^j + 2c_0 e_v^i e_b^i), \quad (3.5.8)$$

where c_2 and c_0 are defined in eq. (3.4.7). Integrating eq. (3.5.7) over the angles by fixing some angular coordinate system we obtain

$$\frac{dE_{\text{rad}}}{d\omega} \Big|_{\omega \rightarrow 0} = \frac{4}{\pi} \frac{(2\gamma^2 - 1)^2}{\gamma^2 - 1} \frac{G^3 m_1^2 m_2^2}{b^2} \mathcal{I}(\gamma) + \mathcal{O}(G^4), \quad (3.5.9)$$

where, following [197], we have introduced

$$\mathcal{I}(\gamma) \equiv -\frac{16}{3} + \frac{2\gamma^2}{\gamma^2 - 1} + \frac{2(2\gamma^2 - 3)}{(\gamma^2 - 1)} \frac{\gamma \operatorname{arccosh}(\gamma)}{\sqrt{\gamma^2 - 1}}. \quad (3.5.10)$$

This result agrees with Refs. [237, 238].

3.5.3 . Emitted angular momentum

The angular momentum lost by the system is another interesting observable as it can be related to the correction to the scattering angle due to radiation reaction [197]. In terms of the asymptotic waveform this is given by [197, 239]

$$J_{\text{rad}}^i = \epsilon^{ijk} \int d\Omega dt_r r^2 \left(2h_{jl} \dot{h}_k^l - x_j \partial_k h_{lm} \dot{h}^{lm} \right). \quad (3.5.11)$$

Decomposing h_{ij} as in eq. (3.4.11) we can rewrite the previous expression as

$$J_{\text{rad}}^i = \epsilon^{ijk} \sum_{\lambda, \lambda'} \int d\Omega dt_r \{ (2\epsilon_{j\ell}(\lambda)\epsilon_k^\ell(\lambda') - [x_j \partial_k \epsilon_{\ell m}(\lambda)]\epsilon^{\ell m}(\lambda')) f_\lambda \dot{f}_{\lambda'} - \epsilon_{\ell m}(\lambda)\epsilon^{\ell m}(\lambda') [x_j \partial_k f_\lambda] \dot{f}_{\lambda'} \}, \quad (3.5.12)$$

where we have put the helicity dependence between parenthesis to make the notation clearer. Recall that we work with the polarization tensors $\lambda = \pm 2$ such that $\epsilon_{ij}^*(+2) = \epsilon_{ij}(-2)$ and normalized as $\epsilon_{ij}(\lambda)\epsilon^{ij}(\lambda') = \delta_{\lambda\lambda'}$. Introducing a system of polar coordinates where $\mathbf{n} = (\sin \theta \cos \phi, \sin \theta \sin \phi, \cos \theta)$ and an orthonormal frame tangent to the sphere, with $\mathbf{e}_\theta = (\cos \theta \cos \phi, \cos \theta \sin \phi, -\sin \theta)$ and $\mathbf{e}_\phi = (-\sin \phi, \cos \phi, 0)$, we can write them as follows where,

$$\epsilon_{ij}(\pm 2) = \epsilon_i^\pm \epsilon_j^\pm, \quad \text{where} \quad \epsilon_i^\pm \equiv \frac{1}{\sqrt{2}}(\pm \mathbf{e}_\theta^i + i \mathbf{e}_\phi^i). \quad (3.5.13)$$

It is then not hard to prove the following identities

$$\sum_{\lambda'=\pm} \epsilon^{ijk} \epsilon_{j\ell}(\lambda)\epsilon_k^{\ell}(\lambda') = -\frac{i\lambda}{2} \delta_{\lambda, \lambda'} n^i, \quad (3.5.14)$$

$$\sum_{\lambda'=\pm} \epsilon^{ijk} [x_j \partial_k \epsilon_{\ell m}(\lambda)]\epsilon^{\ell m}(\lambda') = i\lambda \cot(\theta) e_\theta^i. \quad (3.5.15)$$

Introducing the angular momentum operator $L^i = -i \epsilon^{ijk} x_j \partial_k$, we can finally rewrite the emitted angular momentum as

$$\mathbf{J}_{\text{rad}} = i \sum_{\lambda=\pm} \int d\Omega dt_r \dot{f}_\lambda \{ \lambda(\mathbf{n} + \cot(\theta)\mathbf{e}_\theta) + \mathbf{L} \} f_{\lambda^*}, \quad (3.5.16)$$

where we defined $\lambda^* \equiv -\lambda$.

As pointed out in Ref. [197], the waveform at order $G^{1/2}$ is static and can be pulled out of the time integration, i.e.

$$\mathbf{J}_{\text{rad}} = i \sum_{\lambda=\pm} \int d\Omega \left[\int dt_r \dot{f}_\lambda^{\text{NLO}} \right] \{ \lambda(\mathbf{n} + \cot(\theta)\mathbf{e}_\theta) + \mathbf{L} \} f_{\lambda^*}^{\text{LO}} + \mathcal{O}(G^3). \quad (3.5.17)$$

The quantity inside square brackets in the above equation is the gravitational wave memory. If we write it in terms of the amplitude we have

$$\int dt_r \dot{f}_\lambda^{\text{NLO}} = \frac{i}{4\pi} \int \frac{d\omega}{2\pi} \delta(\omega) \omega \mathcal{A}_\lambda(k). \quad (3.5.18)$$

From the above expression it is clear that only the soft limit amplitude $\mathcal{A}_\lambda(k)_{\omega \rightarrow 0}$ contributes to the emitted angular momentum at this order. As we saw in the previous section, in this region the amplitude does not receive any contributions from the gravitational self-interactions and can then be written explicitly in terms of analytic functions, see eq. (3.5.6).

It has been argued in Refs. [122, 128] that eq. (3.5.11) is valid only in the COM frame. Therefore for the correct computation of the emitted angular momentum we cannot use the amplitude in the form of eq. (3.4.3). For the rest of this section we work in the COM frame defined as in (1.1.1).

In the COM frame we can write

$$f_\lambda^{\text{LO}} = \frac{p_\infty^2}{8\pi m_{\text{P1}}} \left[\frac{1}{n \cdot p_1} + \frac{1}{n \cdot p_2} \right] \epsilon_{ij}^{\lambda*} e_v^i e_v^j. \quad (3.5.19)$$

Moreover, the soft limit amplitude needed for the computation of the gravitational wave memory becomes

$$i\mathcal{A}_\lambda(k)_{\omega \rightarrow 0} = -\frac{2Gm_1m_2}{bm_{\text{P1}}} \frac{(2\gamma^2 - 1)p_\infty}{\sqrt{\gamma^2 - 1}} \frac{\epsilon_{ij}^{*\lambda}}{\omega + i0^+} \left[\left(\frac{1}{n \cdot p_1} + \frac{1}{n \cdot p_2} \right) e_b^i e_v^j + n \cdot e_b \left(\frac{p_\infty}{2(n \cdot p_1)^2} - \frac{p_\infty}{2(n \cdot p_2)^2} \right) e_v^i e_v^j \right]. \quad (3.5.20)$$

Plugging these expressions in (3.5.17), one can perform the angular integral by aligning e_v and e_b along any (mutually orthogonal) directions and eventually obtains

$$\mathbf{J}_{\text{rad}} = \frac{2(2\gamma^2 - 1)}{\sqrt{\gamma^2 - 1}} \frac{G^2 m_1 m_2 J}{b^2} \mathcal{I}(\gamma) (e_b \times e_v), \quad (3.5.21)$$

where J is the angular momentum at infinity, see eq. (1.1.5), and $\mathcal{I}(\gamma)$ is defined in eq. (3.5.10). This result agrees with [197] and [122, 128].

3.6 . Summary of the chapter

In this chapter, we applied the worldline EFT to the computation of radiated observables in the gravitational scattering problem. Using Feynman rules and matching with the action in eq. (1.3.17), we extracted the expression of the stress-energy tensor $T_{\text{NLO}}^{\mu\nu}$ up to NLO in the perturbative expansion. We wrote $T_{\text{NLO}}^{\mu\nu}$ in terms of two sets of integrals presented in eqs. (3.3.3) and (3.3.4).

The stress-energy tensor contains all the information of the radiative dynamics and we used it to compute the asymptotic waveform in direct space, the energy spectrum in the soft limit and the emitted angular momentum. However, since we were not able to completely solve the integrals of eq. (3.3.4), we could not write the stress-energy tensor in terms of known analytic functions. Thus, we found an expression for the emitted four-momentum only in the low-velocities regime.

We shall see in the next chapter how applying the roadmap presented in figure 7 (page 56) allows us to get around this limitation and find an expression for the full radiated momentum.

4 - Leading order radiated momentum

In this chapter we show how to bypass the problem of not having a solution for the stress-energy tensor by rewriting the phase-space integral of the four-momentum as a (cut) two-loop integral. Once we reach this form, we can employ all the powerful techniques shown in section 2.3 and follow the roadmap depicted in figure 7 at page 56.

4.1 . Radiated four-momentum as a two-loop integral

In term of the classical amplitude of graviton emission $\mathcal{A}_\lambda(k)$, the radiated total momentum P_{rad}^μ is given by eq. (1.4.13). Pictorially, this equation can be represented as

$$P_{\text{rad}}^\mu = \sum_\lambda \int_k \delta_+(k^2) k^\mu \left| \mathcal{A}_\lambda \begin{array}{c} k \\ \text{-----} \\ \text{-----} \end{array} \right|^2, \quad (4.1.1)$$

where the on-shell amplitude on the right-hand side is non perturbative in G . Here we focus on the LO emitted momentum and therefore we expand the amplitude in powers of G as

$$\mathcal{A}_\lambda \begin{array}{c} \text{-----} \\ \text{-----} \end{array} = \begin{array}{c} G^{1/2} \\ \bullet \\ \text{-----} \\ \text{-----} \end{array} + \begin{array}{c} G^{1/2} \\ \bullet \\ \text{-----} \\ \text{-----} \\ G^{1/2} \\ \bullet \end{array} + \begin{array}{c} G \\ \bullet \\ \text{-----} \\ \text{-----} \\ G \\ \bullet \end{array} + \begin{array}{c} G^{1/2} \\ \bullet \\ \text{-----} \\ \text{-----} \\ G \\ \bullet \end{array} + \begin{array}{c} G^{1/2} \\ \bullet \\ \text{-----} \\ \text{-----} \\ G^{1/2} \\ \bullet \end{array} + \dots \quad (4.1.2)$$

The first two diagrams on the right-hand side, of order $\mathcal{O}(G^{1/2})$, are static (they are proportional to $\delta(k \cdot u_a)$) and when multiplied by k^μ they do not contribute to the emitted power. Therefore, the LO contribution to the radiated power comes from squaring the last three diagrams, of order $\mathcal{O}(G^{3/2})$,

$$k^\mu \left| \mathcal{A}_\lambda \begin{array}{c} k \\ \text{-----} \\ \text{-----} \end{array} \right|^2 = k^\mu \left| \begin{array}{c} \bullet \\ \text{-----} \\ \text{-----} \\ \bullet \end{array} + \begin{array}{c} \bullet \\ \text{-----} \\ \text{-----} \\ \bullet \end{array} + \begin{array}{c} \bullet \\ \text{-----} \\ \text{-----} \\ \bullet \end{array} \right|^2 + \mathcal{O}(G^4). \quad (4.1.3)$$

As explained above, instead of solving the integrals in eq. (3.2.10) in the momentum of the graviton exchanged between the particles, q^μ , we adopt a different strategy to compute the right-hand side of eq. (4.1.1). Writing explicitly the amplitude in terms of the pseudo stress-energy tensor we have

$$P_{\text{rad}}^\mu = \frac{1}{4m_{\text{Pl}}^2} \int_k \left[\sum_\lambda \epsilon_{\rho\sigma}^{\lambda*} \epsilon_{\alpha\beta}^\lambda \delta_+(k^2) \right] k^\mu \tilde{T}^{\rho\sigma}(k) \tilde{T}^{\alpha\beta}(-k), \quad (4.1.4)$$

where, being $T^{\mu\nu}(x)$ real, we used that $\tilde{T}^{\mu\nu*}(k) = \tilde{T}^{\mu\nu}(-k)$.

At this point we can employ the standard completeness relation

$$\sum_{\lambda=\pm 2} \epsilon_{\alpha\beta}^{\lambda*} \epsilon_{\rho\sigma}^{\lambda} = \mathbb{P}_{\alpha(\rho} \mathbb{P}_{\sigma)\beta} - \frac{1}{2} \mathbb{P}_{\alpha\beta} \mathbb{P}_{\rho\sigma} = P_{\alpha\beta\rho\sigma} + \mathcal{O}(k^2, k^\mu), \quad (4.1.5)$$

where, introducing a time-like unit vector \hat{u}^μ ,

$$\mathbb{P}^{\mu\nu} \equiv \eta_{\mu\nu} + \frac{k^2 \hat{u}^\mu \hat{u}^\nu + k^\mu k^\nu - 2(\hat{u} \cdot k) k^{(\mu} \hat{u}^{\nu)}}{(k \cdot \hat{u})^2 - k^2}. \quad (4.1.6)$$

In eq. (4.1.5) we ignored terms that either vanish on-shell, or are proportional to k^μ and vanish once contracted with the conserved stress-energy tensor.

Having this, we can interpret the quantity inside the squared brackets of eq. (4.1.4) as a cut graviton propagator. Hence, another pictorial depiction of eq. (4.1.1) is

$$P_{\text{rad}}^\mu = \frac{1}{4m_{\text{Pl}}^2} \int_k k^\mu \left(\tilde{T} \right) \overset{k}{\rightsquigarrow} \left(\tilde{T}^* \right). \quad (4.1.7)$$

The modulo squared of the amplitude has been replaced by a vacuum-to-vacuum diagram in the presence of two sources, represented by the pseudo stress-energy tensors. This is essentially the standard optical theorem [215–217]. We also depict explicitly the flow of the momentum k^μ as dictated by the positive energy theta function in $\delta_+(k^2)$.

Contracting the various diagrams represented in eq. (4.1.3), at leading order we expect four different cut topologies on the right-hand side, denoted here by M, N, IY and H type, i.e.,

$$\left(\left(\tilde{T} \right) \overset{k}{\rightsquigarrow} \left(\tilde{T}^* \right) \right)_{\text{LO}} = \begin{array}{c} \text{M} \\ \text{N} \\ \text{IY} \\ \text{H} \end{array} + (1 \leftrightarrow 2), \quad (4.1.8)$$

where we have always considered the upper dot to be object $a = 1$, and the lower dot object $a = 2$. More explicitly, plugging in eq. (4.1.4) the expression of the NLO $\tilde{T}^{\mu\nu}(k)$ given in (3.2.10) we obtain

$$\frac{\tilde{T}^{\rho\sigma}(k) P_{\rho\sigma\alpha\beta} \tilde{T}^{\alpha\beta}(-k)}{4m_{\text{Pl}}^2} = \frac{m_1^2 m_2^2}{64m_{\text{Pl}}^6} \int_{q_1, q_2} \Delta_{1,2}(q_1, k) \Delta_{1,2}(q_2, k) \times \frac{e^{i(q_1 - q_2) \cdot b} \mathcal{N}(q_1, q_2, k)}{q_1^2 q_2^2 (k - q_1)^2 (k - q_2)^2}, \quad (4.1.9)$$

where $\Delta_{1,2}(q, k) \equiv \delta(q \cdot u_1) \delta(q \cdot u_2 - k \cdot u_2)$, and the numerator \mathcal{N} can be organized in terms of the contributions from the four topologies above. It is explicitly defined as

$$\begin{aligned} \mathcal{N}(q_1, q_2, k) \equiv & \left(t_{\uparrow}^{\mu\nu}(q_1, k) + t_{\downarrow}^{\mu\nu}(q_1, k) + t_{\pm}^{\mu\nu}(q_1, k) \right) P_{\mu\nu\rho\sigma} \\ & \times \left(t_{\uparrow}^{\rho\sigma}(q_2, k) + t_{\downarrow}^{\rho\sigma}(q_2, k) + t_{\pm}^{\rho\sigma}(q_2, k) \right)^* . \end{aligned} \quad (4.1.10)$$

Finally, we replace (4.1.9) in eq. (4.1.4) and we rename

$$q_1^\mu = -\ell_1^\mu + q^\mu, \quad q_2^\mu = -\ell_1^\mu, \quad k^\mu = -\ell_1^\mu - \ell_2^\mu + q^\mu. \quad (4.1.11)$$

We then obtain

$$P_{\text{rad}}^\mu = \frac{m_1^2 m_2^2}{64 m_{\text{Pl}}^6} \int_q \delta(q \cdot u_1) \delta(q \cdot u_2) e^{iq \cdot b} Q^\mu, \quad (4.1.12)$$

$$\begin{aligned} Q^\mu \equiv & \int_{\ell_1, \ell_2} \delta_-((\ell_1 + \ell_2 - q)^2) \delta(\ell_1 \cdot u_1) \delta(\ell_2 \cdot u_2) \\ & \times \frac{(-\ell_1^\mu - \ell_2^\mu + q^\mu) \mathcal{N}(\ell_1, \ell_2, q)}{\ell_1^2 \ell_2^2 (\ell_1 - q)^2 (\ell_2 - q)^2} \end{aligned} \quad (4.1.13)$$

We have rewritten the total four-momentum emitted as a cut two-loop integral Q^μ , followed by a Fourier transform from q to b -space.

At this point, we have arrived at a form similar to the one we described for the impulse in section 2.2. As in that case, the advantage of this procedure is that we can now solve the two-loop integral all at once, making use of the powerful computational tools routinely employed in high-energy physics — IBP reduction into master integrals [172, 173, 176] and differential equation methods [180, 182–184] to solve the latter — described in chapter 2 of this work, without the need of deriving the Fourier-space gravitational waveform. This is analogous to the calculations performed in [110, 120, 121]. The difference is that here we start from a purely classical quantity, namely the conserved pseudo stress-energy tensor $\tilde{T}^{\mu\nu}$, while in that references the authors take the classical limit of a full scattering amplitude. For this reason, in our approach we do not have to consider any intermediate quantum or super-classical term.

4.2 . Solving the integral

Before computing the contribution from each of the topologies in eq. (4.1.8) we must discuss the master integrals that we will need to solve the associated two-loop integrals. This is what we turn to now.

4.2.1 . Master integrals

As explained in section 3.5.1, we expect the emitted momentum to be (see eq. (3.5.1))

$$P_{\text{rad}}^\mu = \frac{G^3 m_1^2 m_2^2}{b^3} \frac{u_1^\mu + u_2^\mu}{\gamma + 1} \mathcal{E}_{\text{PP}}(\gamma) + \mathcal{O}(G^4). \quad (4.2.1)$$

Therefore, we can get rid of the free index in Q^μ in eqs. (4.1.12) by contracting with $u_1^\mu + u_2^\mu$. Comparing the final result with (4.2.1) we find the following explicit expression for $\mathcal{E}_{\text{pp}}(\gamma)$

$$\mathcal{E}_{\text{pp}}(\gamma) = 512\pi^3 b^3 \int_q \delta(q \cdot u_1) \delta(q \cdot u_2) e^{iq \cdot b} \sqrt{-q^2} \mathcal{I}_{\text{pp}}(\gamma), \quad (4.2.2)$$

with $\mathcal{I}_{\text{pp}}(\gamma) = Q \cdot (u_1 + u_2)/2$, hence explicitly

$$\begin{aligned} \mathcal{I}_{\text{pp}}(\gamma) &= \frac{1}{2\sqrt{-q^2}} \int_{\ell_1, \ell_2} \delta_-((\ell_1 + \ell_2 - q)^2) \delta(\ell_1 \cdot u_1) \delta(\ell_2 \cdot u_2) \\ &\quad \times \frac{(-\ell_1 \cdot u_2 - \ell_2 \cdot u_1) \mathcal{N}(\ell_1, \ell_2, q)}{\ell_1^2 \ell_2^2 (\ell_1 - q)^2 (\ell_2 - q)^2}. \end{aligned} \quad (4.2.3)$$

Notice that both $\mathcal{E}_{\text{pp}}(\gamma)$ and $\mathcal{I}_{\text{pp}}(\gamma)$ are dimensionless and only dependent on $\gamma = u_1 \cdot u_2$. Indeed, the two-loop integral on the right-hand side of eq. (4.2.3) has dimension one. It can only depend on q^2 and $\gamma = u_1 \cdot u_2$ because $q \cdot u_1 = q \cdot u_2 = 0$ by the delta functions in eq. (4.2.2) and no singular contribution is expected. Since only q is dimensionful, it must scale as $\sqrt{-q^2}$, which is compensated by the prefactor. The integral in eq. (4.2.2) has dimension three and since the only dimensionful parameter is b , it must scale like b^{-3} . This removes the b -dependence on the right-hand side making $\mathcal{E}_{\text{pp}}(\gamma)$ dimensionless.

We now discuss how to simplify and solve the two-loop integral $\mathcal{I}_{\text{pp}}(\gamma)$. Use the notation [110, 112, 121]

$$\rho_1 = 2\ell_1 \cdot u_1, \quad \rho_2 = -2\ell_1 \cdot u_2, \quad \rho_3 = -2\ell_2 \cdot u_1, \quad \rho_4 = 2\ell_2 \cdot u_2, \quad (4.2.4)$$

and

$$\begin{aligned} \rho_5 &= \ell_1^2, & \rho_6 &= \ell_2^2, & \rho_7 &= (\ell_1 + \ell_2 - q)^2, \\ \rho_8 &= (\ell_1 - q)^2, & \rho_9 &= (\ell_2 - q)^2, \end{aligned} \quad (4.2.5)$$

and rewrite it as

$$\mathcal{I}_{\text{pp}}(\gamma) = \frac{1}{\sqrt{-q^2}} \int_{\ell_1, \ell_2} \delta_-(\rho_7) \delta(\rho_1) \delta(\rho_4) \frac{(\rho_2 + \rho_3) \mathcal{N}(\rho_1, \dots, \rho_9)}{\rho_5 \rho_6 \rho_8 \rho_9}. \quad (4.2.6)$$

We use dimensional regularization and extend the four dimensional integration to d space-time dimensions, i.e.

$$\int_{\ell_1, \ell_2} \equiv \int \frac{d^d \ell_1}{(2\pi)^d} \frac{d^d \ell_2}{(2\pi)^d}, \quad d = 4 - 2\varepsilon. \quad (4.2.7)$$

Moreover, reverse unitarity [168–171] allows to treat the three delta functions involving ρ_1 , ρ_4 and ρ_7 as cut propagators and apply IBP identities.

In particular, as explained in chapter 2, we formally replace the three delta functions by cut propagators and we underline them to distinguish from the standard ones,

$$\delta_-(\rho_7) \rightarrow \frac{1}{\underline{\rho_7}}, \quad \delta(\rho_1) \rightarrow \frac{1}{\underline{\rho_1}}, \quad \delta(\rho_4) \rightarrow \frac{1}{\underline{\rho_4}}. \quad (4.2.8)$$

Then, $\mathcal{I}_{\text{pp}}(\gamma)$ is given as a linear combination of integrals of the form

$$G_{\underline{i}_1, \underline{i}_2, \underline{i}_3, \underline{i}_4, \underline{i}_5, \underline{i}_6, \underline{i}_7, \underline{i}_8, \underline{i}_9} = \int_{\ell_1, \ell_2} \frac{1}{\underline{\rho}_1^{i_1} \underline{\rho}_2^{i_2} \underline{\rho}_3^{i_3} \underline{\rho}_4^{i_4} \underline{\rho}_5^{i_5} \underline{\rho}_6^{i_6} \underline{\rho}_7^{i_7} \underline{\rho}_8^{i_8} \underline{\rho}_9^{i_9}}. \quad (4.2.9)$$

With the help of LiteRed [177, 178], we can implement the step two of the roadmap in figure 7, page 56, and reduce $\mathcal{I}_{\text{pp}}(\gamma)$ to a combination of the following four MIs:

$$\begin{aligned} f_1 &\equiv \sqrt{-q^2} G_{2,0,0,\underline{1},0,1,\underline{1},0,1}, & f_2 &\equiv \sqrt{-q^2} G_{2,0,0,\underline{1},0,0,\underline{1},1,1}, \\ f_3 &\equiv \sqrt{-q^2} G_{1,0,1,\underline{1},0,0,\underline{1},1,1}, & f_4 &\equiv \sqrt{-q^2} G_{2,0,0,\underline{1},1,1,\underline{1},1,1}. \end{aligned} \quad (4.2.10)$$

Note that since we are considering a cut two-loop integration, one must use the CutDS option in LiteRed in order to perform the correct IBP reduction. The set of propagators in eqs. (4.2.4) and (4.2.5) and the four MIs above are enough to solve our four topologies in eq. (4.1.8).

At this point, we can use the differential equation methods [180, 182–184] to solve these integrals. To remove the square roots that inevitably appears in the computations, it is convenient to replace again the dependence on γ of the MIs by that on the kinematic variable x , defined by $x \equiv \gamma - \sqrt{\gamma^2 - 1}$ [112], see (2.3.21). Differentiating with respect to x , one realizes that the above integrals satisfy a system of differential equations of the form

$$\partial_x \vec{f}(x, \varepsilon) = F(x, \varepsilon) \vec{f}(x, \varepsilon), \quad \vec{f} = \begin{pmatrix} f_1 \\ f_2 \\ f_3 \\ f_4 \end{pmatrix}. \quad (4.2.11)$$

Here $F(x, \varepsilon)$ is a matrix of rational coefficients. As explained in section 2.3.4, to solve this equation, it is convenient to find a basis $\vec{g} = \{g_1, g_2, g_3, g_4\}$ such that the differential equation is in canonical form [184, 185, 240], i.e.

$$\partial_x \vec{g}(x, \varepsilon) = \varepsilon A(x) \vec{g}(x, \varepsilon). \quad (4.2.12)$$

A system of this form can be trivially solved in terms of polylogarithms as a Laurent series in ε . The transformation between the basis \vec{f} and \vec{g} can be obtained with the help of the package Fuchsia [230, 231], implementing the Lee algorithm [232].

The canonical basis of MIs reads

$$g_1 = \sqrt{-q^2} G_{2,0,0,\underline{1},0,1,\underline{1},0,1}, \quad (4.2.13)$$

$$g_2 = \sqrt{-q^2} G_{2,0,0,\underline{1},0,0,\underline{1},1,1}, \quad (4.2.14)$$

$$g_3 = \varepsilon \sqrt{-q^2} \sqrt{\gamma^2 - 1} G_{1,0,1,\underline{1},0,0,\underline{1},1,1}, \quad (4.2.15)$$

$$\begin{aligned} g_4 &= (\sqrt{-q^2})^5 \frac{\gamma - 1}{8} G_{2,0,0,\underline{1},1,1,\underline{1},1,1} + \sqrt{-q^2} \frac{1 - 2\varepsilon(2 + 3\gamma)}{12(1 + 2\varepsilon)} G_{2,0,0,\underline{1},0,0,\underline{1},1,1} \\ &\quad + \frac{2\varepsilon}{(1 + 2\varepsilon)(1 + \gamma)} \sqrt{-q^2} G_{2,0,0,\underline{1},0,1,\underline{1},0,1}, \end{aligned} \quad (4.2.16)$$

which satisfies the following canonically normalized differential equation,

$$\frac{d}{dx}\vec{g}(x, \varepsilon) = \varepsilon \begin{pmatrix} -\frac{2(1+x^2)}{x(x^2-1)} & 0 & 0 & 0 \\ 0 & \frac{2(1-4x+x^2)}{x(x^2-1)} & 0 & 0 \\ 0 & \frac{1}{x} & 0 & 0 \\ -\frac{4}{x^2-1} & \frac{7+10x+7x^2}{6x(x^2-1)} & 0 & -\frac{4}{x^2-1} \end{pmatrix} \vec{g}(x, \varepsilon), \quad \vec{g} \equiv \begin{pmatrix} g_1 \\ g_2 \\ g_3 \\ g_4 \end{pmatrix}. \quad (4.2.17)$$

This can be equivalently written as

$$d\vec{g} = \varepsilon [A_0 d\log x + A_{+1} d\log(x+1) + A_{-1} d\log(x-1)]\vec{g}, \quad (4.2.18)$$

with

$$A_0 = \begin{pmatrix} -2 & 0 & 0 & 0 \\ 0 & -2 & 0 & 0 \\ 0 & 1 & 0 & 0 \\ 0 & \frac{7}{6} & 0 & 0 \end{pmatrix}, \quad A_{+1} = \begin{pmatrix} 2 & 0 & 0 & 0 \\ 0 & 6 & 0 & 0 \\ 0 & 0 & 0 & 0 \\ 2 & \frac{1}{3} & 0 & 2 \end{pmatrix},$$

$$A_{-1} = \begin{pmatrix} 2 & 0 & 0 & 0 \\ 0 & -2 & 0 & 0 \\ 0 & 0 & 0 & 0 \\ -2 & 2 & 0 & -2 \end{pmatrix}. \quad (4.2.19)$$

As we saw explicitly in section 2.3.4, we can solve this differential equation perturbatively in ε [110], i.e., for each $j = 1, \dots, 4$,

$$g_j(x, \varepsilon) = \frac{1}{(-q^2)^{2\varepsilon}} \sum_k g_j^{(k)}(x) \varepsilon^k. \quad (4.2.20)$$

Each $g_j^{(k)}(x)$ can be found iteratively starting from the $g_j^{(k-1)}(x)$ as we showed explicitly in the one-loop example, see eq. (2.3.27). To understand at which order in k we have to start from, we first need to find the boundary conditions.

4.2.2 . Boundary conditions and solutions for the MIs

The boundary conditions can be found by solving the MIs in the near static limit, i.e. for $\gamma \rightarrow 1$ (or $x \rightarrow 1$). As in section 2.3.5, our MIs \vec{g} are cut two-loop integrals, therefore, it is easier to solve the corresponding uncut scalar integral and then connect the two using Cutkosky's cutting rules [204, 205]. Since this is a delicate point, we show here how this applies to g_1 explicitly, and leave the derivation of all the others BCs in appendix B.

It is helpful to depict the master integrals as diagrams. To do this, for convenience we introduce a "propagator" also for the massive external source, which can be seen as the soft-expanded version of the propagator of a massive scalar field [110, 112, 121]. Note that this is only a convenient pictorial tool useful to solve the Feynman integrals, the compact bodies are external sources and do not propagate. Considering g_1 , we can represent it as in figure 8 (a), where a thick line denotes the "massive propagator" and

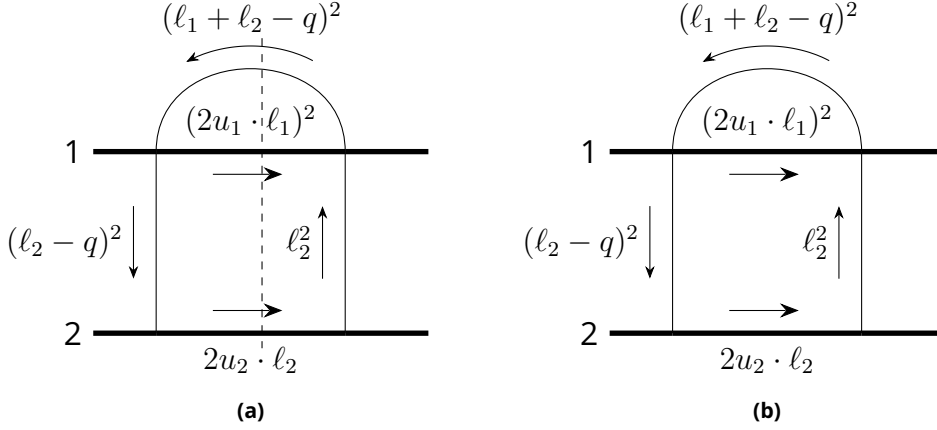


Figure 8: Graphic representation of (a) g_1 and (b) I_1 .

a thin line denotes the massless one. Its uncut version is depicted in figure 8 (b), which corresponds to the following integral

$$i I_1 \equiv (i)^5 (-i)^4 \int_{\ell_1, \ell_2} \frac{\sqrt{-q^2}}{(2\ell_1 \cdot u_1)^2 (2\ell_2 \cdot u_2) \ell_2^2 (\ell_2 - q)^2 (\ell_1 + \ell_2 - q)^2}, \quad (4.2.21)$$

where we have left implicit all the $i0^+$ Feynman prescriptions and included the factor of i and $-i$ coming respectively from the propagators and vertices.

At this point we can apply the Cutkosky cutting rules listed in section 2.3.5, which results in the following pictorial equation

$$= 0. \quad (4.2.22)$$

In terms of g_1 and I_1 , this relation becomes

$$(i I_1)^* + g_1 + (i I_1) = 0 \rightarrow g_1 = 2\text{Im}(I_1). \quad (4.2.23)$$

Thus, to find the boundary conditions of the cut master integral g_1 , it is enough to compute the uncut diagram I_1 in the near static limit and then take twice its imaginary part.

We give an explicit derivation of the other boundary conditions in appendix B and we report here the results:

$$g_1|_{x \rightarrow 1} = g_2|_{x \rightarrow 1} = 12g_4|_{x \rightarrow 1} = -\frac{C_{\text{BC}}}{(4\pi)^{4-2\varepsilon}}, \quad g_3|_{x \rightarrow 1} = 0, \quad (4.2.24)$$

where

$$C_{\text{BC}} = \sin(\pi\varepsilon) \left(\frac{1}{(-q^2)(1-x)} \right)^{2\varepsilon} \frac{\sqrt{\pi} \Gamma(1+\varepsilon) \Gamma(1-\varepsilon) \Gamma(\frac{1}{2}+2\varepsilon) \Gamma(\frac{1}{2}-2\varepsilon)^2}{\varepsilon \Gamma(1-4\varepsilon)}. \quad (4.2.25)$$

We have now all the necessary ingredients to find the solution to the four MIs defined in eqs. (4.2.13) - (4.2.16). For the following computations, we just need the solutions up to order ε in the expansion (4.2.20). These are explicitly given by

$$g_1^{(0)} = -\frac{1}{256\pi}, \quad g_2^{(0)} = -\frac{1}{256\pi}, \quad g_3^{(0)} = 0, \quad g_4^{(0)} = -\frac{1}{3072\pi}, \quad (4.2.26)$$

$$g_1^{(1)} = \frac{\gamma_E - \log(4\pi)}{128\pi} + \frac{1}{128\pi} \left[\log\left(\frac{1-x}{4}\right) - \log(x) + \log\left(\frac{1+x}{2}\right) \right], \quad (4.2.27)$$

$$g_2^{(1)} = \frac{\gamma_E - \log(4\pi)}{128\pi} + \frac{1}{128\pi} \left[\log\left(\frac{1-x}{4}\right) + \log(x) - 3 \log\left(\frac{1+x}{2}\right) \right], \quad (4.2.28)$$

$$g_3^{(1)} = -\frac{1}{256\pi} \log(x), \quad (4.2.29)$$

$$g_4^{(1)} = \frac{\gamma_E - \log(4\pi)}{1536\pi} + \frac{1}{1536\pi} \left[\log\left(\frac{1-x}{4}\right) + 7 \log(x) - 15 \log\left(\frac{1+x}{2}\right) \right], \quad (4.2.30)$$

where γ_E is the Euler-Mascheroni constant. Up to a different normalization of the loop integrals,¹ these agree with [110, 121].

4.3 . Computing the four topologies

We have now all that we need to compute the LO radiated momentum P_{rad}^μ . As mentioned in the previous section, we will focus on computing $\mathcal{E}_{\text{pp}}(\gamma)$ defined eq. (4.2.2), splitting the computation in four contributions coming from the four topologies in eq. (4.1.8), i.e.,

$$\mathcal{E}_{\text{pp}}(\gamma) = \mathcal{E}_{\text{M}}(\gamma) + \mathcal{E}_{\text{N}}(\gamma) + \mathcal{E}_{\text{IY}}(\gamma) + \mathcal{E}_{\text{H}}(\gamma) + (u_1 \leftrightarrow u_2), \quad (4.3.1)$$

where

$$\mathcal{E}_I(\gamma) \equiv 512\pi^3 b^3 \int_q \delta(q \cdot u_1) \delta(q \cdot u_2) e^{iq \cdot b} \sqrt{-q^2} \mathcal{I}_I(\gamma), \quad (4.3.2)$$

with $I = \text{M}, \text{N}, \text{IY}, \text{H}$ and

$$\mathcal{I}_I(\gamma) \equiv \frac{1}{\sqrt{-q^2}} \int_{\ell_1, \ell_2} \frac{(\rho_2 + \rho_3) \mathcal{N}_I(\rho_1, \dots, \rho_9)}{\rho_1 \rho_4 \rho_5 \rho_6 \rho_7 \rho_8 \rho_9}, \quad (4.3.3)$$

The numerators for each topology, \mathcal{N}_I , are defined below. The details of the calculation can be found in the ancillary files accompanying the arXiv submission of [207]. In particular, using xTensor [219] the Mathematica notebook Contractions.nb computes the integrand of eq. (4.3.3) using the stress-energy tensor and prints the results in four different text files. These files are then imported in IBP-Basis1.nb, which performs the needed IBP reductions using LiteRed [177, 178] and computes $\mathcal{E}_I(\gamma)$ for each topology.

¹In the QCD/amplitude literature it is common practice to remove a factor of $i(4\pi)^{\varepsilon-2} e^{-\varepsilon\gamma_E}$ per loop from the normalization of the integrals. Here we do not use this convention.

4.3.1 . M topology

We start from the M topology, i.e. we solve eq. (4.3.2) with

$$\mathcal{N}_M = P_{\mu\nu\rho\sigma} t_{\uparrow}^{\mu\nu} t_{\uparrow}^{*\rho\sigma} . \quad (4.3.4)$$

Performing the contractions and IBP reduction with LiteRed [177, 178], one can eventually write this contribution in terms of a single master integral,

$$\mathcal{I}_M(\gamma, \varepsilon) = C_M(\gamma, \varepsilon) g_1(\gamma, \varepsilon) , \quad (4.3.5)$$

where C_M is a (not very illuminating) function of ε and γ . Here we are interested in the limit $\varepsilon \rightarrow 0$. Since C_M starts at ε^0 , we just need g_1 at order ε^0 , see eq. (4.2.26). After performing the Fourier transform in q in eq. (4.3.2) using eq. (2.1.8) we obtain

$$\mathcal{E}_M(\gamma) = -\frac{\pi}{8} \left(\frac{20\gamma^7 + 16\gamma^6 + 12\gamma^4 - 13\gamma^3 - 24\gamma^2 + 15\gamma + 18}{3\sqrt{\gamma^2 - 1}} \right) . \quad (4.3.6)$$

The final result is unaltered by the exchange $1 \leftrightarrow 2$, therefore the symmetric contribution gives exactly the same result.

Note that the M topology does not contain contributions from the graviton cubic vertex and the involved Fourier-space waveform (the amplitude) can be computed exactly. This means that in this case we can also compute the above contribution in a more ‘‘direct’’ way from eq. (4.1.1), by taking the part of the amplitude that gives the analogous contribution of this topology. Specifically, $\mathcal{E}_M(\gamma)$ can be computed from eq. (4.1.1) as

$$\mathcal{E}_M(\gamma) = 256\pi^3 b^3 \sum_{\lambda} \int_k \delta_+(k^2) k \cdot (u_1 + u_2) \mathcal{A}_{\lambda}^{\uparrow}(k) \mathcal{A}_{\lambda}^{\uparrow}(-k) , \quad (4.3.7)$$

with $\mathcal{A}_{\lambda}^{\uparrow}(k)$ defined in (3.3.5). Working in four dimensions and solving explicitly the integral in q of eq. (3.3.5) as we did in section 3.3, we find the following expression in terms of modified Bessel functions of the second kind K_n ,

$$\begin{aligned} \mathcal{A}_{\lambda}^{\uparrow}(k) = & \frac{\epsilon_{\mu\nu}^{\lambda*}}{4\pi(\gamma^2 - 1)} \left\{ 2i \frac{u_1^{\mu} b^{\nu}}{b} (1 - 2\gamma^2) K_1(z_1) - 2 \frac{u_1^{\mu} u_2^{\nu}}{\sqrt{\gamma^2 - 1}} \gamma (3 - 2\gamma^2) K_0(z_1) \right. \\ & \left. + \frac{u_1^{\mu} u_1^{\nu}}{\sqrt{\gamma^2 - 1}} \left[\left(1 + \gamma(3 - 2\gamma^2) \frac{z_2}{z_1} \right) K_0(z_1) - i(1 - 2\gamma^2) \frac{k \cdot b}{z_1} K_1(z_1) \right] \right\} , \end{aligned} \quad (4.3.8)$$

where, following the notation of that section, we have defined once again, for $a = 1, 2$,

$$z_a \equiv \frac{bk \cdot u_a}{\sqrt{\gamma^2 - 1}} . \quad (4.3.9)$$

Using eq. (4.1.5), we can rewrite eq. (4.3.7) as follows

$$\begin{aligned} \mathcal{E}_M = & \frac{b^2}{2\pi^2 (\gamma^2 - 1)^{5/2}} \int_0^{\infty} d\omega \omega \int d\Omega \frac{z_1 + z_2}{z_1^2} \left\{ K_0^2(z_1) [(z_1 + \gamma(3 - 2\gamma^2)z_2)^2 \right. \\ & + 4z_1\gamma^2(2\gamma^2 - 3)(z_1 - (3 - 2\gamma^2)(z_1 - \gamma z_2))] \\ & \left. + K_1^2(z_1)(1 - 2\gamma^2)^2 [4(1 - \gamma^2)z_1^2 - \mathbf{k} \cdot \mathbf{b}] \right\} , \end{aligned} \quad (4.3.10)$$

where we used that

$$d^4k \delta_+(k^2) = 2\pi d^3\mathbf{k}/(2|\mathbf{k}|)|_{k^0=|\mathbf{k}|} = \pi d\Omega d\omega \omega|_{k^0=\omega}, \quad \omega \equiv |\mathbf{k}|, \quad (4.3.11)$$

with $d\Omega$ denoting the integration over the solid angle. Working again in the frame (3.3.8), one can first solve the integrals in the azimuthal angle ϕ and the frequency ω , then finally in the polar angle θ , eventually recovering eq. (4.3.6). We stress again that such a direct procedure is intractable when the amplitude involves $\mathcal{A}_\lambda^\pm(k)$ (see eq. (3.3.7)).

4.3.2 . N topology

For the N topology the numerator in eq. (4.3.2) is

$$\mathcal{N}_N = P_{\mu\nu\rho\sigma} t_\uparrow^{\mu\nu} t_\downarrow^{*\rho\sigma}. \quad (4.3.12)$$

Performing again the IBP reduction procedure and using the symmetry $u_1 \leftrightarrow u_2$, we find that \mathcal{I}_N can be rewritten in terms of two master integrals, g_2 and g_3 ,

$$\mathcal{I}_N(\gamma, \varepsilon) = C_{N,2}(\gamma, \varepsilon) g_2(\varepsilon, \gamma) + \frac{C_{N,3}(\gamma, \varepsilon)}{\varepsilon \sqrt{\gamma^2 - 1}} g_3(\gamma, \varepsilon), \quad (4.3.13)$$

where $C_{N,2}$ and $C_{N,3}$ are functions starting at order ε^0 . The coefficient in front of g_3 diverges for $\varepsilon \rightarrow 0$ but this is compensated by g_3 that starts at order ε , see eqs. (4.2.26) and (4.2.29). Plugging in the LO solutions for g_2 and g_3 , we eventually find

$$\begin{aligned} \mathcal{E}_N(\gamma) = \frac{\pi}{8} & \left[\frac{4(20\gamma^6 - 64\gamma^5 + 98\gamma^4 - 80\gamma^3 + 28\gamma^2 - 1)}{(\gamma^2 - 1)^{3/2}} \right. \\ & \left. + \frac{4(2\gamma^2 - 3)(2\gamma^4 - 2\gamma^2 + 1)\gamma \operatorname{arccosh}(\gamma)}{(\gamma^2 - 1)^{3/2} \sqrt{\gamma^2 - 1}} \right], \end{aligned} \quad (4.3.14)$$

where we have used eq. (2.3.21) to replace

$$-\log(x) = \operatorname{arccosh} \gamma. \quad (4.3.15)$$

4.3.3 . IY topology

For the IY topology the numerator in eq. (4.3.2) is

$$\mathcal{N}_{IY}(\gamma, \varepsilon) = 2P_{\mu\nu\rho\sigma} \operatorname{Re} [t_\uparrow^{\mu\nu} t_\uparrow^{*\rho\sigma}]. \quad (4.3.16)$$

After the IBP reduction we find that \mathcal{I}_{IY} is given in terms of g_1 , g_2 and g_3 , i.e.

$$\mathcal{I}_{IY}(\gamma, \varepsilon) = C_{IY,1}(\gamma, \varepsilon) g_1(\gamma, \varepsilon) + C_{IY,2}(\gamma, \varepsilon) g_2(\gamma, \varepsilon) + \frac{C_{IY,3}(\gamma, \varepsilon)}{\varepsilon \sqrt{\gamma^2 - 1}} g_3(\gamma, \varepsilon), \quad (4.3.17)$$

Both $C_{IY,1}$ and $C_{IY,2}$ start at order ε^{-1} , leading to a seemingly divergent term for $\varepsilon \rightarrow 0$,

$$\mathcal{I}_{IY}(\gamma) \supset \frac{1}{\varepsilon} \left[\frac{2\gamma^4 - 3\gamma^2 + 3}{8} (g_1 - g_2) - \frac{\gamma(6\gamma^4 + \gamma^2 - 15)}{32\sqrt{\gamma^2 - 1}} g_3 \right]. \quad (4.3.18)$$

However, this is finite because both $g_1 - g_2$ and g_3 start at order ε .

Inserting the solutions for g_1 , g_2 and g_3 given in eqs. (4.2.26)–(4.2.29), we eventually obtain

$$\begin{aligned} \mathcal{E}_{\text{IV}}(\gamma) = & \frac{\pi}{8} \left[\frac{208\gamma^8 + 384\gamma^7 - 64\gamma^6 - 278\gamma^5 + 158\gamma^4 - 5867\gamma^3 + 8349\gamma^2 - 2759\gamma - 83}{12(\gamma + 1)\sqrt{\gamma^2 - 1}} \right. \\ & \left. + \frac{(2\gamma^2 - 3)(3\gamma^2 + 5)\gamma \operatorname{arccosh}(\gamma)}{4\sqrt{\gamma^2 - 1}} - \frac{4(2\gamma^4 - 3\gamma^2 + 3)}{\sqrt{\gamma^2 - 1}} \log\left(\frac{\gamma + 1}{2}\right) \right], \end{aligned} \quad (4.3.19)$$

where we used again eq. (4.3.15) and

$$\log\left(\frac{(x+1)^2}{4x}\right) = \log\left(\frac{\gamma+1}{2}\right). \quad (4.3.20)$$

4.3.4 . H topology

Finally, we need to compute the contribution of the H topology, for which

$$\mathcal{N}_{\text{H}} \equiv \frac{1}{2} P_{\mu\nu\rho\sigma} t_{\pm}^{\mu\nu} t_{\pm}^{*\rho\sigma}. \quad (4.3.21)$$

IBP reducing one last time, we find

$$\mathcal{I}_{\text{H}}(\gamma, \varepsilon) = C_{\text{H},1}(\gamma, \varepsilon) g_1(\gamma, \varepsilon) + C_{\text{H},2}(\gamma, \varepsilon) g_2(\gamma, \varepsilon) + C_{\text{H},4}(\gamma, \varepsilon) g_4(\gamma, \varepsilon). \quad (4.3.22)$$

Once again, the cancellation of divergencies for $\varepsilon \rightarrow 0$ is non-trivial. Before expanding g_1 , g_2 and g_4 we obtain a seemingly divergent term,

$$\begin{aligned} \mathcal{I}_{\text{H}}(\gamma) \supset & \frac{1}{4\varepsilon} \left[\frac{83\gamma^4 - 420\gamma^3 + 738\gamma^2 - 532\gamma + 195}{12} g_2 - \frac{35\gamma^4 - 60\gamma^3 + 90\gamma^2 - 76\gamma + 27}{2} g_4 \right. \\ & \left. - (2\gamma^4 - 15\gamma^3 + 27\gamma^2 - 19\gamma + 7) g_1 \right], \end{aligned} \quad (4.3.23)$$

which however is finite once we use the solutions for g_1 , g_2 and g_4 , eqs. (4.2.26)–(4.2.28) and (4.2.30). Using these, we obtain

$$\begin{aligned} \mathcal{E}_{\text{H}}(\gamma) = & -\frac{\pi}{8} \left[\frac{2(\gamma - 1)(32\gamma^7 + 92\gamma^6 + 60\gamma^5 + 166\gamma^4 - 236\gamma^3 - 1017\gamma^2 + 996\gamma - 261)}{3(\gamma + 1)\sqrt{\gamma^2 - 1}} \right. \\ & \left. + \frac{(\gamma - 1)(19\gamma^3 + 79\gamma^2 - 47\gamma + 29)}{\sqrt{\gamma^2 - 1}} \log\left(\frac{\gamma + 1}{2}\right) \right]. \end{aligned} \quad (4.3.24)$$

4.4 . Final result

Summing up all the above contributions, i.e. eqs. (4.3.6), (4.3.14), (4.3.19) and (4.3.24), and taking into account also the symmetric ones, we eventually obtain

$$\mathcal{E}_{\text{pp}}(\gamma) = \frac{\pi}{8} \left[f_1(\gamma) + f_2(\gamma) \log\left(\frac{\gamma + 1}{2}\right) + f_3(\gamma) \frac{\gamma \operatorname{arccosh}(\gamma)}{2\sqrt{\gamma^2 - 1}} \right], \quad (4.4.1)$$

with

$$f_1(\gamma) = \frac{210\gamma^6 - 552\gamma^5 + 339\gamma^4 - 912\gamma^3 + 3148\gamma^2 - 3336\gamma + 1151}{6(\gamma^2 - 1)^{3/2}}, \quad (4.4.2)$$

$$f_2(\gamma) = -\frac{35\gamma^4 + 60\gamma^3 - 150\gamma^2 + 76\gamma - 5}{\sqrt{\gamma^2 - 1}}, \quad (4.4.3)$$

$$f_3(\gamma) = \frac{(2\gamma^2 - 3)(35\gamma^4 - 30\gamma^2 + 11)}{(\gamma^2 - 1)^{3/2}}. \quad (4.4.4)$$

This agrees with the one derived via different methods [110, 120, 121, 129, 153], and complete the LO radiated sector derived with an EFT worldline approach [206].

From eq. (4.2.1) one can compute the COM radiated energy using eq. (1.4.16), obtaining [120]

$$\Delta E_{\text{hyp}} = \frac{G^3 M^4 \nu^2}{b^3 \Gamma} \mathcal{E}_{\text{pp}}(\gamma) + \mathcal{O}(G^4), \quad (4.4.5)$$

This result has been used to check with the literature in different regimes. For instance, one can compare against post-Newtonian computations up to 2PN [41, 82, 234] by expanding it for small velocities. From eq. (4.4.5), one can also obtain the radiated energy in elliptic orbits in the high ellipticity limit via analytic continuation [114, 192] and compare the small velocity expansion with known 3PN results [21]. We refer to [120, 121, 153, 193] for a more thorough discussion.

4.5 . Summary of the chapter

To summarize, in this chapter we applied the roadmap depicted in figure 7 (page 56) in order to find the LO radiated four-momentum. We recasted the problem as a cut two-loop integral and we divided it in four topologies.

Employing reverse unitarity [121, 168–171] and the IBP identities [172–176], we reduced the problem to the computation of just four MIs given in eqs. (4.2.13)–(4.2.16), that we solved using the differential equation method [180–185]. Finally, to find the suitable boundary conditions, we compute the non cut MIs in the near static limit (see appendix B) and we used Cutkosky’s rules [204, 205, 227, 228] to related these results with the cut MIs.

In the following, we employ again all these steps to go beyond the point-particle approximation and include the effects of tidal deformations and spins.

5 - Beyond point-particle: Tidal deformations

Until now we have studied the dynamics of two point-like massive objects interacting via gravity. While this approximation works well when the objects are far from each other, it misses the influence of their internal structure when they get closer. An important target of current and future observations of GW signals is the measurement of tidal deformations during the coalescence of compact objects [144, 198, 199, 241–247], which may shed light on the internal structure of neutron stars [248], the nature of black holes [249] or the existence of more exotic astrophysical objects [250–252].

Tidal deformations affect the conservative two-body dynamics as well as the emitted energy in GWs. They have been studied employing different analytical techniques, most notably the PN expansion [59–61, 253–255], the effective-one-body approach [212, 256, 257], classical EFT approaches [20, 23–27] and the self-force formalism [258–261]. see [262] for a review of the different approaches and waveform models for tidal deformations.

Tidal effects have been also studied within the PM expansion using on-shell scattering amplitude methods [131–136, 263, 264] as well as worldline approaches [149, 155–158, 265]. These developments concern mainly the conservative sector of the scattering of the two objects. By following a procedure analogous to the one outlined in the previous chapters, we shall here show how to incorporate tidal effects in the radiative sector [155, 167, 208, 263]. In particular, we focus on the leading tidal contributions to the orbital dynamics, i.e. quadrupolar deformations, but this study can be straightforwardly extended to higher multipoles using the same approach.

5.1 . Tidal deformations in the worldline action

In the EFT approach, one can add modifications to the point-particle approximation by adding a set of unknown operators that describe such effects. Since the exact physics that determines the internal structure of the compact objects sourcing the gravitational field is still unknown, it is convenient to parametrize our ignorance of the system at the scale of the objects with suitable operators [20, 26, 144]. We can then match this description with either experimental data or a theory of the physics inside the bodies. In practice, considering one spinless body of mass m as in chapter 1, we can include finite-size effects in eq. (1.2.4) by modifying the mass-shell constraint,

$$\mathcal{H}_m = -e(\lambda) \left[\frac{p^2 - m^2}{2m} + \sum_n \mathcal{O}_n(\lambda) \right], \quad (5.1.1)$$

where λ is the affine parameter describing the worldline. On the right-hand-side, $\mathcal{O}_n(\lambda)$ are a tower of generic operators parametrizing the finite-size effects that satisfy the symmetries of the system far from the object, i.e. invariance under diffeomorphism and re-parametrization of the worldline. They depend on the gravitational field, and we

shall specify their precise form momentarily. Following steps similar to the ones shown in section 1.2 we arrive to the action

$$S_m = -\frac{1}{2} \int d\lambda \frac{1}{e(\lambda)} \left[m \dot{x}^2(\lambda) + e^2(\lambda) \left(m + \sum_n \mathcal{O}_n(\lambda) \right) \right], \quad (5.1.2)$$

where $\dot{x}^2 = g_{\mu\nu} \dot{x}^\mu \dot{x}^\nu$. Note that now $e(\lambda)$ satisfies the equation

$$m \frac{\dot{x}^2(\lambda)}{e^2(\lambda)} - m - \sum_n \mathcal{O}_n(\lambda) = 0. \quad (5.1.3)$$

At this point, we can still choose the affine parameter τ such that $e(\tau) = 1$. Defining again $\mathcal{U}^\mu = dx^\mu/d\tau$, from the previous equation we find that

$$\mathcal{U}^2(\tau) = 1 + \frac{1}{m} \sum_n \mathcal{O}_n(\tau). \quad (5.1.4)$$

This means that in this case τ is not exactly the proper time. In a scattering scenario, the bodies in the far past move freely in empty space, thus we expect

$$\mathcal{O}_n(\tau) \rightarrow 0, \text{ for } \tau \rightarrow -\infty. \quad (5.1.5)$$

This implies that τ is the proper time in the asymptotic past. We shall now employ this affine parameter to describe the worldline. From eq. (5.1.2) we then obtain the action

$$S_m = -\frac{1}{2} \int d\tau \left[m \mathcal{U}^2(\tau) + m + \sum_n \mathcal{O}_n(\tau) \right]. \quad (5.1.6)$$

Let us now focus on the finite-size operators. After discarding redundant couplings involving the Ricci scalar and tensor [20, 26], the operators $\mathcal{O}_n(\tau)$ can be written in terms of contractions of the Weyl or, equivalently, the Riemann tensor. It is convenient to further decompose this into gravito-electric and -magnetic components defined respectively as

$$E_{\mu\nu} \equiv R_{\mu\alpha\nu\beta} \mathcal{U}^\alpha \mathcal{U}^\beta, \quad B_{\mu\nu} \equiv \frac{1}{2} \epsilon_{\alpha\beta\gamma\mu} R^{\alpha\beta}{}_{\delta\nu} \mathcal{U}^\gamma \mathcal{U}^\delta, \quad (5.1.7)$$

where $\epsilon_{\alpha\beta\gamma\mu}$ is the Levi-Civita (pseudo) tensor. They are symmetric and obey

$$g_{\mu\nu} E^{\mu\nu} = 0 = g_{\mu\nu} B^{\mu\nu}, \quad E_{\mu\nu} \mathcal{U}^\nu = 0 = B_{\mu\nu} \mathcal{U}^\nu. \quad (5.1.8)$$

We can then parametrize finite-size effects using symmetric trace-free multipole moments [266]. Going in a locally flat co-moving frame by introducing a vierbein $e^\mu{}_i$ s.t. $e^\mu{}_0 = \mathcal{U}^\mu$ and $e^\mu{}_a e^\nu{}_b g_{\mu\nu} = \eta_{ab}$, we can write this moments as

$$\sum_n \int d\tau \mathcal{O}_n(\tau) = \int d\tau \left(Q_{ab}^E(\tau) E^{ab}(x(\tau)) + Q_{ab}^B(\tau) B^{ab}(x(\tau)) + \dots \right), \quad (5.1.9)$$

where the indices are raised and lower with the flat metric η_{ab} . Here we have written for simplicity only the first deformation given by the electric and magnetic quadrupole moments of the massive object, Q_{ab}^E and Q_{ab}^B , because all of the following discussion can be done analogously for any multipole moment. [26, 198, 199, 212].

let us focus on Q_{ab}^E . We can decompose it into two components

$$Q_{ab}^E = \bar{Q}_{ab}^E + \delta Q_{ab}^E, \quad (5.1.10)$$

where:

- \bar{Q}_{ab}^E is an intrinsic permanent multipole of the body that depends on the physics at the scale of the object;
- δQ_{ab}^E is an induced multipole due to the presence of a long-wavelength interaction.

As we said earlier, here we consider non-rotating bodies for which the multipoles of the first kind are zero, leaving us with only the induced tidal deformations. We shall see in the next chapter an explicit example of a non-zero permanent multipole. Using linear response theory, we can write [20, 26, 131, 212]

$$\delta Q_{ab}^E(\tau) = \int d\tau' G_{\text{ret}}(\tau, \tau') E_{ab}(x(\tau')), \quad (5.1.11)$$

where $G_{\text{ret}}(\tau, \tau')$ is the green function describing the interaction inducing the deformation. We consider local interactions whose frequency ω is larger than the size of the object, i.e. $\omega R_s \ll 1$. We can then go in frequency space in eq. (5.1.11) and write

$$\begin{aligned} \delta Q_{ab}^E(\tau) &= \int d\tau' \int \frac{d\omega}{2\pi} \left(c_{E^2}^{(2,0)} + c_{E^2}^{(2,1)} \omega^2 + \dots \right) e^{-i\omega(\tau-\tau')} E_{ab}(x(\tau')) \\ &= c_{E^2}^{(2,0)} E_{ab}(x(\tau)) - c_{E^2}^{(2,1)} \frac{d^2}{d\tau^2} E_{ab}(x(\tau')) + \dots, \end{aligned} \quad (5.1.12)$$

where we have performed an expansion for small ω of the Fourier transform of $G_{\text{ret}}(\tau, \tau')$ and considered only even power of ω because at this stage the system is still conservative. The constants $c_{E^2}^{(n,l)}$ are unknown Wilson coefficients that contains all the information about the internal structure of the body. Plugging this result in eq. (5.1.9) and integrating by parts, we finally obtain

$$\sum_n \int d\tau \mathcal{O}_n(\tau) = \int d\tau \left(c_{E^2}^{(2,0)} E_{\mu\nu} E^{\mu\nu} + c_{E^2}^{(2,1)} \frac{d}{d\tau} E_{\mu\nu} \frac{d}{d\tau} E^{\mu\nu} + \dots \right), \quad (5.1.13)$$

where we get rid of the flat-frame indices by covariantizing the final result. An analogous discussion holds for $Q_{\mu\nu}^B$.

Following a similar procedure for the other multipole moments, we can describe the full tidal-modified action in eq. (5.1.6) as $S_m = S_{\text{pp}} + S_{\text{tidal}}$, where S_{pp} is the usual point-particle action given in eq. (1.2.7), and

$$S_{\text{tidal}} = \int d\tau \sum_{n=2}^{\infty} \sum_{l=0}^{\infty} \left(c_{E^2}^{(n,l)} E_{\mu_1 \dots \mu_n}^{(l)} E^{(l)\mu_1 \dots \mu_n} + c_{B^2}^{(n,l)} B_{\mu_1 \dots \mu_n}^{(l)} B^{(l)\mu_1 \dots \mu_n} \right), \quad (5.1.14)$$

with the higher rank tensors defined as

$$E_{\mu_1 \dots \mu_n} = \text{Sym}_{\mu_1 \dots \mu_n} \left[\Pi_{\mu_3}^{\nu_3} \dots \Pi_{\mu_n}^{\nu_n} \nabla_{\nu_3} \dots \nabla_{\nu_n} E_{\mu_1 \mu_2} \right], \quad (5.1.15)$$

$$E_{\mu_1 \dots \mu_n}^{(l)} = (u^\alpha \nabla_\alpha)^l E_{\mu_1 \dots \mu_n} = (\partial_\tau)^l E_{\mu_1 \dots \mu_n}, \quad (5.1.16)$$

where $\Pi_{\mu\nu} = g_{\mu\nu} - \mathcal{U}_\mu \mathcal{U}_\nu$ is the \mathcal{U} -orthogonal projector on the worldline, and $\text{Sym}_{\mu_1 \dots \mu_n}$ stands for the symmetrization of all indices μ_1, \dots, μ_n inside the square brackets. An analogous definition goes for the magnetic components. Note that in eq. (5.1.14) we include a factor $1/2$ in the definition of the coefficients $c_{E^2}^{(n,0)}$ and $c_{B^2}^{(n,0)}$.

One can also go beyond the linear response described here and include higher order operators in $E_{\mu\nu}$ and $B_{\mu\nu}$ responsible of non-linear tidal effects, see e.g. [131, 265]. The Wilson coefficients $c_{E^2}^{(n,0)}$ and $c_{B^2}^{(n,0)}$ are linked to the size of the body and the tidal Love numbers [198, 199, 212, 267]. These are dimensionless coefficients that depend on the equation of states of the internal structure of the object and decrease as the compactness increases, reaching zero in the case of a black hole [198, 199, 245, 268]. What we have outlined here for one single object can be easily extended to a binary or even a multi-body system.

5.2 . Tidal effects in the radiative sector

We now describe how to perform computations similar to the one performed in the previous chapter in the presence of tidal deformations. For simplicity, we shall consider only the LO mass and current quadrupole deformation which means that our starting point effective action is given by¹

$$S_{\text{eff},2} = S_{\text{eff},1} + \sum_{a=1,2} \int d\tau_a \left(c_{E_a^2} E_{\mu\nu}^a E_a^{\mu\nu} + c_{B_a^2} B_{\mu\nu}^a B_a^{\mu\nu} \right), \quad (5.2.1)$$

where $S_{\text{eff},1}$ is given in eq. (1.3.1). Note that the Wilson coefficients have mass dimension $[c_{E_a^2}] = [c_{B_a^2}] = -3$. The explicit relation with the relativistic Love numbers $k_a^{(2)}$ and $j_a^{(2)}$ is, respectively [198, 199, 212],

$$c_{E_a^2} = \frac{k_a^{(2)} R_a^5}{6G}, \quad c_{B_a^2} = \frac{j_a^{(2)} R_a^5}{32G}, \quad (5.2.2)$$

with R_a the radius of the object a .

We focus on the radiative sector, therefore we want to find the pseudo stress-energy tensor defined in eq. (1.3.17) including the tidal deformations we have just described. Following again the matching procedure described in the previous chapters, first we expand $g_{\mu\nu} = \eta_{\mu\nu} + h_{\mu\nu}/m_{\text{Pl}}$ in eq. (5.2.1) and find the relevant Feynman rules. All the rules coming from $S_{\text{eff},1}$ have been derived in section 3.1, we need to provide the new

¹For simplicity from now on we call $c_{E^2}^{(2,0)} \equiv c_{E_a^2}$ and $c_{B^2}^{(2,0)} \equiv c_{B_a^2}$.

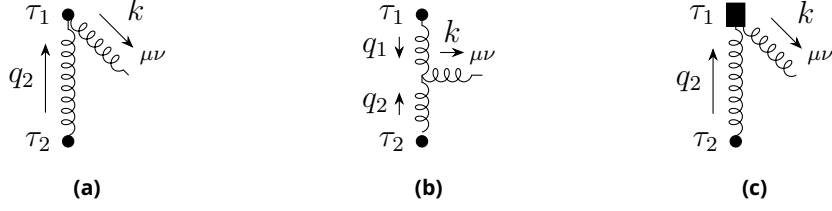


Figure 9: The Feynman diagrams needed for the computation of the stress-energy tensor: (a) and (b) are the point-particle contributions computed in section 3.2, and (c) is the tidal one. The symmetric terms are obtained by exchange of $1 \leftrightarrow 2$.

one coming from tidal contributions. Let us define the following quantities

$$\mathcal{M}_{\mu\nu\alpha\beta}^{E_a}(\ell) \equiv \frac{2\delta E_{\mu\nu}^a}{\delta h^{\alpha\beta}(\ell)} = \eta_{\mu\sigma}\eta_{\nu\rho}u_a^\sigma u_a^\rho \ell_\alpha \ell_\beta + (\ell \cdot u_a)^2 \eta_{\alpha(\mu}\eta_{\nu)\beta} - 2(\ell \cdot u_a)u_a^\rho \eta_{\rho(\mu}\eta_{\nu)\alpha} \ell_\beta + \mathcal{O}(G) , \quad (5.2.3)$$

$$\mathcal{M}_{\mu\nu\alpha\beta}^{B_a}(\ell) \equiv \frac{2\delta B_{\mu\nu}^a}{\delta h^{\alpha\beta}(\ell)} = \frac{1}{2}l^\rho u_a^\sigma \epsilon_{\rho\sigma\alpha(\mu} [\eta_{\nu)\beta}(\ell \cdot u_a) - \eta_{\nu)\rho} u_a^\rho \ell_\beta] + (\alpha \leftrightarrow \beta) + \mathcal{O}(G) , \quad (5.2.4)$$

where we use the flat metric $\eta_{\mu\nu}$ to raise and lower indices. In the above equations we have also expanded the worldlines around straight motion as in eqs. (1.4.7) and (1.4.8), hence u_a^μ are the constant initial velocities of the two objects. We also kept only the needed leading order in the PM expansion. The Feynman rules then reads

$$\tau_a \square = i \sum_{X=E,B} \frac{cX_a^2}{4m_{\text{Pl}}^2} \int d\tau_a e^{i(\ell_1+\ell_2)\cdot(b_a+u_a\tau_a)} \mathcal{M}_{\mu\nu\alpha\beta}^{X_a}(\ell_1) \mathcal{M}_{\kappa\lambda}^{X_a\alpha\beta}(\ell_2) , \quad (5.2.5)$$

On the left-hand side of eq. (5.2.5) we used a square to denotes a tidally-coupled particle evaluated using the straight worldline. We have verified that our expression agrees with the one that can be read off from the 4-point amplitude at leading PM order obtained in Ref. [131].

5.2.1 . Stress-energy tensor with tides

The stress-energy tensor needed to compute the emitted four-momentum is given by the sum of the point-particle and tidal contributions, i.e.,

$$\tilde{T}^{\mu\nu} = \tilde{T}_{\text{pp}}^{\mu\nu} + \tilde{T}_{\text{tid}}^{\mu\nu} , \quad (5.2.6)$$

where, as usual, the tilde denotes the Fourier transform. The stress-energy tensor in the point-particle case has been computed in section 3.2, see eqs. (3.2.2) and (3.2.10).

The contribution of the tidal operators to the stress-energy tensor has no static piece. The leading PM term can be obtained from the diagram (c) in figure 9 and its symmetric

under exchange of the two particles. We obtain

$$\begin{aligned}\tilde{T}_{\text{tid}}^{\mu\nu} &= \frac{m_1 m_2}{4m_{\text{P}1}^2} \int_{q_1, q_2} \delta(q_1 \cdot u_1) \delta(q_2 \cdot u_2) \delta^4(k - q_1 - q_2) \\ &\times \frac{e^{iq_1 \cdot b_1 + iq_2 \cdot b_2}}{q_1^2 q_2^2} \sum_{a=1,2} \sum_{X=E,B} t_{X_a}^{\mu\nu}(q_1, q_2),\end{aligned}\quad (5.2.7)$$

$$t_{X_1}^{\mu\nu} \equiv -2 \frac{c_{X_1}^2}{m_1} q_1^2 \eta^{\mu\alpha} \eta^{\nu\beta} \mathcal{M}_{\alpha\beta\rho\sigma}^{X_1} \mathcal{M}_{\kappa\lambda}^{X_1\rho\sigma} \left(u_2^\kappa u_2^\lambda - \eta^{\kappa\lambda} / 2 \right) \quad (5.2.8)$$

Defining $\beta_\gamma = 2\gamma^2 - 1$ and using eqs. (5.2.3) and (5.2.4), the explicit expressions of $t_{E_1}^{\mu\nu}$ and $t_{B_1}^{\mu\nu}$ is

$$\begin{aligned}t_{E_1}^{\mu\nu} &= \frac{c_{E_1}^2}{m_1} q_1^2 \left[\omega_1^4 \eta^{\mu\nu} - \beta_\gamma \omega_1^2 q_2^\mu q_2^\nu - 2\omega_1^3 q_1^{(\mu} u_1^{\nu)} + 2\omega_1^2 (\gamma(q_1^2 - q_2^2 - k^2) + 2\omega_1 \omega_2) u_1^{(\mu} u_2^{\nu)} \right. \\ &- \omega_1 (\beta_\gamma (q_1^2 - q_2^2 - k^2) + 4\gamma\omega_1 \omega_2 + 2\omega_1^2) q_2^{(\mu} u_1^{\nu)} + 4\gamma\omega_1^3 q_2^{(\mu} u_2^{\nu)} - 2\omega_1^4 u_2^\mu u_2^\nu \\ &\left. - \left(\beta_\gamma \frac{(q_1^2 - q_2^2 - k^2)^2}{4} + 2\gamma\omega_1 \omega_2 (q_1^2 - q_2^2 - k^2) - k^2 \omega_1^2 + 2\omega_1^2 \omega_2^2 \right) u_1^\mu u_1^\nu \right],\end{aligned}\quad (5.2.9)$$

$$\begin{aligned}t_{B_1}^{\mu\nu} &= \frac{c_{B_1}^2}{m_1} q_1^2 \left[\omega_1^2 \left(\frac{q_1^2 - q_2^2 - k^2}{2} + \omega_1^2 \right) \eta^{\mu\nu} - \omega_1 (\beta_\gamma \omega_1 - 2\gamma\omega_2) q_2^\mu q_2^\nu + \omega_1^2 q_1^{(\mu} q_2^{\nu)} \right. \\ &- \left(\frac{(\gamma(q_1^2 - q_2^2 - k^2) + 2\omega_1 \omega_2)^2}{2} - k^2 \omega_1^2 \right) u_1^\mu u_1^\nu - \omega_1^2 (q_1^2 - q_2^2 - k^2 + 2\omega_1^2) u_2^\mu u_2^\nu \\ &- \left(\omega_1 (k^2 + 2\omega_1^2 - 2\omega_2^2 + 4\gamma\omega_1 \omega_2) + \frac{q_1^2 - q_2^2 - k^2}{2} ((1 + 4\gamma^2)\omega_1 - 2\gamma\omega_2) \right) q_2^{(\mu} u_1^{\nu)} \\ &+ \omega_1 (\gamma(q_1^2 - q_2^2 - k^2) + 4\gamma\omega_1^2 - 2\omega_1 \omega_2) q_2^{(\mu} u_2^{\nu)} - \omega_1 \left(\frac{q_1^2 - q_2^2 - k^2}{2} + 2\omega_1^2 \right) q_1^{(\mu} u_1^{\nu)} \\ &\left. + \left(\frac{q_1^2 - q_2^2 - k^2}{2} + 2\omega_1^2 \right) (\gamma(q_1^2 - q_2^2 - k^2) + 2\omega_1 \omega_2) u_1^{(\mu} u_2^{\nu)}. \right]\end{aligned}\quad (5.2.10)$$

Analogous expressions hold for $t_{E_2}^{\mu\nu}$ and $t_{B_2}^{\mu\nu}$ with $(1 \leftrightarrow 2)$. In chapter 3 we saw that $k_\mu \tilde{T}_{\text{pp}}^{\mu\nu} = 0$, therefore here we can focus just on the above quantities. We have verified that the total stress energy tensor including tidal effect is conserved in general, i.e. that $k_\mu \tilde{T}_{\text{tid}}^{\mu\nu} = 0$ for any k^μ . To simplify computations, in the next sections we shall consider the external momentum to be on-shell, i.e. impose $k^2 = 0$ in eqs. (5.2.9) and (5.2.10). We can also discard terms proportional to q_2^2 which give only short-range contributions.

Before proceeding, we find important to write how the tidal contributions to the stress-energy tensor scale w.r.t. the leading point-particle term. Following what we said in Sec. 1.3, neglecting the static piece from eq. (3.2.10) we see that $\tilde{T}_{\text{pp}}^{\mu\nu} \sim Gm^2$. Recalling eq. (5.2.2), for the tidal contribution of eq. (5.2.7) we find

$$\tilde{T}_{\text{tid}}^{\mu\nu} \sim Gm^2 \times (Gmq)^4 \left(\frac{R}{Gm} \right)^4, \quad (5.2.11)$$

where \mathbf{x} denotes either the electric $k^{(2)}$ or the magnetic $j^{(2)}$ love number and R is the typical value of the radius of the scattered objects. According to the scaling outlined

in Sec. 1.3, tidal deformations seems to start being relevant at 5PM order. However, $\tilde{T}_{\text{tid}}^{\mu\nu}$ contains a factor of $(R/Gm)^4$, which means that these effects can be enhanced and enter earlier in the perturbation expansion whenever we look at an objects like neutron stars whose size is bigger than their Schwarzschild radius Gm [59–61, 243, 246].

5.2.2 . Asymptotic waveform

Following the procedure of section 3.4.1, we can find the asymptotic waveform in direct space from the stress-energy tensor we have just computed. Following eq. (3.4.11), we work in the TT gauge and define the contribution of the tidal deformations to the waveform as

$$h_{ij}^{\text{tid}}(x) = \frac{1}{r} \left[\epsilon_{ij}^+ f_{\text{tid}}^{(+)} + \epsilon_{ij}^- f_{\text{tid}}^{(-)} \right] + \mathcal{O}\left(G^{5/2}\right), \quad (5.2.12)$$

where, calling $k^0 = \omega$ and t_r the retarded time,

$$f_{\text{tid}}^{(\pm)} \equiv \frac{1}{8\pi m_{\text{Pl}}} \int \frac{d\omega}{2\pi} e^{-i\omega t_r} \epsilon_{ij}^{\pm*} \tilde{T}_{\text{tid}}^{ij} \Big|_{k^\mu = \omega n^\mu}, \quad (5.2.13)$$

If computed in the COM frame, the results for $f_{\text{tid}}^{(\pm)}$ could be use to compute the emitted angular momentum as in section 3.5.3. Also in this case, for the LO computation one needs only the total gravitational wave-memory of the tidal contribution, i.e.

$$\int dt_r \dot{f}_\lambda^{\text{tid}} = -\frac{i}{8\pi m_{\text{Pl}}} \int \frac{d\omega}{2\pi} \delta(\omega) \omega \epsilon_{ij}^{\pm*} \tilde{T}_{\text{tid}}^{ij}. \quad (5.2.14)$$

From the previous equation we understand that only the soft limit of the stress-energy tensor given in eq. (5.2.7) contributes. It is not hard to see that

$$\epsilon_{ij}^{\pm*} \tilde{T}_{\text{tid}}^{ij} = \mathcal{O}(\omega^3), \quad \text{for } \omega \rightarrow 0, \quad (5.2.15)$$

which implies

$$\int dt_r \dot{f}_\lambda^{\text{tid}} = 0. \quad (5.2.16)$$

This means that the contribution to the emitted angular momentum coming from the leading tidal deformation is at least of order $\mathcal{O}(G^3)$.

Going back to the computation of eq. (5.2.13), plugging in the expression of the $\tilde{T}_{\text{tid}}^{\mu\nu}$ found in the previous section and using manipulations similar to the one described in section 3.4.1, one finds

$$f_{\text{tid}}^{(\pm)} = \sum_{X=E,B} \frac{Gm_2}{m_{\text{Pl}}} \frac{\epsilon_{\mu\nu}^{*\lambda}(\mathbf{n})}{n \cdot u_1} \int_q \frac{\tilde{\delta}(q \cdot u_2) e^{iq \cdot \tilde{b}_1}}{q^2 (k - q)^2} t_{X_1}^{\mu\nu}(k, q) \Big|_{\omega = \frac{q \cdot u_1}{n \cdot u_1}} + (1 \leftrightarrow 2), \quad (5.2.17)$$

where $\tilde{b}_1^\mu \equiv b^\mu + \frac{u_1^\mu}{n \cdot u_1} (t_r - n \cdot b_1)$. We can then choose a frame and remove the remaining delta function by integrating in q^0 . Regardless of the chosen frame, the remaining integral

can be put in the form of the integrals

$$I = \int_{\mathbf{q}} \frac{e^{i\mathbf{q}\cdot\mathbf{b}}}{\mathbf{q}\cdot\mathbf{M}\cdot\mathbf{q}} = \frac{1}{4\pi} \frac{[\mathbf{b}\cdot\mathbf{M}^{-1}\cdot\mathbf{b}]^{-1/2}}{[\det(\mathbf{M})]^{1/2}}, \quad (5.2.18)$$

$$I^{i_1, \dots, i_n} = \int_{\mathbf{q}} \frac{\mathbf{q}^{i_1} \dots \mathbf{q}^{i_n} e^{i\mathbf{q}\cdot\mathbf{b}}}{\mathbf{q}\cdot\mathbf{M}\cdot\mathbf{q}} = \frac{\partial}{i\partial b_{i_1}} \dots \frac{\partial}{i\partial b_{i_n}} I \quad (5.2.19)$$

where \mathbf{M} is a 3×3 matrix. For simplicity, we perform the calculation in the rest frame of particle 2 defined in eq. (3.3.8) obtaining

$$f_{\text{tid}}^{(\pm)} = \frac{15Gm_1m_2}{4\pi m_{\text{Pl}}} \frac{\gamma^2 - 1}{b^5} \sum_{a=1,2} \sum_{X=E,B} \frac{c_{X_a} \epsilon_{ij}^{*\lambda} e_i^j A_{X_a}^{IJ}}{m_a (n \cdot u_a)^3 c_a^{9/2}}, \quad (5.2.20)$$

where we have introduced an extra index $I, J = v, b$, and the functions

$$c_1 = 1 + \frac{\gamma^2 - 1}{\gamma^2 (n \cdot u_1)^2} \left(\frac{t_r}{b} + \mathbf{n} \cdot \mathbf{e}_b \right)^2, \quad c_2 = 1 + (\gamma^2 - 1) \frac{t_r^2}{b^2} \quad (5.2.21)$$

Defining $f_a = 6c_a - 7$, $g_a = \sqrt{c_a - 1}(4c_a - 7)$ and $v = \sqrt{\gamma^2 - 1}/\gamma$ the explicit expressions for $A_{X_a}^{IJ}$ are

$$\begin{aligned} A_{E_a}^{bb} &= (n \cdot u_a)^2 \beta \gamma f_a, \\ A_{E_a}^{vb} &= \gamma (n \cdot u_a) [f_a \beta \gamma v \delta_{a1} \mathbf{e}_b \cdot \mathbf{n} + g_a], \\ A_{E_a}^{vv} &= \frac{(2f_a^2 - 17f_a - 7)}{30} + f_a (\gamma^2 - 1) + v \gamma^2 \delta_{a1} \mathbf{e}_b \cdot \mathbf{n} [f_a \beta \gamma v \delta_{a1} \mathbf{e}_b \cdot \mathbf{n} + 2g_a], \\ A_{B_a}^{bb} &= 2\gamma (n \cdot u_a) \left[\gamma n \cdot u_a - \frac{(n \cdot u_1)(n \cdot u_2)}{n \cdot u_a} \right] f_a, \\ A_{B_a}^{vb} &= f_a \gamma^2 (2\gamma \delta_{a1} n \cdot u_a - 1) v \mathbf{e}_b \cdot \mathbf{n} + g_a \left[\gamma n \cdot u_a - \frac{(n \cdot u_1)(n \cdot u_2)}{n \cdot u_a} \right], \\ A_{B_a}^{vv} &= 2\gamma^2 v \mathbf{e}_b \cdot \mathbf{n} \left[f_a \gamma^2 v \delta_{a1} \mathbf{e}_b \cdot \mathbf{n} + \frac{\gamma \delta_{a1} - \delta_{a2}}{\gamma} g_a \right]. \end{aligned} \quad (5.2.22)$$

One can verify that, performing the low-velocity expansion, the contribution of the magnetic quadrupole enters at 1PN higher than the electric one, as expected. This expression has been recently confirmed in Ref. [167].

5.3 . Radiated four-momentum with tides

The derivation of the emitted linear momentum closely follows the procedure presented in chapter 4. Starting again from eq. (4.1.4) we have

$$P_{\text{rad}}^\mu = \frac{1}{4m_{\text{Pl}}^2} \int_k \tilde{\delta}_+(k^2) k^\mu P_{\alpha\beta\rho\sigma} \left(\tilde{T}_{\text{pp}}^{\alpha\beta} + \tilde{T}_{\text{tid}}^{\alpha\beta} \right) \left(\tilde{T}_{\text{pp}}^{*\rho\sigma} + \tilde{T}_{\text{tid}}^{*\rho\sigma} \right) \quad (5.3.1)$$

$$= P_{\text{pp}}^\mu + \frac{1}{2m_{\text{Pl}}^2} \int_k \tilde{\delta}_+(k^2) k^\mu \text{Re} \left[\tilde{T}_{\text{pp}}^{\alpha\beta} P_{\alpha\beta\rho\sigma} \tilde{T}_{\text{tid}}^{*\rho\sigma} \right] + \dots \quad (5.3.2)$$

In the above equation we considered only the LO terms in the Tidal deformation. Recalling eq. (5.2.11), we see that the contribution quadratic in \tilde{T}_{tid} is further suppressed by $\mathcal{O}(G^4)$ and is thus neglected. P_{pp}^μ is the emitted momentum in the point-particle case computed in chapter 4 and given by eqs. (4.2.1) and (4.4.1). The second term is the first tidal deformation contribution. Ignoring the static piece that does not contribute to the observable, is explicitly given by

$$P_{\text{tid}}^\mu = \frac{1}{2m_{\text{Pl}}^2} \int_k \delta_+(k^2) k^\mu \text{Re} \left[\tilde{T}_{\text{NLO}}^{\alpha\beta}(k) P_{\alpha\beta\rho\sigma} \tilde{T}_{\text{tid}}^{\rho\sigma}(-k) \right], \quad (5.3.3)$$

with $\tilde{T}_{\text{NLO}}^{\mu\nu}$ and $\tilde{T}_{\text{tid}}^{\mu\nu}$ given respectively in eqs. (3.2.10) and (5.2.7). Analogously to eq. (4.1.7), we can interpret the phase-space delta function as a cut propagator, so that the integrand reproduces vacuum-to-vacuum diagrams with a cut, pictorially represented as follows

$$P_{\text{tid}}^\mu = \frac{1}{2m_{\text{Pl}}^2} \sum_{X=E,B} \int_k k^\mu \text{Re} \left[\begin{array}{c} \text{Diagram 1} \\ \text{Diagram 2} \\ \text{Diagram 3} \end{array} \right] + (1 \leftrightarrow 2). \quad (5.3.4)$$

In drawing this we have considered again the upper dot as body $a = 1$ and the lower one as $a = 2$. In contrast with the point-particle case, at LO in the tidal effects we just need to compute three topologies. The H -like diagram is absent, because there are no tidal interactions linear in $h_{\mu\nu}$.

Defining again $\Delta_{1,2}(q, k) \equiv \delta(q \cdot u_1) \delta(q \cdot u_2 - k \cdot u_2)$, we can explicitly write

$$\begin{aligned} \frac{\text{Re} \left[\tilde{T}^{\rho\sigma}(k) P_{\rho\sigma\alpha\beta} \tilde{T}_{\text{tid}}^{\alpha\beta}(-k) \right]}{2m_{\text{Pl}}^2} &= \frac{m_1^2 m_2^2}{32m_{\text{Pl}}^6} \sum_{X=E,B} \int_{q_1, q_2} \Delta_{1,2}(q_1, k) \Delta_{1,2}(q_2, k) \\ &\times \frac{e^{i(q_1 - q_2) \cdot b} \left(\mathcal{N}_{X_1}(q_1, q_2, k) + \mathcal{N}_{X_2}(q_1, q_2, k) \right)}{q_1^2 q_2^2 (k - q_1)^2 (k - q_2)^2}, \end{aligned} \quad (5.3.5)$$

where

$$\mathcal{N}_{X_a}(q_1, q_2, k) \equiv \text{Re} \left[\left(t_{\uparrow}^{\mu\nu}(q_1, k) + t_{\downarrow}^{\mu\nu}(q_1, k) + t_{\pm}^{\mu\nu}(q_1, k) \right) P_{\mu\nu\rho\sigma} \left(t_{X_a}^{\rho\sigma}(q_2, k) \right)^* \right]. \quad (5.3.6)$$

The numerators entering in the computation of the three topologies depicted in eq. (5.3.4) come from the contraction of respectively $t_{\uparrow}^{\mu\nu}$, $t_{\downarrow}^{\mu\nu}$ and $t_{\pm}^{\mu\nu}$ with $(t_{X_a}^{\mu\nu})^*$, as can be seen from the above equation. One must then add the $1 \leftrightarrow 2$ piece. Performing once again

the renaming defined in eq. (4.1.11) one eventually arrives to

$$P_{\text{tid}}^\mu = \frac{m_1^2 m_2^2}{32 m_{\text{Pl}}^6} \int_q \delta(q \cdot u_1) \delta(q \cdot u_2) e^{iq \cdot b} Q_{\text{tid}}^\mu, \quad (5.3.7)$$

$$Q_{\text{tid}}^\mu \equiv \sum_{X=E,B} \int_{\ell_1, \ell_2} \delta_-((\ell_1 + \ell_2 - q)^2) \delta(\ell_1 \cdot u_1) \delta(\ell_2 \cdot u_2) \times \frac{(-\ell_1^\mu - \ell_2^\mu + q^\mu) (\mathcal{N}_{X_1}(\ell_1, \ell_2, q) + \mathcal{N}_{X_2}(\ell_1, \ell_2, q))}{\ell_1^2 \ell_2^2 (\ell_1 - q)^2 (\ell_2 - q)^2}. \quad (5.3.8)$$

Once again, the LO emitted momentum can be recasted as a two-loop integration followed by a Fourier transform from q to b space.

To get rid of the free index in eq. (5.3.3), we can decompose again the emitted momentum using the four-vectors defined in eq. (2.2.8) as in (3.5.1), i.e.

$$P_{\text{tid}}^\mu = \frac{G^3 m_1^2 m_2^2}{b^3} \left(C_{u_1}^{\text{tid}} \check{u}_1^\mu + C_{u_2}^{\text{tid}} u_2^\mu - C_l^{\text{tid}} \hat{l}^\mu - C_b^{\text{tid}} \hat{b}^\mu \right). \quad (5.3.9)$$

The final integral is odd in the exchange

$$(\ell_1 \cdot \hat{b}, \ell_2 \cdot \hat{b}) \rightarrow -(\ell_1 \cdot \hat{b}, \ell_2 \cdot \hat{b}), \quad \text{and} \quad (\ell_1 \cdot \hat{l}, \ell_2 \cdot \hat{l}) \rightarrow -(\ell_1 \cdot \hat{l}, \ell_2 \cdot \hat{l}) \quad (5.3.10)$$

therefore we conclude that $C_l = C_b = 0$. Moreover, $C_{u_2} = C_{u_1}|_{1 \leftrightarrow 2}$. We finally have

$$P_{\text{tid}}^\mu = \frac{15\pi G^3 m_1^2 m_2^2}{64 b^7} \sum_{X=E,B} \left[\left(\frac{c_{X_1^2}}{m_1} \mathcal{E}^X + \frac{c_{X_2^2}}{m_2} \mathcal{F}^X \right) \check{u}_1^\mu + (1 \leftrightarrow 2) \right]. \quad (5.3.11)$$

In the above equation we divided by an extra b^4 w.r.t. the point-particle case to make \mathcal{E}^X and \mathcal{F}^X dimensionless. For convenience, we have also collected an overall numerical coefficient and split into electric and magnetic contributions.

Analogously to the point-particle case described in detail in chapter 4, \mathcal{E}^X and \mathcal{F}^X can be written as Fourier transform of a scalar cut two-loop integral, see eq. (4.2.2). In particular, introducing again the notation of eq. (4.2.4) and (4.2.5) we have

$$\begin{aligned} \mathcal{E}^X(\gamma) &= \frac{2^{17} \pi^2}{15} b^7 \int_q \delta(q \cdot u_1) \delta(q \cdot u_2) e^{iq \cdot b} (-q^2)^{5/2} \mathcal{I}_{\mathcal{E}}^X(\gamma), \\ \mathcal{F}^X(\gamma) &= \frac{2^{17} \pi^2}{15} b^7 \int_q \delta(q \cdot u_1) \delta(q \cdot u_2) e^{iq \cdot b} (-q^2)^{5/2} \mathcal{I}_{\mathcal{F}}^X(\gamma), \end{aligned} \quad (5.3.12)$$

where the cut two-loop integrals $\mathcal{I}_{\mathcal{E}}^X(\gamma)$ and $\mathcal{I}_{\mathcal{F}}^X(\gamma)$ are explicitly

$$\mathcal{I}_{\mathcal{E}}^X = \frac{1}{(-q^2)} \frac{m_1}{c_{X_1^2}} \int_{\ell_1, \ell_2} \delta_-(\rho_7) \delta(\rho_1) \delta(\rho_4) \frac{\rho_3 \mathcal{N}_{X_1}}{\rho_5 \rho_6 \rho_8 \rho_9}, \quad (5.3.13)$$

$$\mathcal{I}_{\mathcal{F}}^X = \frac{1}{(-q^2)} \frac{m_2}{c_{X_2^2}} \int_{\ell_1, \ell_2} \delta_-(\rho_7) \delta(\rho_1) \delta(\rho_4) \frac{\rho_3 \mathcal{N}_{X_2}}{\rho_5 \rho_6 \rho_8 \rho_9}, \quad (5.3.14)$$

f_1^E	$\frac{1}{2(\gamma+1)^3\sqrt{\gamma^2-1}} \left[937\gamma^9 + 1551\gamma^8 - 2463\gamma^7 - 5645\gamma^6 \right. \\ \left. + 20415\gamma^5 + 65965\gamma^4 - 349541\gamma^3 + 535057\gamma^2 - 360356\gamma + 92160 \right]$
f_1^B	$\frac{\gamma-1}{4(\gamma+1)^3\sqrt{\gamma^2-1}} \left[1559\gamma^8 + 3716\gamma^7 - 1630\gamma^6 - 11660\gamma^5 \right. \\ \left. - 28288\gamma^4 + 155292\gamma^3 - 543442\gamma^2 + 535212\gamma - 180775 \right]$
f_2^E	$30\sqrt{\gamma^2-1} (21\gamma^4 - 14\gamma^2 + 9)$
f_2^B	$210(\gamma^2 - 1)^{3/2} (1 + 3\gamma^2)$
f_3^X	$-f_2^X \frac{\gamma(2\gamma^2 - 3)}{4(\gamma^2 - 1)}$
\mathcal{F}^E	$\frac{3(\gamma-1)^2}{(\gamma+1)^3\sqrt{\gamma^2-1}} \left[42\gamma^8 + 210\gamma^7 + 315\gamma^6 - 105\gamma^5 - 944\gamma^4 \right. \\ \left. - 1528\gamma^3 + 22011\gamma^2 - 33201\gamma + 16272 \right]$
\mathcal{F}^B	$-\frac{3(\gamma-1)^3(105\gamma^5 + 630\gamma^4 + 1840\gamma^3 + 3690\gamma^2 - 17769\gamma + 15984)}{(\gamma+1)^3\sqrt{\gamma^2-1}}$

Table I: Functions specifying the radiated four-momentum in eq. (5.3.11).

Following the procedure of chapter 4, making use of reverse unitarity [168–171], we can use IBP identities to express the two-loop integrals $\mathcal{I}_{\mathcal{E},\mathcal{F}}^X$ as linear combinations of simpler master integrals. We perform this reduction using the Mathematica package LiteRed [177, 178], finding that the three integrals defined in eqs. (4.2.13)–(4.2.15) form a complete base. The absence of the integral g_4 defined in eq. (4.2.16) is expected due to the fact that in this computation we do not have the contribution of the H topology. Indeed, from eqs. (4.3.5), (4.3.13), (4.3.17) and (4.3.22), we can see that g_4 entered only in the IBP reduction of the H -like diagram in the point-particle case. Plugging the solutions of the integrals g_1 , g_2 and g_3 inside the IBP reduced version of $\mathcal{I}_{\mathcal{E}}^X$ and $\mathcal{I}_{\mathcal{F}}^X$, we eventually obtain

$$\mathcal{E}^X = f_1^X + f_2^X \log\left(\frac{\gamma+1}{2}\right) + f_3^X \frac{\operatorname{arccosh}(\gamma)}{\sqrt{\gamma^2-1}}, \quad (5.3.15)$$

with f_1^X , f_2^X , f_3^X and \mathcal{F}^X given in Table I.

5.3.1 . Radiated energy and instantaneous flux

From eq. (5.3.11), one can compute the radiated energy in the COM frame from tidal effects, $\Delta E_{\text{hyp}}^{\text{tid}}$. Using eq. (1.4.16) and the notation introduced in section 1.1,

this reads

$$\Delta E_{\text{hyp}}^{\text{tid}} = \frac{15\pi G^7 M^8 \nu^2}{64b^7 \Gamma} \mathcal{G}(\mathcal{E}^X, \mathcal{F}^X), \quad (5.3.16)$$

where

$$\mathcal{G}(\mathcal{E}^X, \mathcal{F}^X) \equiv \sum_{X=E,B} [\kappa_{X^2} \mathcal{E}^X + \lambda_{X^2} (\mathcal{F}^X - \mathcal{E}^X)], \quad (5.3.17)$$

and we have introduced the dimensionless parameters [156]

$$\lambda_{X^2} \equiv \frac{1}{G^4 M^5} \left(\frac{c_{X_1^2} m_2}{m_1} + \frac{c_{X_2^2} m_1}{m_2} \right), \quad (5.3.18)$$

$$\kappa_{X^2} \equiv \frac{1}{G^4 M^4} \left(\frac{c_{X_1^2}}{m_1} + \frac{c_{X_2^2}}{m_2} \right). \quad (5.3.19)$$

Expanding for small relative velocities $v \equiv \sqrt{\gamma^2 - 1}/\gamma$, we find

$$\begin{aligned} \mathcal{E}^E &= 288v^3 + \frac{2143}{7}v^5 + \frac{14542}{21}v^7 + \mathcal{O}(v^9), \\ \mathcal{E}^B &= -98v^5 + \frac{585}{4}v^7 + \mathcal{O}(v^9), \\ \mathcal{F}^E &= 288v^3 + 336v^5 + \frac{3027}{4}v^7 + \mathcal{O}(v^9), \\ \mathcal{F}^B &= -210v^5 - \frac{669}{4}v^7 + \mathcal{O}(v^9), \end{aligned} \quad (5.3.20)$$

which shows that the current (magnetic) quadrupole is 1PN order higher than the mass (electric) one, as expected.

On the other hand, evaluating eq. (5.3.16), for large γ we find

$$\mathcal{E}_{\text{HE}}^X = (a_X + b_X \log \gamma) \gamma^5 + \mathcal{O}(\gamma^3), \quad (5.3.21)$$

$$\mathcal{F}_{\text{HE}}^X = c_X \gamma^6 + d_X \gamma^4 + \mathcal{O}(\gamma^2), \quad (5.3.22)$$

where

$$\begin{aligned} a_E &= 937/2 - 945 \log 2, & a_B &= 1559/4 - 945 \log 2 & b_E &= b_B = 315, \\ c_E &= 126, & c_B &= 0, & d_E &= -504, & d_B &= -315. \end{aligned} \quad (5.3.23)$$

While $\mathcal{E}_{\text{HE}}^E$ and $\mathcal{E}_{\text{HE}}^B$ scale in the same way with γ , $\mathcal{F}_{\text{HE}}^E$ and $\mathcal{F}_{\text{HE}}^B$ behave differently. Moreover, contrary to the point-particle case, we find a $\log \gamma$ divergent term in the large γ limit. This is due again to the absence of an H topology contribution. Our perturbative expansion is valid for $\gamma(GM/b) \ll 1$ [123, 190, 269] (see also [82]). In this regime $\Delta E_{\text{tid}} \ll \Delta E \sim (GM/b)^3 (M/\Gamma) \gamma^3 \ll E$.

The emitted energy from a two-body encounter can be used to derive the energy loss for closed orbits employing the B2B relation [114, 192, 193], see eq. (1.5.18). Expressing the result in terms of the asymptotic angular momentum J , we find

$$\Delta E_{\text{ell}}^{\text{tid}} = \frac{15\pi G^7 M^{15} \nu^9 (1 - \gamma^2)^{7/2}}{64J^7 \Gamma^8} \mathcal{G}(\tilde{\mathcal{E}}^X, \tilde{\mathcal{F}}^X), \quad (5.3.24)$$

where for $X = E, B$

$$\tilde{\mathcal{E}}^X = \tilde{f}_1^X + \tilde{f}_2^X \log\left(\frac{\gamma+1}{2}\right) + \tilde{f}_3^X \frac{\arccos(\gamma)}{\sqrt{1-\gamma^2}}, \quad (5.3.25)$$

with $\tilde{f}_1^X = -2f_1^X$, $\tilde{f}_2^E = -2f_2^E$, $\tilde{f}_2^B = 2f_2^B$, $\tilde{f}_3^E = 2f_3^E$, $\tilde{f}_3^B = -2f_3^B$ and $\tilde{\mathcal{F}}^X = -2\mathcal{F}^X$ subject to the replacement $(\gamma^2-1)^{n/2} \rightarrow (1-\gamma^2)^{n/2}$ for $X = E, B$. In the next section we show that this expression is consistent with known results in the PN approximation.

Following [193], we can use eq. (5.3.16) to reconstruct the instantaneous flux. Using the scattering angle and the B2B map [114, 192], we can reconstruct the Hamiltonian $H(r, \mathbf{p}^2)$ and the radial momentum $\mathbf{p}_r(r, \mathcal{E}) = \sqrt{\mathbf{p}^2(r, \mathcal{E}) - J^2/r^2}$ of the system in the center-of-mass frame and the isotropic gauge, see section 1.5. Recall the definition of \mathcal{E} given in eq. (1.1.3). Then, the total emitted energy can be computed as

$$\Delta E_{\text{hyp}} = \int_{r_{\min}}^{\infty} dr \left(\frac{\partial H(r, \mathbf{p}^2)}{\partial \mathbf{p}^2} \right)^{-1} \frac{F_E(r, \mathcal{E})}{\sqrt{\mathbf{p}^2(r, \mathcal{E}) - J^2/r^2}}, \quad (5.3.26)$$

with r_{\min} the point of closest approach, and $F_E \equiv dE/dt$ the energy flux. For the computations done in the following paragraphs, we only need the straight motion version of these quantities, i.e.

$$r_{\min} = b + \mathcal{O}(G), \quad \left(\frac{\partial H(r, \mathbf{p}^2)}{\partial \mathbf{p}^2} \right)^{-1} = 2M\Gamma\xi + \mathcal{O}(G), \quad \mathbf{p}^2 = p_{\infty}^2 + \mathcal{O}(G), \quad (5.3.27)$$

with $\xi \equiv E_1 E_2 / E$, and E_a the initial asymptotic energy of body $a = 1, 2$. In the PM framework, we have computed the right hand side of this equation

$$\Delta E_{\text{hyp}} = \frac{G^3 M^6 \nu^2}{J^3} \left(\Delta E_{\text{pp}}^{(0)} + \frac{1}{J^4} \Delta E_{\text{tid}}^{(0)} \right) + \mathcal{O}(G^4), \quad (5.3.28)$$

where $\Delta E_{\text{pp}}^{(0)}$ is the emitted energy in the point-particle case computed in the previous chapter, see eq. (4.4.5) and Ref. [110, 120, 121, 129, 153, 207]. The second term in round brackets is the tidal contribution, i.e. $\Delta E_{\text{tid}}^{(0)} = J^7 \Delta E_{\text{hyp}}^{\text{tid}} / (G^3 M^6 \nu^2)$ with $\Delta E_{\text{hyp}}^{\text{tid}}$ given in eq. (5.3.16). We can expand the energy flux in the PM regime as follows

$$F_E(r, \mathcal{E}) = \frac{G^3 M^4}{r^4} \left(\mathcal{F}_{\text{pp}}^{(0)}(\mathcal{E}) + \frac{\mathcal{F}_{\text{tid}}^{(0)}(\mathcal{E})}{r^4} \right) + \mathcal{O}(G^4), \quad (5.3.29)$$

where the dependence on r is fixed by dimensional analysis. Integrating both sides of eq. (5.3.26) and matching order per order in G , we find the same $\mathcal{F}_{\text{pp}}^{(0)}(\mathcal{E})$ written in [193], while for the tidal contribution

$$\frac{G^3 M^4}{r^8} \mathcal{F}_{\text{tid}}^{(0)} = \frac{G^7 M^8}{r^8} \frac{3\nu^3 \sqrt{\gamma^2 - 1}}{4\Gamma^3 \xi} \mathcal{G}(\tilde{\mathcal{E}}^X, \tilde{\mathcal{F}}^X), \quad (5.3.30)$$

As we explain momentarily, also this expression coincides with what is known in the PN literature.

5.3.2 . Consistency checks

We can use eq. (5.3.24) to compare our result for small velocities to the emitted energy in one period derived in the PN expansion in the large eccentricity limit, i.e. to leading order in large J . Expressing eq. (5.3.24) in terms of \mathcal{E} and

$$j = \frac{J}{GM^2\nu}, \quad (5.3.31)$$

the PN expansion of our result, i.e. the limit $\gamma \rightarrow 1$ or $\mathcal{E} \rightarrow 0$ gives

$$\begin{aligned} \frac{\Delta E_{\text{ell}}^{\text{tid}}}{\pi M\nu^2} = & \frac{1}{j^7} \left[\mathcal{E}^5 4320\kappa_{E^2} - \mathcal{E}^6 \frac{30(11\kappa_{E^2}(504\nu - 149) - 209\lambda_{E^2} + 686\kappa_{B^2} + 784\lambda_{B^2})}{7} \right. \\ & + \mathcal{E}^7 \frac{5}{7} (2\kappa_{E^2} (55944\nu^2 - 24585\nu + 19250) + (-6270\nu + 2891)\lambda_{E^2} + \\ & \left. + 21\kappa_{B^2}(980\nu + 977) + \lambda_{B^2}(23520\nu - 16926)) \right] + \mathcal{O}(\mathcal{E}^8). \quad (5.3.32) \end{aligned}$$

We should be able to check this expression with PN result in the large eccentricity, i.e. large angular momentum limit.

The tidal effects on the gravitational wave energy flux for spinless bodies has been computed up to the next-to-next-to-leading order in Ref. [60]. See [59, 61] for a derivation of the equations of motion and Hamiltonian in this case, respectively; see also [263] for a calculation of the PM Hamiltonian and the emitted energy for quasi-circular orbits at leading PN order, with interactions cubic in the curvature and tidal effects. Although in [60] the results were given only for quasi-circular orbits, their authors have kindly provided us with an expression of the flux $F_E^{(\text{PN})}$ and the conserved energy E and angular momentum J for generic orbits, written in terms of r , \dot{r} and $\dot{\phi}$, respectively the two-body distance, the radial velocity and the angular velocity in the COM frame. A dot denote a derivative with respect to the time coordinate that, in the PN regime, is universal.

To find the emitted energy for generic orbits, we shall follow a procedure similar to the one outlined in [270, 271]. Inverting the following relations

$$\left. \begin{aligned} \mathcal{E} &= \frac{E(r, \dot{r}, \dot{\phi}) - M}{M\nu} \\ j &= \frac{J(r, \dot{r}, \dot{\phi})}{GM^2\nu} \end{aligned} \right\} \longrightarrow \begin{cases} \dot{r} = \dot{r}(\mathcal{E}, j, r) \\ \dot{\phi} = \dot{\phi}(\mathcal{E}, j, r) \end{cases}, \quad (5.3.33)$$

we obtain an expression for the radial and angular velocities as a function of \mathcal{E} , j and r . At this point we can find the periastron $r_+(\mathcal{E}, j)$ and apastron $r_-(\mathcal{E}, j)$ as the solution for r of $\dot{r}(\mathcal{E}, j, r) = 0$. The total emitted energy can then be found as

$$\Delta E_{\text{tid}}^{(\text{PN})}(\mathcal{E}, j) = 2 \int_{r_-(\mathcal{E}, j)}^{r_+(\mathcal{E}, j)} \frac{dr}{\dot{r}(\mathcal{E}, j, r)} F_E^{(\text{PN})}(\mathcal{E}, j, r). \quad (5.3.34)$$

We verified that this expression is equivalent to (5.3.32) in the limit of large j . As an extra check, we verified that $\Delta E_{\text{tid}}^{(\text{PN})}(\mathcal{E}, j)$ reduces to that given in [60] for circular orbits, defined by the condition $r_+(\mathcal{E}, j) = r_-(\mathcal{E}, j)$.

We can also directly compare the PN flux $F_E^{(\text{PN})}$ with the low velocity expansion of eq. (5.3.30). Although the leading PM computation is not enough to reconstruct even the complete leading PN term, we can nonetheless check the $\mathcal{O}(G^3)$ terms of $F_E^{(\text{PN})}$. There are two subtleties that we must discuss. The first is that eq. (5.3.30) and the PN flux are in two different gauges, the isotropic and harmonic gauge respectively. However, this gauge difference is 2PM orders higher and can be here neglected. Secondly, the procedure employed to construct $\mathcal{F}_{\text{tid}}^{(0)}$ ignores the contributions of the so-called Schott terms [272], hence eq. (5.3.30) coincides with $F_E^{(\text{PN})}$ only up to total derivatives. Indeed we have verified that, expanding $\mathcal{F}_{\text{tid}}^{(0)}$ for small velocities, i.e. small reduced energy \mathcal{E} , we find

$$\int_{r_-}^{r_+} dr \frac{1}{\dot{r}} \left(\frac{G^3 M^4}{r^8} \mathcal{F}_{E,\text{tid}}^{(0)} - F_E^{(\text{PN})} \right) = 0 + \mathcal{O}(G^5), \quad (5.3.35)$$

hence, the two fluxes coincides at this order in G up to total derivative terms.

5.4 . Summary of the chapter

In this chapter, we went beyond the point-particle approximation and included the effects of tidal deformations on the motion of two compact objects interacting via gravity. In particular, we computed for the first time the influence of such effects in the asymptotic waveform, the emitted four-momentum and the radiated flux at leading PM order. We focused on electric and magnetic-type quadrupole deformations for simplicity, but our computations can be straightforwardly extended to higher multipoles or to higher-orders in the curvature fields. Due to the absence of the H-like topology, the computation of the radiated four momentum required only three of the four MIs we found in the previous chapter.

We have then derived the emitted energy and flux for bound orbits using the B2B dictionary and verified that it is consistent with PN results for eccentric orbits. Moreover, considering the ultra-relativistic limit of the energy loss, we observed that the contributions of the electric and magnetic component scale differently unlike the case of the conservative scattering angle.

We shall now proceed and conclude by modifying again the worldline action to include rotational degrees of freedom, i.e. spin effects.

6 - Beyond point-particle: Spin effects

In the last chapter of this thesis we address the contribution of spin effects in the dynamics of the two bodies. As binary systems with spinning black holes or neutron stars constitute one of the primary sources of gravitational waves, modeling precisely how spin influences a binary's inspiral is essential for making robust detections and performing accurate parameter estimation studies [273–275] and look for possible physics beyond the standard model [252, 273, 276–278].

These effects have been thoroughly investigated in the traditional PN expansion using both explicit solutions to the Einstein equations [54–56, 279, 280], classical EFT methods [26, 57, 58, 200–202] and the self force formalism [68–70, 281]. Together with the EOB formalism [139, 282–285] they form a powerful semi-analytic framework that allows us to construct waveform template needed for the gravitational wave detectors.

The analysis of spin effects on the binary system have also been address recently within the PM expansion using again worldline approaches [159–161, 164, 166] and on-shell scattering amplitude methods [116, 140–143, 286–288]. These advancements concern mainly the conservative sector and the full inclusion of spins in the radiated observables at 3PM was notably absent from the literature. To be precise, the outgoing waveform from a spinning binary has been computed up to 2PM in Ref. [165] and radiation effects on the conservative motion at 3PM have been included in [166, 289].

Following once more the procedure we detailed in the previous chapters, we shall complete the 3PM radiative sector with the computation of the radiated momentum up to quadratic order in spins. Remarkably, we shall see that in order to solve the final loop integration we need once again only the four two-loop integrals we have already computed in the minimal point-particle case, see section 4.2.

6.1 . Spin effects in the wordline action

In this section we review how to include spin degrees of freedom in Einstein gravity, using the EFT approach. In particular, we see how to construct the Routhian describing a spinning extended object [26, 200] starting from a first-order Lagrangian. We redirect to Refs. [26, 57, 58, 159, 200–202, 290–292] and references therein for a more complete discussion on this subject.

6.1.1 . Degrees of freedom

In any generally covariant theory, a spinning particle can be described by a worldline $x^\mu(\lambda)$ and an orthonormal tetrad $e^\mu_A(x(\lambda))$. The first specifies the trajectory of the particle, while the latter may be regarded as the Jacobian $e^\mu_A \equiv \partial x^\mu / \partial y^A$ that transforms between a general coordinate chart x^μ and the particle's body-fixed frame y^A , hence

$$\eta_{AB} = g_{\mu\nu}(x(\lambda))e^\mu_A(x(\lambda))e^\nu_B(x(\lambda)). \quad (6.1.1)$$

This transformation encodes information about the intrinsic rotation of the particle, which proceeds with an angular velocity given by

$$\Omega^{\mu\nu} \equiv \eta^{AB} e^\mu_A \dot{x}^\alpha \nabla_\alpha e^\nu_B, \quad \dot{x}^\mu = \frac{dx^\mu}{d\lambda}. \quad (6.1.2)$$

Note that $\Omega^{\mu\nu}$ is antisymmetric by construction. We call the conjugate momentum p_μ and the spin tensor $\mathcal{S}_{\mu\nu}$; they are defined as

$$p_\mu \equiv -\frac{\delta S_{\text{spin}}}{\delta \dot{x}^\mu}, \quad \mathcal{S}_{\mu\nu} \equiv -\frac{\delta S_{\text{spin}}}{\delta \Omega^{\mu\nu}}, \quad (6.1.3)$$

where the action for the particle is $S_{\text{spin}} = \int d\lambda \mathcal{L}_{\text{spin}}$ and the Lagrangian $\mathcal{L}_{\text{spin}}$ can then be constructed in first-order form as

$$\mathcal{L}_{\text{spin}} = -p_\mu \dot{x}^\mu - \mathcal{S}_{\mu\nu} \Omega^{\mu\nu} - \mathcal{H}_{\text{spin}}. \quad (6.1.4)$$

Analogously to the non-spinning case, see section 1.2, the Hamiltonian will contain the needed constraints that we shall discuss momentarily.

Before proceeding, it is important to write a few more words about $e^\mu_A(\lambda)$. The transformation from the generic coordinates x^μ to the body-fixed frame y^A consists of essentially two steps: first we rescale the metric to go in a locally flat frame, and then we perform a Lorentz transformation to end up in the body-fixed frame. Concretely this means

$$e^\mu_A(x(\lambda)) = \Lambda^a_A(\lambda) e^\mu_a(x(\lambda)). \quad (6.1.5)$$

Here e^μ_a is the vierbein that brings us in the locally flat frame, and Λ^a_A is the final time-dependent Lorentz transformation. In this way, we have explicitly separated the particle's translational (e^μ_a) and rotational (Λ^a_A) degrees of freedom. As a consequence, from eq. (6.1.2) we get [26, 200]

$$e^a_\mu e^b_\nu \Omega^{\mu\nu} = \Omega_\Lambda^{ab} + \dot{x}^\mu \omega_\mu^{ab}, \quad (6.1.6)$$

where we have introduced the angular velocity relative to the rest frame Ω_Λ^{ab} and the spin connection ω_μ^{ab} defined respectively as¹

$$\Omega_\Lambda^{ab} \equiv \eta^{AB} \Lambda^a_A \dot{\Lambda}^b_B, \quad \omega_\mu^{ab} \equiv g^{\rho\sigma} e^b_\rho \nabla_\mu e^a_\sigma. \quad (6.1.7)$$

Introducing the spin tensor in the locally-flat frame, $\mathcal{S}_{ab} = \mathcal{S}_{\mu\nu} e^\mu_a e^\nu_b$, eq. (6.1.4) becomes

$$\mathcal{L}_{\text{spin}} = -\dot{x}^\mu (p_\mu + \mathcal{S}_{ab} \omega_\mu^{ab}) - \mathcal{S}_{ab} \Omega_\Lambda^{ab} - \mathcal{H}_{\text{spin}}. \quad (6.1.8)$$

Because the ‘‘kinetic term’’ $\mathcal{S}_{ab} \Omega_\Lambda^{ab}$ for the rotational degrees of freedom is independent of the metric, we see that a minimal coupling between gravity and spin appears only through an interaction term involving the spin connection.

Let us now go back to the construction of the Hamiltonian. We can see that we need to add some constraints to eq. (6.1.8) by counting the number of degrees of freedom.

¹Note that Λ^a_A depends only on λ , therefore $\dot{x}^\mu \nabla_\mu \Lambda^a_A = \dot{\Lambda}^a_A$.

The coordinate x^μ and the conjugate momentum p_μ contain in total eight degrees of freedom. The Lorentz matrix Λ^a_A and the spin tensor \mathcal{S}_{ab} add another 12 degrees of freedom, bringing the total to twenty. To uniquely describe a spinning point-particle we only need six generalized coordinates (or equivalently twelve phase-space variables), hence we need to impose a commensurate number of constraints. As in the non-spinning case, see section 1.2, the Hamiltonian is made up purely of constraints [210]. In particular we have [290]

$$\mathcal{H}_{\text{spin}} = -\frac{e}{2m}(p^2 - m^2 + m\mathcal{H}_{\text{fs}}) - e\chi_a(\sqrt{p^2}\Lambda^a_0 - p^a) - e\xi^a\mathcal{S}_{ab}p^b, \quad (6.1.9)$$

where the fields $e(\lambda)$, $\chi_a(\lambda)$, and $\xi^a(\lambda)$ serve as Lagrange multipliers. We shall define \mathcal{H}_{fs} momentarily. These three constraints impose

$$C_0 \equiv p^2 - m^2 + m\mathcal{H}_{\text{fs}} \approx 0, \quad (6.1.10)$$

$$C_1^a \equiv \sqrt{p^2}\Lambda^a_0 - p^a \approx 0, \quad (6.1.11)$$

$$C_3^a \equiv \mathcal{S}^{ab}p_b \approx 0. \quad (6.1.12)$$

The hyper-surface in phase-space where all the three conditions above are satisfied is called constraint surface. We use the weak equality symbol, i.e. $a \approx b$ if a and b differ by terms that vanish on the constraint surface [293].

Let us analyze these constraints one by one. The first constraint is the usual mass-shell condition we have imposed also in the non-spinning case. Here we have included possible modifications due to finite-size effects contained in $m\mathcal{H}_{\text{fs}} = \sum_n \mathcal{O}_n$, see section 5.1. We will explain this more explicitly at the end of this section. For a rotating object, the total ADM mass² is in general a function of the spin absolute magnitude [26, 292], i.e. $m^2 = m^2(\mathcal{S}^2)$ where $\mathcal{S}^2 \equiv \mathcal{S}_{ab}\mathcal{S}^{ab}/2$. As we shall see in the next section, specifying the exact dependence of m^2 on \mathcal{S}^2 is actually not necessary because from the EOM one can see that \mathcal{S}^2 is conserved, therefore m^2 remains constant. This constraint removes one degree of freedom.

The second constraint C_1^a imposes $\Lambda^a_0 \approx p^a/\sqrt{p^2}$, which removes the superfluous boosts degrees of freedom of the Lorentz transformation. This basically means that we are setting the timelike vector e^μ_0 parallel to the particle four-momentum [200], which removes three degrees of freedom.

Finally, C_3^a is known as the spin supplementary condition (SSC) [26, 295]. This removes three out of six degrees of freedom from \mathcal{S}_{ab} , leaving us with only the three angles needed to describe the rotation of the body. This constraint is not unique: we choose to work with the so-called covariant SSC, which has the advantage of keeping Lorentz invariant manifest. We redirect the reader to refs. [26, 200, 202, 296] for alternative SSC implementations.

Even with all the constraints we have imposed so far, we are left with one extra redundant degree of freedom. This is associated with the reparametrization invariance;

²For asymptotically flat systems, the ADM mass can be defined, via Noether's theorem, by the asymptotic symmetries at spatial infinity. See e.g. [294].

hence, fixing a gauge for the worldline parameter λ removes the last remaining unphysical degree of freedom.

The last thing we need to discuss are the finite size effects \mathcal{H}_{fs} , that can be written in terms of multipoles as in eq. (5.1.9). Let us consider again the electric quadrupole multipole. As we mentioned in section 5.1, all the multipoles can be decomposed into a permanent part and a response contribution, see eq. (5.1.10). Spinning objects have a non-zero permanent multipole, in particular \bar{Q}_{ab}^E is given by

$$\bar{Q}_{ab}^E = \frac{C_E}{m} \mathcal{S}_{ac} \mathcal{S}^c{}_b. \quad (6.1.13)$$

The Wilson coefficient C_E contains again information about the internal structure of the body. By matching this point-particle theory with the full Kerr solutions, one finds $C_E = 1$ for rotating black holes, while $\bar{Q}_{ab}^B = 0$ for parity reasons. Ignoring the induced tidal deformation that we have analyzed in the previous section, from now on we consider

$$\mathcal{H}_{\text{fs}} = \frac{C_E}{m} \mathcal{S}_{ac} \mathcal{S}^c{}_b E_{ab} + \dots, \quad (6.1.14)$$

and redirect to [202] for an explicit expression of the higher multipoles.

6.1.2 . Consistency condition

The action in eq. (6.1.8), together with eq. (6.1.9), can be use to derive the EOM for the spinning object [200, 295]. For \dot{x}^μ and Ω_Λ^{ab} one explicitly finds

$$me^{-1} \dot{x}^\mu \approx p^\mu - m(\chi_a \Pi^{a\mu} - \xi_a \mathcal{S}^{a\mu}) + \frac{1}{p^2} C_E \mathcal{S}^{ae} \mathcal{S}_e{}^b R_{acbd} p^{(c} \Pi^{d)\mu}, \quad (6.1.15)$$

$$me^{-1} (\Omega_\Lambda^{ab} + \dot{x}^\mu \omega_\mu^{ab}) \approx -\frac{\partial m^2}{\partial \mathcal{S}^2} \mathcal{S}^{ab} + 2m \xi^{[a} p^{b]} + 2C_E E_c^{[a} \mathcal{S}^{b]c}, \quad (6.1.16)$$

where we have introduced the projector $\Pi^\mu{}_\nu \equiv \delta^\mu{}_\nu - p^\mu p_\nu / p^2$. The EOM for \mathcal{S}_{ab} in the locally flat frame is given by

$$\dot{\mathcal{S}}^{ab} = 2e\chi^{[a} p^{b]} - 2\Omega_\Lambda^{c[a} \mathcal{S}^{b]c}. \quad (6.1.17)$$

Notice that $\mathcal{S}_{ab} \dot{\mathcal{S}}^{ab} = d\mathcal{S}^2/d\lambda$ and

$$\frac{d\mathcal{S}^2}{d\lambda} = 2e\chi^{[a} p^{b]} \mathcal{S}_{ab} - 2\Omega_\Lambda^{c[a} \mathcal{S}^{b]c} \mathcal{S}_{ab} = 0. \quad (6.1.18)$$

The first term on the right hand side vanishes because of the covariant SSC, while the last term is zero by means of symmetry. This proves that \mathcal{S}^2 is a constant as we mentioned in the previous section. The equation for the spin tensor can be rewritten in terms of the general coordinates using $e^\mu{}_a$ and eq. (6.1.6). One eventually obtains

$$\dot{x}^\alpha \nabla_\alpha \mathcal{S}_{\mu\nu} = 2e\chi_{[\mu} p_{\nu]} - 2\Omega^\rho{}_{[\mu} \mathcal{S}_{\nu]\rho}. \quad (6.1.19)$$

Using eqs. (6.1.15) and (6.1.16) we finally get

$$\frac{1}{e} \dot{x}^\alpha \nabla_\alpha \mathcal{S}_{\mu\nu} \approx 2p_{[\mu} \dot{x}_{\nu]} + \frac{C_E}{m} \left(\frac{1}{p^2} \mathcal{S}^{ae} \mathcal{S}_e{}^b R_{acb[\mu} p_{\nu]} p^c + E_{a[\mu} \mathcal{S}_{\nu]b} \mathcal{S}^{ab} \right). \quad (6.1.20)$$

Ultimately, the EOM for p_μ can be found by working in normal coordinates around a point where the Christoffel symbols vanish (but their derivatives do not), and then covariantising the result [200]. Doing so, one obtains

$$\frac{1}{e} \dot{x}^\alpha \nabla_\alpha p_\mu \approx -\frac{1}{2e} R_{\mu\nu\rho\sigma} \dot{x}^\nu \mathcal{S}^{\rho\sigma} - \frac{C_E}{2m} \nabla_\mu (E_{ab} \mathcal{S}^{ac} \mathcal{S}_c^b). \quad (6.1.21)$$

Note that for the case of a point-particle, $C_E = 0$, eqs. (6.1.20) and (6.1.21) are the Mathisson-Papapetrou equations [297, 298].

The reason why we wrote down these equation is that they allow us to find some consistency conditions on the constraints C_1^a and C_2^a , which then provide an explicit expression for the Lagrange multipliers χ_a and ξ_a in eq. (6.1.9). We would expect a consistent solution to preserve the constraints under time evolution; hence, we shall additionally require

$$\dot{x}^\alpha \nabla_\alpha C_1^a \approx 0, \quad \dot{x}^\alpha \nabla_\alpha C_2^a \approx 0. \quad (6.1.22)$$

It is worth remarking that, for $n = 1, 2$, if $C_n^a \approx 0$, then for any tensor $T_{aa_1\dots a_k}$ one has $\dot{x}^\alpha \nabla_\alpha (C_n^a T_{aa_1\dots a_k}) \approx 0$. For C_1^a we can then evaluate

$$\eta^{AB} e^\mu{}_A \dot{x}^\alpha \nabla_\alpha \left(\frac{g_{\rho\sigma} e^\rho{}_B e^\sigma{}_a C_1^a}{\sqrt{p^2}} \right) = -\frac{1}{\sqrt{p^2}} \left(\Omega^{\mu\nu} p_\nu + \Pi^{\mu\nu} \dot{x}^\alpha \nabla_\alpha p_\nu \right) \approx 0. \quad (6.1.23)$$

Analogously for C_2^a we can take

$$\dot{x}^\alpha \nabla_\alpha (\eta_{ab} e^b{}_\mu C_2^a) = \dot{x}^\alpha \nabla_\alpha (\mathcal{S}_{\mu\nu} p^\nu) \approx 0. \quad (6.1.24)$$

Using eq. (6.1.19) we can write

$$\dot{x}^\alpha \nabla_\alpha (\mathcal{S}_{\mu\nu} p^\nu) = (2e \chi_{[\mu} p_{\nu]} - 2\Omega^\rho{}_{[\mu} \mathcal{S}_{\nu]\rho}) p^\nu + \mathcal{S}_{\mu\nu} \dot{x}^\alpha \nabla_\alpha p^\nu \approx 0. \quad (6.1.25)$$

Eq. (6.1.23) and the covariant SSC tell us that the second term in the round brackets in the above equation cancels the last one, leaving us with

$$\chi_a \approx 0. \quad (6.1.26)$$

Finally substituting (6.1.16) and (6.1.21) into (6.1.25), and then using $\chi_a \approx 0$ to simplify terms, we find

$$\mathcal{S}_{\mu\nu} \left(e p^2 \xi^\nu - \frac{1}{2} R^\nu{}_{\lambda\alpha\beta} \dot{x}^\lambda \mathcal{S}^{\alpha\beta} \right) \approx 0. \quad (6.1.27)$$

This yields to the solution for ξ^μ , which is explicitly

$$\xi^\mu = \frac{1}{2e p^2} R^\nu{}_{\lambda\alpha\beta} \dot{x}^\lambda \mathcal{S}^{\alpha\beta}. \quad (6.1.28)$$

In the end, plugging eqs. (6.1.26) and (6.1.28) into (6.1.8) with $\mathcal{H}_{\text{spin}}$ given in (6.1.9), we find an explicit expression for the Lagrangian describing a spinning object without any Lagrange multiplier [26, 202]

$$\mathcal{L}_{\text{spin}} = -\dot{x}^\mu (p_\mu + S_{ab}\omega_\mu^{ab}) - \mathcal{S}_{ab}\Omega_\Lambda^{ab} - \mathcal{H}_{\text{spin}}, \quad (6.1.29)$$

$$\mathcal{H}_{\text{spin}} = -\frac{e}{2m}(p^2 - m^2 + C_E \mathcal{S}_{ac} \mathcal{S}_c^b E_{ab}) - \frac{1}{2p^2} p_a \dot{x}^e R_{ebcd} \mathcal{S}^{ab} \mathcal{S}^{cd}. \quad (6.1.30)$$

Having removed all the Lagrange multipliers, we must impose the covariant SSC at the level of the EOM.

6.1.3 . Constructing the Routhian

We have now all the ingredients needed for the construction of the Routhian. In principle, in order to get a canonical Lagrangian that depends only on x^μ , \dot{x}^μ and $\Omega_{\mu\nu}$ we should invert eqs. (6.1.15) and (6.1.16) to find an expression for the conjugate momenta p^μ and $\mathcal{S}_{\mu\nu}$ to plug in (6.1.29). In practice, it is more convenient to remove only the p^μ dependence. As we shall see, the result of this procedure corresponds to perform a partial Legendre transform that allows us to define the Routhian $\mathcal{R}_{\text{spin}}$.

To remove the p^μ dependence in $\mathcal{L}_{\text{spin}}$ we can plug the solutions (6.1.26) and (6.1.28) into eq. (6.1.15) to get

$$\frac{m}{e} \dot{x}^\mu \approx p^\mu + \frac{m}{2e p^2} \dot{x}^e R_{ebcd} \mathcal{S}^{\mu b} \mathcal{S}^{cd} + \frac{1}{p^2} C_E \mathcal{S}^{ae} \mathcal{S}_e^b R_{acbd} p^{(c} \Pi^{d)\mu}. \quad (6.1.31)$$

This relation can be used to find the explicit expression of the conjugate momentum p^μ in terms of \dot{x}^μ and \mathcal{S}_{ab} . Inverting order per order in spins up to $\mathcal{O}(S^2)$, we have

$$p^\mu \approx \frac{m}{e} \dot{x}^\mu - \frac{1}{2e m} \dot{x}^e R_{ebcd} \mathcal{S}^{\mu b} \mathcal{S}^{cd} - \frac{e}{m \dot{x}^2} C_E \mathcal{S}^{ae} \mathcal{S}_e^b R_{acbd} \dot{x}^{(c} U^{d)\mu} + \dots, \quad (6.1.32)$$

where we introduced for convenience the new projector $U^\mu{}_\nu \equiv \delta^\mu{}_\nu - \dot{x}^\mu \dot{x}_\nu / \dot{x}^2$. Plugging this expression in (6.1.29) results in

$$\mathcal{L}_{\text{spin}} = \mathcal{R}_{\text{spin}} - \frac{1}{2} \mathcal{S}_{ab} \Omega_\Lambda^{ab}, \quad (6.1.33)$$

where $\mathcal{R}_{\text{spin}}$ is precisely the Routhian we were looking for

$$\begin{aligned} \mathcal{R}_{\text{spin}} = & -\frac{m}{2e^2} (\dot{x}^2 + e^2) - \frac{1}{2} \dot{x}^\mu \omega_\mu^{ab} \mathcal{S}_{ab} + \frac{1}{2me} \dot{x}_a \dot{x}^e R_{ebcd} \mathcal{S}^{ab} \mathcal{S}^{cd} \\ & + \frac{e}{2m} C_E E_{ab} \mathcal{S}^{ac} \mathcal{S}_c^b + \dots, \end{aligned} \quad (6.1.34)$$

and the electric part of the Riemann tensor is now defined as $E_{ab} = R_{acbd} \dot{x}^c \dot{x}^d / \dot{x}^2$.

The first three terms of eq. (6.1.34) describe the motion of a spinning point-particle in a gravitational field. The last term of this line is there to ensure that the covariant SSC that now reads $\mathcal{S}_{ab} \dot{x}^b = 0 + \mathcal{O}(RS^3)$ holds upon time evolution. On the other hand, the second line describes a quadrupole interaction, i.e. the first term responsible

for the influence of the internal structure of the rotating body. Higher multipoles can be incorporated in a similar way [202].

Being defined as a partial Legendre transform, the Routhian behaves as a Lagrangian for x^μ and as a Hamiltonian for \mathcal{S}_{ab} . The EOM can then be found as follows

$$\frac{\delta}{\delta x^\mu} \int d\lambda \mathcal{R}_{\text{spin}} = 0, \quad \frac{d\mathcal{S}_{ab}}{d\lambda} = \{\mathcal{S}_{ab}, \mathcal{R}_{\text{spin}}\}, \quad (6.1.35)$$

where the only non-trivial Poisson brackets is given by

$$\{\mathcal{S}_{ab}, \mathcal{S}_{cd}\} = 2\eta_{a[d}\mathcal{S}_{c]b} - 2\eta_{b[d}\mathcal{S}_{c]a}. \quad (6.1.36)$$

Finally, analogously to what we did in the point-particle and tidal deformations analysis, we can choose the affine parameter τ such that $e(\tau) = 1$, so that eq. (6.1.34) becomes

$$\begin{aligned} \mathcal{R}_{\text{spin}} = & -\frac{m}{2}(g_{\mu\nu}\mathcal{U}^\mu\mathcal{U}^\nu + 1) - \frac{1}{2}\mathcal{U}^\mu\omega_\mu^{ab}\mathcal{S}_{ab} + \frac{1}{2m}\mathcal{U}_a\mathcal{U}^e R_{ebcd}\mathcal{S}^{ab}\mathcal{S}^{cd} \\ & + \frac{1}{2m}C_E E_{ab}\mathcal{S}^{ac}\mathcal{S}_c{}^b, \end{aligned} \quad (6.1.37)$$

where $\mathcal{U}^\mu \equiv dx^\mu/d\tau$. As in the previous chapter, see eq. (5.1.4), this implies that

$$\mathcal{U}^2(\tau) = 1 + \mathcal{O}(R\mathcal{S}^2). \quad (6.1.38)$$

This means that, in the scattering process we shall study momentarily, τ is the proper time only in the asymptotic past and future.

6.2 . Spin effects in the radiative sector

We have now all the instruments we need to study the scattering of two spinning composite objects interacting via gravity. The starting point is the following effective “action”

$$S_{\text{eff},3} = -\frac{2}{\kappa^2} \int d^d x \sqrt{-g^2} R + \sum_{A=1,2} \int d\tau \mathcal{R}_A, \quad (6.2.1)$$

For reasons that will be clear in the next sections, we work in d dimensions from the beginning and introduce

$$\kappa \equiv \sqrt{32\pi G} = \frac{1}{m_{\text{Pl}}^{(d-2)/2}}. \quad (6.2.2)$$

here we use κ rather than m_{Pl} because its definition does not depend explicitly on d . In (6.2.1) for each body $A = 1, 2$, \mathcal{R}_A is the Routhian given in eq. (6.1.37). We study this system in the PM perturbative regime, hence we expand again $g_{\mu\nu} = \eta_{\mu\nu} + \kappa h_{\mu\nu}$. Recall that in the Routhian we have introduced a vielbein $e^a{}_\mu = \partial y^a / \partial x^\mu$ that brings us in the locally flat frame of each object³, thus \mathcal{R}_A contains both flat-space Latin and curved-space Greek indices. However, In the weak field expansion, it is not hard to find

$$e^a{}_\mu = \eta^{a\rho} \left(\eta_{\mu\rho} + \frac{\kappa}{2} h_{\mu\rho} - \frac{\kappa^2}{8} h_{\mu\sigma} h^\sigma{}_\rho + \dots \right). \quad (6.2.3)$$

³We omit the label A denoting the object to lighten the notation.

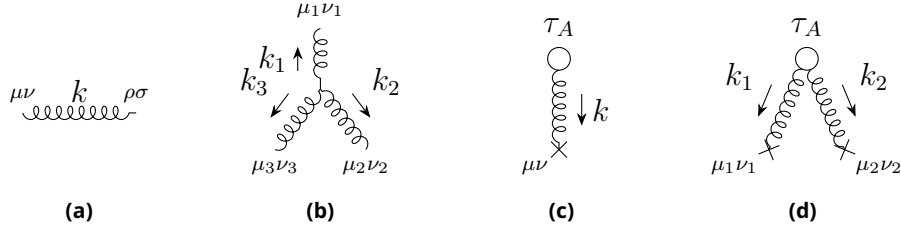


Figure 10: Feynman rules relevant to our computation.

As a consequence, we see that in this expansion Greek and Latin indices are now indistinct. The spin tensors are, nonetheless, still defined in their respective locally flat frames [161].

We are now ready to derive the relevant Feynman rules for computing radiative observables. Once we add the usual de Donder gauge fixing term given in eq. (1.3.7), from the purely gravitational part of $S_{\text{eff},3}$ we get the usual propagator and cubic interaction vertex, see eqs. (3.1.1) and (1.3.10). We draw them once again in figure 10 (a)–(b) for the reader convenience.

From the Routhian in (6.2.1) we obtain the worldline vertices describing graviton emission, sketched in figure 10 (c)–(d). Recall that, in order to completely isolate the power of G , we should also expand the worldline parameters x_A^μ , \mathcal{U}_A^μ and $\mathcal{S}_A^{\mu\nu}$ around straight motion, see section 1.4.1. To keep the expressions more compact, it is more convenient to use the convention introduced in section 1.3, and define the Feynman rules using the non-expanded variables, represented by an empty dot, and then expand to the desired PM order. For instance, the single graviton emission from the worldline is explicitly given by

$$\begin{aligned}
\text{○} \xrightarrow{k} \mu\nu &= -\frac{1}{2} i\kappa \int d\tau_A e^{ik \cdot x_A} \left[m_A \mathcal{U}_A^\mu \mathcal{U}_A^\nu + ik_\rho \mathcal{S}_A^{\rho(\mu} \mathcal{U}_A^{\nu)} \right. \\
&+ \frac{1}{m_A} k_\rho k_\sigma \mathcal{U}_{A\alpha} (\mathcal{U}_A^{(\mu} \mathcal{S}_A^{\nu)\rho} \mathcal{S}_A^{\sigma\alpha} + \mathcal{U}_A^\rho \mathcal{S}_A^{\sigma(\mu} \mathcal{S}_A^{\nu)\alpha}) \\
&+ \frac{1}{2m_A} C_{EA} k_\rho k_\sigma (\mathcal{S}_A^{\rho\alpha} \mathcal{S}_A^{\sigma\alpha} \mathcal{U}_A^\mu \mathcal{U}_A^\nu \\
&\left. + 2\mathcal{U}_A^\rho \mathcal{S}_A^{\sigma\alpha} \mathcal{S}_A^{\alpha(\mu} \mathcal{U}_A^{\nu)} + \mathcal{S}_A^{(\mu\alpha} \mathcal{S}_A^{\nu)\alpha} \mathcal{U}_A^\rho \mathcal{U}_A^\sigma \right]. \quad (6.2.4)
\end{aligned}$$

Expressions for the remaining vertices, which are much lengthier, are presented in appendix C.

Once we have computed the relevant diagrams, we must expand the body variables $X_A \equiv (x_A, \mathcal{U}_A, \mathcal{S}_A)$ about their initial straight-line trajectories as mentioned before. We write [149, 161]

$$X_A(\tau_A) = \bar{X}_A(\tau_A) + \sum_{n=1}^{\infty} \delta^{(n)} X_A(\tau_A), \quad (6.2.5)$$

where once again $\delta^{(n)} X_A$ represents the $\mathcal{O}(G^n)$ deflection away from the initial trajectory \bar{X}_A due to the gravitational pull of the other body. The 1PM deflections $\delta^{(1)} X_A$, which

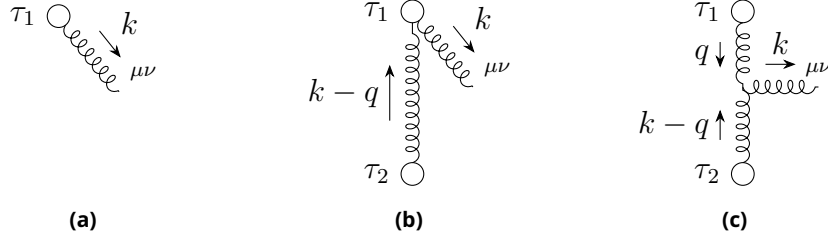


Figure 11: Feynman diagrams contributing to the stress-energy tensor up to next-to-leading order in G . While not drawn explicitly, our calculation includes the mirror inverses of (a) and (b), which are obtained by interchanging the body labels $1 \leftrightarrow 2$ and redefining the loop momentum $q \rightarrow k - q$.

we will need later in our calculation, were previously computed using Eq. (6.1.35) in Refs. [149, 161]. Note that in that references the authors use a different gauge for the gravitons. This difference however does not affect the result for the EOM at this order. As for the straight-motion variables \bar{X}_A , we write

$$\bar{x}_A^\mu = b_A^\mu + u_A^\mu \tau_A, \quad \bar{u}_A^\mu = u_A^\mu, \quad \text{and} \quad \bar{S}_A^{\mu\nu} = m_A s_A^{\mu\nu}, \quad (6.2.6)$$

where the constant vectors u_A^μ and b_A^μ were defined in eqs. (1.4.7) and (1.4.8), while the constant tensor $s_A^{\mu\nu}$ describes the initial spin tensor per unit of mass. Note that $s_A^{\mu\nu} u_{A\nu} = 0$ as per the covariant SSC.

6.2.1 . Stress-energy tensor up to $\mathcal{O}(S^2)$

With the rules given in figure 10 we can then construct all the relevant Feynman diagrams to compute the stress energy tensor via a matching procedure, see section 1.3.2. We compute it up to NLO in G and up to quadratic order in spins. To this end, we need the three diagrams depicted in figure 11.

At leading order in G , only the diagram in figure 11(a), with X_A replaced by \bar{X}_A , contributes. The result is

$$\tilde{T}_{\text{LO}}^{\mu\nu}(k) = \sum_{A=1}^2 \delta(k \cdot u_A) m_A e^{ik \cdot b_A} \left[u_A^\mu u_A^\nu + ik^\rho s_{A\rho}^{(\mu} u_A^{\nu)} - \frac{1}{2} C_{EA} (k_\rho s_A^{\rho\sigma} s_{A\sigma}{}^\alpha k_\alpha) u_A^\mu u_A^\nu \right]. \quad (6.2.7)$$

As it was the case for the point-particle case, $T_{\text{LO}}^{\mu\nu}(k)$ is static and it does not contribute to the emitted energy.

All three diagrams in figure 11 contribute at NLO in G . From figure 11 (a), we extract the $\mathcal{O}(\kappa^2)$ part of the diagram by expanding X_A up to 1PM, whereas for Figs. 11 (b) and 11 (c), it suffices to replace X_A by \bar{X}_A . The total result can be written as

$$\tilde{T}_{\text{NLO}}^{\mu\nu}(k) = \frac{\kappa^2 M^2 \nu}{4} \int_q \frac{\Delta_{12}(q, k)}{q^2 (k - q)^2} t^{\mu\nu}(q, k) e^{iq \cdot b} e^{ik \cdot b_2}, \quad (6.2.8)$$

where we have introduced again $\Delta_{12}(q, k) \equiv \delta(q \cdot u_1) \delta((k - q) \cdot u_2)$. An explicit expression for $t^{\mu\nu}$, accurate to $\mathcal{O}(s^2)$, is presented in appendix C. As a first consistency check of

usual form

$$P_{\text{rad}}^{\mu} = \frac{\kappa^6 M^4 \nu^2}{64} \int_q \delta(q \cdot u_1) \delta(q \cdot u_2) e^{iq \cdot b} Q_S^{\mu}(q). \quad (6.3.4)$$

$$Q_S^{\mu} \equiv \int_{\ell_1, \ell_2} \delta_{-}((\ell_1 + \ell_2 - q)^2) \delta(\ell_1 \cdot u_1) \delta(\ell_2 \cdot u_2) \times \frac{(-\ell_1^{\mu} - \ell_2^{\mu} + q^{\mu}) \mathcal{N}_S(\ell_1, \ell_2, q)}{\ell_1^2 \ell_2^2 (\ell_1 - q)^2 (\ell_2 - q)^2}. \quad (6.3.5)$$

In the presence of spins, we need to perform one additional step before being able to implement the second step represented in figure 7, page 56, i.e. the application of IBP identities.

6.3.1 . Loop integral decomposition and IBP reduction

Let us introduce again the definition of ρ_1, \dots, ρ_9 given in eqs. (4.2.4) and (4.2.5). The quantity $Q_S^{\mu}(q)$ is expressible as a sum of terms in which q^{μ} , u_A^{μ} , and $s_A^{\mu\nu}$ are contracted amongst themselves and with the two-loop integrals

$$G_{n_1 \dots n_9}^{\mu_1 \dots \mu_i \nu_1 \dots \nu_j} \equiv \int_{\ell_1, \ell_2} \frac{\ell_1^{\mu_1} \dots \ell_1^{\mu_i} \ell_2^{\nu_1} \dots \ell_2^{\nu_j}}{\rho_1^{n_1} \rho_2^{n_2} \rho_3^{n_3} \rho_4^{n_4} \rho_5^{n_5} \rho_6^{n_6} \rho_7^{n_7} \rho_8^{n_8} \rho_9^{n_9}}. \quad (6.3.6)$$

Our goal is to write every possible contraction of the loop momenta ℓ_1^{μ} and ℓ_2^{μ} in terms of the scalar products ρ_1, \dots, ρ_9 and q^2 . Similarly to what we saw in section 2.2, to accomplish this we decompose ℓ_A^{μ} ($A \in \{1, 2\}$) in the numerator as

$$\ell_A^{\mu} = (\ell_A \cdot u_1) \check{u}_1^{\mu} + (\ell_A \cdot u_2) \check{u}_2^{\mu} + \frac{(\ell_A \cdot q)}{q^2} q^{\mu} + \ell_{A\perp}^{\mu}, \quad (6.3.7)$$

where \check{u}_1^{μ} and \check{u}_2^{μ} are defined in eq. (2.2.8), and $\ell_{A\perp}^{\mu}$ is the part of ℓ_A^{μ} that is orthogonal to u_1^{μ} , u_2^{μ} , and q^{μ} (recall that q^{μ} is orthogonal to both u_1^{μ} and u_2^{μ}). The three products $(\ell_A \cdot u_1)$, $(\ell_A \cdot u_2)$ and $(\ell_A \cdot q)$ can be easily written in terms of the ρ_1, \dots, ρ_9 defined in (4.2.4) and q^2 , therefore we just need to discuss the orthogonal components $\ell_{A\perp}^{\mu}$.

The fact that the denominator of eq. (6.3.6) is invariant under the exchange

$$(\ell_{1\perp}^{\mu}, \ell_{2\perp}^{\mu}) \rightarrow -(\ell_{1\perp}^{\mu}, \ell_{2\perp}^{\mu}) \quad (6.3.8)$$

implies that any term in the numerator with i powers of $\ell_{1\perp}^{\mu}$ and j powers of $\ell_{2\perp}^{\mu}$ will integrate to zero if $i + j$ is odd. If instead $i + j = 2$, then rotational invariance on the hypersurface orthogonal to u_1 , u_2 , and q allows us to replace

$$\ell_{A\perp}^{\mu} \ell_{B\perp}^{\nu} \rightarrow \frac{(\ell_A^{\rho} \perp_{\rho\sigma} \ell_B^{\sigma})}{d-3} \perp^{\mu\nu}, \quad (6.3.9)$$

under the integral, where the metric on this hypersurface is

$$\perp^{\mu\nu} = \eta^{\mu\nu} - \check{u}_1^{\mu} \check{u}_1^{\nu} - \check{u}_2^{\mu} \check{u}_2^{\nu} - q^{\mu} q^{\nu} / q^2. \quad (6.3.10)$$

Note that the inner product $(\ell_A^\rho \perp_{\rho\sigma} \ell_B^\sigma)$ is easily rewritten solely in terms of the variables $\rho_1, \dots, \rho_9, q^2$, and γ . Analogous replacement rules can be derived for the $i + j = 4$ case by positing the ansatz

$$\ell_{A\perp}^\mu \ell_{B\perp}^\nu \ell_{C\perp}^\rho \ell_{D\perp}^\sigma \rightarrow c_1 \perp^{\mu\nu} \perp^{\rho\sigma} + c_2 \perp^{\mu\rho} \perp^{\nu\sigma} + c_3 \perp^{\mu\sigma} \perp^{\rho\nu} \quad (6.3.11)$$

and then solving for the coefficients $\{c_1, c_2, c_3\}$ by taking appropriate contractions. The same can be done for all $i + j \in 2\mathbb{N}$, although in practice we encounter only integrals with $i + j \leq 5$.

At this point we can explain why we worked in d dimensions from the beginning. The expressions for the coefficients $\{c_1, c_2, c_3\}$ in (6.3.11) are rather long in general, but for e.g. $A = B = 1$ and $C = D = 2$ we see that all of them are proportional to $(d - 4)^{-1}$, hence this decomposition is not well defined in four dimension.

Q_S^μ is now a sum of terms in which different combinations of q^μ , u_A^μ , and $s_A^{\mu\nu}$ are contracted with one another and multiplied by one of the scalar-valued integrals $G_{n_1 \dots n_9}$. At this stage, 3100 different scalar integrals enter into Q_S^μ , but not all of them are independent. Remarkably, after using the LiteRed software package [177, 178] to implement IBP relations between the different integrals, we find that they reduce to the same four master integrals g_1, g_2, g_3 and g_4 we found in the point-particle case, see eqs. (4.2.13) – (4.2.13).

Working in $d = 4 - 2\varepsilon$, we first checked that all the seemingly divergent terms proportional to ε^{-1} coming from either the IBP reduction process or the decomposition in (6.3.11) vanish once we plug the solution for the master integrals. One might expect finite contributions coming from the divergent coefficients inside the decomposition (6.3.11) times the order ε solution of the master integrals, see eqs. (4.2.27) – (4.2.30), which would imply a non trivial contribution coming from the order ε of the stress-energy tensor. We also checked that such contributions actually sum up to zero, meaning that we could have actually worked in $d = 4$ up to eq. (6.3.4), and then solve the loop integrals in $d = 4 - 2\varepsilon$ dimension as explained above. This is consistent with the fact that we expect the final result to be finite in $d = 4$ dimension.

6.3.2 . The radiated four-momentum

Given what we said in the previous section, we can now specializing to four dimensions eq. (6.3.4). It becomes convenient to decompose again onto the complete four-dimensional basis defined in (2.2.8), i.e.

$$P_{\text{rad}}^\mu = \frac{G^3 M^4 \pi \nu^2}{b^3} (C_{u_1} \check{u}_1^\mu + C_{u_2} \check{u}_2^\mu - C_{\hat{b}} \hat{b}^\mu - C_{\hat{l}} \hat{l}^\mu). \quad (6.3.12)$$

Considering $V \in \{u_1, u_2, \hat{b}, \hat{l}\}$, each coefficients C_V is explicitly

$$C_V \equiv 512\pi^2 b^3 \int_q \delta(q \cdot u_1) \delta(q \cdot u_2) e^{iq \cdot b} V_\mu Q_S^\mu. \quad (6.3.13)$$

We can then solve all the (cut) two-loop integrals $V_\mu Q_S^\mu$ as explained in the previous section, and then perform the final Fourier transform using eqs. (2.1.8) and (2.1.10).

$$\begin{aligned}
f_{\text{II}} &= \frac{210\gamma^6 - 356\gamma^5 - 111\gamma^4 - 1627\gamma^3 + 5393\gamma^2 - 4741\gamma + 1352}{16(\gamma+1)(\gamma^2-1)} \\
&\quad - \frac{105\gamma^4 + 345\gamma^3 - 405\gamma^2 + 147\gamma - 48}{8(\gamma+1)} \log\left(\frac{1+\gamma}{2}\right) \\
&\quad + \frac{210\gamma^6 - 405\gamma^4 + 135\gamma^2}{16(\gamma^2-1)^{3/2}} \operatorname{arccosh} \gamma \\
f_{\text{III}} &= \frac{210\gamma^6 - 279\gamma^5 - 219\gamma^4 - 1350\gamma^3 + 4732\gamma^2 - 4243\gamma + 1245}{16(\gamma+1)(\gamma^2-1)} \\
&\quad - \frac{21\gamma^4 + 66\gamma^3 - 84\gamma^2 + 30\gamma - 9}{2(\gamma+1)} \log\left(\frac{1+\gamma}{2}\right) \\
&\quad + \frac{42\gamma^6 - 81\gamma^4 + 27\gamma^2}{4(\gamma^2-1)^{3/2}} \operatorname{arccosh} \gamma \\
f_{\text{IV}} &= -\frac{425\gamma^5 - 1215\gamma^4 + 2491\gamma^3 - 3957\gamma^2 + 2992\gamma - 760}{16(\gamma+1)(\gamma^2-1)^2} \\
&\quad - \frac{84\gamma^6 + 459\gamma^5 - 825\gamma^4 - 138\gamma^3 + 666\gamma^2 - 321\gamma + 75}{8(\gamma+1)(\gamma^2-1)^2} \log\left(\frac{1+\gamma}{2}\right) \\
&\quad + \frac{168\gamma^7 + 78\gamma^6 - 414\gamma^5 - 171\gamma^4 + 261\gamma^3 + 81\gamma^2 - 27\gamma}{16(\gamma+1)(\gamma^2-1)^{5/2}} \operatorname{arccosh} \gamma
\end{aligned}$$

Table I: Functions of the Lorentz factor γ appearing in Eq. (6.3.16).

Note that in this computation we have included also the point-particle contributions given in chapter 4. Isolating this, we can write

$$P_{\text{rad}}^\mu = P_{\text{pp}}^\mu + \frac{G^3 M^4 \pi \nu^2}{b^3} \sum_{s=1}^2 (\mathcal{C}_{u_1}^{(s)} \tilde{u}_1^\mu + \mathcal{C}_{u_2}^{(s)} \tilde{u}_2^\mu - \mathcal{C}_b^{(s)} \hat{b}^\mu - \mathcal{C}_i^{(s)} \hat{l}^\mu), \quad (6.3.14)$$

where s labels the order in spins. In the final result, we trade the asymptotic spin tensors $s_A^{\mu\nu}$ with the corresponding Pauli-Lubanski spin vectors (per unit of mass) defined as

$$s_A^\mu \equiv \frac{1}{2} \epsilon^{\mu\nu\rho\sigma} u_A^\nu s_A^{\rho\sigma}, \quad (6.3.15)$$

then, the components $\mathcal{C}_V^{(s)}$ are dimensionless functions of only the Lorentz factor γ , the two Wilson coefficients C_{E_A} , and the six inner products $(s_A \cdot V)/b$ (there are only six because $s_A \cdot u_A = 0$ by definition).

The fact that P_{rad}^μ is a polar vector strongly constrains which inner products can appear at any given order, and in which combinations. For instance, because $\mathcal{C}_{u_1}^{(1)}$, $\mathcal{C}_{u_2}^{(1)}$, and $\mathcal{C}_b^{(1)}$ must all be even under parity, they can only depend on $(s_A \cdot \hat{l})/b$ at linear order in the spins. Indeed, we find explicitly that

$$\begin{aligned}
\mathcal{C}_{u_1}^{(1)} &= \frac{1}{b} [(s_1 \cdot \hat{l}) f_{\text{II}}(\gamma) + (s_2 \cdot \hat{l}) f_{\text{III}}(\gamma)] + O(s^2), \\
\mathcal{C}_i^{(1)} &= \frac{1}{b} [(s_1 \cdot u_2) + (s_2 \cdot u_1)] f_{\text{IV}}(\gamma) + O(s^2),
\end{aligned} \quad (6.3.16)$$

while $\mathcal{C}_{\hat{b}}^{(1)} = 0 + O(s^2)$. The remaining component $\mathcal{C}_{u_2}^{(1)}$ can be obtained from $\mathcal{C}_{u_1}^{(1)}$ by swapping the body labels $1 \leftrightarrow 2$, since P_{rad}^μ must be symmetric under this interchange. The functions $f_{\text{II}}(\gamma)$, $f_{\text{III}}(\gamma)$ and $f_{\text{IV}}(\gamma)$ are given in table I. An additional 21 functions of γ , with similar analytic structure, appear at $O(s^2)$. These are presented in appendix C. Notice that for $s = 1, 2$, $\mathcal{C}_{\hat{b}}^{(s)}$ and $\mathcal{C}_{\hat{l}}^{(s)}$ both vanish when the spins are aligned along \hat{l} ; hence, for so-called aligned-spin configuration, for the which the binary's motion is confined to a plane, we see that momentum is lost only in the direction of the relative velocity.

6.3.3 . Consistency checks

To validate eq. (6.3.12) against the existing literature, we compare results for the energy ΔE_{hyp} radiated in the center-of-mass frame, computed using eq. (1.4.16). Since \hat{b}^μ and \hat{l}^μ are purely spatial in this frame, $s_A \cdot \hat{b}$ and $s_A \cdot \hat{l}$ are equivalent to the three-dimensional dot products $-s_A \cdot \hat{\mathbf{b}}$ and $-s_A \cdot \hat{\mathbf{l}}$, respectively, and note that $s_1 \cdot u_2 \simeq s_1 \cdot \mathbf{v}$ while $s_2 \cdot u_1 \simeq -s_2 \cdot \mathbf{v}$ after expanding to first order in the relative 3-velocity \mathbf{v} . Having done so, our result for ΔE_{hyp} agrees with that of Ref. [165], which is accurate to leading order in \mathbf{v} and to quadratic order in the spins, once we also replace

$$(\mathbf{b}, \mathbf{s}_A, C_{E_A}) \rightarrow (-\mathbf{b}, -\mathbf{s}_A, 1 - C_{E_A}) \quad (6.3.17)$$

to account for differing conventions.

As a second consistency check, we use analytic continuation by way of the B2B map [114, 192, 193] to convert our result for ΔE_{hyp} into the energy ΔE_{ell} radiated during one period of elliptic-like motion. This is accomplished in three steps. Owing to current limitations of the B2B map, we first specialize to aligned-spin configurations. Next, we must transform from the covariant SSC to the canonical (Newton-Wigner) SSC [296] for the map to work. As explained in [139, 285], this generally entails transforming $(\mathbf{b}, \mathbf{s}_A)$ to new canonical variables $(\mathbf{b}_c, \mathbf{s}_{Ac})$. However, in the aligned-spin case $\mathbf{s}_A \equiv \mathbf{s}_{Ac}$, hence, only the magnitude of the impact parameter must be transformed. The rule is

$$bp_\infty = b_cp_\infty - \frac{E - M}{2E} [E a_+ - (m_1 - m_2)a_-], \quad (6.3.18)$$

where $a_\pm = (\mathbf{s}_1 \pm \mathbf{s}_2) \cdot \hat{\mathbf{l}}$, and we may define $L_c = b_cp_\infty$ as the canonical asymptotic orbital angular momentum. Finally, we obtain ΔE_{ell} from ΔE_{hyp} via [193]

$$\Delta E_{\text{ell}}(\mathcal{E}, L_c, a_\pm) = \Delta E_{\text{hyp}}(\mathcal{E}, L_c, a_\pm) - \Delta E_{\text{hyp}}(\mathcal{E}, -L_c, -a_\pm), \quad (6.3.19)$$

having eliminated γ in favor of \mathcal{E} , see eq. (1.1.3). The l.h.s. follows after analytic continuation from positive to negative values of \mathcal{E} . Expanded in powers of \mathcal{E} , we find that our result in the large-angular-momentum limit agrees with the overlapping terms from PN theory up to 3PN in Ref. [193], and up to 4PN in Refs. [63, 203].

6.4 . Summary of the chapter

We extended the worldline EFT presented in the first chapter to describe spinning compact objects, following Refs. [26, 200, 202, 292].

We then focused once again on the radiative sector and compute the radiated four-momentum at 3PM up to quadratic order in the spins (including the first finite-size effect) and to all orders in the velocity. Remarkably, integrating over the loop momenta required knowledge of only four master integrals, the same four as in the non-spinning case. At low velocities, our radiated energy is consistent with the existing literature, including the case of the energy loss from a bound system during a single orbit, which we derived via analytic continuation using the B2B map.

Conclusions and outlooks

In this thesis, we studied the gravitational two-body problem in the PM perturbative regime using the worldline EFT approach. In chapter 1, we laid out the original description presented in Ref. [149] and we saw how dissipative effects can be included, focusing in particular on the direct computation of radiative observables. We included also a brief presentation of the powerful B2B map [114, 192, 193] that allows to connect the scattering and the bound two-body problems.

We then presented in chapter 2 an explicit application of this EFT: the computation of the 2PM total impulse. This rather simple example allowed us to present in details all the modern integration techniques that we then employed throughout the dissertation, notably reverse unitarity [121, 168–171], IBP identities [172–176], differential equation for Feynman integrals [180–185] and Cutkosky’s rules [204, 205, 227, 228].

Building on [208], we proceeded by considering two point-particles interacting via gravity, and computed the pseudo stress-energy tensor up to NLO in the perturbative expansion. This quantity contains all the relevant information for the computation of radiative observables. We used it explicitly in chapter 3 to compute the asymptotic waveform at NLO, the LO energy spectrum in the soft limit, and the $\mathcal{O}(G^2)$ emitted angular momentum, finding agreements with results known in the literature. However, we were not able to find an expression for the stress-energy tensor in term of analytic known function, and for this reason we could not compute at this stage the full radiated four-momentum at LO.

Then, in chapter 4, we worked around this problem by recasting the computation of the four-momentum as a cut two-loop integral, following [207]. Applying all the modern integration techniques explained in chapter 2, we divided the computation in four topologies that arose naturally from the Feynman rules of the EFT and computed them one by one. This led us to find an explicit expression for the radiated momentum using the classical worldline formalism, filling an important gap.

All these tools can be applied rather straightforwardly to go beyond the current state-of-the-art, by including the influence of the internal structure of the two bodies. In particular, in chapter 5, we analyzed for the first time the radiative scattering dynamics of two compact objects including tidal deformations within the PM expansion [208], and gave explicit expressions for the emitted waveform up to NLO and the emitted momentum due to tidal modifications. Using the map presented in [114, 192, 193], we analytically continued the result to the case of bound orbits and found agreement with the PN literature [59–61].

Finally, we considered a binary system with spinning compact constituents. Starting from the well established EFT for spinning particles [26, 57, 58, 159, 161, 164, 166, 200–202], we computed the LO radiated momentum including spin effects up to quadratic order in spins, and the LO finite-size effect for a rotating body [209]. We found again that our results were in agreement with existing PN results [63, 193, 203]. Remarkably, the

computations done in the simpler point-particle case was essentially enough to compute all these quantities, which explains why the analytic structure of our result is similar in all the studied scenarios. All the results are collected in appendix C.

There are still many important challenges to reach the ambitious goals of future GWs science. Of course, one is the systematic inclusion of radiative effects, in particular in the incomplete 4PM term. In this sense, the worldline approach has recently made some progresses in extending the current systematic framework to include dissipative effects [150, 167], implementing the *in-in* formalism [151].

It is also practically important and theoretically interesting to push the current computations to even higher orders. Indeed, the precision of future GWs experiments [1, 2, 299] requires the improvement of our current state-of-the-art of at least two orders of magnitudes [19]. Moreover, a more systematic inclusion of tidal and spin effects at higher order is also needed to fully test GR and exploring possible physics beyond the standard model [250–252, 300]. Analytic computation of 5PM and 6PM orders could exhibit patterns that might shed light on a possible resummation of the PM series. GW memory effects are expected at 5PM, hence knowledge of this might also help to understand the role of GW memory on the dynamics of the two-body problems and its connection with radiated angular momentum [123, 128] and soft gravitons [301].

Advancements in the efficiency of the perturbative study of the two-body problem can once again come from the synergy between different approaches, in particular EFT and high-energy physics tools. For instance, double copy [94–97] has greatly helped simplifying the computation of gravitational scattering amplitude. Attempts to include this in a worldline formalism can be found in [146–148, 155, 159, 160, 302], for both bound and unbound systems. It would be also interesting to generalize (if possible) the Cutkosky cutting rules used in this thesis to include the use of retarded and advanced propagators, and apply them directly in the context of the *in-in* formalism used in [150, 167].

Another technical and important challenge is improving the current systematic framework used to find solutions for Feynman loop integrals, see also Ref. [303]. The IBP identities explained in chapter 2 becomes computationally more demanding at higher order, thus developments in this sense are crucially required [304–306]. The differential equation method to solve the master integrals found using the aforementioned IBP identities proved to be highly powerful and efficient. Improving the algorithm used to find the canonical basis [184, 185] is vital in view of the increasing number of integrals appearing at each new perturbative order. Moreover, finding the suitable boundary conditions to this differential equations becomes more challenging when higher order in the perturbative series or retarded/advanced propagators are considered [150, 167].

As we underlined in the text of this work, the PM series is suitably adapted to study scattering phenomena. It is definitely interesting to understand whether such hyperbolic encounters could be seen with future detectors [186–189], and in this sense computing waveform for such events is an important goal [163, 206, 307]. It is worth underlying that the analytic structure of the LO waveform in Fourier space and, consequently, of the energy spectrum for a scattering phenomenon is still unknown.

As of today, bound systems' signals are expected to be definitely more abundant. Thus, it is crucial to develop a precise way to map to the bound case all these pieces of information coming from study of the hyperbolic motion. Great progresses has been made especially in the context of the so-called B2B map [114,192,193]. A crucial missing element is the inclusion of non-local effects [31,34,194–196], which have just made their appearance in the PM scheme in the recently obtained 4PM order [129,130,153,154]. While Ref. [193] showed explicitly how to map the local and universal (logarithm) part of the non-local Hamiltonian, the non-universal pieces are still a puzzle that must be addressed in future studies.

Appendices

A - Derivation of the Cutkosky rules

In this appendix, we review the derivation of the Cutkosky cutting rules [204]. We follow the approach of Ref. [205] and derive them using the Veltman largest time equation (see also [228]).

A.1 . The largest time equation

Let us consider a massless scalar field. First of all, we define the following Wightman's functions corresponding to Feynman and anti-Feynman (or Dyson) propagators

$$D(x) = i \int_k \frac{e^{-ik \cdot x}}{k^2 + i0^+}, \quad \bar{D}(x) = -i \int_k \frac{e^{-ik \cdot x}}{k^2 - i0^+}. \quad (\text{A.1.1})$$

Defining also

$$\Delta_{\pm}(x) = \int_k \delta_{\pm}(k^2) e^{-ik \cdot x}, \quad (\text{A.1.2})$$

is not hard to see that

$$D(x) = \vartheta(x^0) \Delta_+(x) + \vartheta(-x^0) \Delta_-(x), \quad (\text{A.1.3})$$

$$\bar{D}(x) = \vartheta(x^0) \Delta_-(x) + \vartheta(-x^0) \Delta_+(x). \quad (\text{A.1.4})$$

The *largest time equation* is essentially a generalization of the following statement:

$$\begin{cases} D(x) = \Delta_+(x) & \text{if } x^0 > 0 \\ D(x) = \Delta_-(x) & \text{if } x^0 < 0 \end{cases}, \quad \begin{cases} \bar{D}(x) = \Delta_-(x) & \text{if } x^0 > 0 \\ \bar{D}(x) = \Delta_+(x) & \text{if } x^0 < 0 \end{cases}. \quad (\text{A.1.5})$$

Let us be more concrete and consider a massless scalar field φ described by the following Lagrangian

$$\mathcal{L} = \frac{1}{2} (\partial_{\mu} \varphi)^2 - \frac{m^2}{2} \varphi^2 + \frac{g}{3!} \varphi^3. \quad (\text{A.1.6})$$

One possible contribution to the two-point correlation function $\langle \varphi(x_1) \varphi(x_2) \rangle$ is given by the following diagram

$$\begin{array}{c} x_1 \quad y_1 \quad \text{---} \quad \text{---} \quad y_2 \quad x_2 \\ \text{---} \quad \text{---} \quad \text{---} \quad \text{---} \quad \text{---} \quad \text{---} \\ \text{---} \quad \text{---} \quad \text{---} \quad \text{---} \quad \text{---} \quad \text{---} \end{array} = (ig)^2 D(y_1 - x_1) (D(y_2 - y_1))^2 D(x_2 - y_2), \quad (\text{A.1.7})$$

where we implied that repeated spacetime coordinates are integrated. Suppose that y_1^0 is the largest time, i.e. $y_1^0 > y_2^0$ and $y_1^0 > x_i^0$ for $i = 1, 2$; then, for eq. (A.1.5) we can write

$$\begin{array}{c} x_1 \quad y_1 \quad \text{---} \quad \text{---} \quad y_2 \quad x_2 \\ \text{---} \quad \text{---} \quad \text{---} \quad \text{---} \quad \text{---} \quad \text{---} \\ \text{---} \quad \text{---} \quad \text{---} \quad \text{---} \quad \text{---} \quad \text{---} \end{array} = (ig)^2 \Delta_+(y_1 - x_1) (\Delta_-(y_2 - y_1))^2 D(x_2 - y_2), \quad (\text{A.1.8})$$

Or, in other words, when y_1^0 is the largest time, the following identity holds

$$D(y_1-x_1)(D(y_2-y_1))^2 D(x_2-y_2) - \Delta_+(y_1-x_1)(\Delta_-(y_2-y_1))^2 D(x_2-y_2) = 0. \quad (\text{A.1.9})$$

The idea now is to generalize this identity for any possible largest time and any diagram. It is convenient to introduce the following diagrammatic convention. For any diagram with n external points and m internal points, we can depict 2^{n+m} decorated diagrams by introducing two distinct vertices represented by black and white dots. Then, the following rules hold

1. For each internal black vertex, multiply by ig , for each internal white vertex, multiply by $-ig$.
2. For each line connecting two black dots x_i, x_j , assign $D(x_j - x_i)$.
3. For each line connecting two white dots x_i, x_j , assign $\bar{D}(x_j - x_i)$.
4. For each line connecting a black (white) dot x_i with a white (black) one x_j , assign $\Delta_+(x_j - x_i)$ ($\Delta_-(x_j - x_i)$).

Let us consider the previous diagram and explain why this decorated representation is essentially the generalization of eq. (A.1.9) to any possible largest time. The diagram in eq. (A.1.7) has 2 internal and external points, hence we need to draw 16 diagrams. Let us sum all of them, i.e., calling $F(x_1, x_2)$ the original non-decorated diagram, we have

$$\begin{aligned}
 \sum_{\text{decorated}} F(x_1, x_2) = & \text{○} \text{---} \text{○} \text{---} \text{○} \text{---} \text{○} + \bullet \text{---} \text{○} \text{---} \text{○} \text{---} \text{○} \\
 + & \text{○} \text{---} \bullet \text{---} \text{○} \text{---} \text{○} + \text{○} \text{---} \text{○} \text{---} \bullet \text{---} \text{○} + \text{○} \text{---} \text{○} \text{---} \text{○} \text{---} \bullet \\
 + & \bullet \text{---} \bullet \text{---} \text{○} \text{---} \text{○} + \bullet \text{---} \text{○} \text{---} \bullet \text{---} \text{○} + \bullet \text{---} \text{○} \text{---} \text{○} \text{---} \bullet \\
 + & \text{○} \text{---} \bullet \text{---} \bullet \text{---} \text{○} + \text{○} \text{---} \bullet \text{---} \text{○} \text{---} \bullet + \text{○} \text{---} \text{○} \text{---} \bullet \text{---} \bullet \\
 + & \bullet \text{---} \bullet \text{---} \bullet \text{---} \text{○} + \bullet \text{---} \bullet \text{---} \text{○} \text{---} \bullet + \bullet \text{---} \text{○} \text{---} \bullet \text{---} \bullet \\
 + & \text{○} \text{---} \bullet \text{---} \bullet \text{---} \bullet + \bullet \text{---} \bullet \text{---} \bullet \text{---} \bullet .
 \end{aligned} \tag{A.1.10}$$

Let us consider again y_1^0 as the largest time. Following the rules listed above and using

eq. (A.1.5), considering the first and the third diagrams we have

$$\text{---} \circ \text{---} \left(\text{---} \circ \text{---} \right) \text{---} \circ = (-ig)^2 \Delta_-(y_1-x_1) (\Delta^+(y_2-y_1)) \bar{D}(x_2-y_2), \quad (\text{A.1.11})$$

$$\text{---} \circ \left(\bullet \text{---} \right) \text{---} \circ = (ig)(-ig) \Delta_-(y_1-x_1) (\Delta^+(y_2-y_1)) \bar{D}(x_2-y_2), \quad (\text{A.1.12})$$

which implies that

$$\text{---} \circ \left(\text{---} \circ \text{---} \right) \text{---} \circ + \text{---} \circ \left(\bullet \text{---} \right) \text{---} \circ = 0. \quad (\text{A.1.13})$$

The same cancellation happens to any pair of diagrams in which the largest time vertex is circled once in black and once in white. This is precisely what we were looking for, i.e. the generalization of eq. (A.1.9) in which any possible vertex is the largest time.

Since the cancellation happens pair by pair, it is not hard to realize that

$$\sum_{\text{decorated}} F(x_1, x_2) = 0. \quad (\text{A.1.14})$$

This is indeed the largest time equation for our considered diagram. This can obviously be generalized to any diagram with n external points and m internal points. We can add then a rule to the four we have listed above

5. If $F(x_1, \dots, x_n)$ is the non-decorated diagram, the sum of all decorated diagrams is zero, i.e.

$$\sum_{\text{decorated}} F(x_1, \dots, x_n) = 0. \quad (\text{A.1.15})$$

We shall see momentarily how this equation derived rather easily in direct space implies non trivial relations between cut and uncut diagrams in momentum space.

A.2 . Largest time equation in momentum space and the Curkosky rules

The Wightman functions of eqs. (A.1.1) and (A.1.2) in momentum space are

$$D(k) = \frac{i}{k^2 + i0^+}, \quad \bar{D}(k) = \frac{i}{k^2 - i0^+}, \quad \Delta_{\pm} = \delta_{\pm}(k^2). \quad (\text{A.2.1})$$

From the rules listed in the previous section we understand that

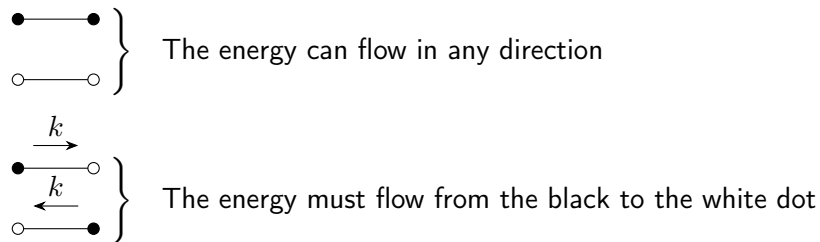




Figure 12: Diagram (a) is inconsistent because all the energy is flowing out of the loop. On the other hand, in (b) all the energy is flowing into the loop.

In this sense, the black dots serve as “sources” and white ones are “sinks”.

From this rather naive consideration, we can actually discard 8 of the 16 diagrams we depicted in (A.1.10) because of energy conservation. For instance, let us consider the two diagrams represented in figure 12 (a) and (b), which are respectively the third and the eight diagrams of eq. (A.1.10). We can immediately discard them because in (a) all the energy is flowing out of the loop, while in (b) all the energy is flowing into the loop [228]. Removing all the diagrams that are inconsistent, we reduce eq. (A.1.10) to

$$\begin{aligned}
 \sum_{\text{decorated}} F(x_1, x_2) = & \text{○} \text{---} \text{○} \text{---} \text{○} \text{---} \text{○} + \bullet \text{---} \text{○} \text{---} \text{○} \text{---} \text{○} \\
 + & \text{○} \text{---} \text{○} \text{---} \bullet + \bullet \text{---} \bullet \text{---} \text{○} \text{---} \text{○} + \text{○} \text{---} \text{○} \text{---} \bullet \text{---} \bullet \\
 + & \bullet \text{---} \bullet \text{---} \bullet \text{---} \text{○} + \text{○} \text{---} \bullet \text{---} \bullet \text{---} \bullet \text{---} \bullet + \bullet \text{---} \bullet \text{---} \bullet \text{---} \bullet = 0.
 \end{aligned}
 \tag{A.2.2}$$

Finally, we can specify the energy flow of the external legs. If we are interested in a scattering phenomenon with an incoming on-shell particle with positive energy (rightmost leg) and an outgoing on-shell particle with positive energies (leftmost leg), then we can further reduce the above equation to

$$\bullet \text{---} \text{○} \text{---} \text{○} \text{---} \text{○} + \bullet \text{---} \bullet \text{---} \text{○} \text{---} \text{○} + \bullet \text{---} \bullet \text{---} \bullet \text{---} \text{○} = 0. \tag{A.2.3}$$

At this point, we can clearly see the connection between these decorated diagrams and the cutting rules listed in section 2.3.5. Given what we said at the beginning of this section we have that

$$\bullet \xrightarrow{k} \text{○} = \frac{\xrightarrow{k}}{\text{---}} = \delta_+(k^2). \tag{A.2.4}$$

Hence, we have derived the first Cutkosky’s rule

- Cut propagators are replaced by on-shell delta functions.

Writing eq. (A.2.5) in terms of cuts, we have



From here we understand another rule given in section 2.3.5:

- The sum of all the cuts in a channel is zero.

Finally, from eq. (A.2.5) and the rules listed in the previous section, we see that on the left-hand side of the cut we have only black dots; thus, we have the usual ig for the vertices and the Feynman propagators for the lines connecting two black dots. On the right hand-side we have only white dots, which implies $-ig$ for the vertices and anti-Feynman propagators. From here we derive the last Cutkosky rule:

- All uncut propagators and vertices on the left-hand side of the cut are unaltered, while the ones on the right-hand side are replaced by the complex conjugate of their usual expressions.

All the rules derived here are valid for any diagrams and any relevant cut in a given channel. For simplicity, we have considered diagrams where no line begins and ends at the same point, but a similar derivation can be carried out in that case considering the renormalized propagator, see e.g. [205, 228]. Of course, the same rules apply whenever one has arbitrary massive or massless fields. Cutkosky's rules are non-perturbative relations, hence, if one expands the diagram in a certain way (e.g. soft expansion), the rules must be valid at each order in this expansion. Finally, we stress that this derivation requires to have only Feynman and anti-Feynman propagators; it would be interesting to see if such rules can be extended to include directly retarded and advanced propagators.

B - Boundary conditions

In this appendix we show how to compute the master integrals defined in eqs. (4.2.13)–(4.2.16) in the near-static limit to obtain the boundary conditions that we wrote in eqs. (4.2.24) and (4.2.25). We are going to follow closely the appendices of Refs. [110, 121].

B.1 . Connecting cut and uncut integrals

In this short section we shall use cutting rules to connect cut and non-cut integrals. For the reader convenience, we rewrite here the four integrals we need to solve to find all the radiated four-momenta computed in this work:

$$g_1 = \sqrt{-q^2} G_{2,0,0,\underline{1},0,1,\underline{1},0,1}, \quad (\text{B.1.1})$$

$$g_2 = \sqrt{-q^2} G_{2,0,0,0,\underline{1},0,0,\underline{1},1,1}, \quad (\text{B.1.2})$$

$$g_3 = \varepsilon \sqrt{-q^2} \sqrt{\gamma^2 - 1} G_{\underline{1},0,1,\underline{1},0,0,0,\underline{1},1,1}, \quad (\text{B.1.3})$$

$$g_4 = (\sqrt{-q^2})^5 \frac{\gamma - 1}{8} G_{2,0,0,\underline{1},1,1,\underline{1},1,1,1} + \sqrt{-q^2} \frac{1 - 2\varepsilon(2 + 3\gamma)}{12(1 + 2\varepsilon)} G_{2,0,0,\underline{1},0,0,\underline{1},1,1} \\ + \frac{2\varepsilon}{(1 + 2\varepsilon)(1 + \gamma)} \sqrt{-q^2} G_{2,0,0,\underline{1},0,1,\underline{1},0,1}, \quad (\text{B.1.4})$$

where we have defined

$$G_{\underline{i}_1, \underline{i}_2, \underline{i}_3, \underline{i}_4, \underline{i}_5, \underline{i}_6, \underline{i}_7, \underline{i}_8, \underline{i}_9} = \int_{\ell_1, \ell_2} \frac{1}{\rho_1^{i_1} \rho_2^{i_2} \rho_3^{i_3} \rho_4^{i_4} \rho_5^{i_5} \rho_6^{i_6} \rho_7^{i_7} \rho_8^{i_8} \rho_9^{i_9}}. \quad (\text{B.1.5})$$

Underlined propagators are cut, see eq. (4.2.8), and the definition of the propagators ρ_1, \dots, ρ_9 is given in eqs. (4.2.4) and (4.2.5). Using a similar diagrammatic convention to the one of section 4.2.2 we can represent g_1, \dots, g_4 as follows

$$g_1 = \text{Diagram 1}, \quad g_2 = \text{Diagram 2}, \quad g_3 = \varepsilon \sqrt{\gamma^2 - 1} \text{Diagram 3}, \quad (\text{B.1.6})$$

$$g_4 = \frac{\gamma - 1}{8} \text{Diagram 4} + \frac{1 - 2\varepsilon(2 + 3\gamma)}{12(1 + 2\varepsilon)} \text{Diagram 5} \\ + \frac{2\varepsilon}{(1 + 2\varepsilon)(1 + \gamma)} \text{Diagram 6}, \quad (\text{B.1.7})$$

where once again thin and thick lines represent respectively massless and massive propagators. Note that we have included in the definition of the graph the power of $\sqrt{-q^2}$

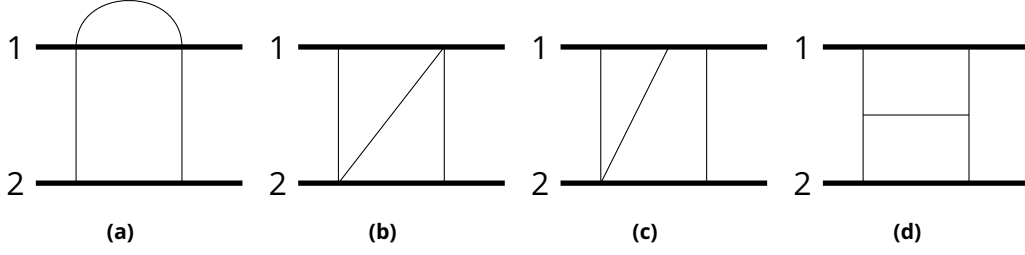


Figure 13: Representation of the topologies of scalar integrals needed to compute the boundary conditions for the four master integrals.

needed to make the integral dimensionless. We want to find boundary conditions for the differential equation given in (4.2.17), thus we need to solve this integrals in the near static limit.

To this end, we can first use the Cutkosky rules listed in 2.3.5 and derived in the previous appendix to connect the cut diagrams pictured above with the non-cut one that we have collected in figure 13. Let us introduce the notion of scalar integrals, which are basically Feynman diagrams in which one isolates all the factors of i coming from the non-cut propagators and the factors of $-i$ coming from the vertices. We can then rewrite the non-cut diagrams in figure 13 as

$$\text{figure 13(a)} \rightarrow i \int_{\ell_1, \ell_2} \frac{\sqrt{-q^2}}{(2\ell_1 \cdot u_1)^2 (2\ell_2 \cdot u_2) \ell_2^2 (\ell_2 - q)^2 (\ell_1 + \ell_2 - q)^2} \equiv i I_1, \quad (\text{B.1.8})$$

$$\text{figure 13(b)} \rightarrow i \int_{\ell_1, \ell_2} \frac{\sqrt{-q^2}}{(2\ell_1 \cdot u_1)^2 (2\ell_2 \cdot u_2) (\ell_1 - q)^2 (\ell_2 - q)^2 (\ell_1 + \ell_2 - q)^2} \equiv i I_2, \quad (\text{B.1.9})$$

$$\text{figure 13(c)} \rightarrow i \int_{\ell_1, \ell_2} \frac{\sqrt{-q^2}}{(2\ell_1 \cdot u_1) (-2\ell_2 \cdot u_1) (2\ell_2 \cdot u_2) (\ell_1 - q)^2 (\ell_2 - q)^2 (\ell_1 + \ell_2 - q)^2} \equiv i I_3, \quad (\text{B.1.10})$$

$$\text{figure 13(d)} \rightarrow i \int_{\ell_1, \ell_2} \frac{(\sqrt{-q^2})^5}{(2\ell_1 \cdot u_1)^2 (2\ell_2 \cdot u_2) \ell_1^2 \ell_2^2 (\ell_1 - q)^2 (\ell_2 - q)^2 (\ell_1 + \ell_2 - q)^2} \equiv i I_4. \quad (\text{B.1.11})$$

Using Cutkosky rules we then obtain

$$g_1 = 2\text{Im}(I_1) \quad (\text{B.1.12})$$

$$g_2 = 2\text{Im}(I_2), \quad (\text{B.1.13})$$

$$g_3 = (\varepsilon \sqrt{\gamma^2 - 1}) 2\text{Im}(I_3) - \varepsilon \sqrt{\gamma^2 - 1} \frac{\text{Im}(\text{Cut})}{\text{Im}(\text{Cut})}, \quad (\text{B.1.14})$$

$$g_4 = \frac{\gamma - 1}{8} 2\text{Im}(I_4) + \frac{1 - 2\varepsilon(2 + 3\gamma)}{12(1 + 2\varepsilon)} 2\text{Im}(I_2) + \frac{2\varepsilon}{(1 + 2\varepsilon)(1 + \gamma)} 2\text{Im}(I_1). \quad (\text{B.1.15})$$

Therefore, to find the solutions of the cut master integrals in the near static limit it is

enough to compute the scalar integrals I_1, \dots, I_4 , and the extra cut diagram in (B.1.14). That is what we do explicitly in the next section.

B.2 . Integrals in the near-static limit

In what follows, unless stated otherwise we will always consider an implicit Feynman prescription $+i0^+$ for all the propagators. We also recall that $q \cdot u_1 = 0 = q \cdot u_2$ in our kinematics.

Integral g_1

Let us start by I_1 defined in eq. (B.1.8). Sending $\ell_1^\mu \rightarrow \ell_1^\mu + q^\mu - \ell_2^\mu$ we can separate the integration in ℓ_1^μ and ℓ_2^μ

$$I_1 = \int_{\ell_2} \frac{\sqrt{-q^2}}{(2\ell_2 \cdot u_2)\ell_2^2(\ell_2 - q)^2} \int_{\ell_1} \frac{1}{\ell_1^2(2\ell_1 \cdot u_1 - 2\ell_2 \cdot u_1)^2}. \quad (\text{B.2.1})$$

We can solve the integral in ℓ_1^μ using eq. (10.25) of Ref. [176],

$$I_1 = -\frac{i}{(4\pi)^{2-\varepsilon}} \Gamma(1-\varepsilon)\Gamma(2\varepsilon) \int_{\ell} \frac{\sqrt{-q^2}}{(-2\ell \cdot u_1)^{2\varepsilon}(2\ell \cdot u_2)\ell^2(\ell - q)^2}. \quad (\text{B.2.2})$$

For simplicity, we now perform a Wick rotation to Euclidean space, i.e., for each vector $v^\mu = (v^0, \mathbf{v}) = (iv_E^0, \mathbf{v}_E)$, and we use the metric $\eta_E^{\mu\nu} = \text{diag}(+, +, +, +)$ to contract the indices. The above equation becomes

$$I_1 = \frac{\sqrt{q_E^2}}{(4\pi)^{2-\varepsilon}} \Gamma(1-\varepsilon)\Gamma(2\varepsilon) \int_{\ell_E} \frac{1}{(2\ell_E \cdot u_1^E)^{2\varepsilon}(-2\ell_E \cdot u_2^E)\ell_E^2(\ell_E - q_E)^2}. \quad (\text{B.2.3})$$

Notice that

$$q_E^2 = -q^2, \quad u_1^E \cdot u_2^E = -\gamma, \quad u_1^E \cdot u_1^E = -1 = u_2^E \cdot u_2^E. \quad (\text{B.2.4})$$

Using Schwinger parametrization we can rewrite the integral over ℓ_E of eq. (B.2.3) as a Gaussian integral, i.e.,

$$\begin{aligned} I_1 &= \frac{\sqrt{q_E^2}}{(4\pi)^{2-\varepsilon}} \Gamma(1-\varepsilon) \int_{\mathbb{R}_+^4} dt_1 dt_2 ds_1 ds_2 t^{2\varepsilon-1} \\ &\quad \times \int_{\ell_E} \exp \left[-t_1(2\ell_E \cdot u_1^E) - t_2(-2\ell_E \cdot u_2^E) - s_1\ell_E^2 - s_2(\ell_E - q_E)^2 \right] \\ &= \frac{\sqrt{-q^2}}{(4\pi)^{4-2\varepsilon}} \Gamma(1-\varepsilon) \int_{\mathbb{R}_+^4} dt_1 dt_2 ds_1 ds_2 \frac{t_1^{2\varepsilon-1}}{(s_1 + s_2)^{2-\varepsilon}} \\ &\quad \times \exp \left[-\frac{s_1 s_2}{s_1 + s_2} (-q^2) - \frac{t_1^2 + t_2^2 - 2\gamma t_1 t_2}{s_1 + s_2} \right]. \end{aligned} \quad (\text{B.2.5})$$

Finally, for $a = 1, 2$, we can split the integrations in t_a and s_a , by simply performing the shift $t_a \rightarrow \sqrt{s_1 + s_2} t_a$, obtaining

$$I_1 = \frac{\sqrt{-q^2}}{(4\pi)^{4-2\varepsilon}} \Gamma(1-\varepsilon) \int_{\mathbb{R}_+^2} ds_1 ds_2 \frac{e^{-\frac{s_1 s_2}{s_1+s_2}(-q^2)}}{(s_1+s_2)^{\frac{3}{2}-2\varepsilon}} \int_{\mathbb{R}_+^2} dt_1 dt_2 t_1^{2\varepsilon-1} e^{-[t_1^2+t_2^2-2\gamma t_1 t_2]}. \quad (\text{B.2.6})$$

The integration over s_1 and s_2 can be performed using standard integration over Feynman parameters. Making the change of variables $s = s_1 + s_2$, $\tilde{s} = s_1/s$ one gets

$$\int_{\mathbb{R}_+^2} ds_1 ds_2 \frac{e^{-\frac{s_1 s_2}{s_1+s_2}(-q^2)}}{(s_1+s_2)^{\frac{3}{2}-2\varepsilon}} = \int_0^1 d\tilde{s} \int_0^\infty \frac{e^{-s[\tilde{s}(1-\tilde{s})(-q^2)]}}{s^{\frac{1}{2}-2\varepsilon}} = \frac{16^\varepsilon \sqrt{\pi}}{(-q^2)^{\frac{1}{2}+2\varepsilon}} \frac{\Gamma(\frac{1}{2}+2\varepsilon) \Gamma(\frac{1}{2}-2\varepsilon)}{\Gamma(1-2\varepsilon)}. \quad (\text{B.2.7})$$

The integration over t_1 and t_2 is a bit more delicate. Changing again variables as follows $t_2 = t t_1$, one can solve the integration over t_1 ,

$$\begin{aligned} \int_{\mathbb{R}_+^2} dt_1 dt_2 t_1^{2\varepsilon-1} e^{-[t_1^2+t_2^2-2\gamma t_1 t_2]} &= \int_0^\infty dt \int_0^\infty dt_1 t_1^{2\varepsilon} e^{-t_1^2[1+t^2-2\gamma t]} \\ &= \frac{\Gamma(\frac{1}{2}+\varepsilon)}{2} \int_0^\infty dt \frac{1}{(1+t^2-2\gamma t)^{\frac{1}{2}+\varepsilon}}. \end{aligned} \quad (\text{B.2.8})$$

Note that the integrand in t is divergent for $t = \gamma - \sqrt{\gamma^2 - 1} = x$ and $t = \gamma + \sqrt{\gamma^2 - 1}$, so one must treat it with care. In the near static limit $x \rightarrow 1$ we obtain

$$\begin{aligned} \int_0^\infty dt \frac{1}{(1+t^2-2\gamma t)^{\frac{1}{2}+\varepsilon}} &= -\frac{1}{2\varepsilon} \\ &+ \frac{\sqrt{\pi}}{(1-x)^{2\varepsilon}} \frac{\Gamma(\frac{1}{2}-\varepsilon)}{\Gamma(1-\varepsilon)} \cos(\pi\varepsilon) (\cot(\pi\varepsilon) - i) + \mathcal{O}(1-x). \end{aligned} \quad (\text{B.2.9})$$

Putting all together we arrive to our final result for I_1 in the near static limit, i.e.,

$$\begin{aligned} I_1 &= \frac{1}{2(4\pi)^{4-2\varepsilon}} \frac{\Gamma(\frac{1}{2}+2\varepsilon) \Gamma(\frac{1}{2}-2\varepsilon)}{(-q^2)^{2\varepsilon} \Gamma(1-2\varepsilon)} \left[-\frac{16^\varepsilon \sqrt{\pi}}{2\varepsilon} \Gamma\left(\frac{1}{2}+\varepsilon\right) \Gamma(1-\varepsilon) \right. \\ &\quad \left. + \frac{16^\varepsilon \pi}{(1-x)^{2\varepsilon}} \Gamma\left(\frac{1}{2}+\varepsilon\right) \Gamma\left(\frac{1}{2}-\varepsilon\right) \cos(\pi\varepsilon) (\cot(\pi\varepsilon) - i) \right] + \mathcal{O}(1-x). \end{aligned} \quad (\text{B.2.10})$$

Using eq. (B.1.12) we can finally find the boundary condition for the master integral g_1 , i.e.,

$$g_1|_{\gamma \rightarrow 1} = -\frac{C_{BC}}{(4\pi)^{4-2\varepsilon}}, \quad (\text{B.2.11})$$

where C_{BC} has been defined in (4.2.25) and we used that

$$16^\varepsilon \pi \frac{\Gamma(\frac{1}{2}+\varepsilon) \Gamma(\frac{1}{2}-\varepsilon) \cos(\pi\varepsilon)}{\Gamma(1-2\varepsilon)} = \frac{\sqrt{\pi} \Gamma(1+\varepsilon) \Gamma(1-\varepsilon) \Gamma(\frac{1}{2}-2\varepsilon)}{\varepsilon \Gamma(1-4\varepsilon)} \sin(\pi\varepsilon). \quad (\text{B.2.12})$$

Integral g_2

Let us now analyse the second scalar integral I_2 defined in eq. (B.1.9). First of all, we perform the shift $\ell_1 \rightarrow \ell_1 + q$ and then go again to Euclidean space for simplicity,

$$I_2 = \sqrt{q_E^2} \int_{\ell_1^E \ell_2^E} \frac{1}{(2\ell_1^E \cdot u_1^E)^2 (-2\ell_2^E \cdot u_2^E) (\ell_1^E)^2 (\ell_2^E - q_E)^2 (\ell_1^E + \ell_2^E)^2}. \quad (\text{B.2.13})$$

Using Schwinger parametrization and then solving the two Gaussian integrals, one eventually arrives to

$$\begin{aligned} I_2 &= \sqrt{q_E^2} \int_{\mathbb{R}_+^5} dt_1 \dots dt_5 \int_{\ell_1^E \ell_2^E} t_4 \exp \left[-t_1 (\ell_1^E)^2 - t_2 (\ell_2^E - q_E)^2 - t_3 (\ell_1^E + \ell_2^E)^2 \right. \\ &\quad \left. - t_4 (2\ell_1^E \cdot u_1^E) - t_5 (-2\ell_2^E \cdot u_2^E) \right] \\ &= \frac{\sqrt{-q^2}}{(4\pi)^{4-2\varepsilon}} \int_{\mathbb{R}_+^5} dt_1 \dots dt_5 \frac{t_4}{T^{2-\varepsilon}} \exp \left[-\frac{t_1 t_2 t_3}{T} (-q^2) - \frac{t_{13} t_4^5 + t_{23} t_5^2 - 2\gamma t_3 t_4 t_5}{T} \right], \end{aligned} \quad (\text{B.2.14})$$

where we have defined [110]

$$t_{13} \equiv t_1 + t_3, \quad t_{23} \equiv t_2 + t_3, \quad T \equiv t_1 t_2 + t_1 t_3 + t_2 t_3. \quad (\text{B.2.15})$$

Now we shift $t_4 \rightarrow \sqrt{T} t_4$ and $t_5 \rightarrow \sqrt{T} t_5$, splitting the computation in two integrals

$$I_2 = \frac{\sqrt{-q^2}}{(4\pi)^{4-2\varepsilon}} \int_{\mathbb{R}_+^3} dt_1 dt_2 dt_3 \frac{e^{-\frac{t_1 t_2 t_3}{T} (-q^2)}}{T^{\frac{1}{2}-\varepsilon}} \int_{\mathbb{R}_+^2} dt_4 dt_5 t_4 e^{-[t_{13} t_4^2 + t_{23} t_5^2 - 2\gamma t_3 t_4 t_5]}. \quad (\text{B.2.16})$$

The integral in t_4 and t_5 can be solve exactly. Changing variables $t_5 = t t_4$ we get

$$\begin{aligned} \int_{\mathbb{R}_+^2} dt_4 dt_5 t_4 e^{-[t_{13} t_4^2 + t_{23} t_5^2 - 2\gamma t_3 t_4 t_5]} &= \int_0^\infty dt \int_0^\infty dt_5 t_4^2 e^{-t_4^2 [t_{23} t^2 + t_{13} - 2\gamma t_3 t]} \\ &= \frac{\sqrt{\pi}}{4} \int_0^\infty dt \frac{1}{(t^2 t_{23} + t_{13} - 2\gamma t_3 t)^{\frac{3}{2}}} = -\frac{\sqrt{\pi}}{4\sqrt{t_{13}}} \frac{\sqrt{T + t_3^2} + \gamma t_3}{(\gamma^2 - 1)t_3^2 - T}, \end{aligned} \quad (\text{B.2.17})$$

so that

$$I_2 = -\frac{\sqrt{\pi}}{4} \frac{\sqrt{-q^2}}{(4\pi)^{4-2\varepsilon}} \int_{\mathbb{R}_+^3} dt_1 dt_2 dt_3 \frac{e^{-\frac{t_1 t_2 t_3}{T} (-q^2)}}{T^{\frac{1}{2}-\varepsilon}} \frac{1}{\sqrt{t_{13}}} \frac{\sqrt{T + t_3^2} + \gamma t_3}{(\gamma^2 - 1)t_3^2 - T}. \quad (\text{B.2.18})$$

At this point we need to take the static limit $\gamma \rightarrow 1$. One possible way is to assume that the three Schwinger parameters do not scale with γ , i.e.,

$$t_1, t_2, t_3 \sim \mathcal{O}(\gamma^0). \quad (\text{B.2.19})$$

However, in this case the resulting solution to the integral is real and, in view of eq. (B.1.13), cannot contribute to the boundary conditions of g_2 . In particular, eq. (B.2.18)

shows that the assumption (B.2.19) does not capture the integration region coming from large values of t_3 . We can choose the following scaling instead [110]

$$t_1 t_2 \sim \mathcal{O}(\gamma^0), \quad t_3 \sim \mathcal{O}(\gamma^2 - 1). \quad (\text{B.2.20})$$

In this limit the integration over t_3 factorizes so that

$$I_2 \simeq -\frac{\sqrt{\pi}}{2(\gamma^2 - 1)} \frac{\sqrt{-q^2}}{(4\pi)^{4-2\varepsilon}} \int_{\mathbb{R}^{+2}} dt_1 dt_2 \frac{e^{-\frac{t_1 t_2}{t_{12}}(-q^2)}}{t_{12}^{\frac{1}{2}-\varepsilon}} \int_0^\infty dt_3 \frac{1}{t_3^{1-\varepsilon} \left(t_3 - \frac{t_{12}}{\gamma^2 - 1}\right)}. \quad (\text{B.2.21})$$

Changing variables, $t_3 = z t_{12}/(\gamma^2 - 1)$, we have

$$I_2 \simeq -\frac{\sqrt{\pi}}{2(1-x)^{2\varepsilon}} \frac{\sqrt{-q^2}}{(4\pi)^{4-2\varepsilon}} \int_{\mathbb{R}^{+2}} dt_1 dt_2 \frac{e^{-\frac{t_1 t_2}{t_{12}}(-q^2)}}{t_{12}^{\frac{3}{2}-2\varepsilon}} \int_0^\infty dz \frac{1}{z^{1-\varepsilon} (z-1)}, \quad (\text{B.2.22})$$

where we used that for $\gamma \rightarrow 1$, $(\gamma^2 - 1)^\varepsilon \sim (1-x)^{2\varepsilon}$. The integral in z can be solved exactly, again taking care of the divergences in 0 and 1, obtaining

$$\int_0^\infty dz \frac{1}{z^{1-\varepsilon} (z-1)} = (-1)^{1-\varepsilon} \frac{\Gamma(1-\varepsilon)\Gamma(1+\varepsilon)}{\varepsilon}. \quad (\text{B.2.23})$$

Instead, the integral in t_1 and t_2 can be solved following a procedure completely analogous to the one of eq. (B.2.7), i.e. changing variables to $t_{12} = t_1 + t_2$ and $\tilde{t} = t_1/t_{12}$. One eventually obtains

$$\int_{\mathbb{R}^{+2}} dt_1 dt_2 \frac{e^{-\frac{t_1 t_2}{t_{12}}(-q^2)}}{t_{12}^{\frac{3}{2}-2\varepsilon}} = \frac{\Gamma\left(\frac{1}{2} + 2\varepsilon\right) \Gamma\left(\frac{1}{2} - 2\varepsilon\right)^2}{(-q^2)^{\frac{1}{2}+2\varepsilon} \Gamma(1-4\varepsilon)}. \quad (\text{B.2.24})$$

Putting these results together and using eq. (B.1.13), we finally arrive to

$$g_2|_{\gamma \rightarrow 1} = -\frac{C_{\text{BC}}}{(4\pi)^{4-2\varepsilon}}. \quad (\text{B.2.25})$$

Integral g_3

As shown by eq. (B.1.14), finding the boundary condition of g_3 requires the solution of \mathcal{I}_3 in the near static limit and also the computation of another cut of figure 13(c). First of all, following a procedure analogous to what shown for I_1 and I_2 , we find

$$I_3 \sqrt{\gamma^2 - 1}|_{\gamma=1} = \frac{i 2^{-2+2\varepsilon} \pi^2}{(4\pi)^{4-2\varepsilon} (-q^2)^{2\varepsilon}} \frac{1}{\varepsilon} \frac{\Gamma\left(\frac{1}{2} - \varepsilon\right) \Gamma\left(\frac{1}{2} - 2\varepsilon\right) \Gamma\left(\frac{1}{2} + 2\varepsilon\right)}{\Gamma\left(\frac{1}{2} - 3\varepsilon\right)}. \quad (\text{B.2.26})$$

To compute g_3 we have to subtract the last term on the right-hand side of eq. (B.1.14). Following the rules described in section B.1, we find

$$\varepsilon \sqrt{\gamma^2 - 1} \int_{\mathbb{R}^{+2}} \frac{1}{t_{12}} = -i\varepsilon \sqrt{\gamma^2 - 1} \sqrt{-q^2} \int_{\ell_2} \delta(2\ell_2 \cdot u_2) \delta(2\ell_2 \cdot u_1) I_L I_R, \quad (\text{B.2.27})$$

where we have defined

$$I_L = \frac{1}{2} \int_{\ell_1} \frac{1}{(2\ell_1 \cdot u_1)(\ell_1 - q)^2(\ell_1 + \ell_2 - q)^2}, \quad (\text{B.2.28})$$

$$I_R = -\frac{1}{(\ell_2 - q)^2}. \quad (\text{B.2.29})$$

The integral I_L is a simple one-loop computation that can be carried out straightforwardly using Schwinger or Feynman parametrization, obtaining

$$I_L = -\frac{i}{(4\pi)^{2-\varepsilon}} \frac{2^{-1+2\varepsilon} \pi}{(-\ell_1^2)^{\frac{1}{2}-\varepsilon}} \frac{\Gamma(\frac{1}{2}-\varepsilon) \Gamma(\frac{1}{2}+\varepsilon)}{\Gamma(1-\varepsilon)}. \quad (\text{B.2.30})$$

Inserting everything in eq. (B.2.27) and solving the two delta functions, one eventually arrives to

$$\begin{aligned} \varepsilon \sqrt{\gamma^2 - 1} \int \frac{d^2 \mathbf{q}}{(2\pi)^{2-\varepsilon}} \frac{1}{(\ell_2)^{\frac{1}{2}+\varepsilon} (\ell_2 + \mathbf{q})^2} &= -\frac{2^{-1+2\varepsilon} \Gamma(\frac{1}{2}-\varepsilon) \Gamma(\frac{1}{2}+\varepsilon)}{(4\pi)^{2-\varepsilon} 4\Gamma(1-\varepsilon)} \int \frac{d^{2-\varepsilon} \ell_2}{(2\pi)^{2-\varepsilon}} \frac{1}{(\ell_2)^{\frac{1}{2}+\varepsilon} (\ell_2 + \mathbf{q})^2} \\ &= \frac{2^{-1+2\varepsilon} \pi^2}{(4\pi)^{4-2\varepsilon} (-q^2)^{2\varepsilon} \varepsilon} \frac{1 \Gamma(\frac{1}{2}-\varepsilon) \Gamma(\frac{1}{2}-2\varepsilon) \Gamma(\frac{1}{2}+2\varepsilon)}{\Gamma(\frac{1}{2}-3\varepsilon)}. \end{aligned} \quad (\text{B.2.31})$$

Using eqs. (B.2.26) and (B.2.31) into (B.1.14), we get

$$g_3|_{\gamma \rightarrow 1} = 0. \quad (\text{B.2.32})$$

Integral g_4

Finally, we discuss the boundary condition for g_4 . Because of the factor $\gamma - 1$ in front of the first term of eq. (B.1.15), I_4 does not contribute to the boundary condition of g_4 , and we do not need to compute it. Using the results computed before for I_1 and I_2 , one can take the near-static limit of (B.1.15), obtaining

$$g_4|_{\gamma \rightarrow 1} = -\frac{1}{12} \frac{C_{\text{BC}}}{(4\pi)^{4-2\varepsilon}}. \quad (\text{B.2.33})$$

C - Explicit expressions

In this last appendix we give an explicit expression for some of the long quantities defined in the text.

C.1 . Radiated Four momentum

We decompose the radiated four momentum as follows

$$P_{\text{rad}}^\mu = \frac{G^3 M^4 \pi \nu^2}{b^3} \left(\mathcal{C}_{u_1} \check{u}_1^\mu + \mathcal{C}_{u_2} \check{u}_2^\mu - \mathcal{C}_l \hat{l}^\mu - \mathcal{C}_b \hat{b}^\mu \right). \quad (\text{C.1.1})$$

Defining $V \in \{\hat{l}, \hat{b}, \check{u}_1, \check{u}_2\}$, in the next tables we give explicit expression for

$$\mathcal{C}_V = \mathcal{C}_V^{(0)} + \frac{1}{b^4} \sum_{X=E,B} \mathcal{C}_V^{X^2} + \frac{1}{b} \sum_{A=1,2} \mathcal{C}_V^{sA} + \frac{1}{b^2} \sum_{A,B=1,2} \mathcal{C}_V^{sAsB}, \quad (\text{C.1.2})$$

The first term is the point-particle computation (chapter 4), the second represents the tidal effects (chapter 5) and the last two are the linear and quadratic in spin contributions (chapter 6).

Table I: Components of the coefficient \mathcal{C}_{u_1} . The components of \mathcal{C}_{u_2} can be obtain from the following expressions by swapping the labels 1 and 2 of the objects.

$$\begin{aligned} \mathcal{C}_{u_1}^{(0)} &= \frac{210\gamma^6 - 552\gamma^5 + 339\gamma^4 - 912\gamma^3 + 3148\gamma^2 - 3336\gamma + 1151}{48(\gamma^2 - 1)^{3/2}} - \frac{35\gamma^4 + 60\gamma^3 - 150\gamma^2 + 76\gamma - 5}{8\sqrt{\gamma^2 - 1}} \log\left(\frac{\gamma+1}{2}\right) \\ &+ \frac{70\gamma^7 - 165\gamma^5 + 112\gamma^3 - 33\gamma}{16(\gamma^2 - 1)^2} \operatorname{arccosh}\gamma \\ \mathcal{C}_{u_1}^{E^2} &= \frac{\mathcal{C}_{E_1^2}}{m_1} \left[\frac{15\sqrt{\gamma^2 - 1} (937\gamma^9 + 1551\gamma^8 - 2463\gamma^7 - 5645\gamma^6 + 20415\gamma^5 + 65965\gamma^4)}{128(\gamma - 1)(\gamma + 1)^4} \right. \\ &- \frac{15\sqrt{\gamma^2 - 1} (349541\gamma^3 - 535057\gamma^2 + 360356\gamma - 92160)}{128(\gamma - 1)(\gamma + 1)^4} \\ &\left. + \frac{225}{32} \sqrt{\gamma^2 - 1} (21\gamma^4 - 14\gamma^2 + 9) \log\left(\frac{\gamma+1}{2}\right) - \frac{225\gamma (2\gamma^2 - 3) (21\gamma^4 - 14\gamma^2 + 9)}{128(\gamma^2 - 1)} \operatorname{arccosh}\gamma \right] \\ &+ \frac{\mathcal{C}_{E_2^2}}{m_2} \frac{45(\gamma - 1)^2 (42\gamma^8 + 210\gamma^7 + 315\gamma^6 - 105\gamma^5 - 944\gamma^4 - 1528\gamma^3 + 22011\gamma^2 - 33201\gamma + 16272)}{64(\gamma + 1)^3 \sqrt{\gamma^2 - 1}} \\ \mathcal{C}_{u_1}^{B^2} &= \frac{\mathcal{C}_{B_1^2}}{m_1} \left[\frac{15\sqrt{\gamma^2 - 1} (1559\gamma^8 + 3716\gamma^7 - 1630\gamma^6 - 11660\gamma^5 + 28288\gamma^4)}{256(\gamma + 1)^4} \right. \\ &+ \frac{15\sqrt{\gamma^2 - 1} (155292\gamma^3 - 543442\gamma^2 + 535212\gamma - 180775)}{256(\gamma + 1)^4} \\ &\left. + \frac{1575}{32} (\gamma^2 - 1)^{3/2} (3\gamma^2 + 1) \log\left(\frac{\gamma+1}{2}\right) - \frac{1575}{128} \gamma (2\gamma^2 - 3) (3\gamma^2 + 1) \operatorname{arccosh}\gamma \right] \\ &- \frac{\mathcal{C}_{B_2^2}}{m_2} \frac{45(\gamma - 1)^3 (105\gamma^5 + 630\gamma^4 + 1840\gamma^3 + 3690\gamma^2 - 17769\gamma + 15984)}{64(\gamma + 1)^3 \sqrt{\gamma^2 - 1}} \end{aligned}$$

$$\begin{aligned}
\mathcal{C}_{u_1}^{s_1} & (s_1 \cdot \hat{l}) \left[\frac{210\gamma^6 - 356\gamma^5 - 111\gamma^4 - 1627\gamma^3 + 5393\gamma^2 - 4741\gamma + 1352}{16(\gamma+1)(\gamma^2-1)} \right. \\
& \quad \left. - \frac{105\gamma^4 + 345\gamma^3 - 405\gamma^2 + 147\gamma - 48}{8(\gamma+1)} \log\left(\frac{\gamma+1}{2}\right) + \frac{210\gamma^6 - 405\gamma^4 + 135\gamma^2}{16(\gamma^2-1)^{3/2}} \operatorname{arccosh}\gamma \right] \\
\mathcal{C}_{u_1}^{s_2} & (s_2 \cdot \hat{l}) \left[\frac{210\gamma^6 - 279\gamma^5 - 219\gamma^4 - 1350\gamma^3 + 4732\gamma^2 - 4243\gamma + 1245}{16(\gamma+1)(\gamma^2-1)} \right. \\
& \quad \left. - \frac{21\gamma^4 + 66\gamma^3 - 84\gamma^2 + 30\gamma - 9}{2(\gamma+1)} \log\left(\frac{\gamma+1}{2}\right) + \frac{42\gamma^6 - 81\gamma^4 + 27\gamma^2}{4(\gamma^2-1)^{3/2}} \operatorname{arccosh}\gamma \right] \\
\mathcal{C}_{u_1}^{s_1 s_2} & (s_1 \cdot u_2)(s_2 \cdot u_1) \left[- \frac{1782\gamma^7 + 2217\gamma^6 - 20532\gamma^5 + 10959\gamma^4 + 75198\gamma^3 - 153537\gamma^2 + 115776\gamma - 31287}{64(\gamma+1)^2(\gamma^2-1)^{5/2}} \right. \\
& \quad \left. + \frac{189\gamma^4 - 531\gamma^3 + 819\gamma^2 - 585\gamma + 144}{4(\gamma+1)(\gamma^2-1)^{3/2}} \log\left(\frac{\gamma+1}{2}\right) - \frac{126\gamma^6 - 243\gamma^4 + 81\gamma^2}{16(\gamma^2-1)^3} \operatorname{arccosh}\gamma \right] \\
& + (s_1 \cdot \hat{b})(s_2 \cdot \hat{b}) \left[- \frac{840\gamma^{10} - 227\gamma^9 - 3696\gamma^8 - 9954\gamma^7 + 44798\gamma^6 - 59952\gamma^5 + 55470\gamma^4 +}{64(\gamma+1)^2(\gamma^2-1)^{5/2}} \right. \\
& \quad \left. + \frac{20398\gamma^3 + 61950\gamma^2 - 90531\gamma + 35462}{64(\gamma+1)^2(\gamma^2-1)^{5/2}} - \frac{168\gamma^7 - 414\gamma^5 + 453\gamma^3 - 315\gamma}{16(\gamma^2-1)^2} \operatorname{arccosh}\gamma \right. \\
& \quad \left. + \frac{42\gamma^7 + 162\gamma^6 - 345\gamma^5 + 27\gamma^4 + 240\gamma^3 - 108\gamma^2 + 63\gamma - 81}{4(\gamma+1)(\gamma^2-1)^{3/2}} \log\left(\frac{\gamma+1}{2}\right) \right] \\
& + (s_1 \cdot \hat{l})(s_2 \cdot \hat{l}) \left[\frac{840\gamma^8 - 1907\gamma^7 - 752\gamma^6 - 6741\gamma^5 + 48430\gamma^4 - 91325\gamma^3 + 79596\gamma^2 - 33947\gamma + 5806}{16(\gamma^2-1)^{5/2}} \right. \\
& \quad \left. - \frac{42\gamma^7 + 162\gamma^6 - 345\gamma^5 + 27\gamma^4 + 195\gamma^3 - 153\gamma^2 + 108\gamma - 36}{(\gamma+1)(\gamma^2-1)^{3/2}} \log\left(\frac{\gamma+1}{2}\right) \right. \\
& \quad \left. + \frac{168\gamma^9 - 582\gamma^7 + 687\gamma^5 - 318\gamma^3 + 45\gamma}{4(\gamma^2-1)^3} \operatorname{arccosh}\gamma \right] \\
\mathcal{C}_{u_1}^{s_1 s_1} & (s_1 \cdot u_2)^2 \left[\frac{1260\gamma^8 + 450\gamma^7 - 5670\gamma^6 + 16530\gamma^5 - 15501\gamma^4 - 30600\gamma^3 + 57822\gamma^2 - 21900\gamma - 2391}{320(\gamma+1)^2(\gamma^2-1)^{5/2}} \right. \\
& \quad \left. + \frac{315\gamma^4 - 1170\gamma^3 + 1620\gamma^2 - 1062\gamma + 297}{32(\gamma+1)(\gamma^2-1)^{3/2}} \log\left(\frac{\gamma+1}{2}\right) + \frac{90\gamma^3 - 135\gamma}{64(\gamma^2-1)^2} \operatorname{arccosh}\gamma \right] \\
& + (s_1 \cdot \hat{b})^2 \left[\frac{2520\gamma^8 + 3310\gamma^7 - 1495\gamma^6 - 5070\gamma^5 + 2868\gamma^4 + 7686\gamma^3 - 15315\gamma^2 + 6674\gamma + 24022}{320(\gamma+1)^4\sqrt{\gamma^2-1}} \right. \\
& \quad \left. - \frac{315\gamma^6 + 1065\gamma^5 + 210\gamma^4 - 1866\gamma^3 - 357\gamma^2 + 801\gamma - 168}{32(\gamma+1)^2\sqrt{\gamma^2-1}} \log\left(\frac{\gamma+1}{2}\right) + \frac{630\gamma^5 - 945\gamma^3}{64(\gamma^2-1)} \operatorname{arccosh}\gamma \right] \\
& + (s_1 \cdot \hat{l})^2 \left[\frac{5670\gamma^6 - 1180\gamma^5 - 16935\gamma^4 - 58250\gamma^3 + 171298\gamma^2 - 131850\gamma + 38447}{320(\gamma+1)^2\sqrt{\gamma^2-1}} \right. \\
& \quad \left. - \frac{315\gamma^6 + 1590\gamma^5 - 975\gamma^4 - 636\gamma^3 + 573\gamma^2 - 954\gamma + 87}{32(\gamma+1)^2\sqrt{\gamma^2-1}} \log\left(\frac{\gamma+1}{2}\right) + \frac{630\gamma^5 - 855\gamma^3 - 135\gamma}{64(\gamma^2-1)} \operatorname{arccosh}\gamma \right] \\
& + C_{E_1}(s_1 \cdot u_2)^2 \left[\frac{1260\gamma^8 + 450\gamma^7 - 3645\gamma^6 + 20580\gamma^5 - 16086\gamma^4 - 125580\gamma^3 + 290877\gamma^2 - 236490\gamma + 70074}{320(\gamma+1)^2(\gamma^2-1)^{5/2}} \right. \\
& \quad \left. + \frac{315\gamma^4 - 1170\gamma^3 + 1620\gamma^2 - 1206\gamma + 297}{32(\gamma+1)(\gamma^2-1)^{3/2}} \log\left(\frac{\gamma+1}{2}\right) + \frac{90\gamma^5 - 81\gamma^3 - 81\gamma}{64(\gamma^2-1)^3} \operatorname{arccosh}\gamma \right] \\
& + C_{E_1}(s_1 \cdot \hat{b})^2 \left[- \frac{4305\gamma^{10} - 3500\gamma^9 - 13415\gamma^8 - 20740\gamma^7 + 117647\gamma^6 - 132330\gamma^5}{320(\gamma+1)^2(\gamma^2-1)^{5/2}} \right.
\end{aligned}$$

$$\begin{aligned}
& - \frac{75309\gamma^4 + 1280\gamma^3 - 127504\gamma^2 + 155290\gamma - 56342}{320(\gamma + 1)^2(\gamma^2 - 1)^{5/2}} \\
& + \frac{525\gamma^7 + 1530\gamma^6 - 2385\gamma^5 - 2220\gamma^4 + 2643\gamma^3 + 834\gamma^2 - 783\gamma - 144}{32(\gamma + 1)(\gamma^2 - 1)^{3/2}} \log\left(\frac{\gamma + 1}{2}\right) \\
& - \frac{1050\gamma^9 - 3675\gamma^7 + 4632\gamma^5 - 2655\gamma^3 + 648\gamma}{64(\gamma^2 - 1)^3} \operatorname{arccosh}\gamma \Big] \\
& + C_{E_1}(s_1 \cdot \hat{l})^2 \Big[\frac{3045\gamma^8 - 10040\gamma^7 + 8525\gamma^6 - 47880\gamma^5 + 217323\gamma^4 - 372936\gamma^3 + 296895\gamma^2 - 108664\gamma + 13732}{320(\gamma^2 - 1)^{5/2}} \\
& - \frac{525\gamma^7 + 1845\gamma^6 - 3555\gamma^5 - 915\gamma^4 + 2607\gamma^3 - 489\gamma^2 + 423\gamma - 441}{32(\gamma + 1)(\gamma^2 - 1)^{3/2}} \log\left(\frac{\gamma + 1}{2}\right) \\
& + \frac{1050\gamma^9 - 3765\gamma^7 + 4803\gamma^5 - 2655\gamma^3 + 567\gamma}{64(\gamma^2 - 1)^3} \operatorname{arccosh}\gamma \Big] \\
C_{u_1}^{s_2 s_2} & (s_2 \cdot u_1)^2 \Big[\frac{2520\gamma^9 + 3150\gamma^8 - 10125\gamma^7 - 8925\gamma^6 + 33999\gamma^5 - 25761\gamma^4 - 32463\gamma^3 + 78777\gamma^2 - 40491\gamma - 681}{640(\gamma + 1)^2(\gamma^2 - 1)^{5/2}} \\
& - \frac{189\gamma^5 + 189\gamma^4 + 1134\gamma^3 - 2682\gamma^2 + 1701\gamma - 531}{64(\gamma + 1)(\gamma^2 - 1)^{3/2}} \log\left(\frac{\gamma + 1}{2}\right) + \frac{378\gamma^5 - 441\gamma^3 - 189\gamma}{128(\gamma^2 - 1)^2} \operatorname{arccosh}\gamma \Big] \\
& + (s_2 \cdot \hat{b})^2 \Big[\frac{1890\gamma^{11} + 5180\gamma^{10} - 12005\gamma^9 - 10125\gamma^8 + 10748\gamma^7 + 4788\gamma^6 + 28686\gamma^5}{640(\gamma + 1)^2(\gamma^2 - 1)^{5/2}} \\
& - \frac{20414\gamma^4 + 4486\gamma^3 + 5496\gamma^2 + 24833\gamma - 26067}{640(\gamma + 1)^2(\gamma^2 - 1)^{5/2}} + \frac{1386\gamma^7 - 3243\gamma^5 + 1524\gamma^3 + 333\gamma}{128(\gamma^2 - 1)^2} \operatorname{arccosh}\gamma \\
& - \frac{693\gamma^7 + 1773\gamma^6 - 1935\gamma^5 - 3999\gamma^4 + 2799\gamma^3 + 1671\gamma^2 - 1557\gamma + 555}{64(\gamma + 1)(\gamma^2 - 1)^{3/2}} \log\left(\frac{\gamma + 1}{2}\right) \Big] \\
& + (s_2 \cdot \hat{l})^2 \Big[\frac{945\gamma^{11} + 5915\gamma^{10} - 3425\gamma^9 - 29070\gamma^8 - 37396\gamma^7 + 175404\gamma^6 - 30792\gamma^5}{320(\gamma + 1)^2(\gamma^2 - 1)^{5/2}} \\
& - \frac{253022\gamma^4 - 182747\gamma^3 - 66537\gamma^2 + 112079\gamma - 34236}{320(\gamma + 1)^2(\gamma^2 - 1)^{5/2}} + \frac{378\gamma^7 - 939\gamma^5 + 552\gamma^3 + 9\gamma}{64(\gamma^2 - 1)^2} \operatorname{arccosh}\gamma \\
& - \frac{189\gamma^7 + 729\gamma^6 - 1755\gamma^5 + 393\gamma^4 + 927\gamma^3 - 957\gamma^2 + 639\gamma - 165}{32(\gamma + 1)(\gamma^2 - 1)^{3/2}} \log\left(\frac{\gamma + 1}{2}\right) \Big] \\
& + C_{E_2}(s_2 \cdot u_1)^2 \Big[\frac{2520\gamma^9 + 3150\gamma^8 - 10125\gamma^7 - 5565\gamma^6 + 42159\gamma^5 -}{640(\gamma + 1)^2(\gamma^2 - 1)^{5/2}} \\
& - \frac{53841\gamma^4 + 99183\gamma^3 - 346377\gamma^2 + 330891\gamma - 108279}{640(\gamma + 1)^2(\gamma^2 - 1)^{5/2}} + \frac{378\gamma^7 - 819\gamma^5 + 540\gamma^3 - 243\gamma}{128(\gamma^2 - 1)^3} \operatorname{arccosh}\gamma \\
& - \frac{189\gamma^5 + 189\gamma^4 + 1134\gamma^3 - 2682\gamma^2 + 1845\gamma - 387}{64(\gamma + 1)(\gamma^2 - 1)^{3/2}} \log\left(\frac{\gamma + 1}{2}\right) \Big] \\
& + C_{E_2}(s_2 \cdot \hat{b})^2 \Big[- \frac{1260\gamma^{11} + 8400\gamma^{10} - 10245\gamma^9 - 24035\gamma^8 - 31168\gamma^7 + 149252\gamma^6 - 88626\gamma^5}{640(\gamma + 1)^2(\gamma^2 - 1)^{5/2}} \\
& - \frac{52014\gamma^4 - 87204\gamma^3 - 96364\gamma^2 + 215983\gamma - 89267}{640(\gamma + 1)^2(\gamma^2 - 1)^{5/2}} - \frac{1974\gamma^9 - 6651\gamma^7 + 7857\gamma^5 - 4089\gamma^3 + 909\gamma}{128(\gamma^2 - 1)^3} \operatorname{arccosh}\gamma \\
& + \frac{987\gamma^7 + 2787\gamma^6 - 4065\gamma^5 - 4113\gamma^4 + 4593\gamma^3 + 1305\gamma^2 - 1515\gamma + 21}{64(\gamma + 1)(\gamma^2 - 1)^{3/2}} \log\left(\frac{\gamma + 1}{2}\right) \Big] \\
& + C_{E_2}(s_2 \cdot \hat{l})^2 \Big[- \frac{630\gamma^9 - 3885\gamma^8 + 5940\gamma^7 - 335\gamma^6 + 36456\gamma^5 - 171341\gamma^4}{320(\gamma^2 - 1)^{5/2}} \\
& - \frac{279868\gamma^3 - 214293\gamma^2 + 76466\gamma - 9506}{320(\gamma^2 - 1)^{5/2}} + \frac{798\gamma^9 - 2727\gamma^7 + 3249\gamma^5 - 1653\gamma^3 + 333\gamma}{64(\gamma^2 - 1)^3} \operatorname{arccosh}\gamma \Big]
\end{aligned}$$

$$- \frac{399\gamma^7 + 1299\gamma^6 - 2505\gamma^5 - 621\gamma^4 + 1941\gamma^3 - 495\gamma^2 + 165\gamma - 183}{32(\gamma+1)(\gamma^2-1)^{3/2}} \log\left(\frac{\gamma+1}{2}\right) \Bigg]$$

Table II: Components of the coefficient $C_{\hat{b}}$.

$$C_{\hat{b}}^{(0)} = C_{\hat{b}}^{E^2} = C_{\hat{b}}^{B^2} = C_{\hat{b}}^{s_1} = C_{\hat{b}}^{s_1} = 0$$

$$C_{\hat{b}}^{s_1 s_2} \left((s_1 \cdot \hat{b})(s_2 \cdot u_1) + (s_1 \cdot u_2)(s_2 \cdot \hat{b}) \right) \left[\frac{42\gamma^4 + 327\gamma^3 - 273\gamma^2 + 141\gamma - 57}{4(\gamma+1)^2 \sqrt{\gamma^2-1}} \log\left(\frac{\gamma+1}{2}\right) \right. \\ \left. - \frac{315\gamma^7 - 1096\gamma^6 - 763\gamma^5 - 15326\gamma^4 + 69709\gamma^3 - 120612\gamma^2 + 103347\gamma - 34230}{64(\gamma+1)^3(\gamma^2-1)^{3/2}} \right. \\ \left. - \frac{168\gamma^6 + 90\gamma^5 - 324\gamma^4 - 153\gamma^3 + 108\gamma^2 + 27\gamma}{16(\gamma+1)(\gamma^2-1)^2} \operatorname{arccosh}\gamma \right]$$

$$C_{\hat{b}}^{s_1 s_1} (s_1 \cdot u_2)(s_1 \cdot \hat{b}) \left[- \frac{1575\gamma^8 + 205\gamma^7 - 8275\gamma^6 + 13925\gamma^5 - 25969\gamma^4 + 5995\gamma^3 - 20797\gamma^2 + 100115\gamma - 61494}{640(\gamma+1)^3(\gamma^2-1)^{3/2}} \right. \\ \left. + \frac{147\gamma^4 + 1044\gamma^3 - 1014\gamma^2 + 468\gamma - 117}{32(\gamma+1)^2 \sqrt{\gamma^2-1}} \log\left(\frac{\gamma+1}{2}\right) \right. \\ \left. - \frac{294\gamma^6 + 114\gamma^5 - 603\gamma^4 - 153\gamma^3 + 243\gamma^2 - 27\gamma}{64(\gamma+1)(\gamma^2-1)^2} \operatorname{arccosh}\gamma \right] \\ + C_{E_1}(s_1 \cdot u_2)(s_1 \cdot \hat{b}) \left[\frac{147\gamma^4 + 1044\gamma^3 - 1014\gamma^2 + 372\gamma - 261}{32(\gamma+1)^2 \sqrt{\gamma^2-1}} \log\left(\frac{\gamma+1}{2}\right) \right. \\ \left. + \frac{1575\gamma^8 + 765\gamma^7 + 6085\gamma^6 + 6305\gamma^5 + 59699\gamma^4 - 430405\gamma^3 + 807067\gamma^2 - 658825\gamma + 204374}{640(\gamma+1)^3(\gamma^2-1)^{3/2}} \right. \\ \left. - \frac{294\gamma^6 + 114\gamma^5 - 603\gamma^4 - 249\gamma^3 + 243\gamma^2 + 117\gamma}{64(\gamma+1)(\gamma^2-1)^2} \operatorname{arccosh}\gamma \right]$$

$$C_{\hat{b}}^{s_2 s_2} \text{ Equal to } -C_{\hat{b}}^{s_1 s_1} \text{ after exchanging the labels 1 and 2.}$$

Table III: Components of the coefficient $C_{\hat{i}}$.

$$C_{\hat{i}}^{(0)} = C_{\hat{i}}^{E^2} = C_{\hat{i}}^{B^2} = 0$$

$$C_{\hat{i}}^{s_1} (s_1 \cdot u_2) \left[- \frac{425\gamma^5 - 1215\gamma^4 + 2491\gamma^3 - 3957\gamma^2 + 2992\gamma - 760}{16(\gamma+1)(\gamma^2-1)^2} \right. \\ \left. - \frac{84\gamma^6 + 459\gamma^5 - 825\gamma^4 - 138\gamma^3 + 666\gamma^2 - 321\gamma + 75}{8(\gamma+1)(\gamma^2-1)^2} \log\left(\frac{\gamma+1}{2}\right) \right. \\ \left. + \frac{168\gamma^7 + 78\gamma^6 - 414\gamma^5 - 171\gamma^4 + 261\gamma^3 + 81\gamma^2 - 27\gamma}{16(\gamma+1)(\gamma^2-1)^{5/2}} \operatorname{arccosh}\gamma \right]$$

$$C_{\hat{i}}^{s_2} \text{ Equal to } C_{\hat{i}}^{s_1} \text{ after exchanging the labels 1 and 2.}$$

$$C_{\hat{i}}^{s_1 s_2} \left((s_1 \cdot \hat{i})(s_2 \cdot u_1) + (s_1 \cdot u_2)(s_2 \cdot \hat{i}) \right) \left[- \frac{42\gamma^4 + 327\gamma^3 - 273\gamma^2 + 141\gamma - 57}{(\gamma+1)^2 \sqrt{\gamma^2-1}} \log\left(\frac{\gamma+1}{2}\right) \right. \\ \left. - \frac{315\gamma^6 + 4714\gamma^5 - 12807\gamma^4 + 52652\gamma^3 - 102963\gamma^2 + 71562\gamma - 16161}{64(\gamma+1)^2(\gamma^2-1)^{3/2}} \right]$$

$$\begin{aligned}
& + \frac{168\gamma^6 + 90\gamma^5 - 324\gamma^4 - 153\gamma^3 + 108\gamma^2 + 27\gamma}{4(\gamma+1)(\gamma^2-1)^2} \operatorname{arccosh}\gamma \Big] \\
C_i^{s_1 s_1} & (s_1 \cdot u_2)(s_1 \cdot \hat{l}) \left[- \frac{147\gamma^4 + 1044\gamma^3 - 1014\gamma^2 + 468\gamma - 117}{8(\gamma+1)^2 \sqrt{\gamma^2-1}} \log\left(\frac{\gamma+1}{2}\right) \right. \\
& - \frac{1575\gamma^7 - 4870\gamma^6 + 19265\gamma^5 - 36520\gamma^4 + 222041\gamma^3 - 461166\gamma^2 + 316159\gamma - 67044}{640(\gamma+1)^2(\gamma^2-1)^{3/2}} \\
& \left. + \frac{294\gamma^6 + 114\gamma^5 - 603\gamma^4 - 153\gamma^3 + 243\gamma^2 - 27\gamma}{16(\gamma+1)(\gamma^2-1)^2} \operatorname{arccosh}\gamma \right] \\
& + C_{E_1}(s_1 \cdot u_2)(s_1 \cdot \hat{l}) \left[\frac{1575\gamma^7 - 2910\gamma^6 - 19975\gamma^5 + 65240\gamma^4 - 207991\gamma^3 + 390746\gamma^2 - 293289\gamma + 73324}{640(\gamma+1)^2(\gamma^2-1)^{3/2}} \right. \\
& - \frac{147\gamma^4 + 1044\gamma^3 - 1014\gamma^2 + 372\gamma - 261}{8(\gamma+1)^2 \sqrt{\gamma^2-1}} \log\left(\frac{\gamma+1}{2}\right) \\
& \left. + \frac{294\gamma^6 + 114\gamma^5 - 603\gamma^4 - 249\gamma^3 + 243\gamma^2 + 117\gamma}{16(\gamma+1)(\gamma^2-1)^2} \operatorname{arccosh}\gamma \right] \\
C_i^{s_2 s_2} & \text{ Equal to } C_i^{s_1 s_1} \text{ after exchanging the labels 1 and 2.}
\end{aligned}$$

C.2 . Stress-energy tensor for spinning object up to $\mathcal{O}(s^2)$

In this section we present the expression for the pseudo-stress energy tensor spin contributions $t^{\mu\nu}$ defined in (6.2.8). Introducing the reduce spin tensors

$$s_A^{\mu\nu} \equiv \frac{S_A^{\mu\nu}}{m_a}, \quad (\text{C.2.1})$$

we decompose it as follows $t^{\mu\nu}$

$$t^{\mu\nu} = t_{(0)}^{\mu\nu} + \sum_{A=1,2} t_{s_A}^{\mu\nu} + \sum_{A,B=1,2} t_{s_A s_B}^{\mu\nu} + \mathcal{O}(s^3). \quad (\text{C.2.2})$$

$t_{(0)}^{\mu\nu}$ is essentially the d dimensional version of the sum of eqs. (3.2.11), (3.2.12) and (3.2.13), while the subscript s_1 denotes the part that is proportional to $s_1^{\mu\nu}$, and so on. For the sake of brevity, we write $\text{Sym}[\dots]$ to denote the action of symmetrizing over all (μ_i, ν_i) index pairs, e.g.

$$\text{Sym}[X^{\mu\nu}] \equiv X^{(\mu\nu)}, \quad \text{Sym}[X^{\mu_1\nu_1\mu_2\nu_2}] \equiv X^{(\mu_1\nu_1)(\mu_2\nu_2)}. \quad (\text{C.2.3})$$

Additionally, we use the shorthands

$$(U \cdot s_A \cdot V) \equiv U^\mu s_{A\mu\nu} V^\nu, \quad (U \cdot s_A \cdot s_A \cdot V) \equiv U^\mu s_{A\mu\nu} s_A^\nu{}_\rho V^\rho, \quad (\text{C.2.4})$$

to represent the scalar contractions between arbitrary vectors U, V and the spin tensor s_A .

$$t_{(0)}^{\mu\nu} \quad \text{Sym} \left[\frac{1}{d-2} [2\gamma(d-2)(k \cdot u_1)(k \cdot u_2) + 2(k \cdot u_1)^2 + 2(k \cdot u_2)^2 + \beta_\gamma(d-2)(k \cdot q)] \right]$$

$$\begin{aligned}
& -\beta_\gamma(d-2)q^2]\eta^{\mu\nu} + 2\beta_\gamma k^\mu k^\nu + \frac{1}{(d-2)(k \cdot u_1)}[2\beta_\gamma(d-2)q^2 - 4(k \cdot u_1)^2]k^\mu u_1^\nu \\
& + 2\beta_\gamma q^\mu q^\nu + \frac{1}{(k \cdot u_2)}[2\beta_\gamma q^2 + 4\gamma(k \cdot u_1)(k \cdot u_2) - 4\beta_\gamma(k \cdot q)]q^\mu u_2^\nu \\
& + \frac{1}{(k \cdot u_1)^2}[2\gamma(k \cdot u_1)(k \cdot u_2)q^2 + 2(k \cdot u_1)^2(k \cdot u_2)^2 + \beta_\gamma(k \cdot q)q^2]u_1^\mu u_1^\nu + [4\gamma(k \cdot q) \\
& - 4\gamma q^2 - 4(k \cdot u_1)(k \cdot u_2)]u_1^\mu u_2^\nu + \frac{1}{(k \cdot u_2)^2}[2\beta_\gamma(k \cdot q)^2 + 2\gamma(k \cdot u_1)(k \cdot u_2)q^2 \\
& + 2(k \cdot u_1)^2(k \cdot u_2)^2 - 4\gamma(k \cdot q)(k \cdot u_1)(k \cdot u_2) - \beta_\gamma(k \cdot q)q^2]u_2^\mu u_2^\nu - 2\beta_\gamma k^\mu q^\nu \\
& - \frac{4}{d-2}[\gamma(d-2)(k \cdot u_1) + (k \cdot u_2)]k^\mu u_2^\nu - \frac{2}{(k \cdot u_1)}[2\gamma(k \cdot u_1)(k \cdot u_2) + \beta_\gamma q^2]q^\mu u_1^\nu \Big]
\end{aligned}$$

$$\begin{aligned}
t_{s_1}^{\mu\nu} \quad & i \text{Sym} \left[\frac{1}{d-2}[(d-2)(k \cdot u_1)(k \cdot u_2)(q \cdot s_1 \cdot u_2) + \gamma(d-2)(k \cdot q)(q \cdot s_1 \cdot u_2) \right. \\
& - 2(k \cdot u_1)(k \cdot s_1 \cdot q) - \gamma(d-2)(k \cdot u_2)(k \cdot s_1 \cdot q) - \gamma(d-2)(q \cdot s_1 \cdot u_2)q^2]\eta^{\mu\nu} \\
& + 2\gamma(q \cdot s_1 \cdot u_2)k^\mu k^\nu + \frac{1}{(d-2)(k \cdot u_1)}[2q^\rho(k \cdot u_1)^2 + \gamma(d-2)(k \cdot u_1)q^2 u_2^\rho \\
& - \beta_\gamma(d-2)k^\rho q^2]k^\mu s_1^\nu{}_\rho + \frac{1}{(d-2)(k \cdot u_1)}[2\gamma(d-2)(q \cdot s_1 \cdot u_2)q^2 + 2(k \cdot u_1)(k \cdot s_1 \cdot q) \\
& - \gamma(d-2)(k \cdot s_1 \cdot u_2)q^2]k^\mu u_1^\nu + [2\gamma(k \cdot s_1 \cdot q) - 2(k \cdot u_1)(q \cdot s_1 \cdot u_2)]k^\mu u_2^\nu \\
& + 2\gamma(q \cdot s_1 \cdot u_2)q^\mu q^\nu + \frac{1}{(k \cdot u_1)}[2\gamma q^\rho(k \cdot u_1)(k \cdot u_2) + \beta_\gamma k^\rho q^2 - \gamma(k \cdot u_1)q^2 u_2^\rho]q^\mu s_1^\nu{}_\rho \\
& + \frac{1}{(k \cdot u_1)}[\gamma(k \cdot s_1 \cdot u_2)q^2 - 2\gamma(q \cdot s_1 \cdot u_2)q^2 - 2(k \cdot u_1)(k \cdot u_2)(q \cdot s_1 \cdot u_2)]q^\mu u_1^\nu \\
& + \frac{1}{(k \cdot u_2)}[2\gamma(q \cdot s_1 \cdot u_2)q^2 + 2(k \cdot u_1)(k \cdot u_2)(q \cdot s_1 \cdot u_2) - 2\gamma(k \cdot u_2)(k \cdot s_1 \cdot q) \\
& - 4\gamma(k \cdot q)(q \cdot s_1 \cdot u_2)]q^\mu u_2^\nu + \frac{1}{(k \cdot u_1)^2}[\gamma(k \cdot q)(k \cdot u_1)q^2 u_2^\rho + (k \cdot u_1)^2(k \cdot u_2)q^2 u_2^\rho \\
& - 2q^\rho(k \cdot u_1)^2(k \cdot u_2)^2 - \beta_\gamma k^\rho(k \cdot q)q^2 - \gamma k^\rho(k \cdot u_1)(k \cdot u_2)q^2 \\
& - \gamma q^\rho(k \cdot u_1)(k \cdot u_2)q^2]s_1^\mu{}_\rho u_1^\nu + [2q^\rho(k \cdot u_1)(k \cdot u_2) + \gamma k^\rho q^2 + \gamma q^\rho q^2 - 2\gamma q^\rho(k \cdot q) \\
& - (k \cdot u_1)q^2 u_2^\rho]s_1^\mu{}_\rho u_2^\nu + \frac{1}{(k \cdot u_1)}[2(k \cdot q)(k \cdot u_1)(q \cdot s_1 \cdot u_2) \\
& + 2(k \cdot u_1)(k \cdot u_2)(k \cdot s_1 \cdot q) + \gamma(k \cdot s_1 \cdot q)q^2 + (k \cdot u_1)(k \cdot s_1 \cdot u_2)q^2 \\
& - 2(k \cdot u_1)(q \cdot s_1 \cdot u_2)q^2]u_1^\mu u_2^\nu + \frac{1}{(k \cdot u_2)^2}[2\gamma(k \cdot q)^2(q \cdot s_1 \cdot u_2) \\
& + 2\gamma(k \cdot q)(k \cdot u_2)(k \cdot s_1 \cdot q) + (k \cdot u_1)(k \cdot u_2)(q \cdot s_1 \cdot u_2)q^2 \\
& - 2(k \cdot q)(k \cdot u_1)(k \cdot u_2)(q \cdot s_1 \cdot u_2) - 2(k \cdot u_1)(k \cdot u_2)^2(k \cdot s_1 \cdot q) \\
& - \gamma(k \cdot q)(q \cdot s_1 \cdot u_2)q^2 - \gamma(k \cdot u_2)(k \cdot s_1 \cdot q)q^2]u_2^\mu u_2^\nu - 2\gamma(q \cdot s_1 \cdot u_2)k^\mu q^\nu \\
& - \frac{q^2}{(k \cdot u_1)^2}[\gamma(k \cdot q)(k \cdot s_1 \cdot u_2) + (k \cdot u_1)(k \cdot u_2)(k \cdot s_1 \cdot u_2) - \gamma(k \cdot q)(q \cdot s_1 \cdot u_2)
\end{aligned}$$

$$- (k \cdot u_1)(k \cdot u_2)(q \cdot s_1 \cdot u_2)]u_1^\mu u_1^\nu \Big]$$

$t_{s_2}^{\mu\nu}$ Equal to $t_{s_1}^{\mu\nu}$ after interchanging the body labels $1 \leftrightarrow 2$ and mapping $q \mapsto k - q$

$$\begin{aligned}
t_{s_1 s_2}^{\mu\nu} \text{ Sym} & \left[\frac{1}{2} [\gamma(k \cdot q)(q \cdot s_1 \cdot s_2 \cdot k) + \gamma(k \cdot s_1 \cdot q)(k \cdot s_2 \cdot q) + \gamma(q \cdot s_1 \cdot s_2 \cdot q)q^2 \right. \\
& + (k \cdot q)(q \cdot s_1 \cdot u_2)(q \cdot s_2 \cdot u_1) + (k \cdot u_1)(k \cdot u_2)(q \cdot s_1 \cdot s_2 \cdot k) \\
& + (k \cdot u_2)(k \cdot s_1 \cdot q)(k \cdot s_2 \cdot u_1) + (k \cdot s_2 \cdot u_1)(q \cdot s_1 \cdot u_2)q^2 - \gamma(k \cdot q)(q \cdot s_1 \cdot s_2 \cdot q) \\
& - \gamma(q \cdot s_1 \cdot s_2 \cdot k)q^2 - (k \cdot q)(k \cdot s_2 \cdot u_1)(q \cdot s_1 \cdot u_2) - (k \cdot u_1)(k \cdot u_2)(q \cdot s_1 \cdot s_2 \cdot q) \\
& - (k \cdot u_1)(k \cdot s_2 \cdot q)(q \cdot s_1 \cdot u_2) - (k \cdot u_2)(k \cdot s_1 \cdot q)(q \cdot s_2 \cdot u_1) \\
& - (q \cdot s_1 \cdot u_2)(q \cdot s_2 \cdot u_1)q^2] \eta^{\mu\nu} + [\gamma(q \cdot s_1 \cdot s_2 \cdot k) + (q \cdot s_1 \cdot u_2)(q \cdot s_2 \cdot u_1) \\
& - \gamma(q \cdot s_1 \cdot s_2 \cdot q) - (k \cdot s_2 \cdot u_1)(q \cdot s_1 \cdot u_2)]k^\mu k^\nu + [\gamma(q \cdot s_1 \cdot s_2 \cdot q) \\
& + (k \cdot s_2 \cdot u_1)(q \cdot s_1 \cdot u_2) - \gamma(q \cdot s_1 \cdot s_2 \cdot k) - (q \cdot s_1 \cdot u_2)(q \cdot s_2 \cdot u_1)]k^\mu q^\nu \\
& + \frac{q^2}{2(k \cdot u_1)} [2\gamma k^\rho (k \cdot s_2 \cdot u_1) + (k \cdot u_1)(q \cdot s_2 \cdot u_1)u_2^\rho - 2\gamma k^\rho (q \cdot s_2 \cdot u_1) \\
& - (k \cdot u_1)(k \cdot s_2 \cdot u_1)u_2^\rho] k^\mu s_1^\nu{}_\rho + \frac{\gamma q^2}{2} (q^\rho - k^\rho) k^\mu s_1^{\nu\sigma} s_{2\rho\sigma} + [\gamma k^\rho (k \cdot s_1 \cdot q) \\
& + q^\rho (k \cdot u_1)(q \cdot s_1 \cdot u_2) - \gamma q^\rho (k \cdot s_1 \cdot q) - k^\rho (k \cdot u_1)(q \cdot s_1 \cdot u_2)] k^\mu s_2^\nu{}_\rho \\
& + \frac{q^2}{2(k \cdot u_1)} [2\gamma(q \cdot s_1 \cdot s_2 \cdot k) + 2(q \cdot s_1 \cdot u_2)(q \cdot s_2 \cdot u_1) + \gamma(k \cdot s_1 \cdot s_2 \cdot q) \\
& + (k \cdot s_1 \cdot u_2)(k \cdot s_2 \cdot u_1) - 2\gamma(q \cdot s_1 \cdot s_2 \cdot q) - 2(k \cdot s_2 \cdot u_1)(q \cdot s_1 \cdot u_2) \\
& - \gamma(k \cdot s_1 \cdot s_2 \cdot k) - (k \cdot s_1 \cdot u_2)(q \cdot s_2 \cdot u_1)] k^\mu u_1^\nu + [(k \cdot u_1)(q \cdot s_1 \cdot s_2 \cdot q) \\
& + (k \cdot s_1 \cdot q)(q \cdot s_2 \cdot u_1) - (k \cdot u_1)(q \cdot s_1 \cdot s_2 \cdot k) - (k \cdot s_1 \cdot q)(k \cdot s_2 \cdot u_1)] k^\mu u_2^\nu \\
& + \frac{\gamma}{2} [2(k \cdot q) - q^2] q^\mu q^\rho s_{1\rho}{}^\sigma s_{2\nu}{}^\sigma + \frac{(k \cdot u_2)}{2} [q^2 - 2(k \cdot q)] q^\rho s_{1\rho}{}^\sigma s_{2\nu}{}^\sigma u_1^\nu \\
& + [\gamma(q \cdot s_1 \cdot s_2 \cdot k) + (q \cdot s_1 \cdot u_2)(q \cdot s_2 \cdot u_1) - \gamma(q \cdot s_1 \cdot s_2 \cdot q) \\
& - (k \cdot s_2 \cdot u_1)(q \cdot s_1 \cdot u_2)] q^\mu q^\nu + \frac{1}{2(k \cdot u_1)} [2\gamma k^\rho (q \cdot s_2 \cdot u_1)q^2 \\
& + 2q^\rho (k \cdot u_1)(k \cdot u_2)(q \cdot s_2 \cdot u_1) + (k \cdot u_1)(k \cdot s_2 \cdot u_1)q^2 u_2^\rho - 2\gamma k^\rho (k \cdot s_2 \cdot u_1)q^2 \\
& - 2\gamma q^\rho (k \cdot u_1)(k \cdot s_2 \cdot q) - 2q^\rho (k \cdot u_1)(k \cdot u_2)(k \cdot s_2 \cdot u_1) \\
& - (k \cdot u_1)(q \cdot s_2 \cdot u_1)q^2 u_2^\rho] q^\mu s_1^\nu{}_\rho + \frac{\gamma q^2}{2} (k^\rho - q^\rho) q^\mu s_1^{\nu\sigma} s_{2\rho\sigma} \\
& + \frac{1}{2(k \cdot u_2)} [2\gamma k^\rho (q \cdot s_1 \cdot u_2)q^2 + 2\gamma q^\rho (k \cdot u_2)(k \cdot s_1 \cdot q) + 2k^\rho (k \cdot u_1)(k \cdot u_2)(q \cdot s_1 \cdot u_2) \\
& + 2(k \cdot q)(k \cdot u_2)(q \cdot s_1 \cdot u_2)u_1^\rho - 2\gamma k^\rho (k \cdot u_2)(k \cdot s_1 \cdot q) \\
& - 2q^\rho (k \cdot u_1)(k \cdot u_2)(q \cdot s_1 \cdot u_2) - 4\gamma k^\rho (k \cdot q)(q \cdot s_1 \cdot u_2) \\
& - (k \cdot u_2)(q \cdot s_1 \cdot u_2)q^2 u_1^\rho] q^\mu s_2^\nu{}_\rho + \frac{1}{2(k \cdot u_1)} [2\gamma(q \cdot s_1 \cdot s_2 \cdot q)q^2 \\
& + 2(k \cdot u_1)(k \cdot u_2)(q \cdot s_1 \cdot s_2 \cdot q) + 2(k \cdot u_1)(k \cdot s_2 \cdot q)(q \cdot s_1 \cdot u_2)
\end{aligned}$$

$$\begin{aligned}
& + 2(k \cdot s_2 \cdot u_1)(q \cdot s_1 \cdot u_2)q^2 + \gamma(k \cdot s_1 \cdot s_2 \cdot k)q^2 + (k \cdot s_1 \cdot u_2)(q \cdot s_2 \cdot u_1)q^2 \\
& - 2\gamma(q \cdot s_1 \cdot s_2 \cdot k)q^2 - 2(k \cdot u_1)(k \cdot u_2)(q \cdot s_1 \cdot s_2 \cdot k) - 2(q \cdot s_1 \cdot u_2)(q \cdot s_2 \cdot u_1)q^2 \\
& - \gamma(k \cdot s_1 \cdot s_2 \cdot q)q^2 - (k \cdot s_1 \cdot u_2)(k \cdot s_2 \cdot u_1)q^2]q^\mu u_1^\nu \\
& + \frac{1}{2(k \cdot u_2)}[2(k \cdot q)(k \cdot s_2 \cdot u_1)(q \cdot s_1 \cdot u_2) + 2(k \cdot u_1)(k \cdot u_2)(q \cdot s_1 \cdot s_2 \cdot k) \\
& + 2(k \cdot u_2)(k \cdot s_1 \cdot q)(k \cdot s_2 \cdot u_1) + 2(q \cdot s_1 \cdot u_2)(q \cdot s_2 \cdot u_1)q^2 + 4\gamma(k \cdot q)(q \cdot s_1 \cdot s_2 \cdot q) \\
& + \gamma(q \cdot s_1 \cdot s_2 \cdot k)q^2 - 2\gamma(k \cdot q)(q \cdot s_1 \cdot s_2 \cdot k) - 2\gamma(q \cdot s_1 \cdot s_2 \cdot q)q^2 \\
& - 2(k \cdot u_1)(k \cdot u_2)(q \cdot s_1 \cdot s_2 \cdot q) - 2(k \cdot u_2)(k \cdot s_1 \cdot q)(q \cdot s_2 \cdot u_1) \\
& - 4(k \cdot q)(q \cdot s_1 \cdot u_2)(q \cdot s_2 \cdot u_1) - (k \cdot s_2 \cdot u_1)(q \cdot s_1 \cdot u_2)q^2]q^\mu u_2^\nu \\
& + \frac{1}{2}[2q^\rho(k \cdot q)(k \cdot u_2)u_1^\sigma + \gamma k^\rho k^\sigma q^2 - 2q^\rho q^\sigma(k \cdot u_1)(k \cdot u_2) - \gamma k^\rho q^\sigma q^2 \\
& - q^\rho(k \cdot u_2)q^2 u_1^\sigma]s_1^\mu{}_\rho s_2^\nu{}_\sigma + \frac{1}{2(k \cdot u_1)^2}[2\gamma k^\rho(k \cdot q)(k \cdot s_2 \cdot u_1)q^2 \\
& + 4q^\rho(k \cdot u_1)^2(k \cdot u_2)(k \cdot s_2 \cdot q) + \gamma k^\rho(k \cdot u_1)(k \cdot s_2 \cdot q)q^2 + \gamma q^\rho(k \cdot u_1)(k \cdot s_2 \cdot q)q^2 \\
& + k^\rho(k \cdot u_1)(k \cdot u_2)(k \cdot s_2 \cdot u_1)q^2 + (k \cdot q)(k \cdot u_1)(q \cdot s_2 \cdot u_1)q^2 u_2^\rho \\
& + q^\rho(k \cdot u_1)(k \cdot u_2)(k \cdot s_2 \cdot u_1)q^2 - 2\gamma k^\rho(k \cdot q)(q \cdot s_2 \cdot u_1)q^2 \\
& - k^\rho(k \cdot u_1)(k \cdot u_2)(q \cdot s_2 \cdot u_1)q^2 - (k \cdot q)(k \cdot u_1)(k \cdot s_2 \cdot u_1)q^2 u_2^\rho \\
& - (k \cdot u_1)^2(k \cdot s_2 \cdot q)q^2 u_2^\rho - q^\rho(k \cdot u_1)(k \cdot u_2)(q \cdot s_2 \cdot u_1)q^2]s_1^\mu{}_\rho u_1^\nu \\
& + \frac{1}{2(k \cdot u_2)}[2\gamma q^\rho(k \cdot q)(k \cdot s_2 \cdot q) + k^\rho(k \cdot u_2)(q \cdot s_2 \cdot u_1)q^2 + q^\rho(k \cdot u_2)(q \cdot s_2 \cdot u_1)q^2 \\
& - 2q^\rho(k \cdot q)(k \cdot u_2)(q \cdot s_2 \cdot u_1) - 2q^\rho(k \cdot u_1)(k \cdot u_2)(k \cdot s_2 \cdot q) - \gamma q^\rho(k \cdot s_2 \cdot q)q^2 \\
& - k^\rho(k \cdot u_2)(k \cdot s_2 \cdot u_1)q^2]s_1^\mu{}_\rho u_2^\nu + \frac{(k \cdot u_1)q^2}{2}(k^\rho - q^\rho)s_1^{\mu\sigma} s_2^{\rho\sigma} u_2^\nu \\
& + \frac{1}{2}[2k^\rho q^\sigma(k \cdot u_1)(k \cdot u_2) + \gamma k^\rho q^\sigma q^2 + q^\rho(k \cdot u_1)q^2 u_2^\sigma - 2\gamma k^\rho q^\sigma(k \cdot q) \\
& - k^\rho(k \cdot u_1)q^2 u_2^\sigma]s_1^\mu{}_\sigma s_2^\nu{}_\rho + \frac{1}{2(k \cdot u_1)}[2k^\rho(k \cdot q)(k \cdot u_1)(q \cdot s_1 \cdot u_2) \\
& + 2k^\rho(k \cdot u_1)(k \cdot u_2)(k \cdot s_1 \cdot q) + \gamma k^\rho(k \cdot s_1 \cdot q)q^2 + k^\rho(k \cdot u_1)(k \cdot s_1 \cdot u_2)q^2 \\
& + q^\rho(k \cdot u_1)(q \cdot s_1 \cdot u_2)q^2 - 2k^\rho(k \cdot u_1)(q \cdot s_1 \cdot u_2)q^2 - 2q^\rho(k \cdot u_1)(k \cdot u_2)(k \cdot s_1 \cdot q) \\
& - \gamma q^\rho(k \cdot s_1 \cdot q)q^2 - q^\rho(k \cdot u_1)(k \cdot s_1 \cdot u_2)q^2]s_2^\mu{}_\rho u_1^\nu \\
& + \frac{1}{2(k \cdot u_2)^2}[2k^\rho(k \cdot u_1)(k \cdot u_2)(q \cdot s_1 \cdot u_2)q^2 + 2q^\rho(k \cdot q)(k \cdot u_1)(k \cdot u_2)(q \cdot s_1 \cdot u_2) \\
& + 4\gamma k^\rho(k \cdot q)^2(q \cdot s_1 \cdot u_2) + 4\gamma k^\rho(k \cdot q)(k \cdot u_2)(k \cdot s_1 \cdot q) \\
& + 4q^\rho(k \cdot u_1)(k \cdot u_2)^2(k \cdot s_1 \cdot q) + \gamma q^\rho(k \cdot u_2)(k \cdot s_1 \cdot q)q^2 \\
& + (k \cdot q)(k \cdot u_2)(q \cdot s_1 \cdot u_2)q^2 u_1^\rho + (k \cdot u_2)^2(k \cdot s_1 \cdot q)q^2 u_1^\rho - 2\gamma k^\rho(k \cdot q)(q \cdot s_1 \cdot u_2)q^2 \\
& - 2\gamma k^\rho(k \cdot u_2)(k \cdot s_1 \cdot q)q^2 - 2\gamma q^\rho(k \cdot q)(k \cdot u_2)(k \cdot s_1 \cdot q) \\
& - 2(k \cdot q)^2(k \cdot u_2)(q \cdot s_1 \cdot u_2)u_1^\rho - 2(k \cdot q)(k \cdot u_2)^2(k \cdot s_1 \cdot q)u_1^\rho \\
& - 4k^\rho(k \cdot q)(k \cdot u_1)(k \cdot u_2)(q \cdot s_1 \cdot u_2) - 4k^\rho(k \cdot u_1)(k \cdot u_2)^2(k \cdot s_1 \cdot q)
\end{aligned}$$

$$\begin{aligned}
& -q^\rho(k \cdot u_1)(k \cdot u_2)(q \cdot s_1 \cdot u_2)q^2]s_2^\mu{}_\rho u_2^\nu + \frac{q^2}{2(k \cdot u_1)^2}[\gamma(k \cdot q)(k \cdot s_1 \cdot s_2 \cdot q) \\
& + \gamma(k \cdot q)(q \cdot s_1 \cdot s_2 \cdot k) + (k \cdot q)(k \cdot s_1 \cdot u_2)(k \cdot s_2 \cdot u_1) + (k \cdot q)(q \cdot s_1 \cdot u_2)(q \cdot s_2 \cdot u_1) \\
& + (k \cdot u_1)(k \cdot u_2)(k \cdot s_1 \cdot s_2 \cdot q) + (k \cdot u_1)(k \cdot u_2)(q \cdot s_1 \cdot s_2 \cdot k) \\
& + (k \cdot u_1)(k \cdot s_1 \cdot u_2)(k \cdot s_2 \cdot q) - \gamma(k \cdot q)(k \cdot s_1 \cdot s_2 \cdot k) - \gamma(k \cdot q)(q \cdot s_1 \cdot s_2 \cdot q) \\
& - (k \cdot q)(k \cdot s_1 \cdot u_2)(q \cdot s_2 \cdot u_1) - (k \cdot q)(k \cdot s_2 \cdot u_1)(q \cdot s_1 \cdot u_2) \\
& - (k \cdot u_1)(k \cdot u_2)(k \cdot s_1 \cdot s_2 \cdot k) - (k \cdot u_1)(k \cdot u_2)(q \cdot s_1 \cdot s_2 \cdot q) \\
& - (k \cdot u_1)(k \cdot s_2 \cdot q)(q \cdot s_1 \cdot u_2)]u_1^\mu u_1^\nu \\
& + \frac{1}{2(k \cdot u_1)(k \cdot u_2)}[2(k \cdot u_1)(k \cdot u_2)(q \cdot s_1 \cdot s_2 \cdot q)q^2 + (k \cdot u_1)(k \cdot u_2)(k \cdot s_1 \cdot s_2 \cdot k)q^2 \\
& + (k \cdot u_1)(k \cdot s_2 \cdot q)(q \cdot s_1 \cdot u_2)q^2 + (k \cdot u_2)(k \cdot s_1 \cdot q)(q \cdot s_2 \cdot u_1)q^2 \\
& - 2(k \cdot q)(k \cdot u_1)(k \cdot u_2)(q \cdot s_1 \cdot s_2 \cdot q) - 2(k \cdot q)(k \cdot u_1)(k \cdot s_2 \cdot q)(q \cdot s_1 \cdot u_2) \\
& - 2(k \cdot u_1)(k \cdot u_2)(k \cdot s_1 \cdot q)(k \cdot s_2 \cdot q) - (k \cdot u_1)(k \cdot u_2)(k \cdot s_1 \cdot s_2 \cdot q)q^2 \\
& - (k \cdot u_1)(k \cdot u_2)(q \cdot s_1 \cdot s_2 \cdot k)q^2 - (k \cdot u_2)(k \cdot s_1 \cdot q)(k \cdot s_2 \cdot u_1)q^2]u_1^\mu u_2^\nu \\
& + \frac{1}{2(k \cdot u_2)^2}[2(k \cdot q)^2(q \cdot s_1 \cdot u_2)(q \cdot s_2 \cdot u_1) + 2(k \cdot q)(k \cdot u_1)(k \cdot u_2)(q \cdot s_1 \cdot s_2 \cdot q) \\
& + 2(k \cdot q)(k \cdot u_2)(k \cdot s_1 \cdot q)(q \cdot s_2 \cdot u_1) + \gamma(k \cdot q)(q \cdot s_1 \cdot s_2 \cdot q)q^2 \\
& - 2\gamma(k \cdot q)^2(q \cdot s_1 \cdot s_2 \cdot q) - (k \cdot q)(q \cdot s_1 \cdot u_2)(q \cdot s_2 \cdot u_1)q^2 \\
& - (k \cdot u_1)(k \cdot u_2)(q \cdot s_1 \cdot s_2 \cdot q)q^2 - (k \cdot u_2)(k \cdot s_1 \cdot q)(q \cdot s_2 \cdot u_1)q^2]u_2^\mu u_2^\nu \\
& - \frac{1}{2(k \cdot u_2)}[2\gamma(k \cdot q)^2 + (k \cdot u_1)(k \cdot u_2)q^2 - 2(k \cdot q)(k \cdot u_1)(k \cdot u_2) \\
& - \gamma(k \cdot q)q^2]q^\rho s_{1\rho}{}^\sigma s_2^\mu{}_\sigma u_2^\nu - \frac{q^2}{2(k \cdot u_1)}[\gamma k^\rho(k \cdot q) + k^\rho(k \cdot u_1)(k \cdot u_2) - \gamma q^\rho(k \cdot q) \\
& - q^\rho(k \cdot u_1)(k \cdot u_2)]s_1^{\mu\sigma} s_{2\rho\sigma} u_1^\nu \Big]
\end{aligned}$$

$$\begin{aligned}
t_{s_1 s_1}^{\mu\nu} \text{Sym} & \left[q^2[(k \cdot s_1 \cdot u_2) - (q \cdot s_1 \cdot u_2)]k^\rho s_1^\mu{}_\rho u_2^\nu + \frac{q^2}{d-2}(q^\sigma - k^\sigma)k^\rho s_1^\mu{}_\rho s_1^\nu{}_\sigma \right. \\
& + \frac{\gamma q^2}{(k \cdot u_1)}[(q \cdot s_1 \cdot u_2) - (k \cdot s_1 \cdot u_2)]k^\mu k^\rho s_1^\nu{}_\rho \\
& + \frac{\gamma q^2}{(k \cdot u_1)}[(k \cdot s_1 \cdot u_2) - (q \cdot s_1 \cdot u_2)]k^\rho q^\mu s_1^\nu{}_\rho \\
& - \frac{q^2}{(d-2)(k \cdot u_1)^2}[(d-2)(k \cdot u_1)(k \cdot u_2)(k \cdot s_1 \cdot u_2) + \gamma(d-2)(k \cdot q)(k \cdot s_1 \cdot u_2) \\
& + (k \cdot u_1)(k \cdot s_1 \cdot q) - (d-2)(k \cdot u_1)(k \cdot u_2)(q \cdot s_1 \cdot u_2) \\
& - \gamma(d-2)(k \cdot q)(q \cdot s_1 \cdot u_2)]k^\rho s_1^\mu{}_\rho u_1^\nu + \beta_\gamma C_{E_1}(q \cdot s_1 \cdot s_1 \cdot q)k^\mu q^\nu + C_{E_1} q^2[\beta_\gamma q^\rho \\
& + \gamma(k \cdot u_1)u_2^\rho - \beta_\gamma k^\rho]k^\mu s_1^{\nu\sigma} s_{1\rho\sigma} + C_{E_1} q^2[\beta_\gamma k^\rho - \beta_\gamma q^\rho - \gamma(k \cdot u_1)u_2^\rho]q^\mu s_1^{\nu\sigma} s_{1\rho\sigma} \\
& + C_{E_1}[2\gamma(q \cdot s_1 \cdot s_1 \cdot q)q^2 + 2(k \cdot u_1)(k \cdot u_2)(q \cdot s_1 \cdot s_1 \cdot q) + \gamma(k \cdot s_1 \cdot s_1 \cdot k)q^2 \\
& - 2\gamma(k \cdot q)(q \cdot s_1 \cdot s_1 \cdot q) - \gamma(k \cdot s_1 \cdot s_1 \cdot q)q^2 - (k \cdot u_1)(k \cdot s_1 \cdot s_1 \cdot u_2)q^2]u_1^\mu u_2^\nu
\end{aligned}$$

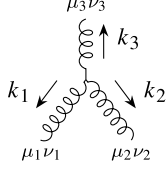
$$\begin{aligned}
& -\beta_\gamma C_{E_1}(q \cdot s_1 \cdot s_1 \cdot q)k^\mu k^\nu - \beta_\gamma C_{E_1}(q \cdot s_1 \cdot s_1 \cdot q)q^\mu q^\nu - C_{E_1}(k \cdot u_1)q^2[\gamma q^\rho \\
& + (k \cdot u_1)u_2^\rho - \gamma k^\rho]s_1^{\mu\sigma}s_{1\rho\sigma}u_2^\nu \\
& + \frac{2C_{E_1}(q \cdot s_1 \cdot s_1 \cdot q)}{d-2}[\gamma(d-2)(k \cdot u_1) + (k \cdot u_2)]k^\mu u_2^\nu - \frac{C_{E_1}(k \cdot u_1)^2 q^2}{d-2}s_1^{\mu\rho}s_{1\nu\rho} \\
& - \frac{C_{E_1}(q \cdot s_1 \cdot s_1 \cdot q)}{2(d-2)}[2\gamma(d-2)(k \cdot u_1)(k \cdot u_2) + 2(k \cdot u_1)^2 + 2(k \cdot u_2)^2 \\
& + \beta_\gamma(d-2)(k \cdot q) - \beta_\gamma(d-2)q^2]\eta^{\mu\nu} + \frac{C_{E_1}}{(k \cdot u_1)}[2\gamma(k \cdot u_1)(k \cdot u_2)(q \cdot s_1 \cdot s_1 \cdot q) \\
& + \beta_\gamma(k \cdot s_1 \cdot s_1 \cdot k)q^2 + \beta_\gamma(q \cdot s_1 \cdot s_1 \cdot q)q^2 - \beta_\gamma(k \cdot s_1 \cdot s_1 \cdot q)q^2 \\
& - \gamma(k \cdot u_1)(k \cdot s_1 \cdot s_1 \cdot u_2)q^2]q^\mu u_1^\nu + \frac{C_{E_1}}{(d-2)(k \cdot u_1)}[2(k \cdot u_1)^2(q \cdot s_1 \cdot s_1 \cdot q) \\
& + \beta_\gamma(d-2)(k \cdot s_1 \cdot s_1 \cdot q)q^2 + \gamma(d-2)(k \cdot u_1)(k \cdot s_1 \cdot s_1 \cdot u_2)q^2 \\
& - \beta_\gamma(d-2)(k \cdot s_1 \cdot s_1 \cdot k)q^2 - \beta_\gamma(d-2)(q \cdot s_1 \cdot s_1 \cdot q)q^2]k^\mu u_1^\nu \\
& + \frac{C_{E_1}q^2}{(d-2)(k \cdot u_1)}[2k^\rho(k \cdot u_1)^2 + \beta_\gamma(d-2)q^\rho(k \cdot q) + (d-2)(k \cdot u_1)^2(k \cdot u_2)u_2^\rho \\
& + \gamma(d-2)(k \cdot q)(k \cdot u_1)u_2^\rho + \gamma(d-2)q^\rho(k \cdot u_1)(k \cdot u_2) - \beta_\gamma(d-2)k^\rho(k \cdot q) \\
& - \gamma(d-2)k^\rho(k \cdot u_1)(k \cdot u_2)]s_1^{\mu\sigma}s_{1\rho\sigma}u_1^\nu \\
& + \frac{C_{E_1}}{2(d-2)(k \cdot u_1)^2}[2\beta_\gamma(d-2)(k \cdot q)(k \cdot s_1 \cdot s_1 \cdot q)q^2 \\
& + 2(d-2)(k \cdot u_1)^2(k \cdot u_2)(k \cdot s_1 \cdot s_1 \cdot u_2)q^2 + 2\gamma(d-2)(k \cdot q)(k \cdot u_1)(k \cdot s_1 \cdot s_1 \cdot u_2)q^2 \\
& + 2\gamma(d-2)(k \cdot u_1)(k \cdot u_2)(k \cdot s_1 \cdot s_1 \cdot q)q^2 + 2(k \cdot u_1)^2(k \cdot s_1 \cdot s_1 \cdot k)q^2 \\
& - 2\beta_\gamma(d-2)(k \cdot q)(k \cdot s_1 \cdot s_1 \cdot k)q^2 - 2(d-2)(k \cdot u_1)^2(k \cdot u_2)^2(q \cdot s_1 \cdot s_1 \cdot q) \\
& - 2\gamma(d-2)(k \cdot u_1)(k \cdot u_2)(k \cdot s_1 \cdot s_1 \cdot k)q^2 - 2\gamma(d-2)(k \cdot u_1)(k \cdot u_2)(q \cdot s_1 \cdot s_1 \cdot q)q^2 \\
& - \beta_\gamma(d-2)(k \cdot q)(q \cdot s_1 \cdot s_1 \cdot q)q^2]u_1^\mu u_1^\nu + \frac{C_{E_1}(q \cdot s_1 \cdot s_1 \cdot q)}{(k \cdot u_2)}[2\beta_\gamma(k \cdot q) \\
& - 2\gamma(k \cdot u_1)(k \cdot u_2) - \beta_\gamma q^2]q^\mu u_2^\nu + \frac{C_{E_1}(q \cdot s_1 \cdot s_1 \cdot q)}{2(k \cdot u_2)^2}[4\gamma(k \cdot q)(k \cdot u_1)(k \cdot u_2) \\
& + \beta_\gamma(k \cdot q)q^2 - 2\beta_\gamma(k \cdot q)^2 - 2\gamma(k \cdot u_1)(k \cdot u_2)q^2 - 2(k \cdot u_1)^2(k \cdot u_2)^2]u_2^\mu u_2^\nu \Big]
\end{aligned}$$

$t_{s_2 s_2}^{\mu\nu}$ Equal to $t_{s_1 s_1}^{\mu\nu}$ after interchanging the body labels $1 \leftrightarrow 2$ and mapping $q \mapsto k - q$

C.3 . Feynman rules

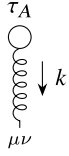
In this section we write the explicit Feynman rules we did not displayed in the main text. In particular we write the graviton cubic vertex in d dimensions. To get the one in four dimension (see (1.3.10)) it is sufficient to replace $\kappa \rightarrow m_{\text{Pl}}^{-1}$. The four-dimensional delta function of momentum conservation is imply. We also display the worldline vertices corresponding to single- and double-graviton emission from the A th spinning body (see

figs. 10 (c) and (d)) in d dimensions. We use again the shorthands defined in eqs. (C.2.3) and (C.2.4), replacing $s_A^{\mu\nu}$ with $\mathcal{S}_A^{\mu\nu}$ in the latter.

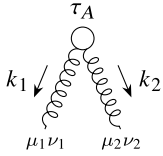


$$\begin{aligned}
& \frac{1}{8} i\kappa \text{Sym} [10k_1^2 \eta^{\mu_1 \mu_2} \eta^{\mu_3 \nu_3} \eta^{\nu_1 \nu_2} + 16(k_1 \cdot k_2) \eta^{\mu_1 \mu_2} \eta^{\mu_3 \nu_3} \eta^{\nu_1 \nu_2} \\
& + 2(k_1 \cdot k_3) \eta^{\mu_1 \mu_2} \eta^{\mu_3 \nu_3} \eta^{\nu_1 \nu_2} + 10k_2^2 \eta^{\mu_1 \mu_2} \eta^{\mu_3 \nu_3} \eta^{\nu_1 \nu_2} \\
& + 2(k_2 \cdot k_3) \eta^{\mu_1 \mu_2} \eta^{\mu_3 \nu_3} \eta^{\nu_1 \nu_2} + 10k_1^2 \eta^{\mu_1 \mu_3} \eta^{\mu_2 \nu_2} \eta^{\nu_1 \nu_3} \\
& + 2(k_1 \cdot k_2) \eta^{\mu_1 \mu_3} \eta^{\mu_2 \nu_2} \eta^{\nu_1 \nu_3} + 16(k_1 \cdot k_3) \eta^{\mu_1 \mu_3} \eta^{\mu_2 \nu_2} \eta^{\nu_1 \nu_3} \\
& + 2(k_2 \cdot k_3) \eta^{\mu_1 \mu_3} \eta^{\mu_2 \nu_2} \eta^{\nu_1 \nu_3} + 10k_3^2 \eta^{\mu_1 \mu_3} \eta^{\mu_2 \nu_2} \eta^{\nu_1 \nu_3} \\
& + 2(k_1 \cdot k_2) \eta^{\mu_1 \nu_1} \eta^{\mu_2 \mu_3} \eta^{\nu_2 \nu_3} + 2(k_1 \cdot k_3) \eta^{\mu_1 \nu_1} \eta^{\mu_2 \mu_3} \eta^{\nu_2 \nu_3} \\
& + 10k_2^2 \eta^{\mu_1 \nu_1} \eta^{\mu_2 \mu_3} \eta^{\nu_2 \nu_3} + 16(k_2 \cdot k_3) \eta^{\mu_1 \nu_1} \eta^{\mu_2 \mu_3} \eta^{\nu_2 \nu_3} + 10k_3^2 \eta^{\mu_1 \nu_1} \eta^{\mu_2 \mu_3} \eta^{\nu_2 \nu_3} \\
& + 9k_1^{\mu_1} k_1^{\mu_2} \eta^{\mu_3 \nu_1} \eta^{\nu_2 \nu_3} + 15k_1^{\mu_1} k_1^{\mu_2} \eta^{\mu_3 \nu_2} \eta^{\nu_1 \nu_3} + 12k_1^{\mu_1} k_1^{\mu_3} \eta^{\mu_2 \nu_1} \eta^{\nu_2 \nu_3} \\
& + 12k_1^{\mu_1} k_1^{\mu_3} \eta^{\mu_2 \nu_3} \eta^{\nu_1 \nu_2} + 16k_1^{\mu_1} k_1^{\nu_1} \eta^{\mu_2 \nu_2} \eta^{\mu_3 \nu_3} + 20k_1^{\mu_1} k_2^{\mu_2} \eta^{\mu_3 \nu_1} \eta^{\nu_2 \nu_3} \\
& + 12k_1^{\mu_1} k_2^{\mu_2} \eta^{\mu_3 \nu_2} \eta^{\nu_1 \nu_3} + 12k_1^{\mu_1} k_2^{\mu_3} \eta^{\mu_2 \nu_1} \eta^{\nu_2 \nu_3} + 4k_1^{\mu_1} k_2^{\mu_3} \eta^{\mu_2 \nu_3} \eta^{\nu_1 \nu_2} \\
& + 12k_1^{\mu_1} k_2^{\nu_1} \eta^{\mu_2 \nu_2} \eta^{\mu_3 \nu_3} + 10k_1^{\mu_1} k_3^{\mu_2} \eta^{\mu_3 \nu_1} \eta^{\nu_2 \nu_3} + 6k_1^{\mu_1} k_3^{\mu_2} \eta^{\mu_3 \nu_2} \eta^{\nu_1 \nu_3} \\
& + 24k_1^{\mu_1} k_3^{\mu_3} \eta^{\mu_2 \nu_1} \eta^{\nu_2 \nu_3} + 8k_1^{\mu_1} k_3^{\mu_3} \eta^{\mu_2 \nu_3} \eta^{\nu_1 \nu_2} + 12k_1^{\mu_1} k_3^{\nu_1} \eta^{\mu_2 \nu_2} \eta^{\mu_3 \nu_3} \\
& + 4k_1^{\mu_2} k_1^{\nu_2} \eta^{\mu_1 \mu_3} \eta^{\nu_1 \nu_3} + 4k_1^{\mu_2} k_2^{\mu_3} \eta^{\mu_1 \nu_1} \eta^{\nu_2 \nu_3} + 12k_1^{\mu_2} k_2^{\nu_2} \eta^{\mu_1 \nu_1} \eta^{\mu_3 \nu_3} \\
& + 4k_1^{\mu_2} k_3^{\mu_1} \eta^{\mu_3 \nu_3} \eta^{\nu_1 \nu_2} + 8k_1^{\mu_2} k_3^{\mu_3} \eta^{\mu_1 \nu_2} \eta^{\nu_1 \nu_3} + 8k_1^{\mu_2} k_3^{\mu_3} \eta^{\mu_1 \nu_3} \eta^{\nu_1 \nu_2} \\
& + 16k_1^{\mu_2} k_3^{\nu_2} \eta^{\mu_1 \mu_3} \eta^{\nu_1 \nu_3} + 4k_1^{\mu_3} k_1^{\nu_3} \eta^{\mu_1 \mu_2} \eta^{\nu_1 \nu_2} + 4k_1^{\mu_3} k_2^{\mu_1} \eta^{\mu_2 \nu_2} \eta^{\nu_1 \nu_3} \\
& + 8k_1^{\mu_3} k_2^{\mu_2} \eta^{\mu_1 \nu_2} \eta^{\nu_1 \nu_3} + 8k_1^{\mu_3} k_2^{\mu_2} \eta^{\mu_1 \nu_3} \eta^{\nu_1 \nu_2} + 16k_1^{\mu_3} k_2^{\nu_3} \eta^{\mu_1 \mu_2} \eta^{\nu_1 \nu_2} \\
& + 4k_1^{\mu_3} k_3^{\mu_2} \eta^{\mu_1 \nu_1} \eta^{\nu_2 \nu_3} + 12k_1^{\mu_3} k_3^{\nu_3} \eta^{\mu_1 \nu_1} \eta^{\mu_2 \nu_2} + 9k_2^{\mu_1} k_2^{\mu_2} \eta^{\mu_3 \nu_1} \eta^{\nu_2 \nu_3} \\
& + 15k_2^{\mu_1} k_2^{\mu_2} \eta^{\mu_3 \nu_2} \eta^{\nu_1 \nu_3} + 4k_2^{\mu_1} k_2^{\nu_1} \eta^{\mu_2 \mu_3} \eta^{\nu_2 \nu_3} + 4k_2^{\mu_1} k_3^{\mu_2} \eta^{\mu_3 \nu_3} \eta^{\nu_1 \nu_2} \\
& + 12k_2^{\mu_1} k_3^{\mu_3} \eta^{\mu_2 \nu_1} \eta^{\nu_2 \nu_3} + 4k_2^{\mu_1} k_3^{\mu_3} \eta^{\mu_2 \nu_3} \eta^{\nu_1 \nu_2} + 16k_2^{\mu_1} k_3^{\nu_1} \eta^{\mu_2 \mu_3} \eta^{\nu_2 \nu_3} \\
& + 12k_2^{\mu_2} k_2^{\mu_3} \eta^{\mu_1 \nu_2} \eta^{\nu_1 \nu_3} + 12k_2^{\mu_2} k_2^{\mu_3} \eta^{\mu_1 \nu_3} \eta^{\nu_1 \nu_2} + 16k_2^{\mu_2} k_2^{\nu_2} \eta^{\mu_1 \nu_1} \eta^{\mu_3 \nu_3} \\
& + 10k_2^{\mu_2} k_3^{\mu_1} \eta^{\mu_3 \nu_1} \eta^{\nu_2 \nu_3} + 6k_2^{\mu_2} k_3^{\mu_1} \eta^{\mu_3 \nu_2} \eta^{\nu_1 \nu_3} + 16k_2^{\mu_2} k_3^{\mu_3} \eta^{\mu_1 \nu_2} \eta^{\nu_1 \nu_3} \\
& + 16k_2^{\mu_2} k_3^{\mu_3} \eta^{\mu_1 \nu_3} \eta^{\nu_1 \nu_2} + 12k_2^{\mu_2} k_3^{\nu_2} \eta^{\mu_1 \nu_1} \eta^{\mu_3 \nu_3} + 4k_2^{\mu_3} k_2^{\nu_3} \eta^{\mu_1 \mu_2} \eta^{\nu_1 \nu_2} \\
& + 4k_2^{\mu_3} k_3^{\mu_1} \eta^{\mu_2 \nu_2} \eta^{\nu_1 \nu_3} + 12k_2^{\mu_3} k_3^{\nu_3} \eta^{\mu_1 \nu_1} \eta^{\mu_2 \nu_2} + 12k_3^{\mu_1} k_3^{\mu_3} \eta^{\mu_2 \nu_1} \eta^{\nu_2 \nu_3} \\
& + 12k_3^{\mu_1} k_3^{\mu_3} \eta^{\mu_2 \nu_3} \eta^{\nu_1 \nu_2} + 4k_3^{\mu_1} k_3^{\nu_1} \eta^{\mu_2 \mu_3} \eta^{\nu_2 \nu_3} + 12k_3^{\mu_2} k_3^{\mu_3} \eta^{\mu_1 \nu_2} \eta^{\nu_1 \nu_3} \\
& + 12k_3^{\mu_2} k_3^{\mu_3} \eta^{\mu_1 \nu_3} \eta^{\nu_1 \nu_2} + 4k_3^{\mu_2} k_3^{\nu_2} \eta^{\mu_1 \mu_3} \eta^{\nu_1 \nu_3} + 16k_3^{\mu_3} k_3^{\nu_3} \eta^{\mu_1 \nu_1} \eta^{\mu_2 \nu_2} \\
& - 6k_1^2 \eta^{\mu_1 \mu_2} \eta^{\mu_3 \nu_1} \eta^{\nu_2 \nu_3} - 6(k_1 \cdot k_2) \eta^{\mu_1 \mu_2} \eta^{\mu_3 \nu_1} \eta^{\nu_2 \nu_3} \\
& - 6(k_1 \cdot k_3) \eta^{\mu_1 \mu_2} \eta^{\mu_3 \nu_1} \eta^{\nu_2 \nu_3} - 6k_2^2 \eta^{\mu_1 \mu_2} \eta^{\mu_3 \nu_1} \eta^{\nu_2 \nu_3} \\
& - 6(k_2 \cdot k_3) \eta^{\mu_1 \mu_2} \eta^{\mu_3 \nu_1} \eta^{\nu_2 \nu_3} - 6k_3^2 \eta^{\mu_1 \mu_2} \eta^{\mu_3 \nu_1} \eta^{\nu_2 \nu_3} - 10k_1^2 \eta^{\mu_1 \mu_2} \eta^{\mu_3 \nu_2} \eta^{\nu_1 \nu_3} \\
& - 10(k_1 \cdot k_2) \eta^{\mu_1 \mu_2} \eta^{\mu_3 \nu_2} \eta^{\nu_1 \nu_3} - 10(k_1 \cdot k_3) \eta^{\mu_1 \mu_2} \eta^{\mu_3 \nu_2} \eta^{\nu_1 \nu_3} \\
& - 10k_2^2 \eta^{\mu_1 \mu_2} \eta^{\mu_3 \nu_2} \eta^{\nu_1 \nu_3} - 10(k_2 \cdot k_3) \eta^{\mu_1 \mu_2} \eta^{\mu_3 \nu_2} \eta^{\nu_1 \nu_3} - 10k_3^2 \eta^{\mu_1 \mu_2} \eta^{\mu_3 \nu_2} \eta^{\nu_1 \nu_3} \\
& - 4k_1^2 \eta^{\mu_1 \nu_1} \eta^{\mu_2 \nu_2} \eta^{\mu_3 \nu_3} - 4(k_1 \cdot k_2) \eta^{\mu_1 \nu_1} \eta^{\mu_2 \nu_2} \eta^{\mu_3 \nu_3} \\
& - 4(k_1 \cdot k_3) \eta^{\mu_1 \nu_1} \eta^{\mu_2 \nu_2} \eta^{\mu_3 \nu_3} - 4k_2^2 \eta^{\mu_1 \nu_1} \eta^{\mu_2 \nu_2} \eta^{\mu_3 \nu_3} \\
& - 4(k_2 \cdot k_3) \eta^{\mu_1 \nu_1} \eta^{\mu_2 \nu_2} \eta^{\mu_3 \nu_3} - 4k_3^2 \eta^{\mu_1 \nu_1} \eta^{\mu_2 \nu_2} \eta^{\mu_3 \nu_3} - 20k_1^{\mu_1} k_1^{\mu_2} \eta^{\mu_3 \nu_3} \eta^{\nu_1 \nu_2}
\end{aligned}$$

$$\begin{aligned}
& -20k_1^{\mu_1} k_1^{\mu_3} \eta^{\mu_2\nu_2} \eta^{\nu_1\nu_3} - 32k_1^{\mu_1} k_1^{\nu_1} \eta^{\mu_2\mu_3} \eta^{\nu_2\nu_3} - 32k_1^{\mu_1} k_2^{\mu_2} \eta^{\mu_3\nu_3} \eta^{\nu_1\nu_2} \\
& - 8k_1^{\mu_1} k_2^{\mu_3} \eta^{\mu_2\nu_2} \eta^{\nu_1\nu_3} - 20k_1^{\mu_1} k_2^{\nu_1} \eta^{\mu_2\mu_3} \eta^{\nu_2\nu_3} - 8k_1^{\mu_1} k_3^{\mu_2} \eta^{\mu_3\nu_3} \eta^{\nu_1\nu_2} \\
& - 32k_1^{\mu_1} k_3^{\mu_3} \eta^{\mu_2\nu_2} \eta^{\nu_1\nu_3} - 20k_1^{\mu_1} k_3^{\nu_1} \eta^{\mu_2\mu_3} \eta^{\nu_2\nu_3} - 4k_1^{\mu_2} k_2^{\mu_3} \eta^{\mu_1\nu_2} \eta^{\nu_1\nu_3} \\
& - 4k_1^{\mu_2} k_2^{\mu_3} \eta^{\mu_1\nu_3} \eta^{\nu_1\nu_2} - 20k_1^{\mu_2} k_2^{\nu_2} \eta^{\mu_1\mu_3} \eta^{\nu_1\nu_3} - 5k_1^{\mu_2} k_3^{\mu_1} \eta^{\mu_3\nu_1} \eta^{\nu_2\nu_3} \\
& - 3k_1^{\mu_2} k_3^{\mu_1} \eta^{\mu_3\nu_2} \eta^{\nu_1\nu_3} - 8k_1^{\mu_2} k_3^{\mu_3} \eta^{\mu_1\nu_1} \eta^{\nu_2\nu_3} - 8k_1^{\mu_2} k_3^{\nu_2} \eta^{\mu_1\nu_1} \eta^{\mu_3\nu_3} \\
& - 6k_1^{\mu_3} k_2^{\mu_1} \eta^{\mu_2\nu_1} \eta^{\nu_2\nu_3} - 2k_1^{\mu_3} k_2^{\mu_1} \eta^{\mu_2\nu_3} \eta^{\nu_1\nu_2} - 8k_1^{\mu_3} k_2^{\mu_2} \eta^{\mu_1\nu_1} \eta^{\nu_2\nu_3} \\
& - 8k_1^{\mu_3} k_2^{\nu_3} \eta^{\mu_1\nu_1} \eta^{\mu_2\nu_2} - 4k_1^{\mu_3} k_3^{\mu_2} \eta^{\mu_1\nu_2} \eta^{\nu_1\nu_3} - 4k_1^{\mu_3} k_3^{\mu_2} \eta^{\mu_1\nu_3} \eta^{\nu_1\nu_2} \\
& - 20k_1^{\mu_3} k_3^{\nu_3} \eta^{\mu_1\mu_2} \eta^{\nu_1\nu_2} - 20k_2^{\mu_1} k_2^{\mu_2} \eta^{\mu_3\nu_3} \eta^{\nu_1\nu_2} - 5k_2^{\mu_1} k_3^{\mu_2} \eta^{\mu_3\nu_1} \eta^{\nu_2\nu_3} \\
& - 3k_2^{\mu_1} k_3^{\mu_2} \eta^{\mu_3\nu_2} \eta^{\nu_1\nu_3} - 8k_2^{\mu_1} k_3^{\mu_3} \eta^{\mu_2\nu_2} \eta^{\nu_1\nu_3} - 8k_2^{\mu_1} k_3^{\nu_1} \eta^{\mu_2\nu_2} \eta^{\mu_3\nu_3} \\
& - 20k_2^{\mu_2} k_2^{\mu_3} \eta^{\mu_1\nu_1} \eta^{\nu_2\nu_3} - 32k_2^{\mu_2} k_2^{\nu_2} \eta^{\mu_1\mu_3} \eta^{\nu_1\nu_3} - 8k_2^{\mu_2} k_3^{\mu_1} \eta^{\mu_3\nu_3} \eta^{\nu_1\nu_2} \\
& - 32k_2^{\mu_2} k_3^{\mu_3} \eta^{\mu_1\nu_1} \eta^{\nu_2\nu_3} - 20k_2^{\mu_2} k_3^{\nu_2} \eta^{\mu_1\mu_3} \eta^{\nu_1\nu_3} - 6k_2^{\mu_3} k_3^{\mu_1} \eta^{\mu_2\nu_1} \eta^{\nu_2\nu_3} \\
& - 2k_2^{\mu_3} k_3^{\mu_1} \eta^{\mu_2\nu_3} \eta^{\nu_1\nu_2} - 20k_2^{\mu_3} k_3^{\nu_3} \eta^{\mu_1\mu_2} \eta^{\nu_1\nu_2} - 20k_3^{\mu_1} k_3^{\mu_3} \eta^{\mu_2\nu_2} \eta^{\nu_1\nu_3} \\
& - 20k_3^{\mu_2} k_3^{\mu_3} \eta^{\mu_1\nu_1} \eta^{\nu_2\nu_3} - 32k_3^{\mu_3} k_3^{\nu_3} \eta^{\mu_1\mu_2} \eta^{\nu_1\nu_2}]
\end{aligned}$$



$$\begin{aligned}
& -\frac{1}{2}i\kappa \int d\tau_A e^{ik \cdot x_A} \text{Sym} \left[m_A \mathcal{U}_A^\mu \mathcal{U}_A^\nu + ik_\rho \mathcal{S}_A^{\rho\mu} \mathcal{U}_A^\nu + \frac{1}{m_A} k_\rho k_\sigma \mathcal{U}_A^\alpha \right. \\
& \left. (\mathcal{U}_A^\mu \mathcal{S}_A^{\nu\rho} \mathcal{S}_A^{\sigma\alpha} + \mathcal{U}_A^\rho \mathcal{S}_A^{\sigma\mu} \mathcal{S}_A^{\nu\alpha}) + \frac{1}{2m_A} C_{EA} k_\rho k_\sigma (\mathcal{S}_A^{\rho\alpha} \mathcal{S}_A^\sigma{}_\alpha \mathcal{U}_A^\mu \mathcal{U}_A^\nu \right. \\
& \left. + 2\mathcal{U}_A^\rho \mathcal{S}_A^{\sigma\alpha} \mathcal{S}_A^\mu{}_\alpha \mathcal{U}_A^\nu + \mathcal{S}_A^\mu{}_\alpha \mathcal{S}_A^{\nu\alpha} \mathcal{U}_A^\rho \mathcal{U}_A^\sigma) \right]
\end{aligned}$$



$$\begin{aligned}
& \frac{1}{8}i\kappa^2 \int d\tau_A e^{i(k_1+k_2) \cdot x_A} \text{Sym} \left[i[(k_1 \cdot \mathcal{U}_A) - (k_2 \cdot \mathcal{U}_A)] \eta^{\mu_1\mu_2} \mathcal{S}_A^{\nu_1\nu_2} \right. \\
& - 2ik_1^\rho \eta^{\mu_1\mu_2} \mathcal{S}_A^{\nu_2}{}_\rho \mathcal{U}_A^{\nu_1} - 2ik_1^{\mu_2} \mathcal{S}_A^{\mu_1\nu_2} \mathcal{U}_A^{\nu_1} - 2ik_2^\rho \eta^{\mu_1\mu_2} \mathcal{S}_A^{\nu_1}{}_\rho \mathcal{U}_A^{\nu_2} \\
& - 2ik_2^{\mu_1} \mathcal{S}_A^{\mu_2\nu_1} \mathcal{U}_A^{\nu_2} + \frac{2}{m_A} \{ [(k_1 \cdot \mathcal{S}_A \cdot k_2) \mathcal{U}_A^\rho + k_2^\rho (k_1 \cdot \mathcal{S}_A \cdot \mathcal{U}_A) \\
& + k_2^\rho (k_2 \cdot \mathcal{S}_A \cdot \mathcal{U}_A)] \eta^{\mu_1\mu_2} \mathcal{S}_A^{\nu_1}{}_\rho \mathcal{U}_A^{\nu_2} \\
& + [(k_1 \cdot \mathcal{S}_A \cdot \mathcal{U}_A)(k_2 \cdot \mathcal{U}_A) - (k_1 \cdot \mathcal{U}_A)(k_2 \cdot \mathcal{S}_A \cdot \mathcal{U}_A)] \eta^{\mu_1\mu_2} \mathcal{S}_A^{\nu_1\nu_2} \\
& + [k_1^\rho (k_1 \cdot \mathcal{S}_A \cdot \mathcal{U}_A) + k_1^\rho (k_2 \cdot \mathcal{S}_A \cdot \mathcal{U}_A) - (k_1 \cdot \mathcal{S}_A \cdot k_2) \mathcal{U}_A^\rho] \eta^{\mu_1\mu_2} \mathcal{S}_A^{\nu_2}{}_\rho \mathcal{U}_A^{\nu_1} \\
& + (k_1^\rho + k_2^\rho) k_1^{\mu_2} \mathcal{S}_A^{\mu_1}{}_\rho \mathcal{S}_A^{\nu_2}{}_\sigma \mathcal{U}_A^{\nu_1} \mathcal{U}_A^\sigma \\
& + [(k_1 \cdot \mathcal{S}_A \cdot \mathcal{U}_A) + (k_2 \cdot \mathcal{S}_A \cdot \mathcal{U}_A)] k_1^{\mu_2} \mathcal{S}_A^{\mu_1\nu_2} \mathcal{U}_A^{\nu_1} \\
& + (k_1^\rho + k_2^\rho) k_2^{\mu_1} \mathcal{S}_A^{\mu_2}{}_\rho \mathcal{S}_A^{\nu_1}{}_\sigma \mathcal{U}_A^{\nu_2} \mathcal{U}_A^\sigma \\
& + [(k_1 \cdot \mathcal{S}_A \cdot \mathcal{U}_A) + (k_2 \cdot \mathcal{S}_A \cdot \mathcal{U}_A)] k_2^{\mu_1} \mathcal{S}_A^{\mu_2\nu_1} \mathcal{U}_A^{\nu_2} \\
& + (k_1^\rho k_1^\sigma + k_2^\rho k_2^\sigma) \mathcal{S}_A^{\mu_1}{}_\rho \mathcal{S}_A^{\mu_2}{}_\sigma \mathcal{U}_A^{\nu_1} \mathcal{U}_A^{\nu_2} \\
& + [k_1^\rho (k_1 \cdot \mathcal{U}_A) + (k_1 \cdot k_2) \mathcal{U}_A^\rho] \mathcal{S}_A^{\mu_1\mu_2} \mathcal{S}_A^{\nu_1}{}_\rho \mathcal{U}_A^{\nu_2} - [k_1^\rho (k_1 \cdot \mathcal{U}_A) \\
& + k_2^\rho (k_1 \cdot \mathcal{U}_A) + k_2^\rho (k_2 \cdot \mathcal{U}_A)] \eta^{\mu_1\mu_2} \mathcal{S}_A^{\nu_1}{}_\rho \mathcal{S}_A^{\nu_2}{}_\sigma \mathcal{U}_A^\sigma - [k_1^\rho (k_1 \cdot \mathcal{U}_A) \\
& + k_1^\rho (k_2 \cdot \mathcal{U}_A) + k_2^\rho (k_2 \cdot \mathcal{U}_A)] \eta^{\mu_1\mu_2} \mathcal{S}_A^{\nu_1}{}_\sigma \mathcal{S}_A^{\nu_2}{}_\rho \mathcal{U}_A^\sigma
\end{aligned}$$

$$\begin{aligned}
& - k_1^\rho k_2^{\mu_1} \mathcal{S}_A^{\mu_2 \rho} \mathcal{S}_A^{\nu_2 \sigma} \mathcal{U}_A^{\nu_1} \mathcal{U}_A^\sigma - k_1^{\mu_2} k_2^\rho \mathcal{S}_A^{\mu_1 \rho} \mathcal{S}_A^{\nu_1 \sigma} \mathcal{U}_A^{\nu_2} \mathcal{U}_A^\sigma \\
& - [(k_1 \cdot \mathcal{U}_A) + (k_2 \cdot \mathcal{U}_A)] k_1^{\mu_2} \mathcal{S}_A^{\mu_1 \nu_2} \mathcal{S}_A^{\nu_1 \rho} \mathcal{U}_A^\rho \\
& - [(k_1 \cdot \mathcal{U}_A) + (k_2 \cdot \mathcal{U}_A)] k_2^{\mu_1} \mathcal{S}_A^{\mu_2 \nu_1} \mathcal{S}_A^{\nu_2 \rho} \mathcal{U}_A^\rho \\
& - [(k_1 \cdot k_2) \mathcal{U}_A^\rho + k_2^\rho (k_2 \cdot \mathcal{U}_A)] \mathcal{S}_A^{\mu_1 \mu_2} \mathcal{S}_A^{\nu_2 \rho} \mathcal{U}_A^{\nu_1} \} + \frac{C_{EA}}{m_A} \{ 2[k_2^\rho (k_1 \cdot \mathcal{U}_A) \\
& - 2k_1^\rho (k_2 \cdot \mathcal{U}_A) - k_2^\rho (k_2 \cdot \mathcal{U}_A)] \eta^{\mu_1 \mu_2} \mathcal{S}_A^{\nu_1 \sigma} \mathcal{S}_A^{\rho \sigma} \mathcal{U}_A^{\nu_2} + 2[(k_1 \cdot \mathcal{U}_A)^2 \\
& + (k_1 \cdot \mathcal{U}_A)(k_2 \cdot \mathcal{U}_A) + (k_2 \cdot \mathcal{U}_A)^2] \eta^{\mu_1 \mu_2} \mathcal{S}_A^{\nu_1 \rho} \mathcal{S}_A^{\nu_2 \rho} \\
& + 2(k_1^\rho + k_2^\rho) k_1^{\mu_2} \mathcal{S}_A^{\nu_2 \sigma} \mathcal{S}_A^{\rho \sigma} \mathcal{U}_A^{\mu_1} \mathcal{U}_A^{\nu_1} + 2(k_2 \cdot \mathcal{U}_A) k_1^{\mu_2} \mathcal{S}_A^{\mu_1 \rho} \mathcal{S}_A^{\nu_1 \rho} \mathcal{U}_A^{\nu_2} \\
& + 2(k_1^\rho + k_2^\rho) k_2^{\mu_1} \mathcal{S}_A^{\nu_1 \sigma} \mathcal{S}_A^{\rho \sigma} \mathcal{U}_A^{\mu_2} \mathcal{U}_A^{\nu_2} + 2(k_1 \cdot \mathcal{U}_A) k_2^{\mu_1} \mathcal{S}_A^{\mu_2 \rho} \mathcal{S}_A^{\nu_2 \rho} \mathcal{U}_A^{\nu_1} \\
& + 2(k_1 \cdot k_2) \mathcal{S}_A^{\mu_1 \rho} \mathcal{S}_A^{\mu_2 \rho} \mathcal{U}_A^{\nu_1} \mathcal{U}_A^{\nu_2} - 2[2k_2^\rho (k_1 \cdot \mathcal{U}_A) + k_1^\rho (k_1 \cdot \mathcal{U}_A) \\
& - k_1^\rho (k_2 \cdot \mathcal{U}_A)] \eta^{\mu_1 \mu_2} \mathcal{S}_A^{\nu_2 \sigma} \mathcal{S}_A^{\rho \sigma} \mathcal{U}_A^{\nu_1} - 2(k_1 \cdot \mathcal{S}_A \cdot \mathcal{S}_A \cdot k_2) \eta^{\mu_1 \mu_2} \mathcal{U}_A^{\nu_1} \mathcal{U}_A^{\nu_2} \\
& - 2k_1^\rho k_2^{\mu_1} \mathcal{S}_A^{\mu_2 \sigma} \mathcal{S}_A^{\rho \sigma} \mathcal{U}_A^{\nu_1} \mathcal{U}_A^{\nu_2} - 2k_1^{\mu_2} k_2^\rho \mathcal{S}_A^{\mu_1 \sigma} \mathcal{S}_A^{\rho \sigma} \mathcal{U}_A^{\nu_1} \mathcal{U}_A^{\nu_2} \\
& - 2[(k_1 \cdot \mathcal{U}_A) + (k_2 \cdot \mathcal{U}_A)] k_1^{\mu_2} \mathcal{S}_A^{\mu_1 \rho} \mathcal{S}_A^{\nu_2 \rho} \mathcal{U}_A^{\nu_1} \\
& - 2[(k_1 \cdot \mathcal{U}_A) + (k_2 \cdot \mathcal{U}_A)] k_2^{\mu_1} \mathcal{S}_A^{\mu_2 \rho} \mathcal{S}_A^{\nu_1 \rho} \mathcal{U}_A^{\nu_2} \\
& - (k_1 \cdot k_2) \mathcal{S}_A^{\mu_1 \rho} \mathcal{S}_A^{\nu_1 \rho} \mathcal{U}_A^{\mu_2} \mathcal{U}_A^{\nu_2} - (k_1 \cdot k_2) \mathcal{S}_A^{\mu_2 \rho} \mathcal{S}_A^{\nu_2 \rho} \mathcal{U}_A^{\mu_1} \mathcal{U}_A^{\nu_1} \} \Big]
\end{aligned}$$

Bibliography

- [1] **LISA** Collaboration, P. Amaro-Seoane *et. al.*, “Laser Interferometer Space Antenna,” [1702.00786](#).
- [2] M. Punturo *et. al.*, “The Einstein Telescope: A third-generation gravitational wave observatory,” *Class. Quant. Grav.* **27** (2010) 194002.
- [3] D. Reitze *et. al.*, “Cosmic Explorer: The U.S. Contribution to Gravitational-Wave Astronomy beyond LIGO,” *Bull. Am. Astron. Soc.* **51** (2019), no. 7 035, [1907.04833](#).
- [4] E. Barausse, “The evolution of massive black holes and their spins in their galactic hosts,” *Mon. Not. Roy. Astron. Soc.* **423** (2012) 2533–2557, [1201.5888](#).
- [5] E. Berti *et. al.*, “Testing General Relativity with Present and Future Astrophysical Observations,” *Class. Quant. Grav.* **32** (2015) 243001, [1501.07274](#).
- [6] **LIGO Scientific, Virgo** Collaboration, R. Abbott *et. al.*, “Tests of general relativity with binary black holes from the second LIGO-Virgo gravitational-wave transient catalog,” *Phys. Rev. D* **103** (2021), no. 12 122002, [2010.14529](#).
- [7] E. Barausse *et. al.*, “Prospects for Fundamental Physics with LISA,” *Gen. Rel. Grav.* **52** (2020), no. 8 81, [2001.09793](#).
- [8] **LISA Cosmology Working Group** Collaboration, P. Auclair *et. al.*, “Cosmology with the Laser Interferometer Space Antenna,” [2204.05434](#).
- [9] **LISA** Collaboration, K. G. Arun *et. al.*, “New horizons for fundamental physics with LISA,” *Living Rev. Rel.* **25** (2022), no. 1 4, [2205.01597](#).
- [10] T. Callister, M. Fishbach, D. Holz, and W. Farr, “Shouts and Murmurs: Combining Individual Gravitational-Wave Sources with the Stochastic Background to Measure the History of Binary Black Hole Mergers,” *Astrophys. J. Lett.* **896** (2020), no. 2 L32, [2003.12152](#).
- [11] A. Buonanno and T. Damour, “Effective one-body approach to general relativistic two-body dynamics,” *Phys. Rev. D* **59** (1999) 084006, [gr-qc/9811091](#).
- [12] A. Buonanno and T. Damour, “Transition from inspiral to plunge in binary black hole coalescences,” *Phys. Rev. D* **62** (2000) 064015, [gr-qc/0001013](#).
- [13] M. Khalil, A. Buonanno, J. Steinhoff, and J. Vines, “Energetics and scattering of gravitational two-body systems at fourth post-Minkowskian order,” *Phys. Rev. D* **106** (2022), no. 2 024042, [2204.05047](#).

- [14] F. Pretorius, “Evolution of binary black hole spacetimes,” *Phys. Rev. Lett.* **95** (2005) 121101, [gr-qc/0507014](#).
- [15] M. Campanelli, C. O. Lousto, P. Marronetti, and Y. Zlochower, “Accurate evolutions of orbiting black-hole binaries without excision,” *Phys. Rev. Lett.* **96** (2006) 111101, [gr-qc/0511048](#).
- [16] J. G. Baker, J. Centrella, D.-I. Choi, M. Koppitz, and J. van Meter, “Gravitational wave extraction from an inspiraling configuration of merging black holes,” *Phys. Rev. Lett.* **96** (2006) 111102, [gr-qc/0511103](#).
- [17] F. Foucart, P. Laguna, G. Lovelace, D. Radice, and H. Witek, “Snowmass2021 Cosmic Frontier White Paper: Numerical relativity for next-generation gravitational-wave probes of fundamental physics,” [2203.08139](#).
- [18] M. Pürrer and C.-J. Haster, “Gravitational waveform accuracy requirements for future ground-based detectors,” *Phys. Rev. Res.* **2** (2020), no. 2 023151, [1912.10055](#).
- [19] A. Buonanno, M. Khalil, D. O’Connell, R. Roiban, M. P. Solon, and M. Zeng, “Snowmass White Paper: Gravitational Waves and Scattering Amplitudes,” in *2022 Snowmass Summer Study*, 4, 2022. [2204.05194](#).
- [20] W. D. Goldberger and I. Z. Rothstein, “An Effective field theory of gravity for extended objects,” *Phys. Rev. D* **73** (2006) 104029, [hep-th/0409156](#).
- [21] L. Blanchet, “Gravitational Radiation from Post-Newtonian Sources and Inspiralling Compact Binaries,” *Living Rev. Rel.* **17** (2014) 2, [1310.1528](#).
- [22] L. Blanchet, “Analytic Approximations in GR and Gravitational Waves,” *Int. J. Mod. Phys. D* **28** (2019), no. 06 1930011, [1812.07490](#).
- [23] W. D. Goldberger, “Les Houches lectures on effective field theories and gravitational radiation,” in *Les Houches Summer School - Session 86: Particle Physics and Cosmology: The Fabric of Spacetime*, 1, 2007. [hep-ph/0701129](#).
- [24] I. Z. Rothstein, “Progress in effective field theory approach to the binary inspiral problem,” *Gen. Rel. Grav.* **46** (2014) 1726.
- [25] S. Foffa and R. Sturani, “Effective field theory methods to model compact binaries,” *Class. Quant. Grav.* **31** (2014), no. 4 043001, [1309.3474](#).
- [26] R. A. Porto, “The effective field theorist’s approach to gravitational dynamics,” *Phys. Rept.* **633** (2016) 1–104, [1601.04914](#).
- [27] M. Levi, “Effective Field Theories of Post-Newtonian Gravity: A comprehensive review,” *Rept. Prog. Phys.* **83** (2020), no. 7 075901, [1807.01699](#).

- [28] W. D. Goldberger, “Effective field theories of gravity and compact binary dynamics: A Snowmass 2021 whitepaper,” [2206.14249](#).
- [29] A. Einstein, L. Infeld, and B. Hoffmann, “The Gravitational equations and the problem of motion,” *Annals Math.* **39** (1938) 65–100.
- [30] A. Einstein and L. Infeld, “The Gravitational equations and the problem of motion. 2.,” *Annals Math.* **41** (1940) 455–464.
- [31] T. Damour, P. Jaranowski, and G. Schäfer, “Nonlocal-in-time action for the fourth post-Newtonian conservative dynamics of two-body systems,” *Phys. Rev. D* **89** (2014), no. 6 064058, [1401.4548](#).
- [32] P. Jaranowski and G. Schäfer, “Derivation of local-in-time fourth post-Newtonian ADM Hamiltonian for spinless compact binaries,” *Phys. Rev. D* **92** (2015), no. 12 124043, [1508.01016](#).
- [33] T. Marchand, L. Bernard, L. Blanchet, and G. Faye, “Ambiguity-Free Completion of the Equations of Motion of Compact Binary Systems at the Fourth Post-Newtonian Order,” *Phys. Rev. D* **97** (2018), no. 4 044023, [1707.09289](#).
- [34] C. R. Galley, A. K. Leibovich, R. A. Porto, and A. Ross, “Tail effect in gravitational radiation reaction: Time nonlocality and renormalization group evolution,” *Phys. Rev. D* **93** (2016) 124010, [1511.07379](#).
- [35] R. A. Porto and I. Z. Rothstein, “Apparent ambiguities in the post-Newtonian expansion for binary systems,” *Phys. Rev. D* **96** (2017), no. 2 024062, [1703.06433](#).
- [36] J. Blümlein, A. Maier, P. Marquard, and G. Schäfer, “Fourth post-Newtonian Hamiltonian dynamics of two-body systems from an effective field theory approach,” *Nucl. Phys. B* **955** (2020) 115041, [2003.01692](#).
- [37] S. Foffa, R. A. Porto, I. Rothstein, and R. Sturani, “Conservative dynamics of binary systems to fourth Post-Newtonian order in the EFT approach II: Renormalized Lagrangian,” *Phys. Rev. D* **100** (2019), no. 2 024048, [1903.05118](#).
- [38] S. Foffa and R. Sturani, “Conservative dynamics of binary systems to fourth Post-Newtonian order in the EFT approach I: Regularized Lagrangian,” *Phys. Rev. D* **100** (2019), no. 2 024047, [1903.05113](#).
- [39] T. Marchand, Q. Henry, F. Larrouturou, S. Marsat, G. Faye, and L. Blanchet, “The mass quadrupole moment of compact binary systems at the fourth post-Newtonian order,” *Class. Quant. Grav.* **37** (2020), no. 21 215006, [2003.13672](#).

- [40] L. Blanchet, G. Faye, and F. Larrouturou, “The quadrupole moment of compact binaries to the fourth post-Newtonian order: from source to canonical moment,” *Class. Quant. Grav.* **39** (2022), no. 19 195003, [2204.11293](#).
- [41] L. Blanchet and G. Schaefer, “Higher order gravitational radiation losses in binary systems,” *Mon. Not. Roy. Astron. Soc.* **239** (1989) 845–867. [Erratum: *Mon. Not. Roy. Astron. Soc.* 242, 704 (1990)].
- [42] L. Blanchet and G. Schaefer, “Gravitational wave tails and binary star systems,” *Class. Quant. Grav.* **10** (1993) 2699–2721.
- [43] L. Blanchet, B. R. Iyer, and B. Joguet, “Gravitational waves from inspiralling compact binaries: Energy flux to third postNewtonian order,” *Phys. Rev. D* **65** (2002) 064005, [gr-qc/0105098](#). [Erratum: *Phys. Rev. D* 71, 129903 (2005)].
- [44] L. Blanchet, G. Faye, B. R. Iyer, and B. Joguet, “Gravitational wave inspiral of compact binary systems to $7/2$ postNewtonian order,” *Phys. Rev. D* **65** (2002) 061501, [gr-qc/0105099](#). [Erratum: *Phys. Rev. D* 71, 129902 (2005)].
- [45] L. Blanchet and B. R. Iyer, “Hadamard regularization of the third post-Newtonian gravitational wave generation of two point masses,” *Phys. Rev. D* **71** (2005) 024004, [gr-qc/0409094](#).
- [46] L. Blanchet, T. Damour, G. Esposito-Farese, and B. R. Iyer, “Gravitational radiation from inspiralling compact binaries completed at the third post-Newtonian order,” *Phys. Rev. Lett.* **93** (2004) 091101, [gr-qc/0406012](#).
- [47] T. Marchand, L. Blanchet, and G. Faye, “Gravitational-wave tail effects to quartic non-linear order,” *Class. Quant. Grav.* **33** (2016), no. 24 244003, [1607.07601](#).
- [48] D. Bini, T. Damour, and A. Geralico, “Novel approach to binary dynamics: application to the fifth post-Newtonian level,” *Phys. Rev. Lett.* **123** (2019), no. 23 231104, [1909.02375](#).
- [49] J. Blümlein, A. Maier, P. Marquard, and G. Schäfer, “The fifth-order post-Newtonian Hamiltonian dynamics of two-body systems from an effective field theory approach: potential contributions,” *Nucl. Phys. B* **965** (2021) 115352, [2010.13672](#).
- [50] G. L. Almeida, S. Foffa, and R. Sturani, “Tail contributions to gravitational conservative dynamics,” *Phys. Rev. D* **104** (2021), no. 12 124075, [2110.14146](#).
- [51] J. Blümlein, A. Maier, P. Marquard, and G. Schäfer, “The 6th post-Newtonian potential terms at $O(G_N^4)$,” *Phys. Lett. B* **816** (2021) 136260, [2101.08630](#).
- [52] J. Blümlein, A. Maier, P. Marquard, and G. Schäfer, “Testing binary dynamics in gravity at the sixth post-Newtonian level,” *Phys. Lett. B* **807** (2020) 135496, [2003.07145](#).

- [53] D. Bini, T. Damour, and A. Geralico, "Sixth post-Newtonian local-in-time dynamics of binary systems," *Phys. Rev. D* **102** (2020), no. 2 024061, [2004.05407](#).
- [54] A. Bohé, G. Faye, S. Marsat, and E. K. Porter, "Quadratic-in-spin effects in the orbital dynamics and gravitational-wave energy flux of compact binaries at the 3PN order," *Class. Quant. Grav.* **32** (2015), no. 19 195010, [1501.01529](#).
- [55] L. Blanchet, A. Buonanno, and G. Faye, "Third post-Newtonian spin-orbit effect in the gravitational radiation flux of compact binaries," *ASP Conf. Ser.* **467** (2013) 215, [1210.0764](#).
- [56] J. Steinhoff, S. Hergt, and G. Schaefer, "On the next-to-leading order gravitational spin(1)-spin(2) dynamics," *Phys. Rev. D* **77** (2008) 081501, [0712.1716](#).
- [57] R. A. Porto, A. Ross, and I. Z. Rothstein, "Spin induced multipole moments for the gravitational wave amplitude from binary inspirals to 2.5 Post-Newtonian order," *JCAP* **09** (2012) 028, [1203.2962](#).
- [58] R. A. Porto, A. Ross, and I. Z. Rothstein, "Spin induced multipole moments for the gravitational wave flux from binary inspirals to third Post-Newtonian order," *JCAP* **03** (2011) 009, [1007.1312](#).
- [59] Q. Henry, G. Faye, and L. Blanchet, "Tidal effects in the equations of motion of compact binary systems to next-to-next-to-leading post-Newtonian order," *Phys. Rev. D* **101** (2020), no. 6 064047, [1912.01920](#).
- [60] Q. Henry, G. Faye, and L. Blanchet, "Tidal effects in the gravitational-wave phase evolution of compact binary systems to next-to-next-to-leading post-Newtonian order," *Phys. Rev. D* **102** (2020), no. 4 044033, [2005.13367](#).
- [61] Q. Henry, G. Faye, and L. Blanchet, "Hamiltonian for tidal interactions in compact binary systems to next-to-next-to-leading post-Newtonian order," *Phys. Rev. D* **102** (2020), no. 12 124074, [2009.12332](#).
- [62] G. Cho, B. Pardo, and R. A. Porto, "Gravitational radiation from inspiralling compact objects: Spin-spin effects completed at the next-to-leading post-Newtonian order," *Phys. Rev. D* **104** (2021), no. 2 024037, [2103.14612](#).
- [63] G. Cho, R. A. Porto, and Z. Yang, "Gravitational radiation from inspiralling compact objects: Spin effects to fourth Post-Newtonian order," [2201.05138](#).
- [64] Y. Mino, M. Sasaki, and T. Tanaka, "Gravitational radiation reaction to a particle motion," *Phys. Rev. D* **55** (1997) 3457–3476, [gr-qc/9606018](#).

- [65] T. C. Quinn and R. M. Wald, “An Axiomatic approach to electromagnetic and gravitational radiation reaction of particles in curved space-time,” *Phys. Rev. D* **56** (1997) 3381–3394, [gr-qc/9610053](#).
- [66] L. Barack and A. Pound, “Self-force and radiation reaction in general relativity,” *Rept. Prog. Phys.* **82** (2019), no. 1 016904, [1805.10385](#).
- [67] A. Pound, B. Wardell, N. Warburton, and J. Miller, “Second-Order Self-Force Calculation of Gravitational Binding Energy in Compact Binaries,” *Phys. Rev. Lett.* **124** (2020), no. 2 021101, [1908.07419](#).
- [68] A. Antonelli, C. Kavanagh, M. Khalil, J. Steinhoff, and J. Vines, “Gravitational spin-orbit coupling through third-subleading post-Newtonian order: from first-order self-force to arbitrary mass ratios,” *Phys. Rev. Lett.* **125** (2020), no. 1 011103, [2003.11391](#).
- [69] A. Antonelli, C. Kavanagh, M. Khalil, J. Steinhoff, and J. Vines, “Gravitational spin-orbit and aligned spin₁-spin₂ couplings through third-subleading post-Newtonian orders,” *Phys. Rev. D* **102** (2020) 124024, [2010.02018](#).
- [70] M. Khalil, “Gravitational spin-orbit dynamics at the fifth-and-a-half post-Newtonian order,” *Phys. Rev. D* **104** (2021), no. 12 124015, [2110.12813](#).
- [71] B. Bertotti, “On gravitational motion,” *Nuovo Cim.* **4** (1956), no. 4 898–906.
- [72] B. Bertotti and J. Plebanski, “Theory of gravitational perturbations in the fast motion approximation,” *Annals Phys.* **11** (1960), no. 2 169–200.
- [73] P. Havas and J. N. Goldberg, “Lorentz-Invariant Equations of Motion of Point Masses in the General Theory of Relativity,” *Phys. Rev.* **128** (1962) 398–414.
- [74] M. Portilla, “SCATTERING OF TWO GRAVITATING PARTICLES: CLASSICAL APPROACH,” *J. Phys. A* **13** (1980) 3677–3683.
- [75] L. Bel, T. Damour, N. Deruelle, J. Ibanez, and J. Martin, “Poincaré-invariant gravitational field and equations of motion of two pointlike objects: The postlinear approximation of general relativity,” *Gen. Rel. Grav.* **13** (1981) 963–1004.
- [76] K. Westpfahl, “High-Speed Scattering of Charged and Uncharged Particles in General Relativity,” *Fortsch. Phys.* **33** (1985), no. 8 417–493.
- [77] K. Westpfahl and M. Goller, “GRAVITATIONAL SCATTERING OF TWO RELATIVISTIC PARTICLES IN POSTLINEAR APPROXIMATION,” *Lett. Nuovo Cim.* **26** (1979) 573–576.
- [78] P. C. Peters, “Relativistic gravitational bremsstrahlung,” *Phys. Rev. D* **1** (1970) 1559–1571.

- [79] K. S. Thorne and S. J. Kovacs, "The Generation of Gravitational Waves. 1. Weak-field sources," *Astrophys. J.* **200** (1975) 245–262.
- [80] R. J. Crowley and K. S. Thorne, "The Generation of Gravitational Waves. 2. The Postlinear Formalism Revisited," *Astrophys. J.* **215** (1977) 624–635.
- [81] S. Kovacs and K. Thorne, "The Generation of Gravitational Waves. 3. Derivation of Bremsstrahlung Formulas," *Astrophys. J.* **217** (1977) 252–280.
- [82] S. Kovacs and K. Thorne, "The Generation of Gravitational Waves. 4. Bremsstrahlung," *Astrophys. J.* **224** (1978) 62–85.
- [83] M. Turner and C. M. Will, "Post-Newtonian gravitational bremsstrahlung," *Astrophys. J.* **220** (1978) 1107–1124.
- [84] D. Amati, M. Ciafaloni, and G. Veneziano, "Higher Order Gravitational Deflection and Soft Bremsstrahlung in Planckian Energy Superstring Collisions," *Nucl. Phys. B* **347** (1990) 550–580.
- [85] D. Amati, M. Ciafaloni, and G. Veneziano, "Planckian scattering beyond the semiclassical approximation," *Phys. Lett. B* **289** (1992) 87–91.
- [86] M. J. G. Veltman, "Quantum Theory of Gravitation," *Conf. Proc. C* **7507281** (1975) 265–327.
- [87] B. S. DeWitt, "Quantum Theory of Gravity. 1. The Canonical Theory," *Phys. Rev.* **160** (1967) 1113–1148.
- [88] B. S. DeWitt, "Quantum Theory of Gravity. 2. The Manifestly Covariant Theory," *Phys. Rev.* **162** (1967) 1195–1239.
- [89] B. S. DeWitt, "Quantum Theory of Gravity. 3. Applications of the Covariant Theory," *Phys. Rev.* **162** (1967) 1239–1256.
- [90] J. F. Donoghue, "General relativity as an effective field theory: The leading quantum corrections," *Phys. Rev. D* **50** (1994) 3874–3888, [gr-qc/9405057](#).
- [91] N. E. J. Bjerrum-Bohr, J. F. Donoghue, and B. R. Holstein, "Quantum gravitational corrections to the nonrelativistic scattering potential of two masses," *Phys. Rev. D* **67** (2003) 084033, [hep-th/0211072](#). [Erratum: *Phys.Rev.D* 71, 069903 (2005)].
- [92] Y. Iwasaki, "Fourth-order gravitational potential based on quantum field theory," *Lett. Nuovo Cim.* **1** (1971) 783–786.
- [93] Y. Iwasaki, "Quantum theory of gravitation vs. classical theory. - fourth-order potential," *Prog. Theor. Phys.* **46** (1971) 1587–1609.

- [94] Z. Bern, J. J. M. Carrasco, and H. Johansson, “New Relations for Gauge-Theory Amplitudes,” *Phys. Rev. D* **78** (2008) 085011, [0805.3993](#).
- [95] Z. Bern, J. J. M. Carrasco, and H. Johansson, “Perturbative Quantum Gravity as a Double Copy of Gauge Theory,” *Phys. Rev. Lett.* **105** (2010) 061602, [1004.0476](#).
- [96] Z. Bern, J. J. Carrasco, M. Chiodaroli, H. Johansson, and R. Roiban, “The Duality Between Color and Kinematics and its Applications,” [1909.01358](#).
- [97] A. Brandhuber, G. Chen, G. Travaglini, and C. Wen, “A new gauge-invariant double copy for heavy-mass effective theory,” *JHEP* **07** (2021) 047, [2104.11206](#).
- [98] Z. Bern, L. J. Dixon, D. C. Dunbar, and D. A. Kosower, “One loop n point gauge theory amplitudes, unitarity and collinear limits,” *Nucl. Phys. B* **425** (1994) 217–260, [hep-ph/9403226](#).
- [99] Z. Bern, L. J. Dixon, D. C. Dunbar, and D. A. Kosower, “Fusing gauge theory tree amplitudes into loop amplitudes,” *Nucl. Phys. B* **435** (1995) 59–101, [hep-ph/9409265](#).
- [100] R. Britto, F. Cachazo, and B. Feng, “Generalized unitarity and one-loop amplitudes in N=4 super-Yang-Mills,” *Nucl. Phys. B* **725** (2005) 275–305, [hep-th/0412103](#).
- [101] D. Neill and I. Z. Rothstein, “Classical Space-Times from the S Matrix,” *Nucl. Phys. B* **877** (2013) 177–189, [1304.7263](#).
- [102] N. E. J. Bjerrum-Bohr, J. F. Donoghue, and P. Vanhove, “On-shell Techniques and Universal Results in Quantum Gravity,” *JHEP* **02** (2014) 111, [1309.0804](#).
- [103] A. Luna, I. Nicholson, D. O’Connell, and C. D. White, “Inelastic Black Hole Scattering from Charged Scalar Amplitudes,” *JHEP* **03** (2018) 044, [1711.03901](#).
- [104] N. E. J. Bjerrum-Bohr, P. H. Damgaard, G. Festuccia, L. Planté, and P. Vanhove, “General Relativity from Scattering Amplitudes,” *Phys. Rev. Lett.* **121** (2018), no. 17 171601, [1806.04920](#).
- [105] S. Mougiakakos and P. Vanhove, “Schwarzschild-Tangherlini metric from scattering amplitudes in various dimensions,” *Phys. Rev. D* **103** (2021), no. 2 026001, [2010.08882](#).
- [106] M. Beneke and V. A. Smirnov, “Asymptotic expansion of Feynman integrals near threshold,” *Nucl. Phys. B* **522** (1998) 321–344, [hep-ph/9711391](#).
- [107] C. Cheung, I. Z. Rothstein, and M. P. Solon, “From Scattering Amplitudes to Classical Potentials in the Post-Minkowskian Expansion,” *Phys. Rev. Lett.* **121** (2018), no. 25 251101, [1808.02489](#).

- [108] A. Cristofoli, N. E. J. Bjerrum-Bohr, P. H. Damgaard, and P. Vanhove, "Post-Minkowskian Hamiltonians in general relativity," *Phys. Rev. D* **100** (2019), no. 8 084040, [1906.01579](#).
- [109] A. Koemans Collado, P. Di Vecchia, and R. Russo, "Revisiting the second post-Minkowskian eikonal and the dynamics of binary black holes," *Phys. Rev. D* **100** (2019), no. 6 066028, [1904.02667](#).
- [110] P. Di Vecchia, C. Heissenberg, R. Russo, and G. Veneziano, "The eikonal approach to gravitational scattering and radiation at $\mathcal{O}(G^3)$," *JHEP* **07** (2021) 169, [2104.03256](#).
- [111] P. Di Vecchia, C. Heissenberg, R. Russo, and G. Veneziano, "Universality of ultra-relativistic gravitational scattering," *Phys. Lett. B* **811** (2020) 135924, [2008.12743](#).
- [112] J. Parra-Martinez, M. S. Ruf, and M. Zeng, "Extremal black hole scattering at $\mathcal{O}(G^3)$: graviton dominance, eikonal exponentiation, and differential equations," *JHEP* **11** (2020) 023, [2005.04236](#).
- [113] N. E. J. Bjerrum-Bohr, A. Cristofoli, and P. H. Damgaard, "Post-Minkowskian Scattering Angle in Einstein Gravity," *JHEP* **08** (2020) 038, [1910.09366](#).
- [114] G. Kälin and R. A. Porto, "From Boundary Data to Bound States," *JHEP* **01** (2020) 072, [1910.03008](#).
- [115] D. A. Kosower, B. Maybee, and D. O'Connell, "Amplitudes, Observables, and Classical Scattering," *JHEP* **02** (2019) 137, [1811.10950](#).
- [116] B. Maybee, D. O'Connell, and J. Vines, "Observables and amplitudes for spinning particles and black holes," *JHEP* **12** (2019) 156, [1906.09260](#).
- [117] Z. Bern, C. Cheung, R. Roiban, C.-H. Shen, M. P. Solon, and M. Zeng, "Scattering Amplitudes and the Conservative Hamiltonian for Binary Systems at Third Post-Minkowskian Order," *Phys. Rev. Lett.* **122** (2019), no. 20 201603, [1901.04424](#).
- [118] Z. Bern, C. Cheung, R. Roiban, C.-H. Shen, M. P. Solon, and M. Zeng, "Black Hole Binary Dynamics from the Double Copy and Effective Theory," *JHEP* **10** (2019) 206, [1908.01493](#).
- [119] C. Cheung and M. P. Solon, "Classical gravitational scattering at $\mathcal{O}(G^3)$ from Feynman diagrams," *JHEP* **06** (2020) 144, [2003.08351](#).
- [120] E. Herrmann, J. Parra-Martinez, M. S. Ruf, and M. Zeng, "Gravitational Bremsstrahlung from Reverse Unitarity," *Phys. Rev. Lett.* **126** (2021), no. 20 201602, [2101.07255](#).

- [121] E. Herrmann, J. Parra-Martinez, M. S. Ruf, and M. Zeng, “Radiative classical gravitational observables at $\mathcal{O}(G^3)$ from scattering amplitudes,” *JHEP* **10** (2021) 148, [2104.03957](#).
- [122] P. Di Vecchia, C. Heissenberg, and R. Russo, “Angular momentum of zero-frequency gravitons,” *JHEP* **08** (2022) 172, [2203.11915](#).
- [123] P. Di Vecchia, C. Heissenberg, R. Russo, and G. Veneziano, “The eikonal operator at arbitrary velocities I: the soft-radiation limit,” *JHEP* **07** (2022) 039, [2204.02378](#).
- [124] N. E. J. Bjerrum-Bohr, P. H. Damgaard, L. Planté, and P. Vanhove, “Classical gravity from loop amplitudes,” *Phys. Rev. D* **104** (2021), no. 2 026009, [2104.04510](#).
- [125] N. E. J. Bjerrum-Bohr, P. H. Damgaard, L. Planté, and P. Vanhove, “The amplitude for classical gravitational scattering at third Post-Minkowskian order,” *JHEP* **08** (2021) 172, [2105.05218](#).
- [126] N. E. J. Bjerrum-Bohr, L. Planté, and P. Vanhove, “Post-Minkowskian radial action from soft limits and velocity cuts,” *JHEP* **03** (2022) 071, [2111.02976](#).
- [127] A. Brandhuber, G. Chen, G. Travaglini, and C. Wen, “Classical gravitational scattering from a gauge-invariant double copy,” *JHEP* **10** (2021) 118, [2108.04216](#).
- [128] A. V. Manohar, A. K. Ridgway, and C.-H. Shen, “Radiated Angular Momentum and Dissipative Effects in Classical Scattering,” *Phys. Rev. Lett.* **129** (2022), no. 12 121601, [2203.04283](#).
- [129] Z. Bern, J. Parra-Martinez, R. Roiban, M. S. Ruf, C.-H. Shen, M. P. Solon, and M. Zeng, “Scattering Amplitudes and Conservative Binary Dynamics at $\mathcal{O}(G^4)$,” *Phys. Rev. Lett.* **126** (2021), no. 17 171601, [2101.07254](#).
- [130] Z. Bern, J. Parra-Martinez, R. Roiban, M. S. Ruf, C.-H. Shen, M. P. Solon, and M. Zeng, “Scattering Amplitudes, the Tail Effect, and Conservative Binary Dynamics at $\mathcal{O}(G^4)$,” *Phys. Rev. Lett.* **128** (2022), no. 16 161103, [2112.10750](#).
- [131] Z. Bern, J. Parra-Martinez, R. Roiban, E. Sawyer, and C.-H. Shen, “Leading Nonlinear Tidal Effects and Scattering Amplitudes,” *JHEP* **05** (2021) 188, [2010.08559](#).
- [132] C. Cheung and M. P. Solon, “Tidal Effects in the Post-Minkowskian Expansion,” *Phys. Rev. Lett.* **125** (2020), no. 19 191601, [2006.06665](#).
- [133] M. Accattulli Huber, A. Brandhuber, S. De Angelis, and G. Travaglini, “Eikonal phase matrix, deflection angle and time delay in effective field theories of gravity,” *Phys. Rev. D* **102** (2020), no. 4 046014, [2006.02375](#).

- [134] K. Haddad and A. Helset, "Tidal effects in quantum field theory," *JHEP* **12** (2020) 024, [2008.04920](#).
- [135] R. Aoude, K. Haddad, and A. Helset, "On-shell heavy particle effective theories," *JHEP* **05** (2020) 051, [2001.09164](#).
- [136] C. Cheung, N. Shah, and M. P. Solon, "Mining the Geodesic Equation for Scattering Data," *Phys. Rev. D* **103** (2021), no. 2 024030, [2010.08568](#).
- [137] N. Arkani-Hamed, T.-C. Huang, and Y.-t. Huang, "Scattering amplitudes for all masses and spins," *JHEP* **11** (2021) 070, [1709.04891](#).
- [138] M.-Z. Chung, Y.-T. Huang, J.-W. Kim, and S. Lee, "The simplest massive S-matrix: from minimal coupling to Black Holes," *JHEP* **04** (2019) 156, [1812.08752](#).
- [139] J. Vines, J. Steinhoff, and A. Buonanno, "Spinning-black-hole scattering and the test-black-hole limit at second post-Minkowskian order," *Phys. Rev. D* **99** (2019), no. 6 064054, [1812.00956](#).
- [140] Z. Bern, A. Luna, R. Roiban, C.-H. Shen, and M. Zeng, "Spinning black hole binary dynamics, scattering amplitudes, and effective field theory," *Phys. Rev. D* **104** (2021), no. 6 065014, [2005.03071](#).
- [141] A. Guevara, A. Ochirov, and J. Vines, "Scattering of Spinning Black Holes from Exponentiated Soft Factors," *JHEP* **09** (2019) 056, [1812.06895](#).
- [142] Z. Bern, D. Kosmopoulos, A. Luna, R. Roiban, and F. Teng, "Binary Dynamics Through the Fifth Power of Spin at $\mathcal{O}(G^2)$," [2203.06202](#).
- [143] F. Febres Cordero, M. Kraus, G. Lin, M. S. Ruf, and M. Zeng, "Conservative Binary Dynamics with a Spinning Black Hole at $\mathcal{O}(G^3)$ from Scattering Amplitudes," [2205.07357](#).
- [144] W. D. Goldberger and I. Z. Rothstein, "Dissipative effects in the worldline approach to black hole dynamics," *Phys. Rev. D* **73** (2006) 104030, [hep-th/0511133](#).
- [145] M. M. Riva, "Effective Field Theory for Gravitational Radiation in General Relativity and beyond," other thesis, 11, 2021.
- [146] W. D. Goldberger and A. K. Ridgway, "Radiation and the classical double copy for color charges," *Phys. Rev. D* **95** (2017), no. 12 125010, [1611.03493](#).
- [147] W. D. Goldberger and A. K. Ridgway, "Bound states and the classical double copy," *Phys. Rev. D* **97** (2018), no. 8 085019, [1711.09493](#).

- [148] C.-H. Shen, “Gravitational Radiation from Color-Kinematics Duality,” *JHEP* **11** (2018) 162, [1806.07388](#).
- [149] G. Kälin and R. A. Porto, “Post-Minkowskian Effective Field Theory for Conservative Binary Dynamics,” *JHEP* **11** (2020) 106, [2006.01184](#).
- [150] G. Kälin, J. Neef, and R. A. Porto, “Radiation-Reaction in the Effective Field Theory Approach to Post-Minkowskian Dynamics,” [2207.00580](#).
- [151] C. R. Galley, “Classical Mechanics of Nonconservative Systems,” *Phys. Rev. Lett.* **110** (2013), no. 17 174301, [1210.2745](#).
- [152] G. Kälin, Z. Liu, and R. A. Porto, “Conservative Dynamics of Binary Systems to Third Post-Minkowskian Order from the Effective Field Theory Approach,” *Phys. Rev. Lett.* **125** (2020), no. 26 261103, [2007.04977](#).
- [153] C. Dlapa, G. Kälin, Z. Liu, and R. A. Porto, “Dynamics of binary systems to fourth Post-Minkowskian order from the effective field theory approach,” *Phys. Lett. B* **831** (2022) 137203, [2106.08276](#).
- [154] C. Dlapa, G. Kälin, Z. Liu, and R. A. Porto, “Conservative Dynamics of Binary Systems at Fourth Post-Minkowskian Order in the Large-Eccentricity Expansion,” *Phys. Rev. Lett.* **128** (2022), no. 16 161104, [2112.11296](#).
- [155] W. D. Goldberger and J. Li, “Strings, extended objects, and the classical double copy,” *JHEP* **02** (2020) 092, [1912.01650](#).
- [156] G. Kälin, Z. Liu, and R. A. Porto, “Conservative Tidal Effects in Compact Binary Systems to Next-to-Leading Post-Minkowskian Order,” *Phys. Rev. D* **102** (2020) 124025, [2008.06047](#).
- [157] W. D. Goldberger and I. Z. Rothstein, “Horizon radiation reaction forces,” *JHEP* **10** (2020) 026, [2007.00731](#).
- [158] W. D. Goldberger, J. Li, and I. Z. Rothstein, “Non-conservative effects on spinning black holes from world-line effective field theory,” *JHEP* **06** (2021) 053, [2012.14869](#).
- [159] W. D. Goldberger, J. Li, and S. G. Prabhu, “Spinning particles, axion radiation, and the classical double copy,” *Phys. Rev. D* **97** (2018), no. 10 105018, [1712.09250](#).
- [160] J. Li and S. G. Prabhu, “Gravitational radiation from the classical spinning double copy,” *Phys. Rev. D* **97** (2018), no. 10 105019, [1803.02405](#).
- [161] Z. Liu, R. A. Porto, and Z. Yang, “Spin Effects in the Effective Field Theory Approach to Post-Minkowskian Conservative Dynamics,” *JHEP* **06** (2021) 012, [2102.10059](#).

- [162] G. Mogull, J. Plefka, and J. Steinhoff, "Classical black hole scattering from a worldline quantum field theory," *JHEP* **02** (2021) 048, [2010.02865](#).
- [163] G. U. Jakobsen, G. Mogull, J. Plefka, and J. Steinhoff, "Classical Gravitational Bremsstrahlung from a Worldline Quantum Field Theory," *Phys. Rev. Lett.* **126** (2021), no. 20 201103, [2101.12688](#).
- [164] G. U. Jakobsen, G. Mogull, J. Plefka, and J. Steinhoff, "SUSY in the sky with gravitons," *JHEP* **01** (2022) 027, [2109.04465](#).
- [165] G. U. Jakobsen, G. Mogull, J. Plefka, and J. Steinhoff, "Gravitational Bremsstrahlung and Hidden Supersymmetry of Spinning Bodies," *Phys. Rev. Lett.* **128** (2022), no. 1 011101, [2106.10256](#).
- [166] G. U. Jakobsen and G. Mogull, "Conservative and Radiative Dynamics of Spinning Bodies at Third Post-Minkowskian Order Using Worldline Quantum Field Theory," *Phys. Rev. Lett.* **128** (2022), no. 14 141102, [2201.07778](#).
- [167] G. U. Jakobsen, G. Mogull, J. Plefka, and B. Sauer, "All Things Retarded: Radiation-Reaction in Worldline Quantum Field Theory," [2207.00569](#).
- [168] C. Anastasiou and K. Melnikov, "Higgs boson production at hadron colliders in NNLO QCD," *Nucl. Phys. B* **646** (2002) 220–256, [hep-ph/0207004](#).
- [169] C. Anastasiou, L. J. Dixon, and K. Melnikov, "NLO Higgs boson rapidity distributions at hadron colliders," *Nucl. Phys. B Proc. Suppl.* **116** (2003) 193–197, [hep-ph/0211141](#).
- [170] C. Anastasiou, L. J. Dixon, K. Melnikov, and F. Petriello, "Dilepton rapidity distribution in the Drell-Yan process at NNLO in QCD," *Phys. Rev. Lett.* **91** (2003) 182002, [hep-ph/0306192](#).
- [171] C. Anastasiou, C. Duhr, F. Dulat, E. Furlan, F. Herzog, and B. Mistlberger, "Soft expansion of double-real-virtual corrections to Higgs production at N³LO," *JHEP* **08** (2015) 051, [1505.04110](#).
- [172] F. V. Tkachov, "A Theorem on Analytical Calculability of Four Loop Renormalization Group Functions," *Phys. Lett. B* **100** (1981) 65–68.
- [173] K. G. Chetyrkin and F. V. Tkachov, "Integration by Parts: The Algorithm to Calculate beta Functions in 4 Loops," *Nucl. Phys. B* **192** (1981) 159–204.
- [174] S. Laporta and E. Remiddi, "The Analytical value of the electron (g-2) at order alpha**3 in QED," *Phys. Lett. B* **379** (1996) 283–291, [hep-ph/9602417](#).
- [175] S. Laporta, "High precision calculation of multiloop Feynman integrals by difference equations," *Int. J. Mod. Phys. A* **15** (2000) 5087–5159, [hep-ph/0102033](#).

- [176] V. A. Smirnov, *Analytic tools for Feynman integrals*, vol. 250 of *Springer Tracts in Modern Physics*. Springer, Berlin, Heidelberg, 2012.
- [177] R. N. Lee, “Presenting LiteRed: a tool for the Loop InTEgrals REDuction,” [1212.2685](#).
- [178] R. N. Lee, “LiteRed 1.4: a powerful tool for reduction of multiloop integrals,” *J. Phys. Conf. Ser.* **523** (2014) 012059, [1310.1145](#).
- [179] A. V. Smirnov and F. S. Chuharev, “FIRE6: Feynman Integral REDuction with Modular Arithmetic,” *Comput. Phys. Commun.* **247** (2020) 106877, [1901.07808](#).
- [180] A. V. Kotikov, “Differential equations method: New technique for massive Feynman diagrams calculation,” *Phys. Lett. B* **254** (1991) 158–164.
- [181] A. V. Kotikov, “Differential equation method: The Calculation of N point Feynman diagrams,” *Phys. Lett. B* **267** (1991) 123–127. [Erratum: *Phys.Lett.B* 295, 409–409 (1992)].
- [182] Z. Bern, L. J. Dixon, and D. A. Kosower, “Dimensionally regulated one loop integrals,” *Phys. Lett. B* **302** (1993) 299–308, [hep-ph/9212308](#). [Erratum: *Phys.Lett.B* 318, 649 (1993)].
- [183] T. Gehrmann and E. Remiddi, “Differential equations for two loop four point functions,” *Nucl. Phys. B* **580** (2000) 485–518, [hep-ph/9912329](#).
- [184] J. M. Henn, “Multiloop integrals in dimensional regularization made simple,” *Phys. Rev. Lett.* **110** (2013) 251601, [1304.1806](#).
- [185] S. Caron-Huot and J. M. Henn, “Iterative structure of finite loop integrals,” *JHEP* **06** (2014) 114, [1404.2922](#).
- [186] B. Kocsis, M. E. Gaspar, and S. Marka, “Detection rate estimates of gravity-waves emitted during parabolic encounters of stellar black holes in globular clusters,” *Astrophys. J.* **648** (2006) 411–429, [astro-ph/0603441](#).
- [187] S. Capozziello, M. De Laurentis, F. De Paolis, G. Ingrosso, and A. Nucita, “Gravitational waves from hyperbolic encounters,” *Mod. Phys. Lett. A* **23** (2008) 99–107, [0801.0122](#).
- [188] K. Kremer, C. S. Ye, N. Z. Rui, N. C. Weatherford, S. Chatterjee, G. Fragione, C. L. Rodriguez, M. Spera, and F. A. Rasio, “Modeling Dense Star Clusters in the Milky Way and Beyond with the CMC Cluster Catalog,” *Astrophys. J. Suppl.* **247** (2020), no. 2 48, [1911.00018](#).

- [189] S. Mukherjee, S. Mitra, and S. Chatterjee, “Gravitational wave observatories may be able to detect hyperbolic encounters of black holes,” *Mon. Not. Roy. Astron. Soc.* **508** (2021), no. 4 5064–5073, [2010.00916](#).
- [190] T. Damour, “Classical and quantum scattering in post-Minkowskian gravity,” *Phys. Rev. D* **102** (2020), no. 2 024060, [1912.02139](#).
- [191] P. H. Damgaard and P. Vanhove, “Remodeling the effective one-body formalism in post-Minkowskian gravity,” *Phys. Rev. D* **104** (2021), no. 10 104029, [2108.11248](#).
- [192] G. Kälin and R. A. Porto, “From boundary data to bound states. Part II. Scattering angle to dynamical invariants (with twist),” *JHEP* **02** (2020) 120, [1911.09130](#).
- [193] G. Cho, G. Kälin, and R. A. Porto, “From boundary data to bound states. Part III. Radiative effects,” *JHEP* **04** (2022) 154, [2112.03976](#).
- [194] D. Bini and T. Damour, “Analytical determination of the two-body gravitational interaction potential at the fourth post-Newtonian approximation,” *Phys. Rev. D* **87** (2013), no. 12 121501, [1305.4884](#).
- [195] T. Damour, P. Jaranowski, and G. Schäfer, “Conservative dynamics of two-body systems at the fourth post-Newtonian approximation of general relativity,” *Phys. Rev. D* **93** (2016), no. 8 084014, [1601.01283](#).
- [196] L. Blanchet, “Time asymmetric structure of gravitational radiation,” *Phys. Rev. D* **47** (1993) 4392–4420.
- [197] T. Damour, “Radiative contribution to classical gravitational scattering at the third order in G ,” *Phys. Rev. D* **102** (2020), no. 12 124008, [2010.01641](#).
- [198] T. Damour and A. Nagar, “Relativistic tidal properties of neutron stars,” *Phys. Rev. D* **80** (2009) 084035, [0906.0096](#).
- [199] T. Binnington and E. Poisson, “Relativistic theory of tidal Love numbers,” *Phys. Rev. D* **80** (2009) 084018, [0906.1366](#).
- [200] R. A. Porto, “Post-Newtonian corrections to the motion of spinning bodies in NRGR,” *Phys. Rev. D* **73** (2006) 104031, [gr-qc/0511061](#).
- [201] R. A. Porto and I. Z. Rothstein, “Spin(1)Spin(2) Effects in the Motion of Inspiralling Compact Binaries at Third Order in the Post-Newtonian Expansion,” *Phys. Rev. D* **78** (2008) 044012, [0802.0720](#). [Erratum: *Phys. Rev. D* 81, 029904 (2010)].
- [202] M. Levi and J. Steinhoff, “Spinning gravitating objects in the effective field theory in the post-Newtonian scheme,” *JHEP* **09** (2015) 219, [1501.04956](#).

- [203] G. Cho, G. Kälin, and R. A. Porto (private communication).
- [204] R. E. Cutkosky, "Singularities and discontinuities of Feynman amplitudes," *J. Math. Phys.* **1** (1960) 429–433.
- [205] M. J. G. Veltman, *Diagrammatica: The Path to Feynman rules*, vol. 4. Cambridge University Press, 5, 2012.
- [206] S. Mougiakakos, M. M. Riva, and F. Vernizzi, "Gravitational Bremsstrahlung in the post-Minkowskian effective field theory," *Phys. Rev. D* **104** (2021), no. 2 024041, [2102.08339](#).
- [207] M. M. Riva and F. Vernizzi, "Radiated momentum in the post-Minkowskian worldline approach via reverse unitarity," *JHEP* **11** (2021) 228, [2110.10140](#).
- [208] S. Mougiakakos, M. M. Riva, and F. Vernizzi, "Gravitational Bremsstrahlung with Tidal Effects in the Post-Minkowskian Expansion," *Phys. Rev. Lett.* **129** (2022), no. 12 121101, [2204.06556](#).
- [209] M. M. Riva, F. Vernizzi, and L. K. Wong, "Gravitational bremsstrahlung from spinning binaries in the post-Minkowskian expansion," *Phys. Rev. D* **106** (2022), no. 4 044013, [2205.15295](#).
- [210] M. Henneaux and C. Teitelboim, *Quantization of gauge systems*. Princeton University Press, 1992.
- [211] D. Tong, "String Theory," [0908.0333](#).
- [212] D. Bini, T. Damour, and G. Faye, "Effective action approach to higher-order relativistic tidal interactions in binary systems and their effective one body description," *Phys. Rev. D* **85** (2012) 124034, [1202.3565](#).
- [213] C. R. Galley and R. A. Porto, "Gravitational self-force in the ultra-relativistic limit: the "large- N " expansion," *JHEP* **11** (2013) 096, [1302.4486](#).
- [214] A. Kuntz, "Half-solution to the two-body problem in General Relativity," *Phys. Rev. D* **102** (2020), no. 6 064019, [2003.03366](#).
- [215] M. E. Peskin and D. V. Schroeder, *An Introduction to quantum field theory*. Addison-Wesley, Reading, USA, 1995.
- [216] M. Srednicki, *Quantum field theory*. Cambridge University Press, 1, 2007.
- [217] M. D. Schwartz, *Quantum Field Theory and the Standard Model*. Cambridge University Press, 3, 2014.
- [218] D. Brizuela, J. M. Martín-García, and G. A. Mena Marugán, "xPert: Computer algebra for metric perturbation theory," *Gen. Rel. Grav.* **41** (2009) 2415–2431, [0807.0824](#).

- [219] J. M. Martín-García, “xAct: Efficient tensor computer algebra for the Wolfram Language.” <http://xact.es/index.html>.
- [220] L. V. Keldysh, “Diagram technique for nonequilibrium processes,” *Zh. Eksp. Teor. Fiz.* **47** (1964) 1515–1527.
- [221] C. R. Galley and A. K. Leibovich, “Radiation reaction at 3.5 post-Newtonian order in effective field theory,” *Phys. Rev. D* **86** (2012) 044029, [1205.3842](#).
- [222] L. Abbott, “Introduction to the Background Field Method,” *Acta Phys. Polon. B* **13** (1982) 33.
- [223] T. Damour, “Gravitational scattering, post-Minkowskian approximation and Effective One-Body theory,” *Phys. Rev. D* **94** (2016), no. 10 104015, [1609.00354](#).
- [224] M. Maggiore, *Gravitational Waves. Vol. 1: Theory and Experiments*. Oxford Master Series in Physics. Oxford University Press, 2007.
- [225] O. B. Firsov, “Determination of the forces acting between atoms using the differential effective cross-section for elastic scattering,” *Journal of Experimental and Theoretical Physics (ZhETP)* **24** (1953) 279.
- [226] L. Landau and E. Lifshitz, *Mechanics (Mekhanika)*. Volume 1 of A Course of Theoretical Physics. Pergamon Press, 1969.
- [227] G. 't Hooft and M. J. G. Veltman, “DIAGRAMMAR,” *NATO Sci. Ser. B* **4** (1974) 177–322.
- [228] D. Meltzer and A. Sivaramakrishnan, “CFT unitarity and the AdS Cutkosky rules,” *JHEP* **11** (2020) 073, [2008.11730](#).
- [229] B. Grinstein, “Lectures on heavy quark effective theory,” in *Workshop on High-energy Phenomenology (CINVESTAV)*, 12, 1991.
- [230] O. Gituliar and V. Magerya, “Fuchsia and master integrals for splitting functions from differential equations in QCD,” *PoS* **LL2016** (2016) 030, [1607.00759](#).
- [231] O. Gituliar and V. Magerya, “Fuchsia: a tool for reducing differential equations for Feynman master integrals to epsilon form,” *Comput. Phys. Commun.* **219** (2017) 329–338, [1701.04269](#).
- [232] R. N. Lee, “Reducing differential equations for multiloop master integrals,” *JHEP* **04** (2015) 108, [1411.0911](#).
- [233] W. D. Goldberger and A. Ross, “Gravitational radiative corrections from effective field theory,” *Phys. Rev. D* **81** (2010) 124015, [0912.4254](#).

- [234] D. Bini, T. Damour, and A. Geralico, “Sixth post-Newtonian nonlocal-in-time dynamics of binary systems,” *Phys. Rev. D* **102** (2020), no. 8 084047, [2007.11239](#).
- [235] S. Weinberg, “Photons and Gravitons in S -Matrix Theory: Derivation of Charge Conservation and Equality of Gravitational and Inertial Mass,” *Phys. Rev.* **135** (1964) B1049–B1056.
- [236] S. Weinberg, “Infrared photons and gravitons,” *Phys. Rev.* **140** (1965) B516–B524.
- [237] L. Smarr, “Gravitational Radiation from Distant Encounters and from Headon Collisions of Black Holes: The Zero Frequency Limit,” *Phys. Rev. D* **15** (1977) 2069–2077.
- [238] P. Di Vecchia, C. Heissenberg, R. Russo, and G. Veneziano, “Radiation Reaction from Soft Theorems,” *Phys. Lett. B* **818** (2021) 136379, [2101.05772](#).
- [239] K. S. Thorne, “Multipole Expansions of Gravitational Radiation,” *Rev. Mod. Phys.* **52** (1980) 299–339.
- [240] J. M. Henn, “Lectures on differential equations for Feynman integrals,” *J. Phys. A* **48** (2015) 153001, [1412.2296](#).
- [241] T. Damour, M. Soffel, and C.-m. Xu, “General relativistic celestial mechanics. 4: Theory of satellite motion,” *Phys. Rev. D* **49** (1994) 618–635.
- [242] T. Hinderer, “Tidal Love numbers of neutron stars,” *Astrophys. J.* **677** (2008) 1216–1220, [0711.2420](#).
- [243] E. E. Flanagan and T. Hinderer, “Constraining neutron star tidal Love numbers with gravitational wave detectors,” *Phys. Rev. D* **77** (2008) 021502, [0709.1915](#).
- [244] T. Hinderer, B. D. Lackey, R. N. Lang, and J. S. Read, “Tidal deformability of neutron stars with realistic equations of state and their gravitational wave signatures in binary inspiral,” *Phys. Rev. D* **81** (2010) 123016, [0911.3535](#).
- [245] B. Kol and M. Smolkin, “Black hole stereotyping: Induced gravito-static polarization,” *JHEP* **02** (2012) 010, [1110.3764](#).
- [246] T. Damour, A. Nagar, and L. Villain, “Measurability of the tidal polarizability of neutron stars in late-inspiral gravitational-wave signals,” *Phys. Rev. D* **85** (2012) 123007, [1203.4352](#).
- [247] M. Favata, “Systematic parameter errors in inspiraling neutron star binaries,” *Phys. Rev. Lett.* **112** (2014) 101101, [1310.8288](#).

- [248] L. Baiotti and L. Rezzolla, “Binary neutron star mergers: a review of Einstein’s richest laboratory,” *Rept. Prog. Phys.* **80** (2017), no. 9 096901, [1607.03540](#).
- [249] L. Barack *et. al.*, “Black holes, gravitational waves and fundamental physics: a roadmap,” *Class. Quant. Grav.* **36** (2019), no. 14 143001, [1806.05195](#).
- [250] A. Buonanno and B. S. Sathyaprakash, *Sources of Gravitational Waves: Theory and Observations*. Cambridge University Press, 10, 2015. [1410.7832](#).
- [251] V. Cardoso and P. Pani, “Testing the nature of dark compact objects: a status report,” *Living Rev. Rel.* **22** (2019), no. 1 4, [1904.05363](#).
- [252] D. Baumann, H. S. Chia, R. A. Porto, and J. Stout, “Gravitational Collider Physics,” *Phys. Rev. D* **101** (2020), no. 8 083019, [1912.04932](#).
- [253] T. Mora and C. M. Will, “A PostNewtonian diagnostic of quasiequilibrium binary configurations of compact objects,” *Phys. Rev. D* **69** (2004) 104021, [gr-qc/0312082](#). [Erratum: *Phys.Rev.D* 71, 129901 (2005)].
- [254] J. E. Vines and E. E. Flanagan, “Post-1-Newtonian quadrupole tidal interactions in binary systems,” *Phys. Rev. D* **88** (2013) 024046, [1009.4919](#).
- [255] J. Vines, E. E. Flanagan, and T. Hinderer, “Post-1-Newtonian tidal effects in the gravitational waveform from binary inspirals,” *Phys. Rev. D* **83** (2011) 084051, [1101.1673](#).
- [256] T. Damour and A. Nagar, “Effective One Body description of tidal effects in inspiralling compact binaries,” *Phys. Rev. D* **81** (2010) 084016, [0911.5041](#).
- [257] J. Steinhoff, T. Hinderer, A. Buonanno, and A. Taracchini, “Dynamical Tides in General Relativity: Effective Action and Effective-One-Body Hamiltonian,” *Phys. Rev. D* **94** (2016) 104028, [1608.01907](#).
- [258] D. Bini and T. Damour, “Gravitational self-force corrections to two-body tidal interactions and the effective one-body formalism,” *Phys. Rev. D* **90** (2014), no. 12 124037, [1409.6933](#).
- [259] D. Bini and A. Geralico, “Gravitational self-force corrections to tidal invariants for spinning particles on circular orbits in a Schwarzschild spacetime,” *Phys. Rev. D* **98** (2018), no. 8 084021, [1806.03495](#).
- [260] D. Bini and A. Geralico, “Gravitational self-force corrections to tidal invariants for particles on eccentric orbits in a Schwarzschild spacetime,” *Phys. Rev. D* **98** (2018), no. 6 064026, [1806.06635](#).
- [261] D. Bini and A. Geralico, “Gravitational self-force corrections to tidal invariants for particles on circular orbits in a Kerr spacetime,” *Phys. Rev. D* **98** (2018), no. 6 064040, [1806.08765](#).

- [262] T. Dietrich, T. Hinderer, and A. Samajdar, “Interpreting Binary Neutron Star Mergers: Describing the Binary Neutron Star Dynamics, Modelling Gravitational Waveforms, and Analyzing Detections,” *Gen. Rel. Grav.* **53** (2021), no. 3 27, [2004.02527](#).
- [263] M. Accettulli Huber, A. Brandhuber, S. De Angelis, and G. Travaglini, “From amplitudes to gravitational radiation with cubic interactions and tidal effects,” *Phys. Rev. D* **103** (2021), no. 4 045015, [2012.06548](#).
- [264] M. Accettulli Huber, A. Brandhuber, S. De Angelis, and G. Travaglini, “From amplitudes to gravitational radiation with cubic interactions and tidal effects,” *Phys. Rev. D* **103** (2021), no. 4 045015, [2012.06548](#).
- [265] D. Bini, T. Damour, and A. Geralico, “Scattering of tidally interacting bodies in post-Minkowskian gravity,” *Phys. Rev. D* **101** (2020), no. 4 044039, [2001.00352](#).
- [266] A. Ross, “Multipole expansion at the level of the action,” *Phys. Rev. D* **85** (2012) 125033, [1202.4750](#).
- [267] A. E. H. Love, *Some Problems of Geodynamics*. Cambridge University Press, 1911.
- [268] H. Fang and G. Lovelace, “Tidal coupling of a Schwarzschild black hole and circularly orbiting moon,” *Phys. Rev. D* **72** (2005) 124016, [gr-qc/0505156](#).
- [269] P. D. D’Eath, “High Speed Black Hole Encounters and Gravitational Radiation,” *Phys. Rev. D* **18** (1978) 990.
- [270] T. Damour and N. Deruelle, “General relativistic celestial mechanics 1. the post-newtonian motion,” *Ann. Inst. Henri Poincaré* **43** (1985) 107–132.
- [271] G. Schäfer and N. Wex, “Second post-newtonian motion of compact binaries,” *Physics Letters A* **174** (1993), no. 3 196–205.
- [272] D. Bini and T. Damour, “Gravitational radiation reaction along general orbits in the effective one-body formalism,” *Phys. Rev. D* **86** (2012) 124012, [1210.2834](#).
- [273] S. Vitale, R. Lynch, J. Veitch, V. Raymond, and R. Sturani, “Measuring the spin of black holes in binary systems using gravitational waves,” *Phys. Rev. Lett.* **112** (2014), no. 25 251101, [1403.0129](#).
- [274] **LIGO Scientific, Virgo** Collaboration, T. D. Abbott *et. al.*, “Improved analysis of GW150914 using a fully spin-precessing waveform Model,” *Phys. Rev. X* **6** (2016), no. 4 041014, [1606.01210](#).

- [275] **LIGO Scientific, Virgo** Collaboration, R. Abbott *et. al.*, “GW190412: Observation of a Binary-Black-Hole Coalescence with Asymmetric Masses,” *Phys. Rev. D* **102** (2020), no. 4 043015, [2004.08342](#).
- [276] D. Baumann, H. S. Chia, and R. A. Porto, “Probing Ultralight Bosons with Binary Black Holes,” *Phys. Rev. D* **99** (2019), no. 4 044001, [1804.03208](#).
- [277] A. Arvanitaki and S. Dubovsky, “Exploring the String Axiverse with Precision Black Hole Physics,” *Phys. Rev. D* **83** (2011) 044026, [1004.3558](#).
- [278] **LIGO Scientific, VIRGO, KAGRA** Collaboration, R. Abbott *et. al.*, “All-sky search for gravitational wave emission from scalar boson clouds around spinning black holes in LIGO O3 data,” *Phys. Rev. D* **105** (2022), no. 10 [2111.15507](#).
- [279] G. Faye, L. Blanchet, and A. Buonanno, “Higher-order spin effects in the dynamics of compact binaries. I. Equations of motion,” *Phys. Rev. D* **74** (2006) 104033, [gr-qc/0605139](#).
- [280] L. Blanchet, A. Buonanno, and G. Faye, “Higher-order spin effects in the dynamics of compact binaries. II. Radiation field,” *Phys. Rev. D* **74** (2006) 104034, [gr-qc/0605140](#). [Erratum: *Phys.Rev.D* 75, 049903 (2007), Erratum: *Phys.Rev.D* 81, 089901 (2010)].
- [281] A. Antonelli, M. van de Meent, A. Buonanno, J. Steinhoff, and J. Vines, “Quasicircular inspirals and plunges from nonspinning effective-one-body Hamiltonians with gravitational self-force information,” *Phys. Rev. D* **101** (2020), no. 2 024024, [1907.11597](#).
- [282] T. Damour, P. Jaranowski, and G. Schaefer, “Effective one body approach to the dynamics of two spinning black holes with next-to-leading order spin-orbit coupling,” *Phys. Rev. D* **78** (2008) 024009, [0803.0915](#).
- [283] A. Nagar, “Effective one body Hamiltonian of two spinning black-holes with next-to-next-to-leading order spin-orbit coupling,” *Phys. Rev. D* **84** (2011) 084028, [1106.4349](#). [Erratum: *Phys.Rev.D* 88, 089901 (2013)].
- [284] E. Barausse and A. Buonanno, “Extending the effective-one-body Hamiltonian of black-hole binaries to include next-to-next-to-leading spin-orbit couplings,” *Phys. Rev. D* **84** (2011) 104027, [1107.2904](#).
- [285] J. Vines, “Scattering of two spinning black holes in post-Minkowskian gravity, to all orders in spin, and effective-one-body mappings,” *Class. Quant. Grav.* **35** (2018), no. 8 084002, [1709.06016](#).
- [286] A. Guevara, A. Ochirov, and J. Vines, “Black-hole scattering with general spin directions from minimal-coupling amplitudes,” *Phys. Rev. D* **100** (2019), no. 10 104024, [1906.10071](#).

- [287] W.-M. Chen, M.-Z. Chung, Y.-t. Huang, and J.-W. Kim, “The 2PM Hamiltonian for binary Kerr to quartic in spin,” *JHEP* **08** (2022) 148, [2111.13639](#).
- [288] R. Aoude, K. Haddad, and A. Helset, “Classical gravitational spinning-spinless scattering at $\mathcal{O}(G^2S^\infty)$,” [2205.02809](#).
- [289] F. Alessio and P. Di Vecchia, “Radiation reaction for spinning black-hole scattering,” *Phys. Lett. B* **832** (2022) 137258, [2203.13272](#).
- [290] J. Steinhoff and G. Schaefer, “Canonical formulation of self-gravitating spinning-object systems,” *EPL* **87** (2009), no. 5 50004, [0907.1967](#).
- [291] P. Brax, A.-C. Davis, S. Melville, and L. K. Wong, “Spin-orbit effects for compact binaries in scalar-tensor gravity,” *JCAP* **10** (2021) 075, [2107.10841](#).
- [292] J. Steinhoff, “Spin gauge symmetry in the action principle for classical relativistic particles,” [1501.04951](#).
- [293] P. A. M. Dirac, *Lectures on Quantum Mechanics*. Yeshiva University, New York, 1964.
- [294] S. M. Carroll, *Spacetime and Geometry*. Cambridge University Press, 7, 2019.
- [295] A. J. Hanson and T. Regge, “The Relativistic Spherical Top,” *Annals Phys.* **87** (1974) 498.
- [296] T. D. Newton and E. P. Wigner, “Localized states for elementary systems,” *Rev. Mod. Phys.* **21** (Jul, 1949) 400–406.
- [297] A. Papapetrou, “Spinning test particles in general relativity. 1.,” *Proc. Roy. Soc. Lond. A* **209** (1951) 248–258.
- [298] W. G. Dixon, “Dynamics of extended bodies in general relativity. I. Momentum and angular momentum,” *Proc. Roy. Soc. Lond. A* **314** (1970) 499–527.
- [299] **KAGRA, LIGO Scientific, Virgo, VIRGO** Collaboration, B. P. Abbott *et. al.*, “Prospects for observing and localizing gravitational-wave transients with Advanced LIGO, Advanced Virgo and KAGRA,” *Living Rev. Rel.* **21** (2018), no. 1 3, [1304.0670](#).
- [300] E. Berti, V. Cardoso, Z. Haiman, D. E. Holz, E. Mottola, S. Mukherjee, B. Sathyaprakash, X. Siemens, and N. Yunes, “Snowmass2021 Cosmic Frontier White Paper: Fundamental Physics and Beyond the Standard Model,” in *2022 Snowmass Summer Study*, 3, 2022. [2203.06240](#).
- [301] A. Strominger and A. Zhiboedov, “Gravitational Memory, BMS Supertranslations and Soft Theorems,” *JHEP* **01** (2016) 086, [1411.5745](#).

- [302] C. Shi and J. Plefka, "Classical double copy of worldline quantum field theory," *Phys. Rev. D* **105** (2022), no. 2 026007, [2109.10345](#).
- [303] J. L. Bourjaily *et. al.*, "Functions Beyond Multiple Polylogarithms for Precision Collider Physics," in *2022 Snowmass Summer Study*, 3, 2022. [2203.07088](#).
- [304] Z. Bern, M. Enciso, H. Ita, and M. Zeng, "Dual Conformal Symmetry, Integration-by-Parts Reduction, Differential Equations and the Nonplanar Sector," *Phys. Rev. D* **96** (2017), no. 9 096017, [1709.06055](#).
- [305] P. Mastrolia and S. Mizera, "Feynman Integrals and Intersection Theory," *JHEP* **02** (2019) 139, [1810.03818](#).
- [306] H. Frellesvig, F. Gasparotto, M. K. Mandal, P. Mastrolia, L. Mattiazzi, and S. Mizera, "Vector Space of Feynman Integrals and Multivariate Intersection Numbers," *Phys. Rev. Lett.* **123** (2019), no. 20 201602, [1907.02000](#).
- [307] A. Cristofoli, R. Gonzo, D. A. Kosower, and D. O'Connell, "Waveforms from amplitudes," *Phys. Rev. D* **106** (2022), no. 5 056007, [2107.10193](#).